



Title	Enantioselective C-H Functionalization using Chiral Carboxylic Acid and d6 Transition Metal Complexes
Author(s)	黄, 竜涛; Huang, Longtao
Degree Grantor	北海道大学
Degree Name	博士(薬科学)
Dissertation Number	甲第15611号
Issue Date	2023-09-25
DOI	https://doi.org/10.14943/doctoral.k15611
Doc URL	https://hdl.handle.net/2115/90921
Type	doctoral thesis
File Information	Longtao_Huang.pdf



博士学位論文

**Enantioselective C–H Functionalization using Chiral Carboxylic Acid and
d6 Transition Metal Complexes**

(キラルカルボン酸と d6 型遷移金属錯体を用いたエナンチオ選択的 C-H
官能基化)

HUANG LONGTAO

北海道大学大学院生命科学院
生命科学専攻 生命医薬科学コース
薬品製造化学研究室

2023 年 9 月

Abbreviation

Pd	Palladium
Ru	Ruthenium
Rh	Rhodium
Ir	Iridium
Co	Cobalt
CCA	chiral carboxylic acid
Cp* /Cp*	pentamethylcyclopentadienyl
*	chiral
DG	directing groups
FG	functional groups
BINOL	2,2'-dihydroxy-1,1'-binaphthyl
KIE	kinetic isotope effects
NMR	nuclear magnetic resonance
CMD	concerted metalation deprotonation
DCE	1,2-dichloroethane
TFE	2,2,2-trifluoroethanol
HFIP	hexafluoro-2-propanol
HPLC	high performance liquid chromatography
Ac	acetyl
er	enantiomeric ratio
equiv	equivalent
h	hour
0.1 M	0.1 mol/L
Me	methyl
Ph	phenyl
<i>t</i> -Bu	tertiary butyl
r.t.	room temperature
MS 3A	molecular sieves 3A
MS 13X	molecular sieves 13X

IR	infrared spectroscopy
HRMS	high resolution mass spectrum
<i>i</i> Pr	isopropyl
Cy	cyclohexyl
oDCB	1,2-dichlorobenzene
R_f	retention factor
MPAA	mono- <i>N</i> -protected amino acid
cTDG	chiral transient directing group

Acknowledgement

I would like to express my sincere appreciation to my supervisor-Prof Shigeki Matsunaga, Tatsuhiko Yoshino sensei and Masahiro Kojima sensei for their generous, endless and strict encouragement during my study. I am sure that their enthusiasm for chemistry influenced greatly on my research style.

I also thank Dr. Luqing Lin, Dr. Shun Satake, Dr. Seiya Fukagawa, Dr. Yoshimi Kato, Mr. Yuki Hirata, Mr. Yuta Kitakawa, Mr. Kodai Yamada, Mr. Futa Kamiyama, Mr. Daichi Sekine for their kind discussion on my research project. They often gave me clues to overcome difficulties in the research.

I want to express my thank to Mr. Takumaru Kurihara, Mr. Ryo Tanaka, Mr. Tomoyuki Sekino, Mr. Yuji Kamei, Mr. Junpei Hirose, Mr. Kazuki Ikeda, Mr. Shunta Sato and others in Prof Matsunaga's lab for their help in my research/daily life, which let me adjust to life in Japan quickly.

I am grateful to Prof Zheng Wang, he told me how attractive chemistry is when I was an undergraduate student. I also thank Dr. Fei Cao, Dr. Huihong Wang, Mr. Yi Jiang and others in Prof Wang's lab.

I acknowledge the Global Facility Center of Hokkaido University, for measuring various spectral data. I would like to thank the operators of the Center's Instrumental Analysis Contract Department for their support. I also thank the financial support of Hokkaido University DX Doctoral Fellowship.

Finally, I would like to express my sincere appreciation to my parents and family for their continuous support.

2023, summer.

Table of contents

1. Chapter 1. Cp*M(III)-catalyzed Enantioselective C–H Functionalization by Chiral Cp Ligand	
1-1. Introduction of C–H Bond Functionalization	1
1-2. Cp*M(III) Catalysts and Chiral Cp*M(III) Catalysts for C–H Functionalization	1
2. Chapter 2. Cp*M(III)-catalyzed Enantioselective C-H Activation by Chiral Carboxylic Acid	
2-1. Application of Carboxylate in Transition Metal Catalyzed C-H Activation	7
2-2. Enantioselective C(sp ²)-H Functionalization Reaction.....	9
2-3. Enantioselective C(sp ³)-H Functionalization Reaction.....	10
2-4. Enantioselective C-H Functionalization Reactions by Other New CCA.....	12
3. Chapter 3. Cp*Rh(III)-Catalyzed Conjugate Addition of C-H Bonds to α,β -Unsaturated Compounds	
3-1. Introduction of Cp*Rh(III)-Catalyzed Conjugate Addition to α,β -Unsaturated Ketones.....	13
3-2. Cp*Rh(III)-catalyzed Conjugate Addition of C(sp ²)-H Bonds to α,β -Unsaturated Carbonyl Compounds	13
3-3. Cp*Rh(III)-Catalyzed Conjugate Addition of C(sp ³)-H Bonds to α,β -Unsaturated Ketones ...	15
3-4. Cp*M(III)-Catalyzed Asymmetric Addition of C–H Bonds to Electron-deficient Alkenes .	16
4. Chapter 4. First Work: Cp*Rh(III)-Catalyzed Asymmetric Conjugate Addition of C(sp ³)-H Bonds to α,β -Unsaturated Ketones	
4-1. Screening of Cationic Ag Salt	19
4-2. Screening of Solvent	20
4-3. Screening of Ligand	21
4-4. Influence of Acidity	22
4-5. Screening of Reaction Temperature	25
4-6. Scope of Substrates	26
4-7. H/D Exchange Experiment	29
4-8. Proposed Reaction Mechanism.....	30
4-9. Determination of Absolute Configuration.....	31
5. Chapter 5. Arene Ru(II)-Catalyzed Enantioselective C–H Functionalization	
5-1. Introduction of Arene Ru(II)-Catalyzed C–H Bond Functionalization	33
5-2. Introduction of Chiral Arene-Ru(II)-catalyzed Enantioselective C–H Bond Functionalization	34
5-3. Introduction of Arene-Ru(II)/cTDG-Catalyzed Enantioselective C–H Bond Functionalization	36

6. Chapter 6. Arene-Ru(II)-catalyzed Enantioselective C–H Functionalization by Chiral Carboxylic Acid	
6-1. The two modes of Arene-Ru(II)/CCA-Catalyzed Enantioselective C–H Bond Functionalization	38
6-2. Arene-Ru(II)/CCA-Catalyzed Enantioselective C–H Bond Functionalization	38
7. Chapter 7. Aza Analogues of Sulfones - Sulfoximine and TM Catalyzed C–H Activation of Sulfoximine to C–C Formation	
7-1. Importance of Sulfur(VI)-Containing Motifs in Pharmaceutical and Medicinal Chemistry	41
7-2. TM Catalyzed C–H Alkenylation of Sulfoximines	43
7-3. TM Catalyzed C-H Enantioselective C–H Functionalization of Sulfoximines	44
8. Chapter 8. Second work: Ru(II)/Chiral Carboxylic Acid-Catalyzed Enantioselective C–H Functionalization of Sulfoximines	
8-1. Optimization of Reaction Condition	47
8-2. Screening of CCA	49
8-3. Scope of Sulfoximines and Sulfoxonium Ylides	50
8-4. Proposed Mechanism	51
9. Chapter 9. Third work: Enantioselective Synthesis of 1,2-Benzothiazine 1-Imines via Ru(II)/Chiral Carboxylic Acid-Catalyzed C–H Alkylation/Cyclization	
9-1. Screening of CCA and The Synthesis Route of New CCA	55
9-2. Optimization of M⁺ Salt	56
9-3. Scope of Sulfonylimines and Sulfoxonium Ylides	57
9-4. Kinetic Resolution of Racemic Sulfonylimine	59
9-5. Parallel Kinetic Resolution	60
9-6. The Experiment for Mechanism	60
10. Experimental Section	63
11. Reference	173

Chapter 1. Cp^xM(III)-catalyzed Enantioselective C–H Functionalization by Chiral Cp Ligand

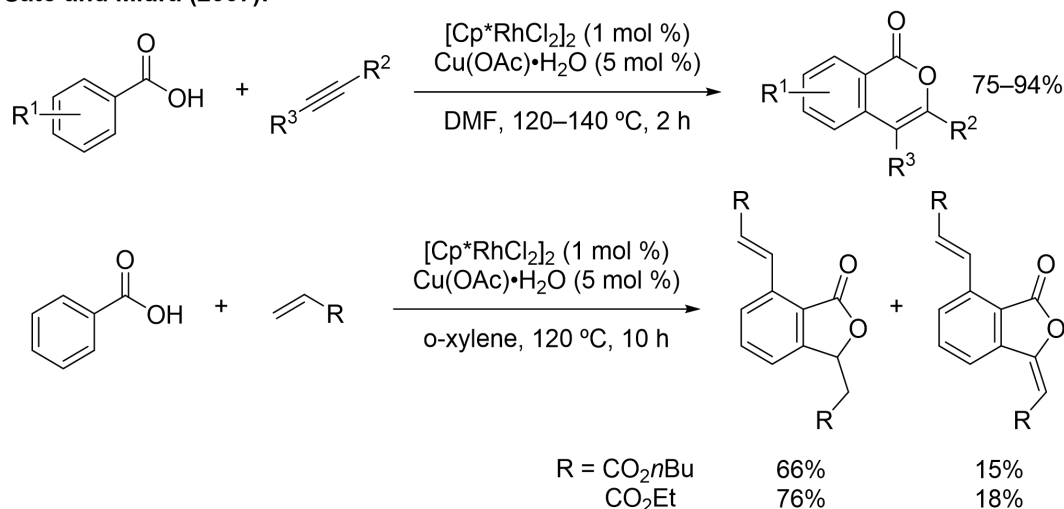
1-1 Introduction of C–H Bond Functionalization

Organic compounds are collections of carbon-carbon, carbon-hydrogen, carbon-heteroatom, and other bonds.¹ Many transition metal-catalyzed synthetic methods have been intensively investigated since the middle of the 20th century, and the activation and transformation of various chemical bonds has become possible.¹ In recent years, the variation of bonds that can be activated has been tremendously expanded and currently even non-activated carbon-hydrogen bonds can be efficiently cleaved and functionalized under transition metal catalysis.¹ These reactions are generally called C–H functionalization (or C–H activation, when focusing on C-H bond cleavage step) and have become one of the most advanced studies in synthetic organic chemistry, representing economic and ecological advantages, because carbon-carbon or carbon-hetero atom bonds can be formed without additional synthetic steps for replacing the less reactive C–H bonds with highly reactive functional groups in advance. Therefore, C–H functionalization strategy can simplify and streamline synthetic routes. In addition, C–H activation is also applicable to some compounds that are often difficult and/or impossible to be pre-functionalized, which will expand the accessible chemical space by C-H functionalization strategy.

1-2 Cp^xM(III) Catalysts and Chiral Cp^xM(III) Catalysts for C–H Functionalization

C–H functionalization reactions using cationic group 9 transition metals such as Rh(III), Ir(III), and Co(III) with a pentamethylcyclopentadienyl (Cp^{*}) ligand have been widely developed and studied since the pioneering work by Sato and Miura *et al.* in 2007 (Scheme 1).^{2a)} These reactions exhibit good substrate versatility, functional group compatibility, and high catalyst turnover. In these reactions, C–H bonds near a coordinating functional group, often called as a directional group (DG) are selectively cleaved. (Scheme 1).

Sato and Miura (2007):



Scheme 1. Oxidative Coupling Reactions Using a Cp^{*}Rh(III) Catalyst

Despite the considerable potential of C-H functionalization strategy, however, the corresponding enantioselective processes remain largely underexplored, which would be in part due to the half-sandwich structure and the limited number of vacant coordination sites of Cp*M(III) complexes (**Figure 1**).³ Usually, the reactions using this type of catalyst require to use all three remaining coordination sites for substrates and reactants; thus the Cp-type ligand can be regarded as the sole permanent ligand on the metal during a catalytic cycle. Most intermediates are coordinatively saturated 18-electron complexes with no remaining site for additional ligands. Therefore, if an enantio-determining step is present after C-H bond cleavage (**Figure 1**, Process B or C), it is difficult for Cp*M(III)-catalyzed reaction to be achieved with enantiocontrol by external chiral ligands, such as chiral phosphines.

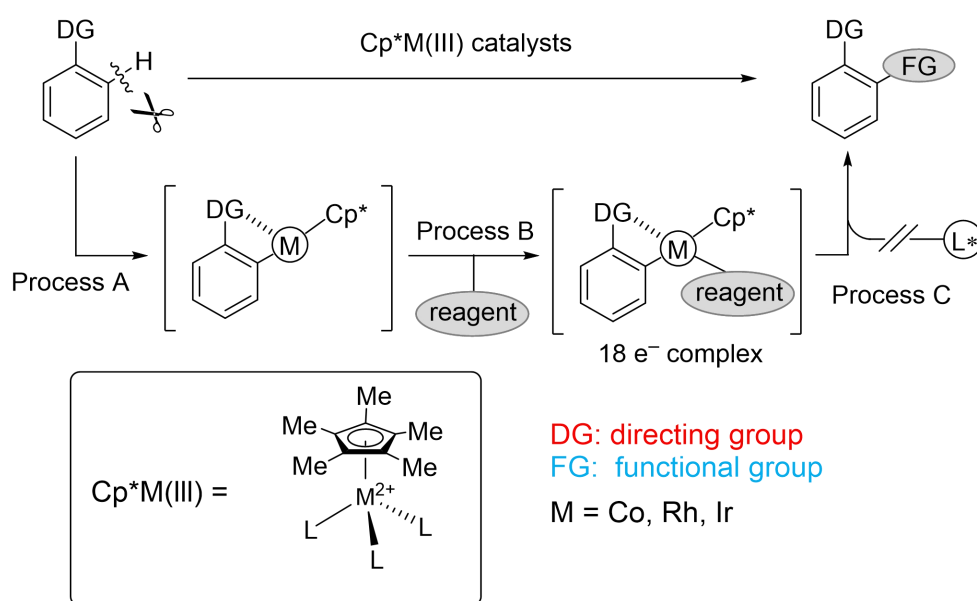
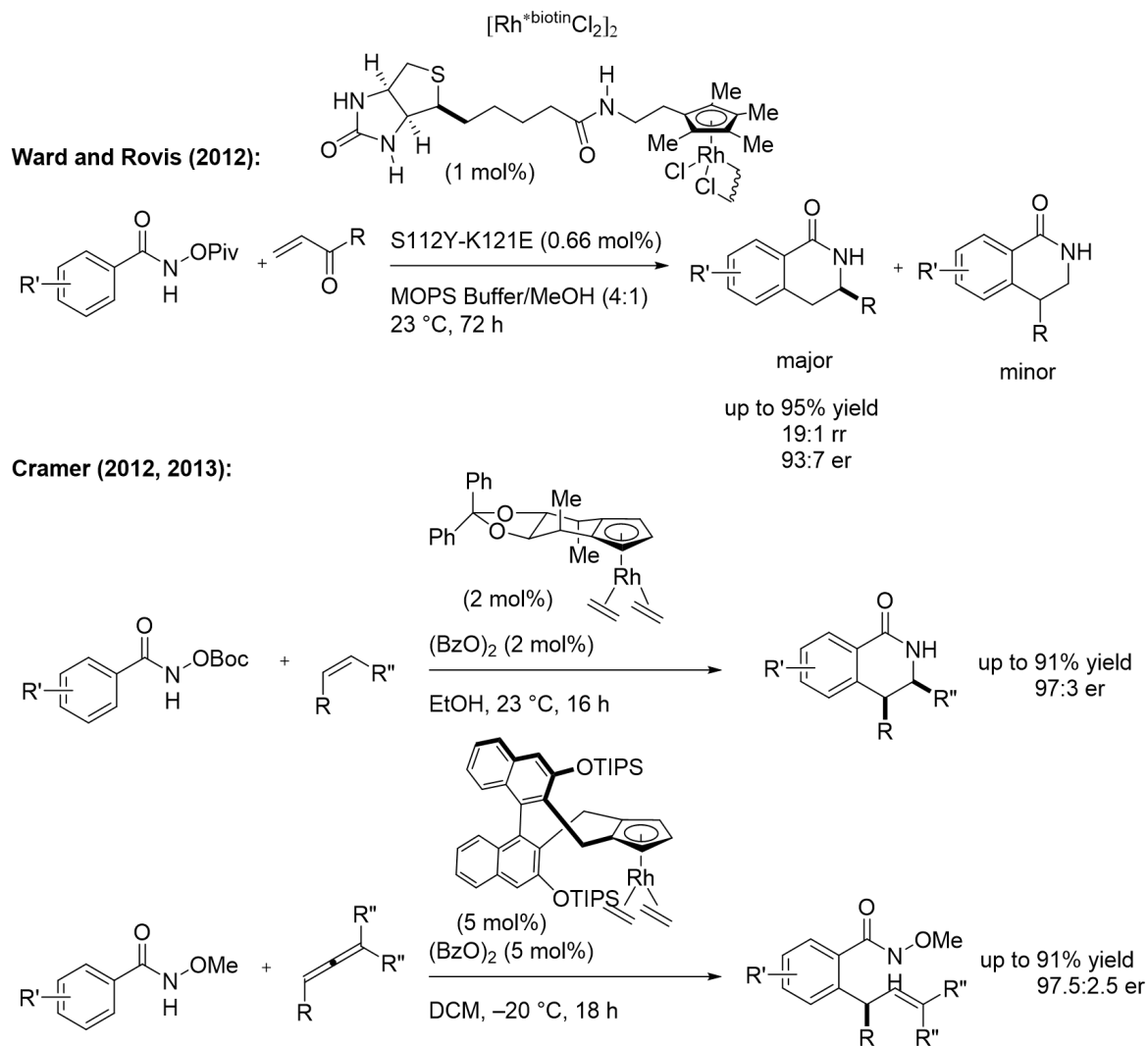


Figure 1. Cp*M(III)-Catalyzed C-H Functionalization

In 2012, Ward and Rovis et al. successfully developed a Rh(III) catalyst with a biotin-derived Cp ligand, which was combined with a modified streptavidin and enabled enantioselective C-H functionalization reactions.⁴⁾ Meanwhile, Cramer et al. reported Rh catalysts with a chiral Cp ligand derived from tartaric acid or BINOL, which exhibit high enantioselectivity in similar reactions.⁵⁾ These are the first reports on highly enantioselective C-H functionalization reactions using high-valent group 9 metal catalysts with a Cp-type ligand (**Scheme 2**).



Scheme 2. First Examples of Enantioselective C–H Functionalization Reactions Using Chiral Cp^xM(III) Catalysts

In the above-mentioned cases, the enantio-determining step is the insertion of the reagent (alkene/allene, **Figure 1**, Process B). In order to achieve high levels of stereoselectivity, Cramer proposed that three key issues should be satisfied when designing chiral Cp ligands (**Figure 2**). 1) Chiral Cp derivatives should be C₂-symmetric to avoid the generation of complex conformational isomers; 2) Cp ligand should limit the rotation of other ligands (substrates; S_L and S_S) coordinated with the metal atom; 3) The direction of the coordination of the reagent (R_c) should be controlled. If these points are satisfied, it eventually causes the Cp complex to form a pocket-like structure, by which the direction of the substrates and reagent attack is precisely controlled.

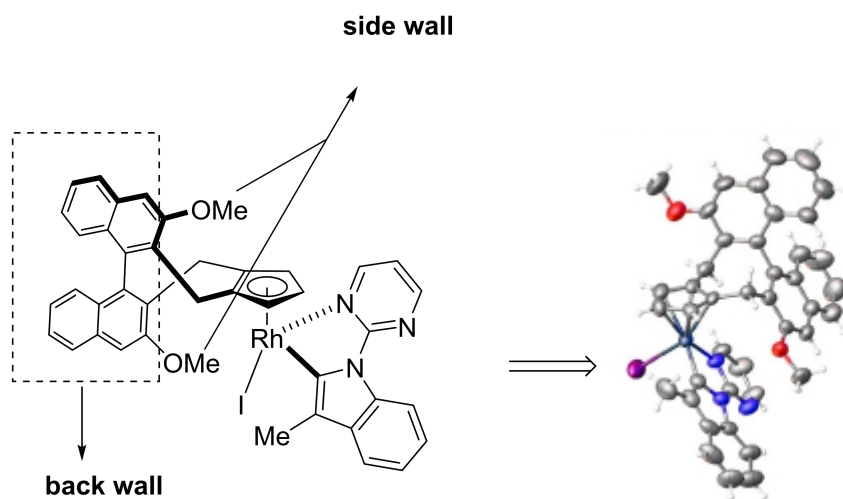
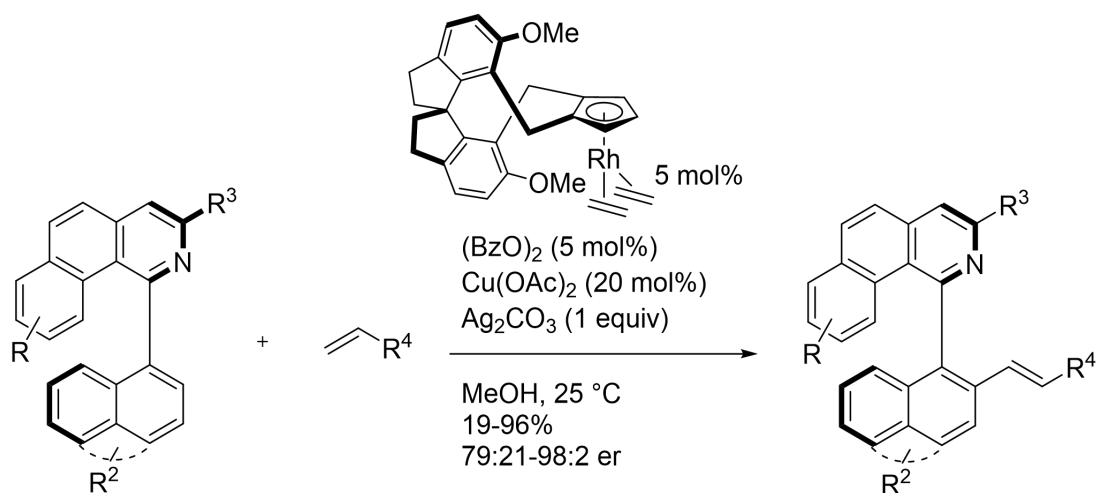


Figure 3. X-ray Structure of The Metallacycle Intermediate Bearing a Chiral Cp^x ligand, Supporting the Cramer's Stereochemical Model.

You's group reported a different class of chiral Cp ligands based on a spirocyclic scaffold, which they referred to as SCp ligands, and their Rh complexes (**Scheme 3**).⁷⁾

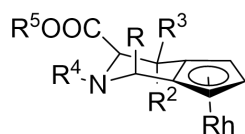
You (2016):



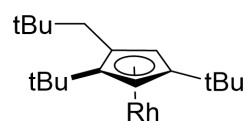
Scheme 3. You's Chiral Cp Complex

Antonchick and Waldmann, as well as Perekalin also developed chiral Cp^xRh(III) catalysts based on a different chiral scaffold (**Figure 4**).^{8a,8b)} Most of chiral Cp ligand was based on BINOL scaffold.¹⁾ In addition, Cramer also developed chiral BINOL Cp ligand with Co(III) or Ir(III) catalyst.^{8c,8d)}

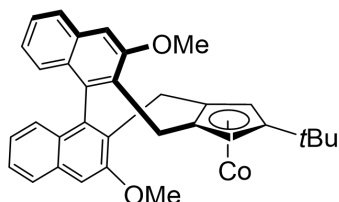
Antonchick and Waldmann (2016)



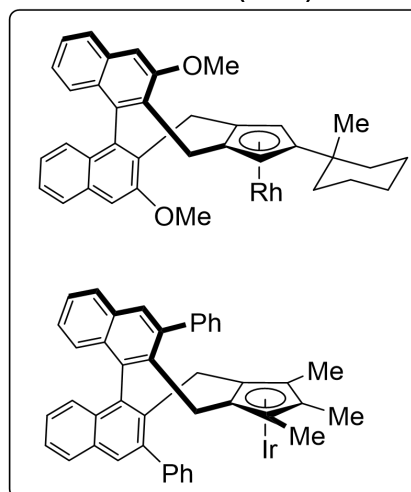
Perekalin (2018)



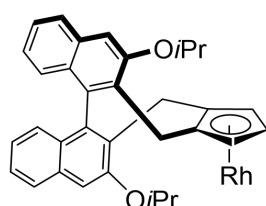
Cramer (2019)



Cramer (2020)



Li (2019)



You (2020)

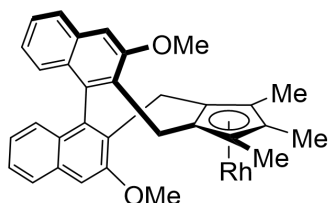


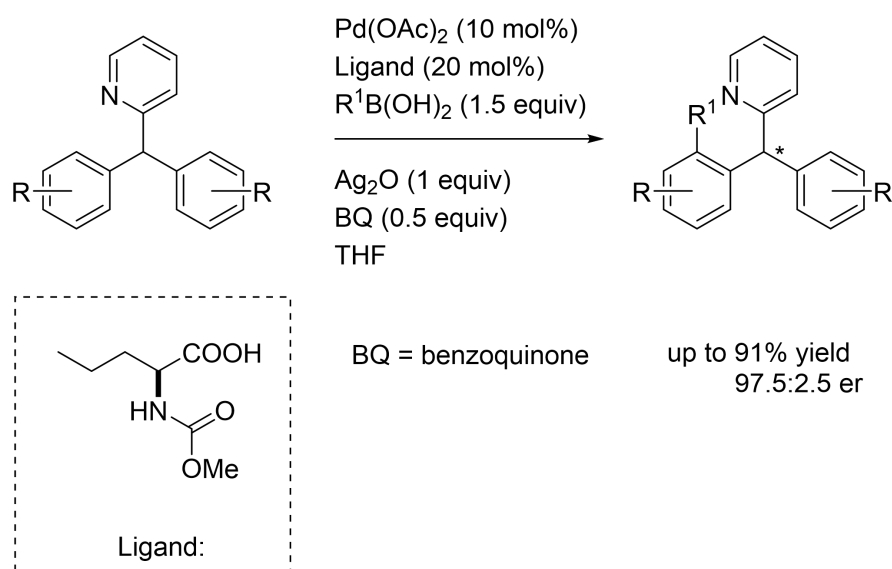
Figure 4. Other Chiral Cp Complexes

As explained above, since Rovis' and Cramer's work in 2012, several chiral Cp complexes have been developed, and highly enantioselective C–H functionalization reactions have been achieved. However, the synthesis of precisely designed Cp ligands and their metal complexes often suffers from lengthy synthetic routes, the requirement of optical resolution, and low yield. Recently, improved synthetic methods for chiral Cp ligands as well as simpler and more accessible CpRh(III) complexes have been reported. Nevertheless, there is still an urgent need to develop new strategies for asymmetric C–H functionalization reactions using Cp*M(III) catalysts.

Chapter 2. Cp*M(III)-catalyzed Enantioselective C–H Activation by Chiral Carboxylic Acid

2-1 Application of Carboxylate in Transition Metal Catalyzed C–H Activation

A carboxylate additive is widely employed as a base to promote C–H bond metalation via a concerted base-assisted deprotonation mechanism, often called concerted metalation-deprotonation (CMD). Such a C–H activation process has been well studied in Pd-catalyzed C–H functionalization, in which Pd(OAc)₂ is frequently employed. As a carboxylate can participate in a C–H activation step, the introduction of chiral carboxylates or related ligands enable enantioselective C–H bond cleavage. Yu et al. reported many examples of Pd(II)-catalyzed enantioselective C–H activation reactions, in which a mono-*N*-protected amino acid (MPAA) or related ligand is used (Scheme 4).^{9c, 9d, 10a}



Scheme 4. Pd(II)-Catalyzed Enantioselective C–H Activation by Using MPAA

Although these MPAA type bidentate κ^2 ligands are successful in Pd catalysis, the application of them to group 9 metals is not promising (Figure 5). While Pd(II) complexes adopt a square-planar geometry, Cp*M(III) (M = Co, Rh, Ir) complexes adopt a pseudo-octahedral geometry with a Cp ligand and lack a vacant coordination site for an external chiral ligand.^{10b} Therefore, seeking a different class of chiral carboxylic acid or other ligands are crucial to achieve enantioselective C–H functionalization using a Cp*M(III) catalyst.

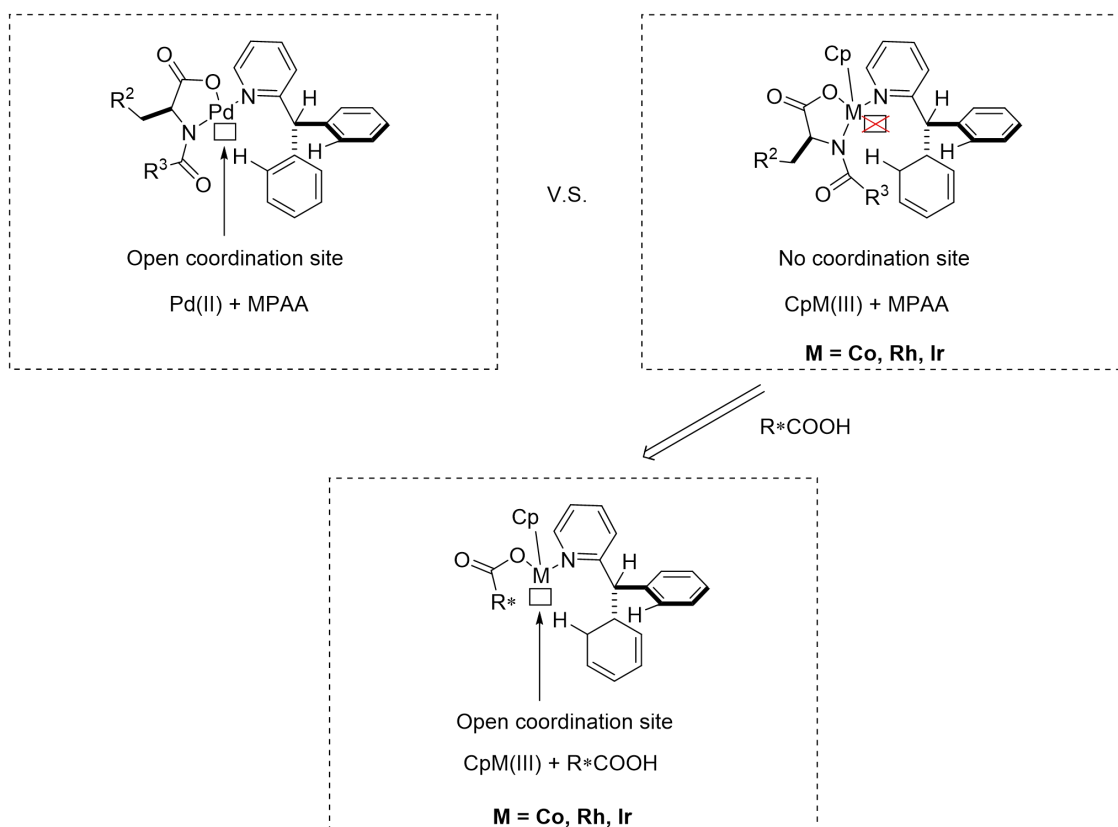
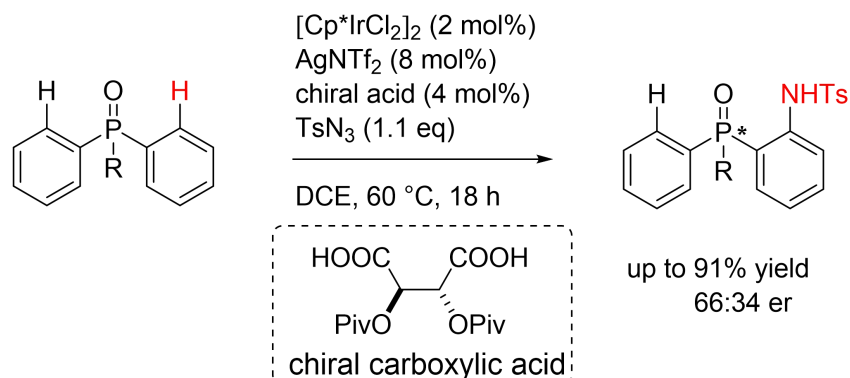


Figure 5. Difference Between Pd(II) and Cp*M(III) (M = Co, Rh, Ir) Complexes with a MPAA or CCA Ligand.

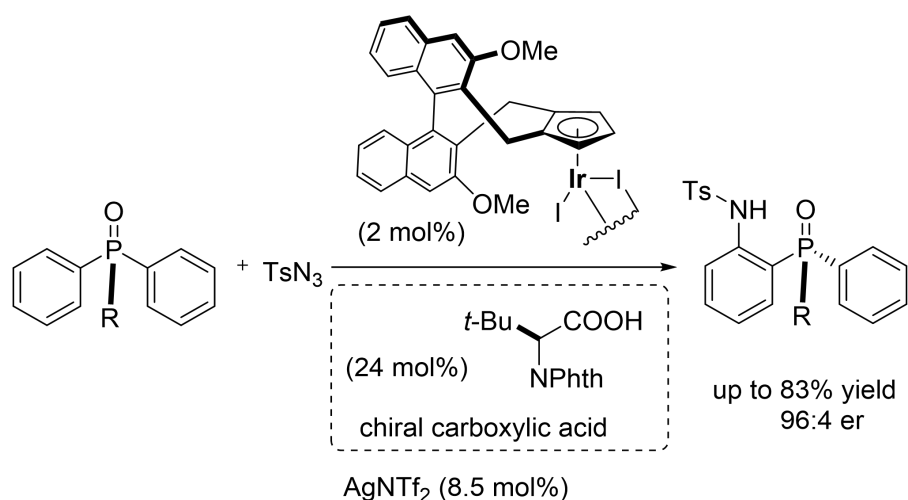
In 2015, Chang discovered that the reactivity of C-H amidation of triphenylphosphine oxide under Cp*Ir(III) catalysis was dramatically increased when AcOH was added (Scheme 5).¹¹⁾ The authors reported the asymmetric amidation reaction by using a chiral carboxylic acid and Cp*Ir(III) catalyst. Although the enantiomeric ratio remains low (66:34), for the first time, they demonstrated that a chiral acid can realize enantioselective C-H activation with a Cp*M(III) catalyst (Scheme 5).



Scheme 5. Ir-Catalyzed C(sp²)-H Amidation of a Phosphine Oxide Using a Chiral Acid

Cramer reported the enantioselective C-H amidation of diphenyl cyclohexyl phosphine oxides with a tosyl azide by using both chiral Cp ligand and chiral carboxylic acid (Scheme 6).¹²⁾ The result demonstrates

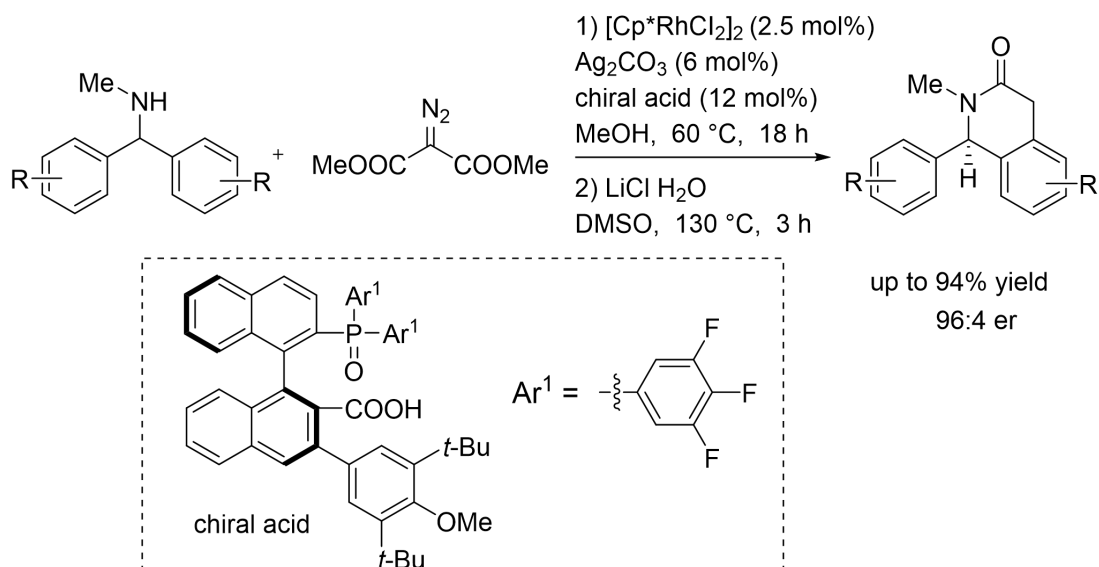
the cooperative effect on the enantioselectivity between the chiral Cp ligand and chiral carboxylic acid.



Scheme 6. Cooperation Between Chiral Cp Ligand and Chiral Carboxylic Acid

2-2 Enantioselective $\text{C}(\text{sp}^2)\text{-H}$ Functionalization Reactions

A few years after the pioneering work of Chang,¹¹⁾ Lin, Yoshino and Matsunaga reported the $\text{Cp}^*\text{Rh(III)}$ -catalyzed enantioselective C-H alkylation/cyclization reactions of diarylmethylamines with a diazomalonate to afford dihydroisoquinolones (**Scheme 7**).¹⁴⁾ The authors developed a highly sterically demanding chiral carboxylic acid based on a BINOL scaffold, which exhibited high enantioselectivity in this reaction without a chiral Cp ligand.



Scheme 7. Enantioselective $\text{C}(\text{sp}^2)\text{-H}$ Alkylation/Cyclization Reactions of Diarylmethylamines by $[\text{Cp}^*\text{RhCl}_2]_2$ / Chiral Carboxylic Acid

The reaction mechanism for this enantioselective C-H functionalization is shown in **Figure 6**. The active species $[\text{Cp}^*\text{Rh}(\text{OCOR}^*)]$ is generated from $[\text{Cp}^*\text{RhCl}_2]_2$, chiral carboxylic acid, and Ag_2CO_3 . After coordination of the amino group of a substrate, enantioselective C-H bond cleavage would occur via chiral carboxylate-assisted concerted metalation-deprotonation to afford chiral rhodacycle **B**. Subsequent coordination of diazomalonate (**C**) is followed by the formation of Rh-carbenoid with the release of N_2 and aryl migration, affording **D**. Finally, protonation of **D** and the lactam formation would furnish intermediate **E** with the regeneration of the active species $[\text{Cp}^*\text{Rh}(\text{OCOR}^*)]$. Intermediate **E** undergoes decarboxylation to provide **F** under Krapcho conditions using LiCl .¹⁴⁾

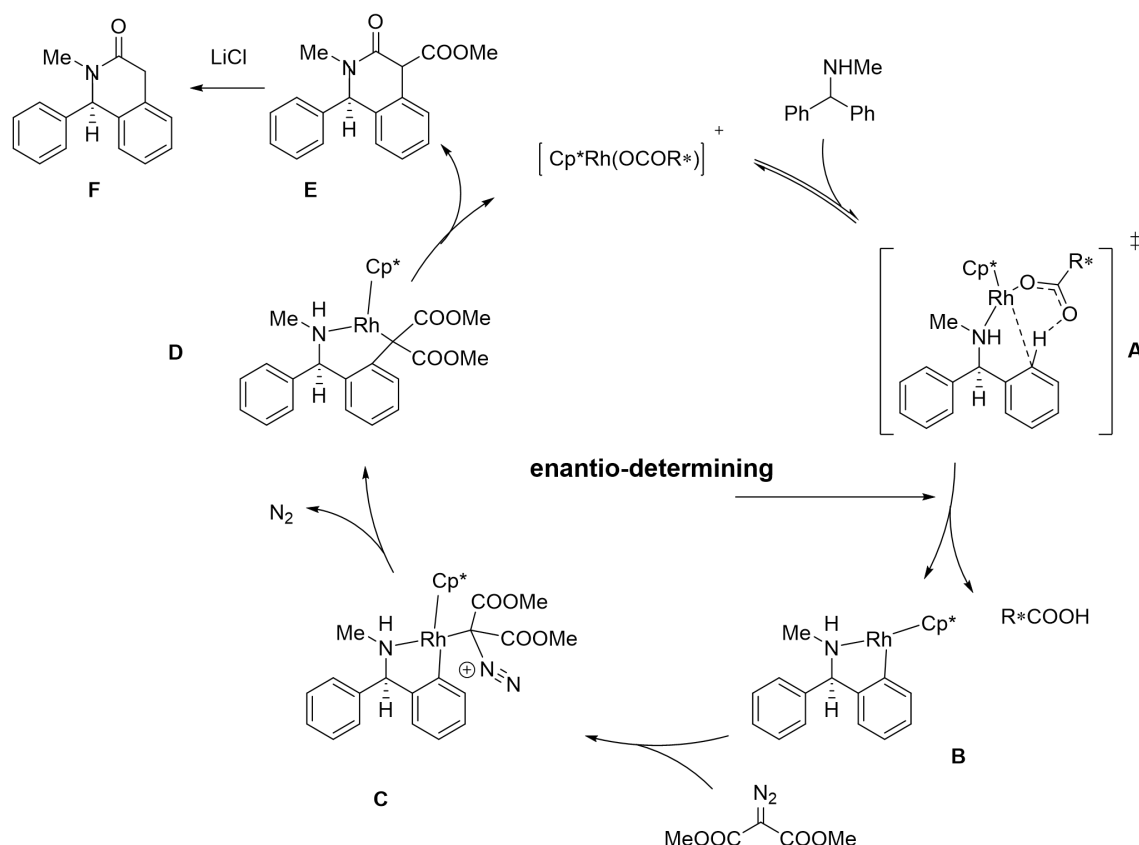
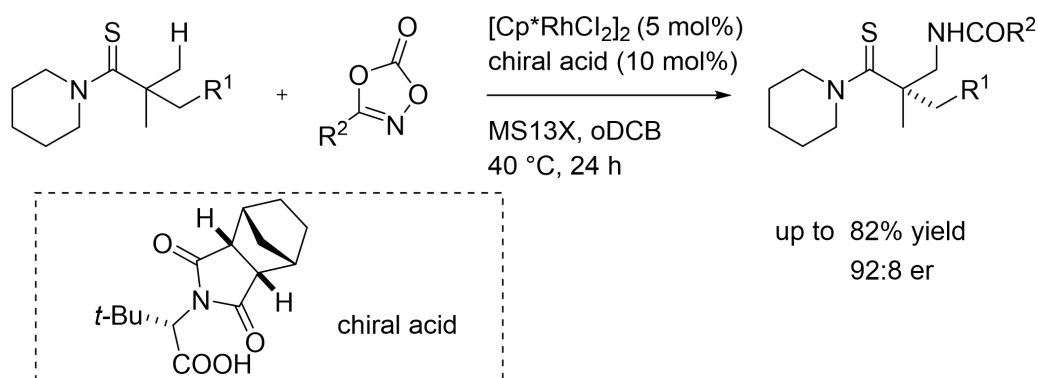


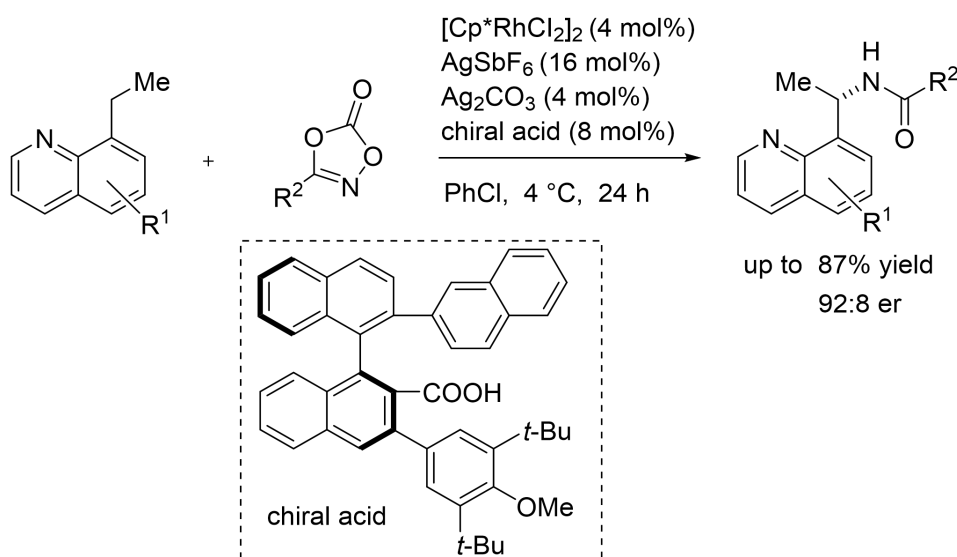
Figure 6. Mechanism of Enantioselective C(sp²)-H Alkylation/cyclization Reactions of Diarylmethylamines

2-3 Enantioselective C(sp³)-H Functionalization Reactions

C(sp³)-H bond activation by a transition metal catalyst is far more challenging than the activation of C(sp²)-H bonds due to the low acidity of C(sp³)-H bonds and the lack of π -electrons that can interact with the metal center. In 2019, Yoshino and Matsunaga achieved enantioselective C(sp³)-H amidation reactions of thioamides (**Scheme 8**).^{16,18)} Furthermore, they reported enantioselective C(sp³)-H amidation of 8-alkylquinolines under $\text{Cp}^*\text{Rh}(\text{III})$ /chiral carboxylic acid catalysis (**Scheme 9**).^{17a,18)}

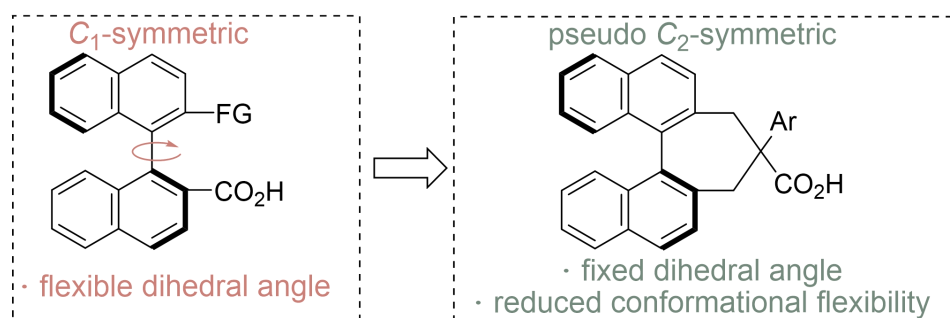


Scheme 8. Enantioselective C(sp³)-H Amidation Reactions of Thioamides



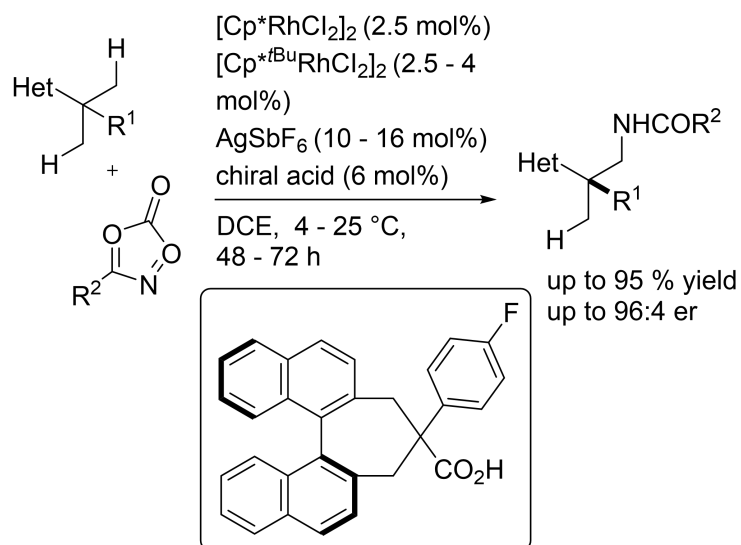
Scheme 9. Enantioselective Methylene C(sp³)-H Amidation Reactions of 8-Ethylquinolines

Although the aforementioned C₁-symmetric binaphthyl CCAs are highly tunable and have been applied to several reactions, the unfixed, flexible rotating dihedral angle between the two naphthyl rings can cause additional internal conformational flexibility, which, in combination with the conformational flexibility between the metal and substrate, can lead to an unfavorably large number of possible transition-state structures for C–H activation (**Scheme 10**). Their fixed structure and can reduce the conformational flexibility and potentially be beneficial in recognizing the structure of some substrates.



Scheme 10. Comparison of C₁-Symmetric and Pseudo-C₂-Symmetric CCAs

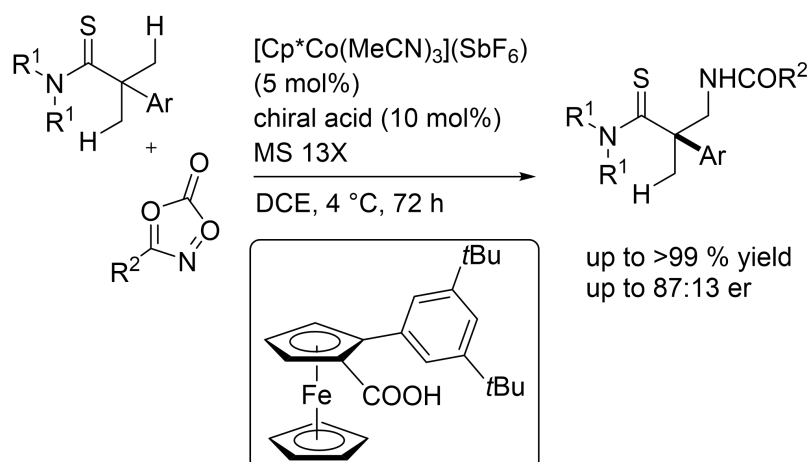
In 2021, Yoshino, Matsunaga, and coworkers more recently reported binaphthyl-based pseudo-C₂-symmetric CCAs for enantioselective C–H functionalization and exhibited high enantioselectivity in the enantioselective C(sp³)–H amidation of 2-alkylpyridines and related heteroaromatic compounds.^{17b)}



Scheme 11. Heteroaryl-Directed Enantioselective C(sp³)–H Amidation Using Pseudo-C₂-Symmetric CCA

2-4 Enantioselective C–H Functionalization Reactions by Other New CCA

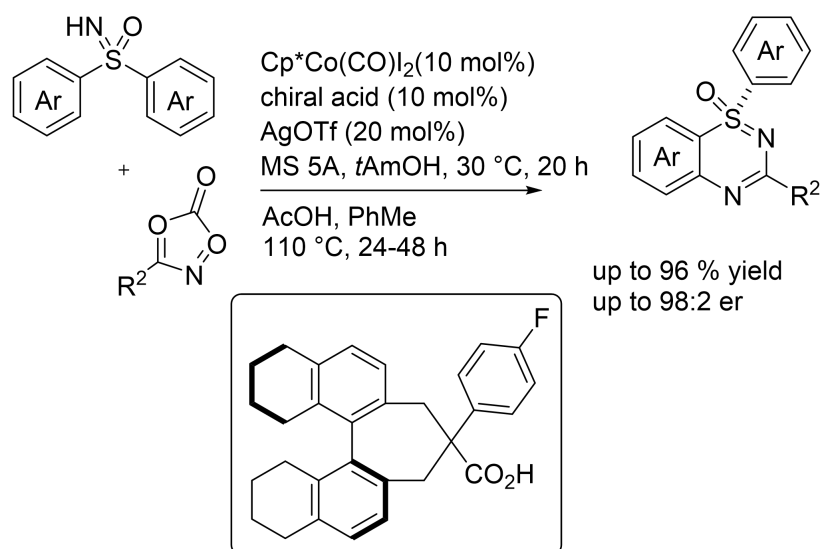
Yoshino and Matsunaga also studied on the planar chirality of 1,2-disubstituted ferrocenes as a platform for CCAs. A modular synthetic route for optically active 2-aryl-ferrocene carboxylic acids have been developed, and the synthesized CCAs were applied to the Co(III)-catalyzed enantioselective C(sp³)–H amidation of thioamides.^{17c)}



Scheme 12. Planar-Chiral Ferrocene Carboxylic Acids for Enantioselective C(sp³)–H Amidation of

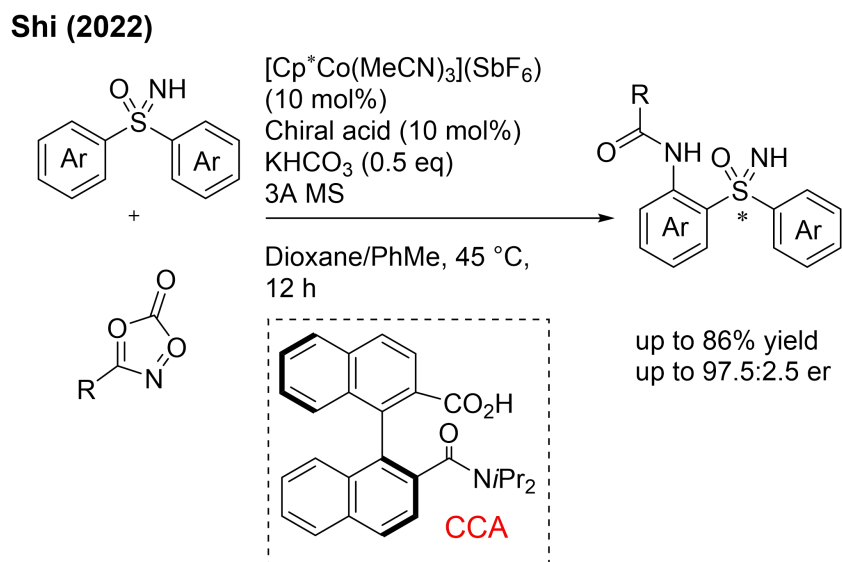
α -Aryl Thioamides

Chiral carboxylic acids were also successfully used for the enantioselective C(sp²)-H amidation of sulfoximines with a Cp*Co(III) catalyst. A chiral acid with an H₈-binaphthyl backbone resulted in higher enantioselectivity than the corresponding binaphthyl derivative.^{17d,18)}



Scheme 13. Cp*Co(III)-Catalyzed Enantioselective Synthesis of Benzothiadiazine-1-oxides via C-H Activation with H₈-BINOL CCA

At the same time, Shi et al. reported the synthesis of sulfur-stereogenic sulfoximines via Co(III)/chiral carboxylic acid (CCA)-catalyzed enantioselective C-H amidation.^{17e)}



Scheme 14. CpCo(III)/CCA Catalyzed C-H Activation of Sulfoximines

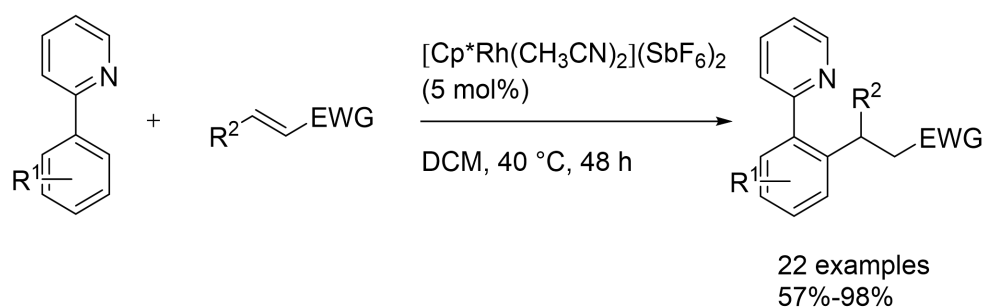
Chapter 3. Cp*Rh(III)-Catalyzed Conjugate Addition of C–H Bonds to α,β -Unsaturated Compounds

3-1 Introduction of Cp*Rh(III)-Catalyzed Conjugate Addition to α,β -Unsaturated Ketones

In 1997, Miyaura reported that Rh(I) complexes catalyze the 1,4-addition of aryl and alkenyl boronic acids to enones in excellent yield.^{20b)} This type of reaction proceeds under mild reaction conditions and show good functional group compatibility, and has become one of the most important and powerful C–C bond forming strategies. They also have been applied widely to the synthesis of natural products. However, as the key intermediates are generated from stoichiometric amounts of organometallic reagents, this process usually has some drawbacks: 1) the tedious pre-functionalization steps, 2) the requirement of anaerobic manipulations, 3) unwanted formation of stoichiometric salt wastes, which lead to lower atom efficiency from the viewpoints of overall reaction processes. As alternative methods, transition-metal-catalyzed conjugate addition of C–H bonds to α,β -unsaturated ketones has been demonstrated to be a simple and atom-economical protocol for the construction of C–C bond frameworks. Various C–H bonds, e.g., aryl, olefinic, and aldehydic C–H bonds, have been used in this type of addition reactions.

3-2 Cp*Rh(III)-catalyzed Conjugate Addition of C(sp²)–H Bonds to α,β -Unsaturated Carbonyl Compounds

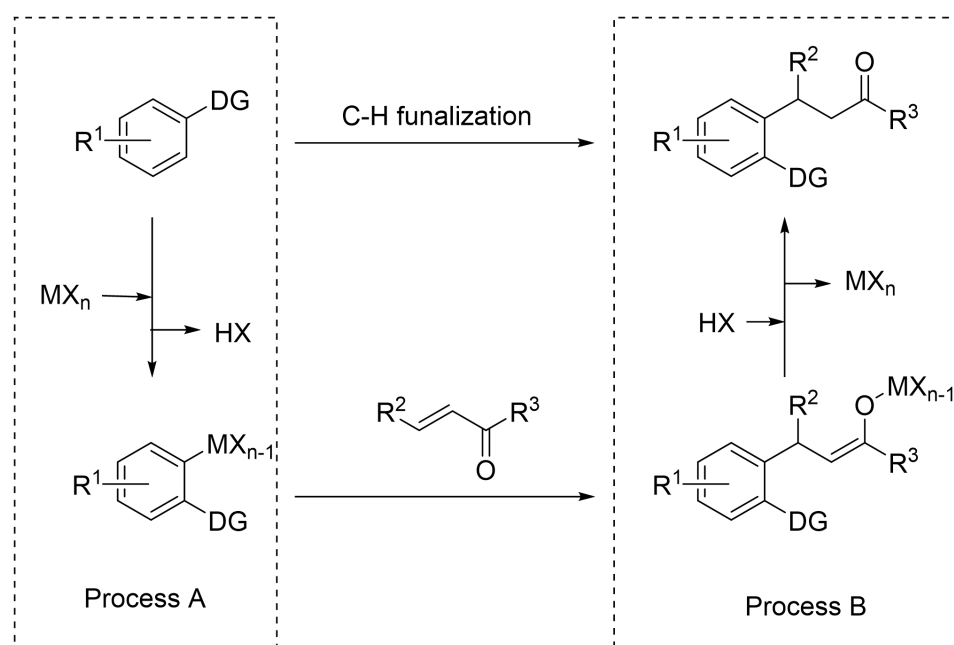
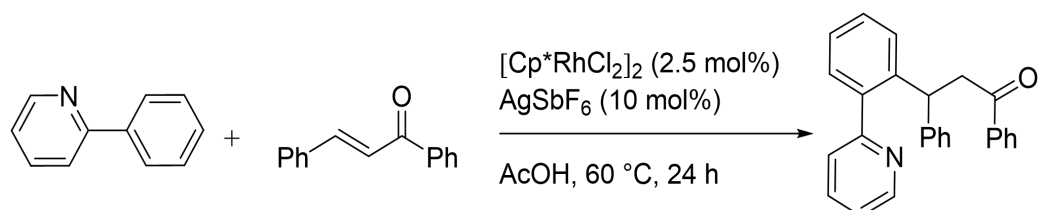
Li and coworkers reported the first Cp*Rh(III)-catalyzed conjugate addition of C–H bonds to electron-deficient alkenes.^{20c)} The reaction proceeded under very mild conditions without pre-functionalization of nucleophiles (Scheme 15).



Scheme 15. First Cp*Rh(III)-Catalyzed Conjugate Addition of C–H Bonds

The reaction mechanism of high-valent metal-catalyzed conjugate addition of C–H bonds is summarized in **Figure 7**, in which two proton-transfer steps are involved. The first proton transfer step is the C–H activation step (**Figure 7, Process A**), which may require a base for the removal of a proton generated in the reversible C–H metalation process. The second proton transfer is the protonation of a metal-enolate intermediate (**Figure 7, Process B**), which would be preferred under acidic conditions. Therefore, for the whole catalytic process, careful control of the balance between the acidity and basicity of the reaction conditions would be crucial for the reaction. By selecting a solvent with an appropriate acidity,

the rate balance of these two proton-transfer processes can be optimized. Based on this hypothesis, Huang and co-workers developed an efficient and mild Cp*Rh(III)-catalyzed C-H conjugate addition reactions, in which AcOH was used as the solvent. Using the combination of [Cp*RhCl₂]₂ and AgSbF₆ as the catalyst and AcOH as the solvent, various arenes with a heterocyclic directing group and enones were successfully employed, providing the desired conjugate addition products in good to excellent yields under mild conditions (**Figure 7**).²²⁾



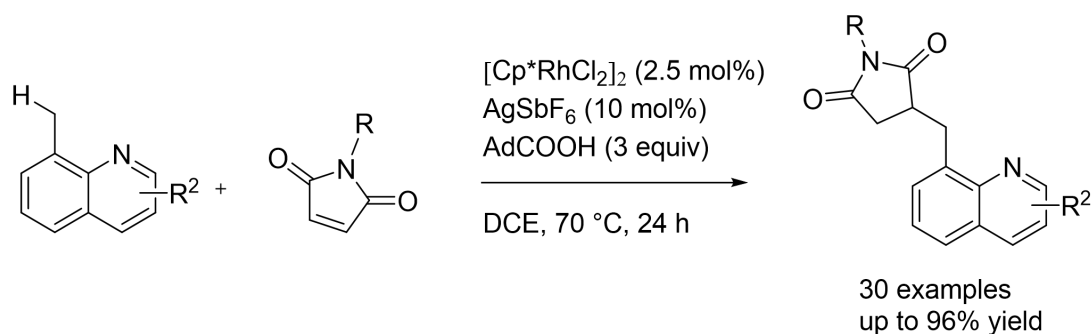
Process A: basic condition may promote deprotonative C-H activation
 Process B: acidic condition would keep metal-enolate intermediate stable

Figure 7. A hypothesis: Influence of Acidity and Basicity on C–H Conjugate Addition Reactions

3-3 Cp*Rh(III)-Catalyzed Conjugate Addition of C(sp³)–H Bonds to α,β -Unsaturated Ketones

Compared with the conjugate addition reactions of C(sp²)–H bonds to α,β -unsaturated ketones, the addition reactions of C(sp³)–H bonds are far more challenging. Although activation of C(sp³)–H bonds leading to hetero-functionalization and arylation have been reported using Cp*Rh(III) and Cp*Ir(III) catalysts,²³⁾ redox-neutral addition of C(sp³)–H bond to unsaturated C–C bond remains less studied probably due to the low reactivity of the M–C(alkyl) species as well as the difficulty of C(sp³)–H activation.

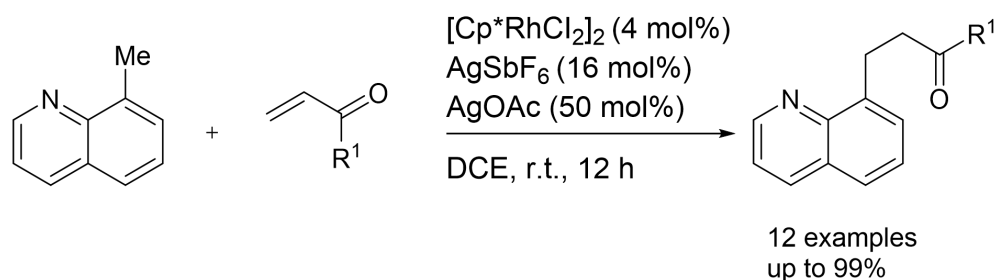
In 2016, Kim reported the addition of C(sp³)-H bond of 8-methylquinolines to maleimides (**Scheme 16**).^{24a)}



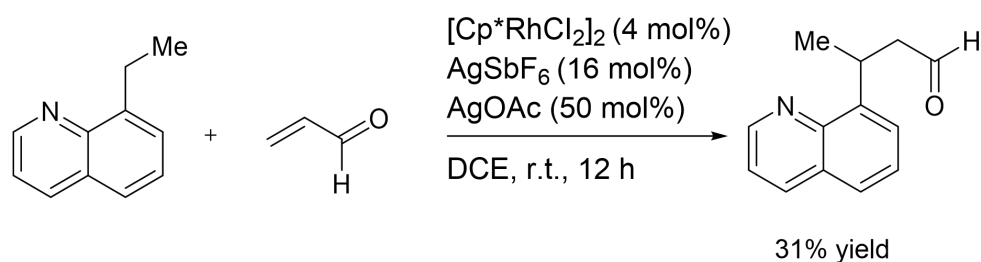
Scheme 16. Cp^{*}Rh(III)-Catalyzed Addition of C(sp³)-H Bonds to Maleimides

In 2017, Li and his co-workers reported Cp^{*}Rh(III)-catalyzed addition reactions of C(sp³)-H bonds of 8-alkylquinolines to enones.^{24b)} 8-Ethylquinoline, which requires the activation of a methylene C(sp³)-H bond, resulted in low yield (**Scheme 17**).

(a) Methyl C(sp³)-H activation



(b) Methylene C(sp³)-H activation



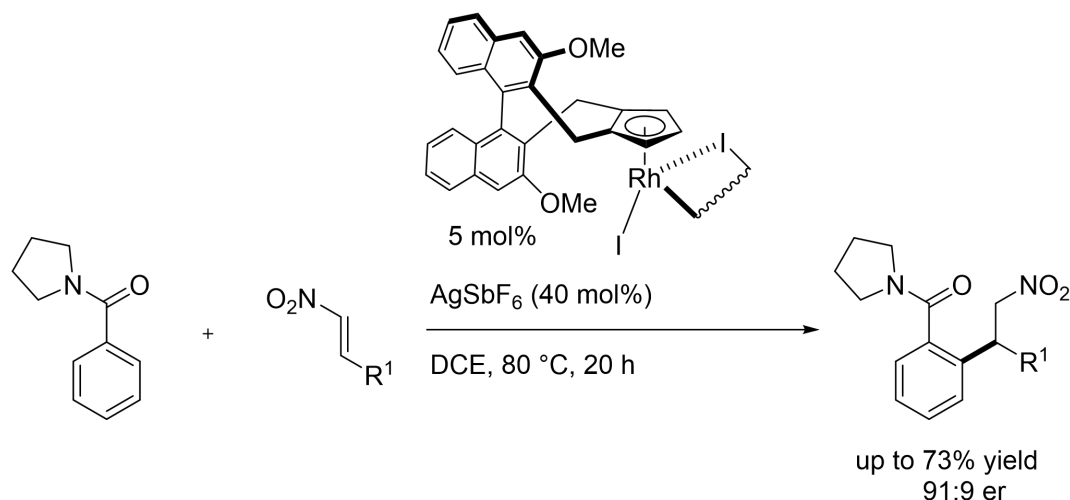
Scheme 17. Cp^{*}Rh(III)-Catalyzed Addition of C(sp³)-H Bonds to α,β -Unsaturated Ketones

Li's group also reported Cp^{*}Rh(III)-catalyzed addition reactions of 8-methylquinoline to enones.^{24c)} More recently, Sharma and co-workers reported [RuCl₂(*p*-cymene)]₂/[Cp^{*}RhCl₂]₂-catalyzed direct alkylation of C(sp³)-H bond of 8-methylquinolines with alkenes.^{24d)}

3-4 Cp^{*}M(III)-Catalyzed Asymmetric Addition of C-H Bonds to Electron-deficient Alkenes.

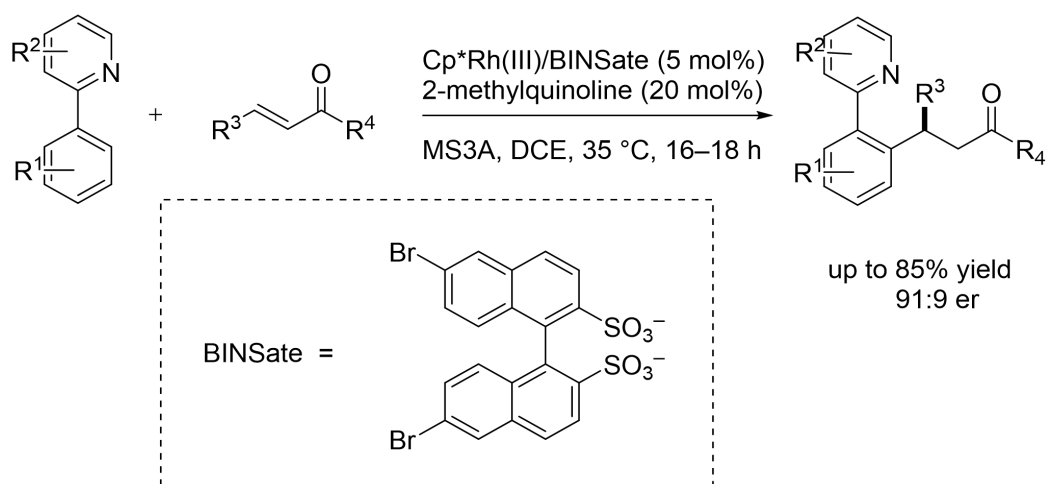
During the past few years, some attention has been paid to Cp^{*}M(III)-catalyzed asymmetric addition of C-H bonds to electron-deficient alkenes. In 2017, Ellman and his co-workers reported the asymmetric addition of a benzamide to a nitroalkene by using a Cramer's chiral Cp ligand (**Scheme 18**).^{15c)} The

enantio-determining step of this reaction is the insertion of the nitroalkene, which is controlled by the chiral Cp ligand.



Scheme 18. Chiral Cp^{*}Rh(III)-Catalyzed Asymmetric Conjugate Addition via C(sp²)-H Activation

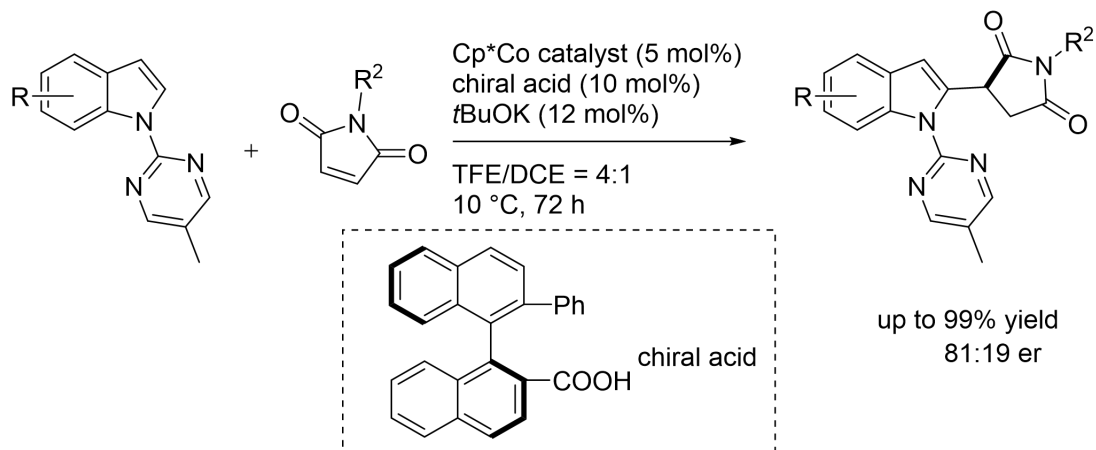
Yoshino and Matsunaga developed enantioselective C-H alkylation reactions of 2-phenylpyridines and 6-arylpyridines with α,β -unsaturated ketones catalyzed by Cp^{*}Rh(III)/chiral disulfonate catalysts (Scheme 19).^{15a)} A proposed mechanism for the enantio-induction would be the reversible insertion of an enone and selective proto-demetalation by a chiral proton source generated from a chiral disulfonate anion would realize the enantioselective process. The same mechanism is proposed by Ackermann and co-workers in C-H enantioselective alkylation reactions using a Cp^{*}Co(III)/chiral carboxylic acid catalyst.



Scheme 19. Cp^{*}Rh(III)/Chiral Disulfonate-Catalyzed Asymmetric Conjugate Addition via C(sp²)-H Activation

Yoshino and Matsunaga developed an enantioselective Cp^{*}Co(III)/chiral carboxylic acid-catalyzed 1,4-addition reaction of indoles to maleimides, which proceeds via a C-H activation process.^{15b)} In this reaction, a chiral carboxylic acid derived from BINOL serves as the sole chiral source for the enantioselective addition, albeit the observed enantioselectivity leaves room for improvement (Scheme

20).^{15b)} The same mechanism is proposed by Ackermann and co-workers in C–H enantioselective alkylation reactions using a Cp*Co(III)/chiral carboxylic acid catalyst. The insertion of the C–C double bond is expected to be reversible, while a selective protonation by the chiral carboxylic acid would proceed to furnish the product in an enantioselective fashion.



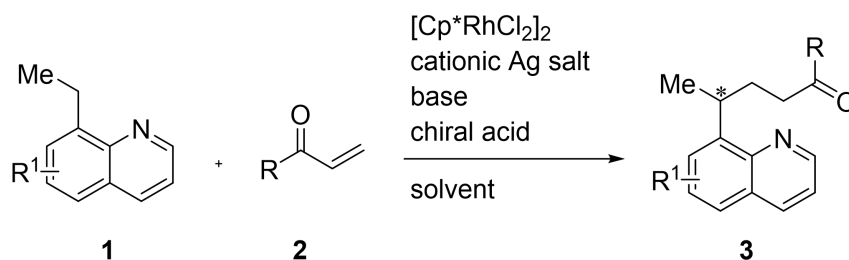
Scheme 20. Cp*Co(III)-Catalyzed Asymmetric Conjugate Addition via C(sp²)-H Activation

Chapter 4. First Work: Cp^{*}Rh(III)-Catalyzed Asymmetric Conjugate

Addition of C(sp³)-H Bonds to α,β -Unsaturated Ketones⁵¹⁾

Although the introduction of chiral Cp^x ligands, chiral carboxylic acids (CCAs), and other chiral sources has enabled various enantioselective C(sp²)-H functionalization reactions, there have been fewer reports on enantioselective functionalization of less reactive C(sp³)-H bonds. In this context, Matsunaga group recently reported the Co(III)/CCA-catalyzed C-H amidation of thioamides and the Rh(III)/CCA-catalyzed amidation of 8-alkylquinolines, as discussed in **Chapter 2**. However, the enantioselective C-C bond-forming reactions via C(sp³)-H activation using high-valent group 9 metal catalysts for the construction of carbon skeletons of chiral organic molecules have not yet been reported.

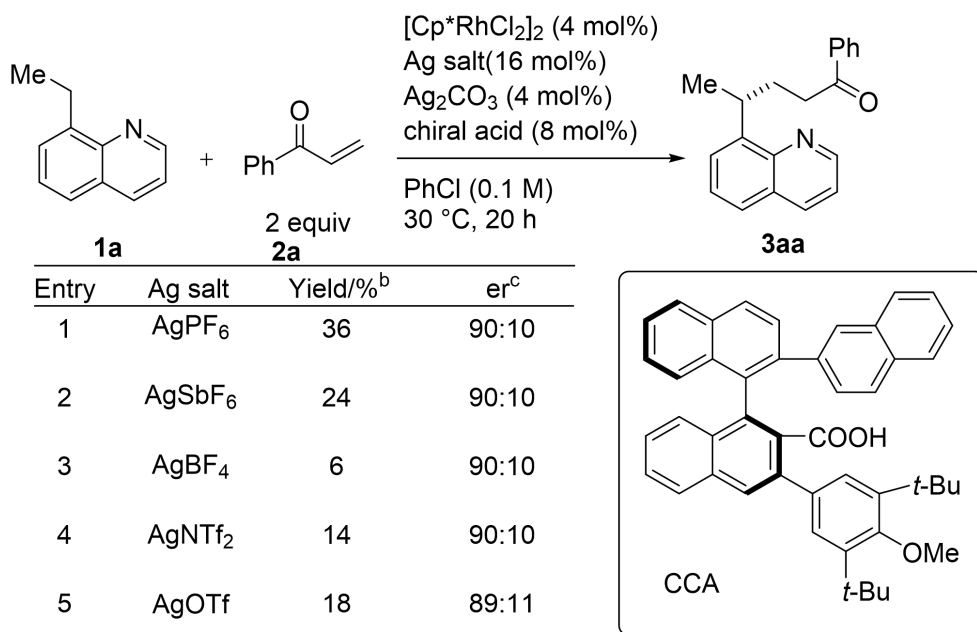
Based on these previous studies in Matsunaga group as well as racemic reactions explained in **Chapter 3**, I decided to explore Cp^{*}M(III)-catalyzed asymmetric conjugate addition of C(sp³)-H bond to α,β -unsaturated ketones by using a chiral carboxylic acid (**Scheme 21**).



Scheme 21. My work: Cp^{*}Rh(III)-Catalyzed Asymmetric Conjugate Addition to α,β -Unsaturated Ketones via C(sp³)-H Activation

4-1. Screening of Ag Salt

My investigation into enantioselective methylene C-H addition of 8-ethylquinoline **1a** to phenyl vinyl ketone **2a** to afford the product **3aa** started with attempting to identify appropriate reaction conditions under Cp^{*}Rh(III) catalysis. Based on the optimized conditions for the enantioselective C-H amidation reactions (**Chapter 2, Scheme 8**), I selected [Cp^{*}RhCl₂]₂ as a Rh catalyst and CCA **4** as a chiral acid, and initially screened Ag salts. The best yield was observed when using AgPF₆ (**Table 1**, entry 2), while other examined silver salts are less effective. On the other hand, there is no difference in the enantioselectivity (**Table 1**).

Table 1. Screening of Cationic Ag Salts^a

a) Scale: 0.05 mmol **1a**

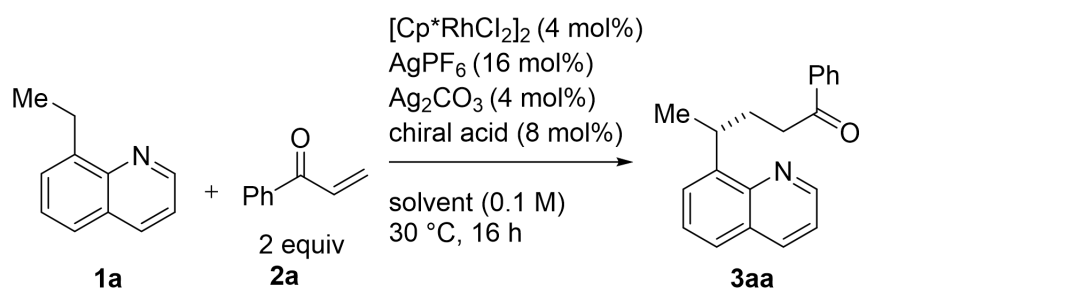
b) Determined by ¹H NMR analysis of the crude mixture using 1,1,2,2-tetrabromoethane as an internal standard.

c) Determined by HPLC analysis.

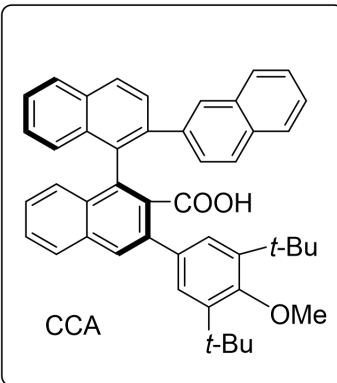
4-2. Screening of Solvent

I next investigated the solvent effects (**Table 2**). Among the solvents screened, PhCl afforded the best yield (entry 3, 35%) and enantiomeric ratio (89:11). Because toluene also gave the relatively promising result compared to other solvents, aromatic solvents would be suitable for this reaction.

Table 2. Screening of Solvent^a



Entry	Solvent	Yield/% ^b	er ^c
1	DCE	10	87:13
2	Toluene	21	89:11
3	PhCl	35	89:11
4	Hexane	N.D	–
5	Dioxane	N.D	–
6	TFE	N.D	–



a) Scale: 0.05 mmol **1a**

b) Determined by ¹H NMR analysis of the crude mixture using 1,1,2,2-tetrabromoethane as an internal standard.

c) Determined by HPLC analysis.

4-3. Screening of Cp Ligand

Then, I examined the steric effects of the Cp^xRh(III) catalyst (**Table 3**). Among the catalysts screened, only Cp^{Me4}Rh(III) (**Table 3, entry 1**) and Cp^{*iPr}Rh(III) (**Table 3, entry 2**) afforded over 10% yield, and the enantiomeric ratios were lower than that observed when using a standard Cp^{*}Rh(III) catalyst. On the other hand, Cp^{Et}Rh(III) (**Table 3, entry 5**) and Cp^{Ind}Rh(III) (**Table 3, entry 8**) showed slightly better enantioselectivity (90:10 er), but the yield was very low. Other catalysts did not provide the desired product at all. Considering the reactivity and selectivity, a standard Cp^{*}Rh(III) catalyst was selected for the further investigation.

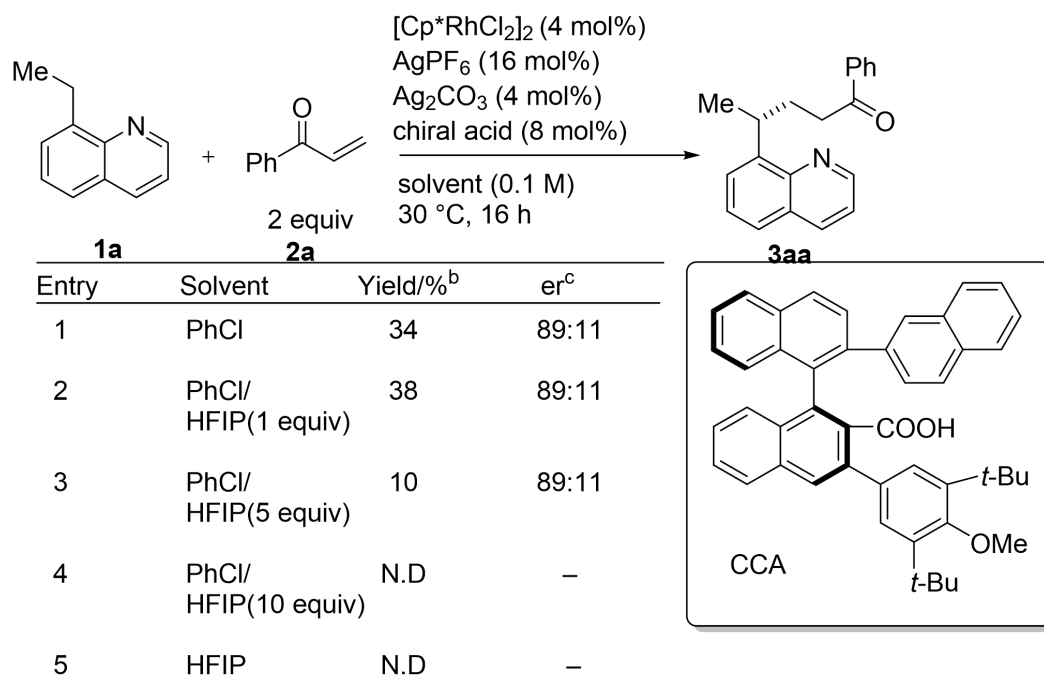
Table 3. Screening of Cp Ligand^a

Entry	Cp ^x	Yield/% ^b	er ^c
1	Cp ^{Me4} (R = H)	23	87:13
2	Cp ^{iPr} (R = iPr)	20	87:13
3	Cp ^{Ph} (R = Ph)	N.D	–
4	Cp ^{tBu} (R = tBu)	N.D	–
5	Cp ^{Et}	5	90:10
6	Cp ^t	N.D	–
7	Cp ^A	N.D	–
8	Cp ^{Ind}	trace	90:10

a) Scale: 0.05 mmol **1a**
 b) Determined by ¹H NMR analysis of the crude mixture using 1,1,2,2-tetrabromoethane as an internal standard.
 c) Determined by HPLC analysis.

4-4. Influence of Acidity

There are two proton-transfer steps involved in the 1,4-conjugate addition reaction, and the balance of acidity and basicity of the reaction media would be important as discussed in **Chapter 3**. I began to screen the acidity of the solvent. To increase the acidity, I used HFIP as an acid additive (**Table 4**). When I used one equivalent of HFIP, the yield was slightly improved (**Table 4**, entry 2). However, as the amount of HFIP increased, the yield significantly decreased and an unknown byproduct was observed (**Table 4**, entries 3-5).

Table 4. Effects of HFIP^a

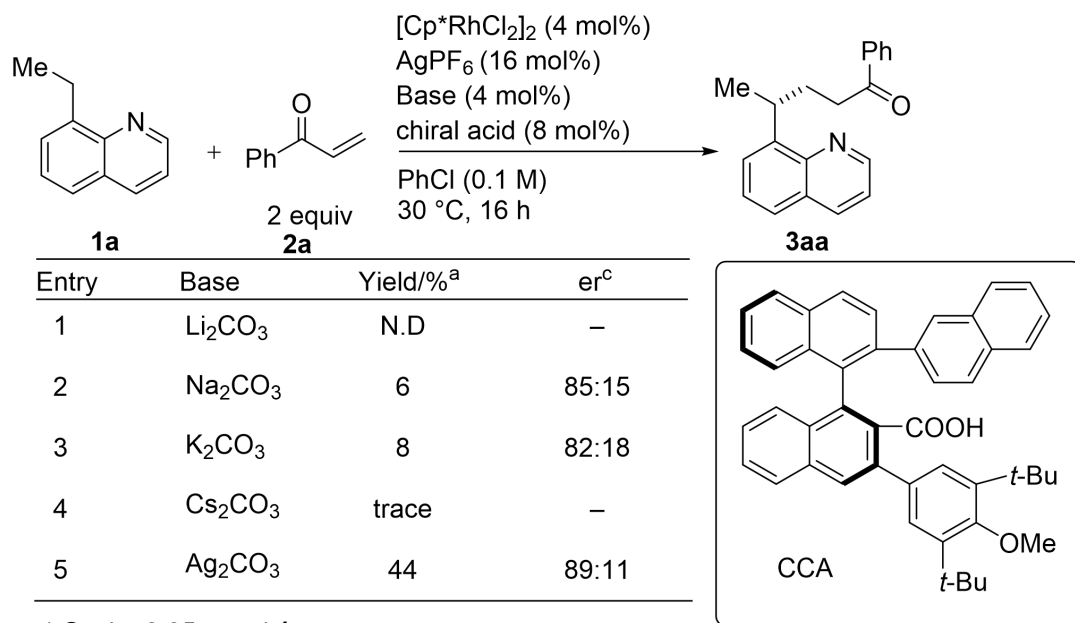
a) Scale: 0.05 mmol **1a**

b) Determined by ¹H NMR analysis of the crude mixture using 1,1,2,2-tetrabromoethane as an internal standard.

c) Determined by HPLC analysis.

As the addition of an acid resulted in the negative effects, I next examined the influence of bases. Although I screened different carbonate bases other than Ag₂CO₃, only lower reactivity was observed (**Table 5**, entries 1-4). On the other hand, in the subsequent exploration of the amount of Ag₂CO₃ (**Table 6**), the yield was increased up to 50% when 28 mol% of Ag₂CO₃ was used (**Table 6**, entry 6).

Table 5. Screening of Carbonate Bases^a

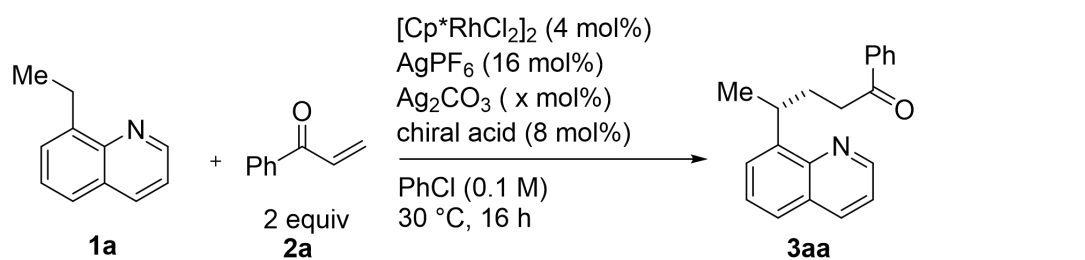


a) Scale: 0.05 mmol **1a**

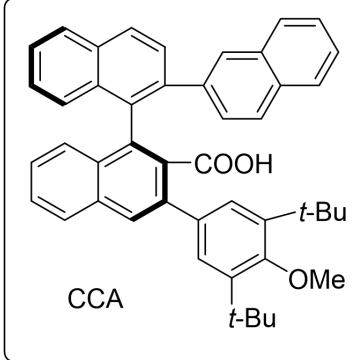
b) Determined by ¹H NMR analysis of the crude mixture using 1,1,2,2-tetrabromoethane as an internal standard.

c) Determined by HPLC analysis.

Table 6. Effects of the Amount of Ag₂CO₃^a



Entry	Ag ₂ CO ₃ /mol%	Yield/% ^b	er ^c
1	2	16	89:11
2	4	34	89:11
3	10	40	89:11
4	20	44	89:11
5	25	43	89:11
6	28	50	89:11
7	35	33	89:11
8	40	35	89:11
9	50	35	89:11



CCA

a) Scale: 0.05 mmol **1a**
b) Determined by ¹H NMR analysis of the crude mixture using 1,1,2,2-tetrabromoethane as an internal standard.
c) Determined by HPLC analysis.

The results in **Tables 4-6** suggest that the acidity of the reaction conditions can affect the reactivity, which fits the hypothesis (**Chapter 3, Figure 7**). Although an acid, such as HFIP, can promote the protonation of the enolate intermediate, it may inhibit the deprotonative C–H activation step. The C–H activation step would be preferred relatively under basic conditions. As a whole, increasing the acid may inhibit the reaction while the increasing the amount of Ag₂CO₃ was effective in the current case. However, in the screening of bases, only Ag₂CO₃ afforded good yield, which implies that Ag₂CO₃ may work as not only the base but also play another role.

From **Table 5** and **Table 6**, Ag₂CO₃ show a very important role in reactivity. In my opinion, Ag₂CO₃ could hold the balance between R*COOH and R*COO⁻. In my proposed mechanism, R*COO⁻ plays main role on coordinating with Rh complex. From **Table 4**, high acidity could reduce the yield. In a word, the balance between RCOOH and RCOO⁻ is very important to reactivity and Ag₂CO₃ and Ag⁺ are very suitable for the dissociation of RCOOH.

4-5. Screening of Reaction Temperature

Finally, I examined the effects of the reaction temperature (**Table 7**). At lower temperatures (-10 °C to 0 °C, entries 1 and 2), the selectivity was improved but the reactivity was not satisfactory. The best result was obtained when the reaction was performed at 20 °C or 30 °C (**Table 7**, entries 4 and 5), while higher

temperatures led to lower yields (**Table 7**, entries 6 and 7), despite that the decomposition of phenyl vinyl ketone **2a** was not evident.

Table 7. Screening of The Reaction Temperature^a

Entry	Temp/°C	Yield/% ^b	Recov. 1a ^b / 2a ^d	er ^c
1	-10	24	86%/160%	91:9
2	0	30	78%/156%	91:9
3	10	30	74%/150%	89:11
4	20	48	53%/140%	89:11
5	30	47	55%/146%	89:11
6	40	30	80%/144%	89:11
7	60	20	89%/154%	89:11

a) Scale: 0.05 mmol **1a**

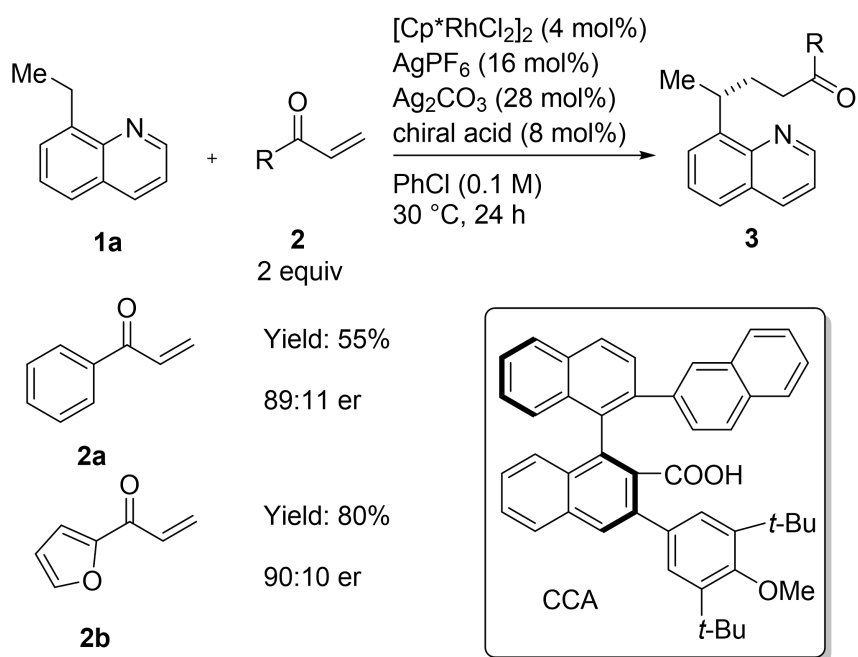
b) Determined by ¹H NMR analysis of the crude mixture using 1,1,2,2-tetrabromoethane as an internal standard.

c) Determined by HPLC analysis.

d) "**1a**"= 8-ethylquinoline (100%); "**2a**"= phenyl vinyl ketone (200%).

4-6 Scope of Substrates

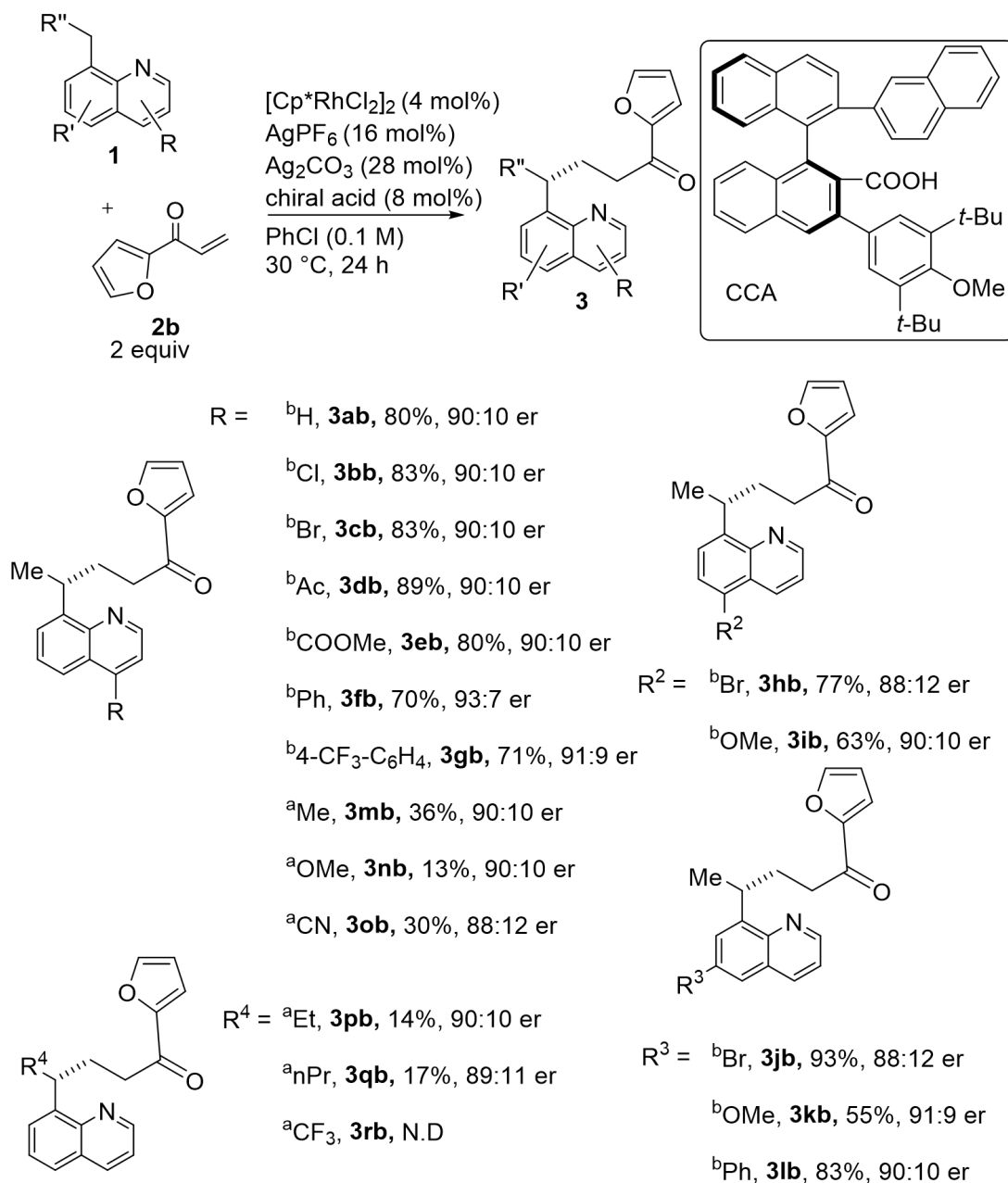
With the optimal conditions in hands, I turned my attention to the substrate scope. Firstly, I investigated 2-furylyl vinyl ketone **2b**, and found that the better yield was obtained (80%) with the comparable selectivity (**Scheme 22**). For further examination of other 8-methylquinoline **1**, **2b** was used as the electrophile.



Scheme 22. Higher Reactivity of Heterocyclic Enone

Then various substituted 8-alkylquinolines **1** were investigated as the substrate and reacted with 2-furyl vinyl ketone **2b** (Scheme 23). Several 8-ethylquinolines bearing an electron-withdrawing group (**3bb-3gb**) at the 4-position all reacted in good yield (>69%) and high enantioselectivity (>90:10 er) except for that bearing a CN group (**3ob**). Furthermore, 5 or 6-substituted quinolines (**3hb-3lb**) were also applicable, furnishing the desired product in moderate yield (40%-69%). In contrast, 8-methylquinolines bearing an electron-donating group at the 4-position (**3mb, 3nb**) resulted in lower yields (<40%). The reactions using 8-alkylquinoline bearing a longer alkyl group (**3pb-3rb**) exhibited low reactivity (<20%).

From Scheme 23, 8-ethylquinoline bearing electron-donating groups slow down the reaction. In my opinion, EDG could enhance the electron density of N and it will compete binding to Rh with RCOOH, which inhibit the enantio-determining step (see: Figure 7).



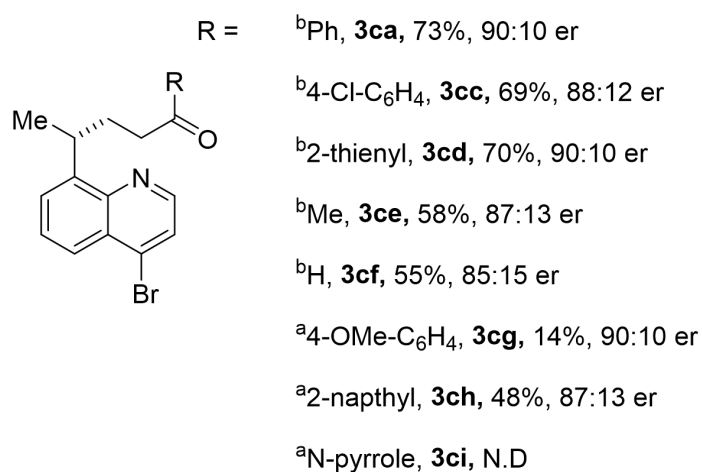
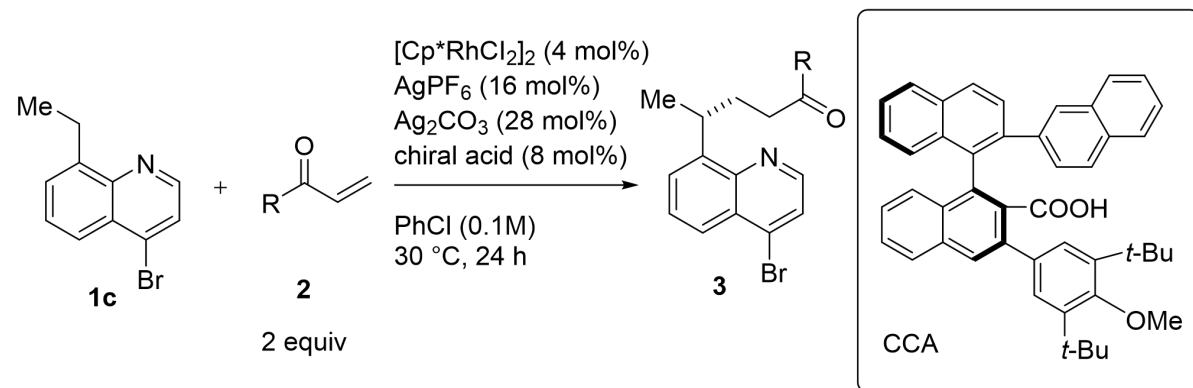
a) Scale: 0.05 mmol **1** Yield: Determined by ¹H NMR analysis of the crude mixture using 1,1,2,2-tetrabromoethane as an internal standard.

b) Scale: 0.2 mmol **1** Yield: isolated yield (by silic column); er: Determined by HPLC analysis.

Scheme 23. Scope of Quinolines

Next, the scope of enones was examined using **1c** as the substrate (**Scheme 24**). While aryl vinyl ketones bearing an electron-withdrawing group (**3ca**, **3ce**) afforded moderate yield and good enantioselectivity (45%-70% yield, >88:12 er). Aryl vinyl ketones bearing an electron-donating group (**3cg**) afforded low yield, but still in good enantioselectivity. On the other hand, substituted alkyl vinyl ketones (**3ce**, **3cf**) reacted smoothly in the reaction system with moderate yield (about 50%) and moderate enantioselectivity (85:15–87:13 er). 2-Thienyl vinyl ketone (**3cd**) and phenyl vinyl ketone (**3ca**) afforded good results.

From **Scheme 24**, different β -substituted enones could also make very big influence on yield. It may be from the electron density of O in carbonyl group and C=C. High electron density of C=C may improve the reactivity by coordinating with Rh. High electron density or low steric effect on C=O may compete binding to Rh with RCOOH to inhibit the enantio-determining step.

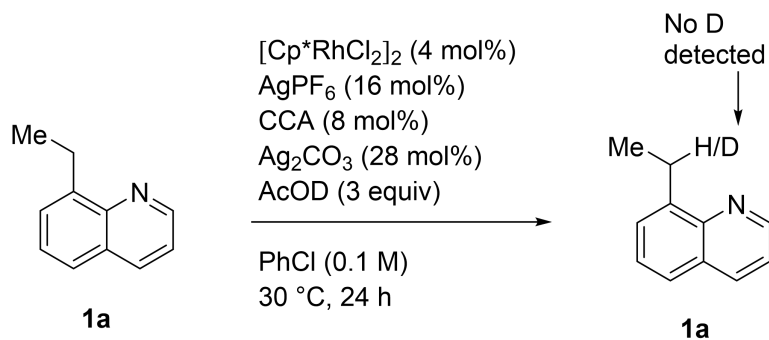


a) Scale: 0.05 mmol **1** Yield:
Determined by ¹H NMR analysis
of the crude mixture using
1,1,2,2-tetrabromoethane as an
internal standard.
b) Scale: 0.2 mmol **1** Yield:
isolated yield (by silic column)
er: Determined by HPLC analysis.

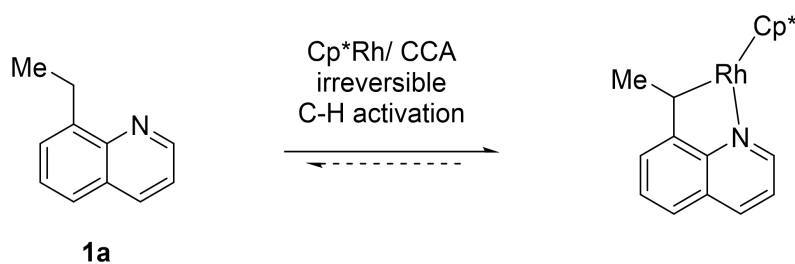
Scheme 24. Scope of α,β -Unsaturated Compounds

4-7 H/D Exchange Experiment

To confirm the enantio-determining step of these reactions, the reversibility of the C–H activation was examined (**Scheme 25**). When **1a** was reacted with AcOD under the optimized reaction conditions except that enone **2** was omitted, almost no H/D exchange was observed, indicating that the C–H activation is irreversible and determines the enantioselectivity (**Scheme 26**).



Scheme 25. H/D Exchange Experiment



Scheme 26. Irreversible C–H Activation

4-8 Proposed Reaction Mechanism.

A proposed reaction mechanism is shown in **Figure 8**. First, $[Cp^*RhCl_2]_2$ reacts with AgPF₆, Ag₂CO₃, and a chiral carboxylic acid to produce an active and chiral Rh catalyst. Next, 8-ethylquinoline **1** coordinates to the Rh center, and C–H bond cleavage proceeds via concerted metalation deprotonation (CMD) assisted by the chiral carboxylate, which is the enantio-determining step. This C–H activation is irreversible as discussed above, and thus other following steps are not relevant to the enantioselectivity. Then the coordination of an α,β -unsaturated carbonyl compound to the rhodium center (**B**) is followed by the insertion of the C–C double bond into the Rh–C(sp³) bond to give an enolate intermediate **C**. Finally, protonolysis of **C** gives product **3** and regenerates the active rhodium species (**Figure 8**).

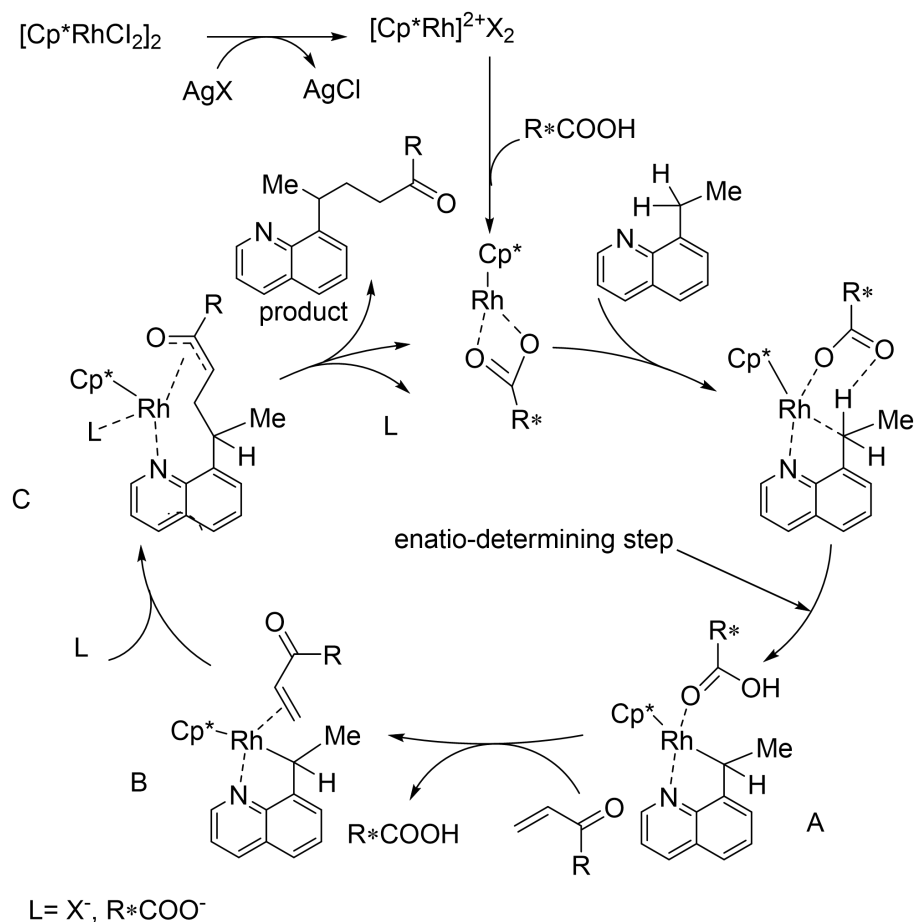


Figure 8. Proposed mechanism

4-9 Determination of Absolute Configuration

The absolute configuration of **3** was unambiguously confirmed by the single crystal X-ray diffraction analysis of **3ja** to be the same as that observed for the C–H amidation of 8-ethylquinolines **1a** in the previous study using the same CCA (the data are shown in Experiment section).¹⁸). These results, the observed similar enantioselectivity with the same CCA as the previous C–H amidation reactions and the irreversibility of the C–H activation all suggest that the enantioselectivity is almost determined in the C–H activation step.

Summary

I developed Cp*Rh(III)/CCA-catalyzed enantioselective addition of C(sp³)–H bonds of 8-ethylquinolines **1** to α,β -unsaturated carbonyl compounds **2**. The reactions proceeded under mild conditions with good functional group compatibility and exhibited good enantioselectivity. The results demonstrate further utility of the combination of a high-valent group 9 metal catalyst and a chiral carboxylic acid (CCA) for the selective functionalization of enantiotopic C(sp³)–H bonds to furnish C–C bonds, which complements the previously established C–N bond-forming reactions.

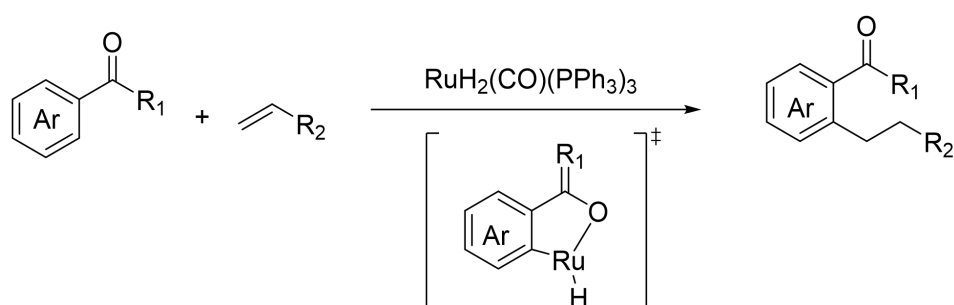
However, there are some points to further explore: 1) the limited scope of electrophiles, 2) the limited scope of 8-alkylquinolines: 8-alkylquinolines bearing a longer alkyl group resulted in low yield (**3pa-3ra**). 3) the requirement of large equivalents of silver additives (almost 0.5 equiv), which may not conform to the economic chemistry.

Chapter 5. Arene Ru(II)-Catalyzed Enantioselective C–H Functionalization

5-1 Introduction of Arene Ru(II)-Catalyzed C–H Bond Functionalization

Ruthenium (Ru) is relatively inexpensive (21.2 USD/g) compared to other widely used metals for C–H activation such as rhodium (491.2 USD/g) and palladium (63.0 USD/g), and also occupies an important position. The use of Ru(0) catalyst precursors, especially with the contribution of the Murai–Chatani–Kakiuchi group since 1993,²⁶⁾ has led to the discovery of new reactions based on initial Ru(0) insertion into the C–H bond and further reactivity of generated C–Ru–H species especially via unsaturated substrate insertion processes (**Scheme 27**).

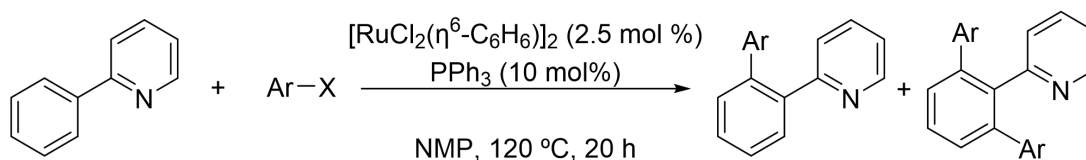
OMurai–Chatani–Kakiuchi (1993):



Scheme 27. Ru(0)-Catalyzed C–H Bond Activation

In 2001, Oi and Inoue demonstrated C–H arylation with aryl halides catalyzed by [RuCl₂(C₆H₆)₂].²⁷⁾ In the following two decades, Ru(II)-catalyzed C–H activation has achieved great success by Ackermann, Bruneau, Dixneuf, and others (**Scheme 28**).²⁵⁾

Oi and Inoue (2001):



Scheme 28. Ru(II)-Catalyzed C–H Bond Activation

Arene-Ru(II) complexes are very successful among Ru-complexes, and the reason may be from their easy transformation into cyclometalated species via C–H bond cleavage; Ru(II) also shows its good compatibility with currently used oxidants and the stability of some of them to both air and water. In addition, the ease of preparation and low price are also its attractive advantages. However, the example of enantioselective Ru(II)-catalyzed C–H functionalization remains less than Pd and Rh (**Figure 9**).

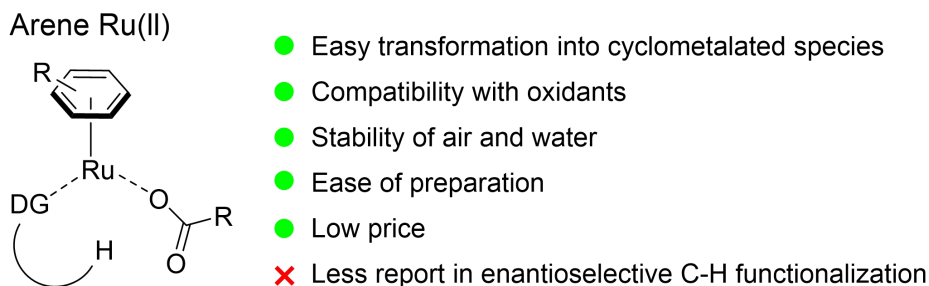


Figure 9. Arene-Ru(II) Complex

5-2 Introduction of Chiral Arene-Ru(II)-catalyzed Enantioselective C–H Bond Functionalization

The catalytic control of the enantioselectivity of Ru(II)-catalyzed C–H functionalization reactions remains a challenging problem. On the basis of the structure of arene Ru(II) complexes, there are three possible strategies to make Ru(II)-catalyzed asymmetric C–H activation feasible.

The first one is to develop Ru(II) catalysts bearing precisely designed chiral arene ligands. This strategy has been applied in enantioselective group 9 $Cp^xM(III)$ ($M = Co, Rh, Ir$) catalyzed C–H functionalization with tailor-made chiral Cp^x ligands, and it showed good result. What's more, the arene-Ru(II) complex has similar features to group 9 $[Cp^*M(III)]$ complexes. They possess a dicationic d^6 metal center and a half-sandwich structure with three available coordination sites. However, some additional challenges exist for the enantiocontrol in the Ru(II) catalysis. First, the stability of such arene ruthenium complexes could be poor as arene would dissociate from a metal center facily. In fact, Larrosa and co-workers found that *p*-cymene ligand dissociated from the ruthenium(II) catalyst in their C–H arylation reaction.²⁹⁾ Second, the design of chiral arene ligands is not trivial because most of the privileged chiral ligand scaffolds (e. g. 1,1'-bi-2-naphthol, 1,1'-spirobiindane-7,7'-diol) contains multi arene motifs, which may raise serious problems in chemoselectivity and diastereoselectivity of their complexation with ruthenium (**Figure 10**).

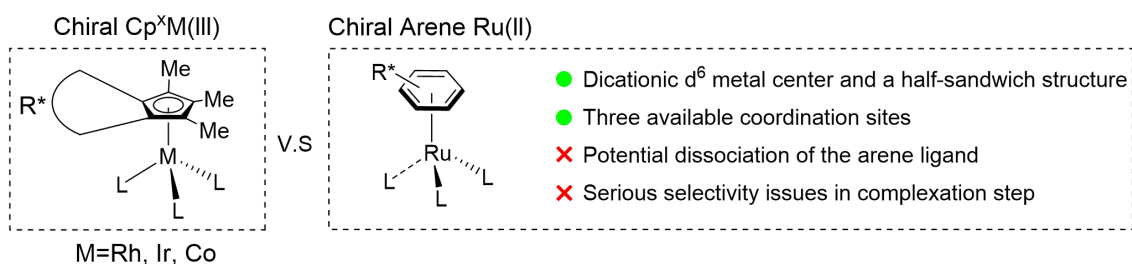
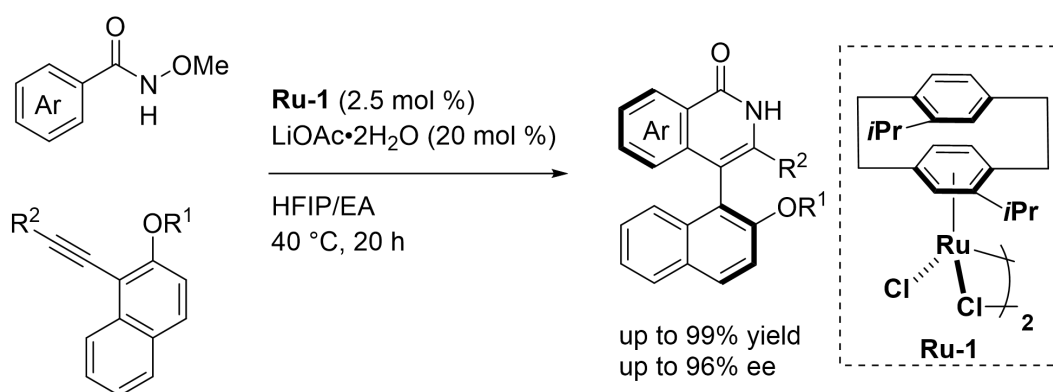


Figure 10. Chiral Arene-Ru(II) Complex

Wang and co-workers made an important progress in this chemistry by rationally designing a C_2 -symmetric chiral arene ligand based on the [2.2]paracyclophane skeleton.³⁰⁾ Their chiral Ru(II) catalyst was proved to be highly efficient for enantioselective C–H functionalization of *N*-methoxy amides with sterically hindered alkynes, affording various axially chiral isoquinolones in excellent yield with good to high enantioselectivity. Significantly, Wang demonstrated that the chiral arene-Ru(II) could catalyze enantioselective C–H functionalization to control the enantioselectivity.

Wang (2022):



Scheme 29. Chiral Arene-Ru(II) Catalyzed Enantioselectivity C–H Functionalization

First, as shown in structure A in **Figure 11**, the strained structure of [2.2]paracyclophane and its C₂ symmetry would preclude the registration and stereoisomerism created in the complexation step. Secondly, steric repulsion from the uncoordinated alkene ring would force the substituent R to shift to the metal side, resulting in a well-defined chiral environment around the metal center (**Figure 11**, structure B). Thirdly, protection of the coordinated aromatic from any possible nucleophilic attack and trans-ring electronic interactions of the uncoordinated aromatic should improve the stability of the aromatic metal complex (**Figure 10**, structures C and D).

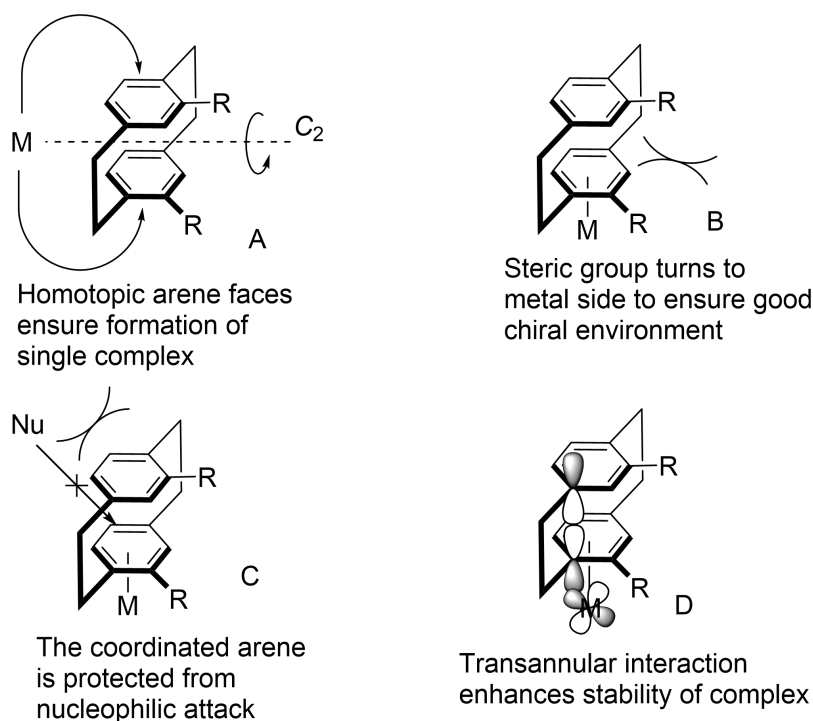


Figure 11. Design of [2.2]paracyclophane-Based Chiral Arene Ligands.

In 2021, Perekalin and co-workers also reported the chiral cyclohexa-1,3-diene ligand with Ru(II) complex.³¹⁾ However, the development of enantioselective C–H activation was only partially successful;

only 68% ee was achieved in their report. Many attempts to apply this chiral arene-Ru(II) complex to catalytic C–H activation failed, which was attributed to its facile decomposition under the reaction conditions.

5-3 Introduction of Arene-Ru(II)/cTDG-Catalyzed Enantioselective C–H Bond Functionalization

Enantioselective C–H activation facilitated by a chiral transient guidance group (cTDG) is a process in which a chiral guidance group is formed in situ and induces diastereoselective C–H activation.^{25,28} cTDG is cleaved automatically, releasing the enantiomer-rich product. (Figure 12). Loading of chiral reagents to generate cTDG in situ is usually substoichiometric or catalytic. This elegant strategy was pioneered by Yu, who used chiral amino acids or amino amides to achieve palladium-catalyzed enantioselective benzylic C(sp³)–H arylation of ortho-alkyl-substituted benzaldehyde.

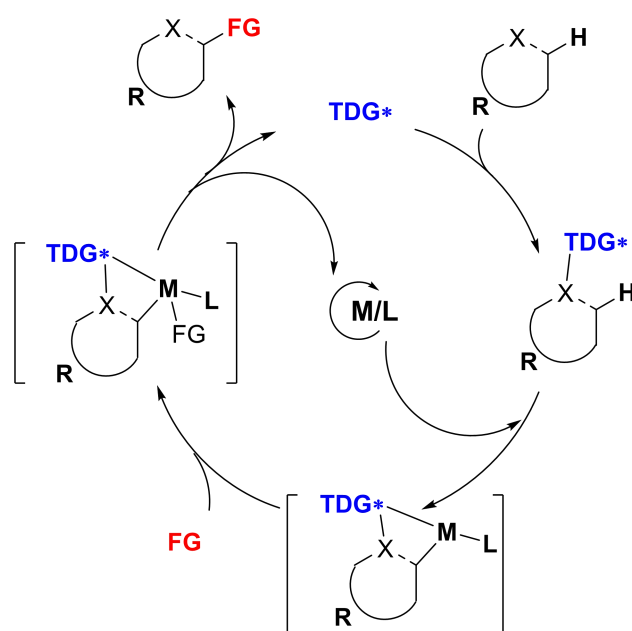


Figure 12. Transition Metal Catalyzed Enantioselective C–H Functionalization with cTDG.

Mechanistically, amino acids and amino amides are incompatible with d⁶ metal complexes featuring piano stool configurations (e.g., CpRh^{III}, arene-Ru^{II}), which have one less available coordinating sites compared to Pd(II) (Figure 13). Thereby, monodentate transient directing group would be required.

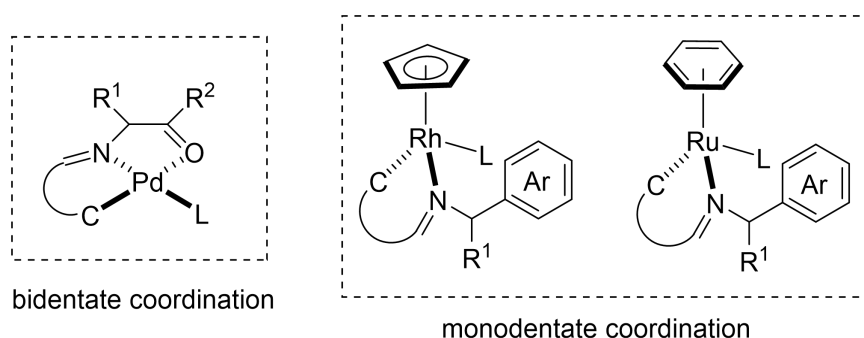
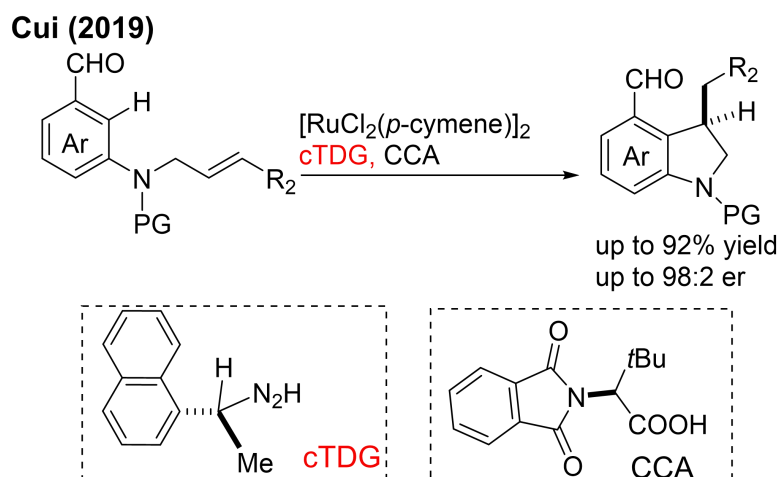


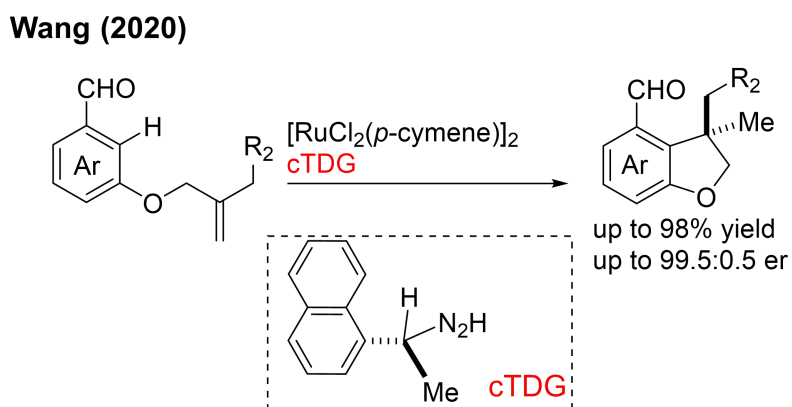
Figure 13. Monodentate Coordination Between Ru(II) and cTDG.

In 2019, Cui and co-workers successfully developed a Ru(II)(*p*-cymene)-catalyzed enantioselective intramolecular C–H functionalization of aldehydes bearing an olefinic side chain by the transient chiral directing group strategy, affording chiral indolines in up to 92% yield with up to 96% ee (**Scheme 30**). In this work, besides (*R*)-1-(naphthalen-1-yl)ethan-1-amine (cTDG), an 1-*tert*-leucine derived chiral carboxylic acid (CCA) was found to be vital to achieve high enantioselectivity.³²⁾



Scheme 30. Arene-Ru(II)/cTDG Catalyzed Enantioselectivity C–H Functionalization by Cui

In 2020, Wang and his co-workers also reported that the use of (*R*)-1-(naphthalen-1-yl)ethan-1-amine as the cTDG, the Ru(II)(*p*-cymene)-catalyzed intramolecular enantioselective C–H activation of aldehydes bearing an olefin side chain was successfully realized (**Scheme 31**).³³⁾



Scheme 31. Arene-Ru(II)/cTDG Catalyzed Enantioselectivity C–H Functionalization by Wang

Chapter 6. Arene-Ru(II)-catalyzed Enantioselective C–H Functionalization by Chiral Carboxylic Acid

6-1 The two modes of Arene-Ru(II)/CCA-Catalyzed Enantioselective C–H Bond Functionalization

Chiral carboxylic acids (CCAs) as chiral inducers have been proved to be an effective strategy to accomplish enantioselective C–H activation under d^6 metal catalysis with piano stool configurations, such as Cp Group 9 metal with CCA. In terms of Ru(II)-catalyzed enantioselective C–H functionalization, two modes have been disclosed. First, when C–H activation is the enantiodetermining step, chiral carboxylate can assist the selective activation of enantiotopic C–H bonds. The resulting chiral ruthenacyclic intermediate then undergoes further functionalization to furnish enantiomerically enriched product. Second, the chiral carboxylic acid (CCA) enables enantioselective proto-demetalation step (**Figure 14**).

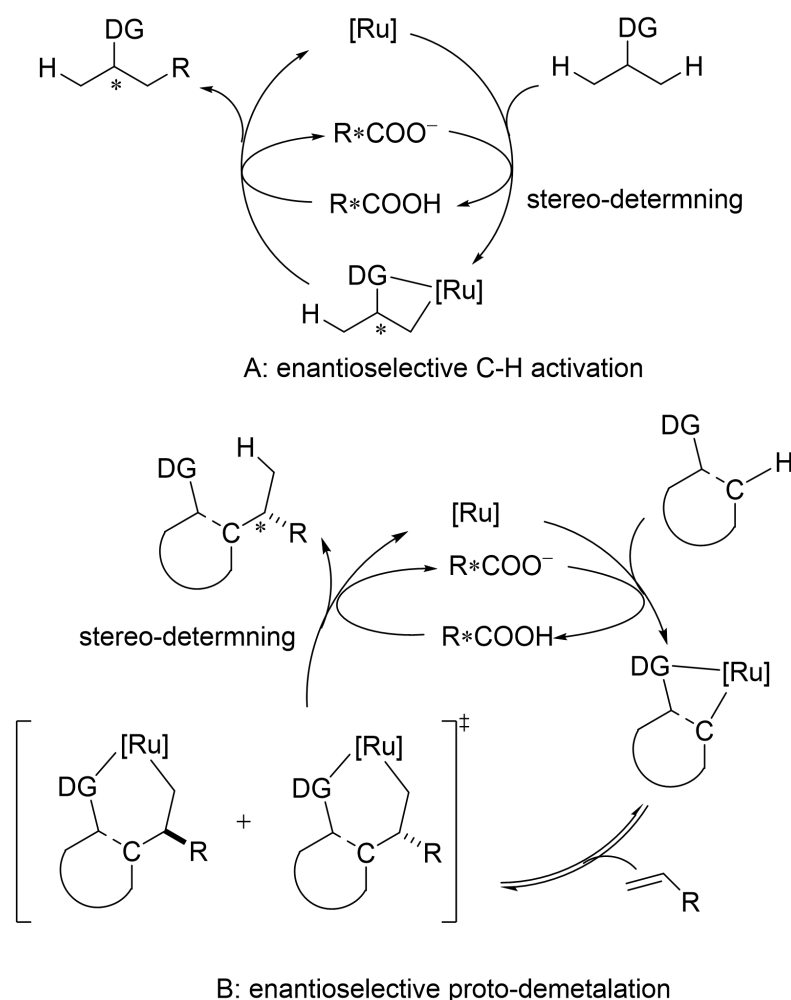


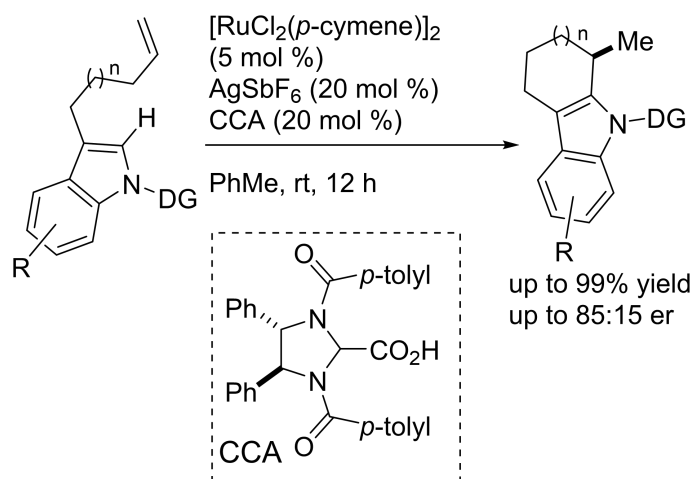
Figure 14. The Two Modes of Arene-Ru(II)/CCA-catalyzed Enantioselective C–H Functionalization

6-2 Arene-Ru(II)/CCA-Catalyzed Enantioselective C–H Bond Functionalization

In 2021, Ackermann and co-workers reported a chiral carboxylic acid-assisted arene-Ru(II)-catalyzed intramolecular enantioselective C–H cyclization (**Scheme 32**).³⁴⁾ Under the chiral carboxylic acid (CCA),

indole substrates were transformed to chiral indole derivatives in moderate to high yield (up to 99 %) with moderate enantioselectivity (up to 72 %). In the computational and experimental mechanistic studies, the result indicated the migratory insertion step was reversible and the proto-demetalation step was the enantio-determining step.

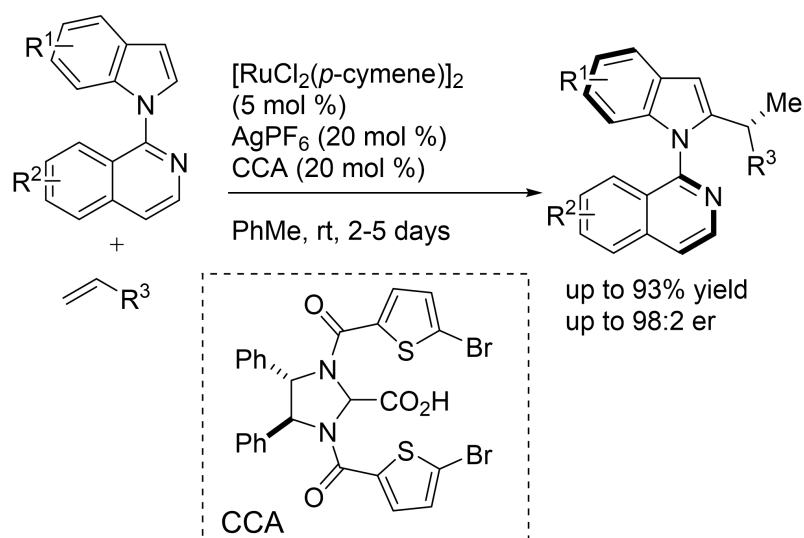
Ackermann (2021)



Scheme 32. Arene-Ru(II)/CCA Catalyzed Enantioselective C–H Alkylation by Ackermann

Ackermann continued this investigation, and reported an intermolecular version of above reaction later in 2022 (Scheme 33).³⁵ In the presence of the chiral carboxylic acid (CCA), they afforded chiral indole derivatives with central and axial chirality in high yield (up to 93% yield) and high regio-, diastereo- and enantioselectivity (up to 96% ee). DFT calculation indicated the proto-demetalation step was the stereo-determining step.

Ackermann (2022)



Scheme 33. Arene-Ru(II)/CCA Catalyzed Intermolecular Enantioselective C–H Alkylation by Ackermann

In 2021, Shi and co-workers reported a highly enantioselective Ru(II)(*p*-cymene)-catalyzed C–H

Chapter 7. Aza Analogues of Sulfones - Sulfoximine and TM Catalyzed C–H Activation of Sulfoximine to C–C Formation

7-1 Importance of Sulfur(VI)-Containing Motifs in Pharmaceutical and Medicinal Chemistry

Sulfur(VI) compounds, especially sulfones, sulfonamides and their analogues, have showed broad range of bioactivity, and those compounds show a high structural diversity, which is crucial for medicinal chemistry research.²⁵ The development of new less toxic, low cost, and highly active sulfonamides containing analogues are important in medicinal chemistry. Now, more than 150 FDA approved sulfur(VI)-based drugs are available in the market, and they are widely used to treat various diseases, such as anti-inflammatory, anti-viral, antidiabetic, anti-leishmanial, anti-cancer, and others (**Figure 15**).

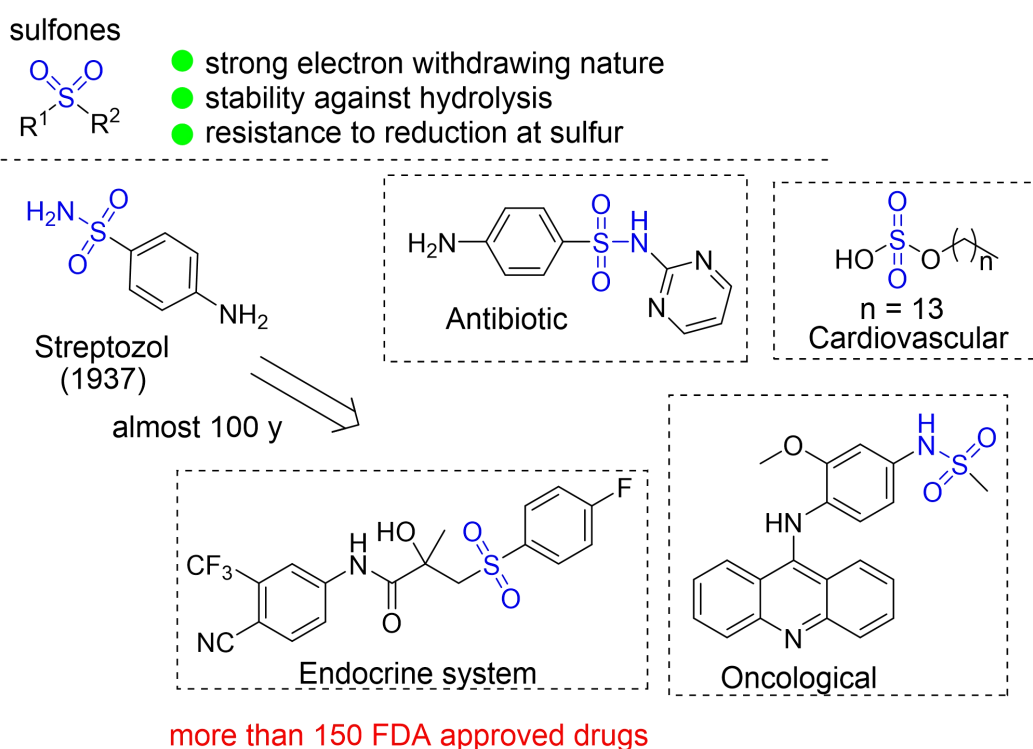


Figure 15. Pharmaceutical and Medicinal Significance of Sulfones and Sulfonamides

Sulfoximines are the aza analogues of sulfones. In the case the two carbon substituents are different, the replacement of the oxygen of sulfones with a nitrogen atom will result in a chiral tetrahedral sulfur atom (**Figure 16**). Compared with sulfones, sulfoximines have an additional substitution site (N-R³) that could be modified by various functional groups. In addition, it has great potential to construct cyclic sulfoximines by connecting substituents R¹ and R³. The NH moiety of sulfoximines is weakly basic, and the protonated form has a *pK*_a of 2.7.²⁵ The basicity of the nitrogen atom is also sufficient to coordinate with metals or form salts with acids. The acidity of the NH moiety (*pK*_a = 24) is comparable to the acidity of alcohol (*pK*_a in DMSO, MeOH: 29; *i*-PrOH: 30.2; *t*-BuOH: 33).²⁵ It has been confirmed in the literature that sulfoximine can be used as an isostere of alcohols in the studies of HIV-1 protease inhibitors.

The NH group is nucleophilic and can be replaced by a variety of functional groups. The nature of the

substituents on the nitrogen atom greatly affects its properties as an acid and base. The NMR studies indicated that a sulfoximine group has higher electron-withdrawing ability than a sulfone group. The heteroatoms bonded to the sulfur center function as hydrogen bond acceptors. In the absence of any substituent at the NH moiety ($R^3 = H$), the sulfoximine has the dual functions as both hydrogen bond donor and hydrogen bond acceptor. Compared with sulfones or sulfonamide, sulfoximines showed better solubility in protic solvents. Sulfoximines are constitutionally and configurationally stable compounds that can be handled without special attention. Based on these promising properties, interest in this functional group, which is underrepresented in drug research and development, has clearly increased.

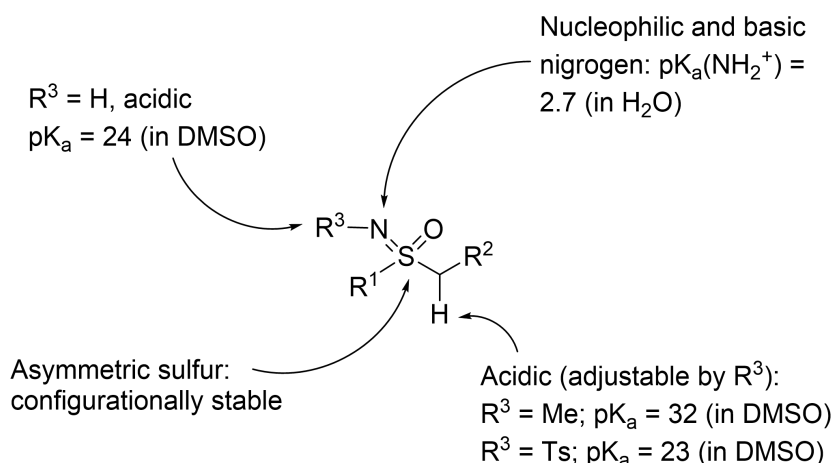


Figure 16. General Properties of The Sulfoximine Group

Generally, the modifications of sulfoximines are categorized into two classes, that is, N–H functionalization and C–H functionalization. Selective C–H functionalization reactions of *S*-aryl substituents of sulfoximine and its analogue with the nitrogen atom working as a directing group are efficient synthetic methods for increasing the diversity of available sulfoximine derivatives. In the following part, I will discuss selective C–H functionalization reactions of sulfoximines (**Figure 17**).

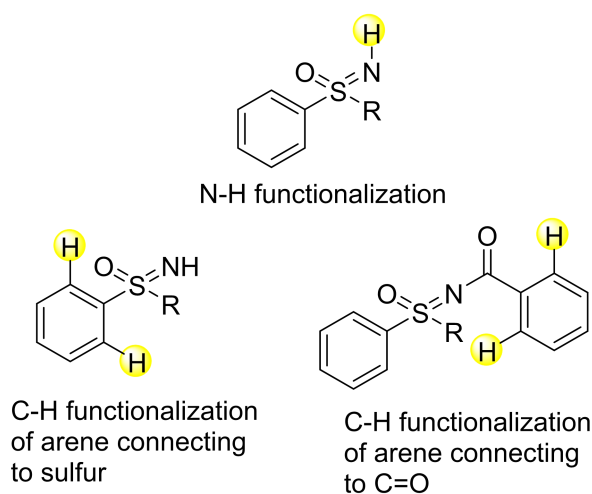
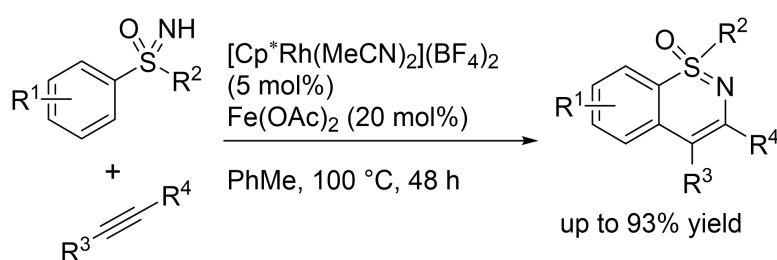


Figure 17. Overview of N–H and C–H Functionalization of Sulfoximines and Their Analogues

7-2 TM Catalyzed C–H Alkenylation of Sulfoximines

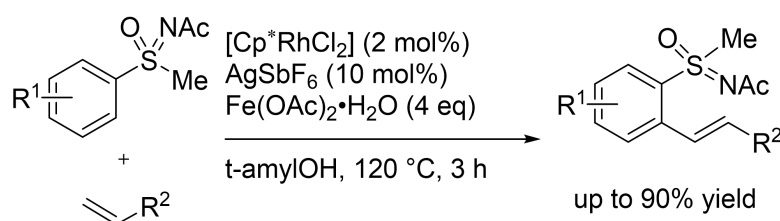
One of the seminal examples of oxidative C–H/N–H annulation of NH-sulfoximines with alkynes to afford 1,2-benzothiazine was reported by Bolm and co-workers (**Scheme 35**).³⁹⁾ They screened various metal catalyst and found that 5 mol% of $[\text{Cp}^*\text{Rh}(\text{MeCN})_3](\text{BF}_4)_2$ in presence of 20 mol% of $\text{Fe}(\text{OAc})_2$ as an activator in toluene under oxygen atmosphere at 100 °C resulted in excellent yield of the desired products with good functional compatibility.



Scheme 35. Rh Catalyzed Oxidative C–H/N–H Annulations of Alkyne with Sulfoximine

Bolm and coworkers also reported a Rh(III)-catalyzed directed C–H alkenylation of sulfoximines with acyl protecting group at the nitrogen for the synthesis of mono- and bis-alkenylated derivatives in reasonable efficiency (**Scheme 36**).⁴⁰⁾

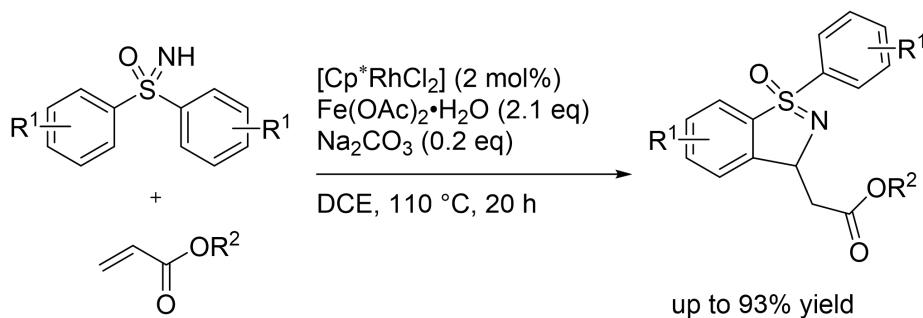
Bolm (2014)



Scheme 36. Rh-Catalyzed C–H Alkenylation of N–Ac/aroyl with Sulfoximine

Dong et al. reported the synthesis of biologically active benzoisothiazole 1-oxide through Rh(III)-catalyzed N-directed ortho C–H activation/tandem intramolecular aza-Michael cyclization reaction between NH-sulfoximines and various olefins (**Scheme 37**).⁴¹⁾

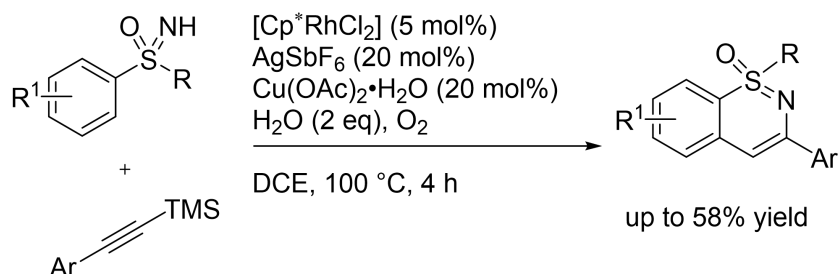
Dong (2017)



Scheme 37. Rh Catalyzed C–H Alkenylation/aza-Michael Cyclization with Sulfoximine

Prabhu and co-workers reported a Rh(III)-catalyzed oxidative synthesis of 1,2-benzothiazine derivatives utilizing silyl alkynes through a desilylative route (**Scheme 38**).⁴²⁾

Prabhu (2019)

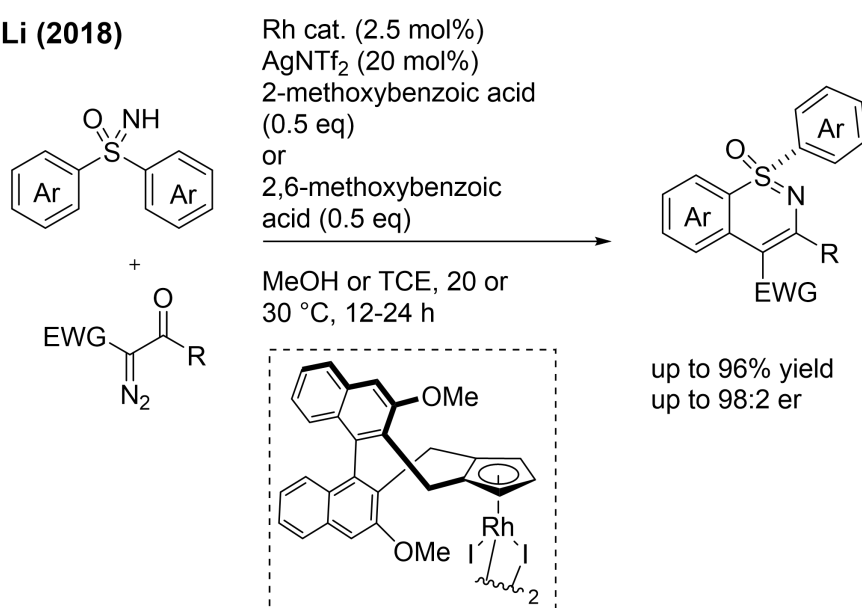


Scheme 38. Rh Catalyzed C–H Oxidative Annulation of Sulfoximines with Silyl Alkynes.

7-3 TM Catalyzed C–H Enantioselective C–H Functionalization of Sulfoximines

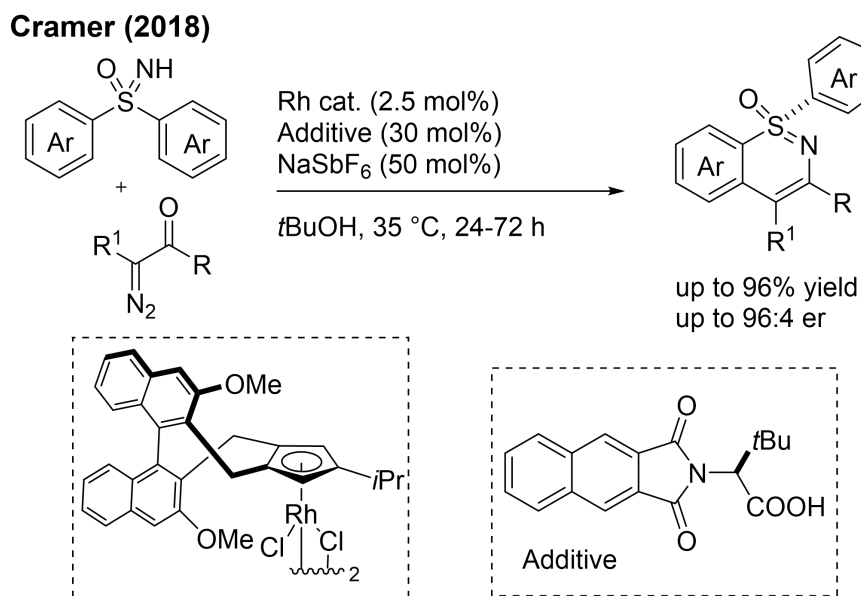
Enantioselective C–H Functionalization of sulfoximines have been developed using chiral metal catalysts or chiral carboxylic acid co-catalysts. Li and co-workers described an unprecedented enantiodivergent [4+2] annulative coupling of sulfoximines with α -diazocarbonyl compounds via chiral Rh(III)-catalyzed desymmetrizing C–H activation (**Scheme 39**).⁴³⁾

Li (2018)



Scheme 39. Chiral Rh(III)-Catalyzed [4+2] Annulative Coupling of Sulfoximines with Diazo Compounds

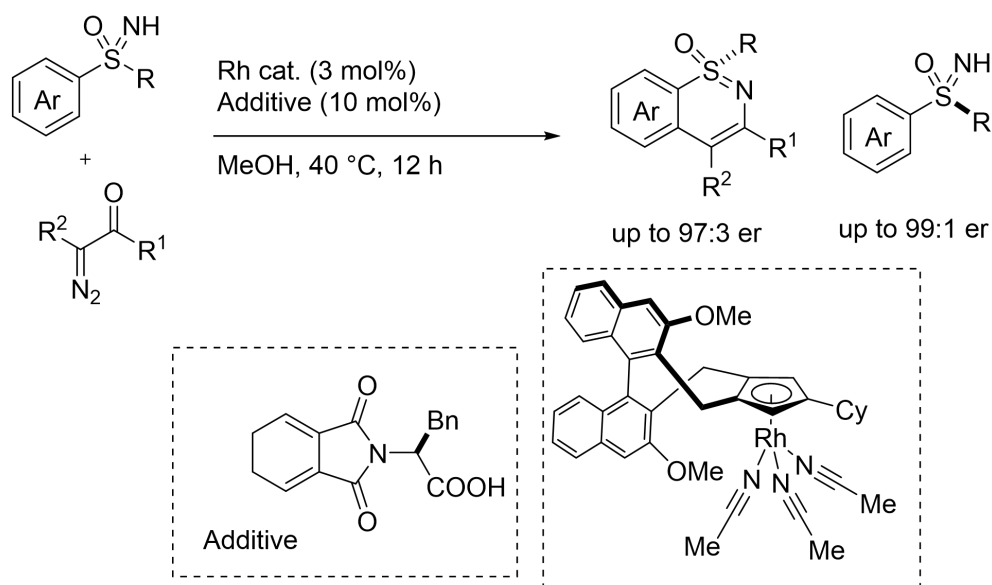
Simultaneously, another independent work has been reported from the Cramer's group to expedite the access of *S*-chiral 1,2-benzothiazines with good enantioselectivities (**Scheme 40**).⁴⁴⁾



Scheme 40. Chiral Rh(III)-Catalyzed [4+2] Annulative Coupling by Cramer et al.

One year later, the same team disclosed an effective kinetic resolution methodology of racemic sulfoximines, which allowed in accessing the acyclic enantioenriched aryl alkyl sulfoximines along with optically active 1,2-benzothiazines through Rh(III)-catalyzed C–H functionalization (**Scheme 41**).⁴⁵⁾

Cramer (2019)

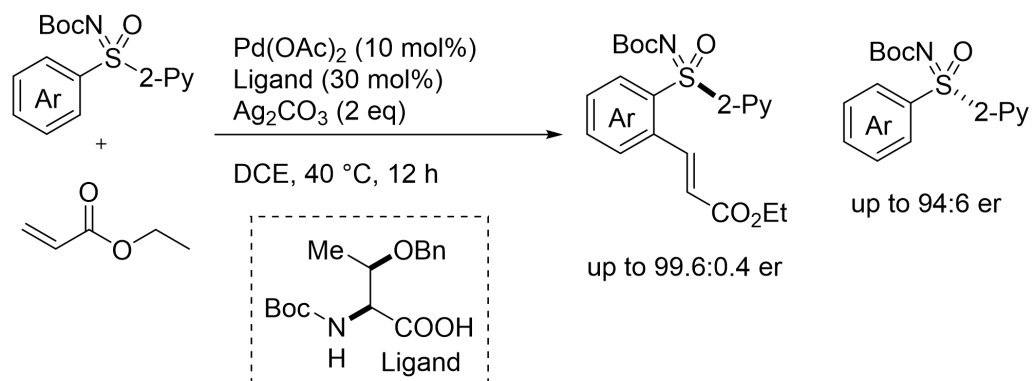


Scheme 41. Chiral Rh(III) Catalyzed [4+2] Annulative Coupling with Racemic Sulfoximines

A direct Pd(II)-catalyzed kinetic resolution of heteroaryl sulfoximines through an ortho-C–H alkenylation/arylation has been developed by Sahoo and co-workers (**Scheme 42**).⁴⁶⁾ The coordination of the 2-pyridyl unit and the chiral amino acid ligand to the Pd(II)-catalyst controls the enantio-selective C–H cleavage. The method provided access to a wide range of enantiomerically enriched unreacted aryl-pyridyl-sulfoximines and C–H alkenylation/arylation products in good yields with high

enantioselectivity (up to >99% ee). Selectivity factor in kinetic resolution reached up to >200.

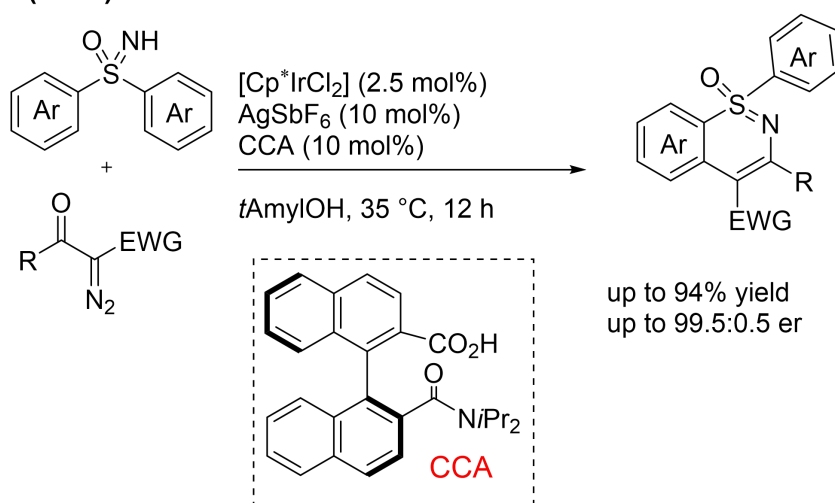
Sahoo (2021)



Scheme 42. Pd(II)/MPAA Catalyzed C-H Activation of Racemic Sulfoximines

Shi and co-workers reported the Ir(III)-catalyzed asymmetric C–H activation/annulation of sulfoximines with diazo compounds using an achiral iridium catalyst and a chiral carboxylic acid combination (**Scheme 43**).⁴⁷⁾ Various types of sulfur-stereogenic sulfoximines were obtained in high yields with excellent enantioselectivities. In 2022, Xu have developed an iridium-catalyzed enantioselective C–H borylation of *N*-silyl diaryl sulfoximines.⁴⁸⁾

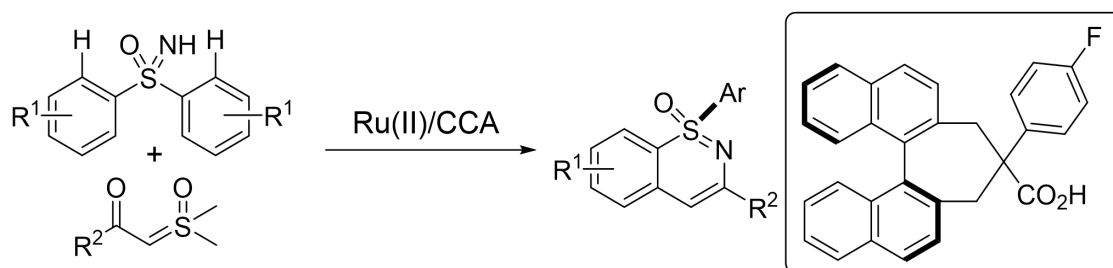
Shi (2022)



Scheme 43. Cp*Ir(III)/CCA-Catalyzed C–H Activation with Sulfoximine

Chapter 8. Second work: Ru(II)/Chiral Carboxylic Acid-Catalyzed Enantioselective C–H Functionalization of Sulfoximines⁵²⁾

When C–H bonds are cleaved by using an electrophilic high-valent metal catalyst, carboxylates and other basic anionic ligands would participate in the C–H bond cleavage step via either an ambiphilic metal–ligand activation (AMLA), a concerted metalation-deprotonation (CMD), or a base-assisted internal electrophilic substitution (BIES) mechanism. Therefore, enantio-induction can be achieved by using a chiral carboxylic acid (CCA) or a related ligand. The strategy was first introduced to the field of Pd(II) catalysis by the Yu group and was recently expanded to be used with group 9 metal catalysts. Matsunaga, Yoshino and coworkers have been engaged in the development of the enantioselective C–H functionalization of prochiral substrates using Co(III)/CCA and Rh(III)/CCA systems. When considering the similarity between Ru(II) catalysis and Cp*M(III) catalysis, I wonder the possibility of achiral Ru(II) and chiral carboxylic acids system for enantioselective C–H bond cleavage. Thus, I decided to investigate the possibility of enantioselective C–H bond cleavage using a Ru(II) catalyst and a CCA. In 2021³⁶⁾, during the course of my PhD study, Shi and co-workers also reported enantioselective C–H alkylation/cyclization reactions between sulfoximines and sulfoxonium ylides using $[\text{RuCl}_2(p\text{-cymene})]_2$ and a C₁-symmetric binaphthyl CCA. In this chapter, I describe my own study demonstrating that a pseudo-C₂-symmetric binaphthyl CCA that was recently developed in Matsunaga/Yoshino group for group 9 metals is suitable for Ru(II)-catalyzed enantioselective C–H bond cleavage of prochiral sulfoximines (**Scheme 44**).



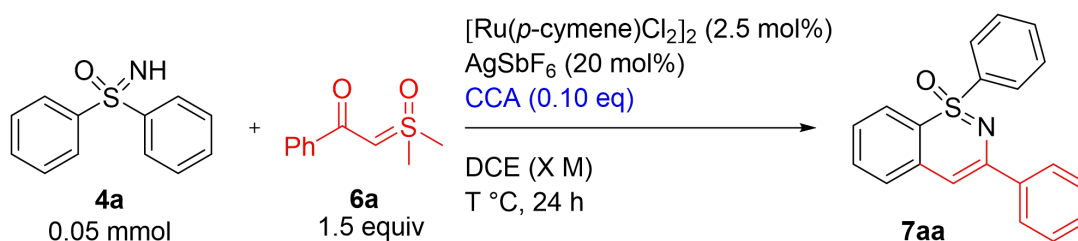
Scheme 44. Second work: Ru(II)/Chiral Carboxylic Acid-Catalyzed Enantioselective C – H Functionalization of Sulfoximines

8-1 Optimization of Reaction Condition

I initiated my investigation by optimizing the coupling of the sulfoximine **4a** and sulfoxonium ylide **6a** (**Table 8**). It afforded quantitative yield and good er. (**entry 4**) Meanwhile, reaction temperature (from 0 to 80 °C) could make a large influence on reactivity but almost no impact on enantioselectivity (**entries 1-6**). Low temperature (below 35 °C) clearly decreased the reactivity and resulted in moderate yield; In high temperature (from 35 to 80 °C), the conversion could achieve almost 100% and no two-component/rearrangement byproduct were detected. In the concentration effect, too high concentration is negative to this reaction (**entry 8**); the similar situation also happened in **entry 9** when I added more sulfoxonium ylide. These two results in entry 8 and entry 9 suggested that high concentration of

sulfoxonium ylide may inhibit the catalytic process of this reaction. Another questionable point (**Table 8, entry 10**) is the reaction time. Too prolonged reaction time led to the lower yield, which could be ascribed to the instability of desired product. (I later found that desired product **7aa** could transform into unknown compound slowly in CHCl₃.)

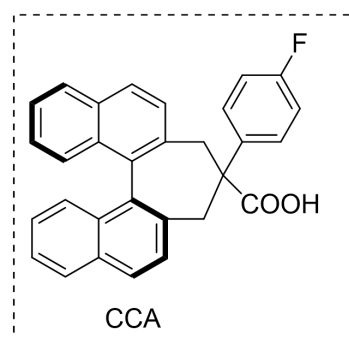
Table 8. Optimization of The Reaction Temperature and Concentration^a



Entry	T/°C	X/ M	TM% ^c	Er ^d
1	5	0.05	22	14:86
2	20	0.05	38	14:86
3	30	0.05	80	14:86
4	35	0.05	>99	14:86
5	40	0.05	>99	14:86
6	80	0.05	>99	17:83

7	35	0.10	>99	14:86
8	35	0.30	23	15:85

9 ^a	35	0.05	23	14:86
10 ^b	35	0.05	77	14:86

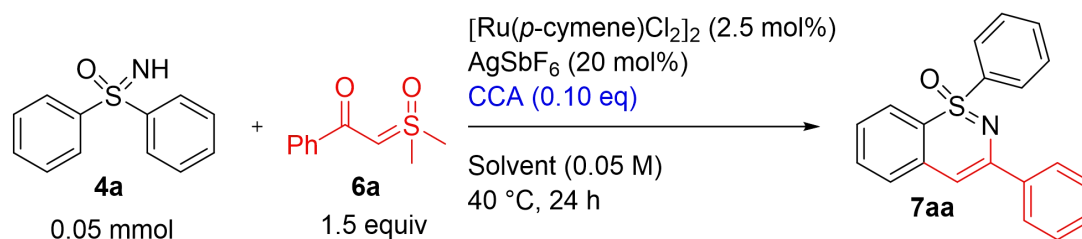


^aelectrophiles (3.0 eq), ^breaction time (48 h),

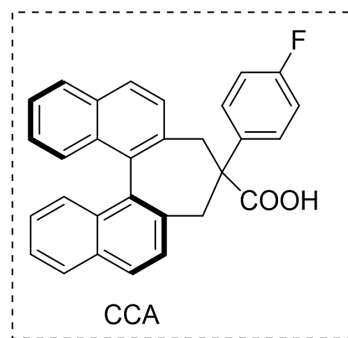
^cDetermined by ¹H NMR analysis of the crude mixture using; 1,1,2,2-tetrabromoethane as an internal standard.

^dDetermined by HPLC analysis.

In the screening of solvent, halogenated solvent afforded excellent yield and good er even though the desired product may be unstable in these solvents (**Table 9**). Among these results, CHCl₃ (**entry 2**) was selected as the best solvent, especially based on the positive impact on enantioselectivity.

Table 9. Solvent Effect^a

Entry	Solvent	TM% ^a	Er ^b
1	DCE	95	13:87
2	CHCl ₃	97	10:90
3	DCM	90	12:88
4	MeOH	88	13:87
5	HFIP	74	24:76
6	1,4-dioxane	36	17:83
7	toluene	50	13:87
8	PhCl	56	11:89
9	acetone	56	16:84
10	DMF	30	36:64
11	CH ₃ CN	17	19:81
12	NMP	N.D	–
13	hexane	N.D	–

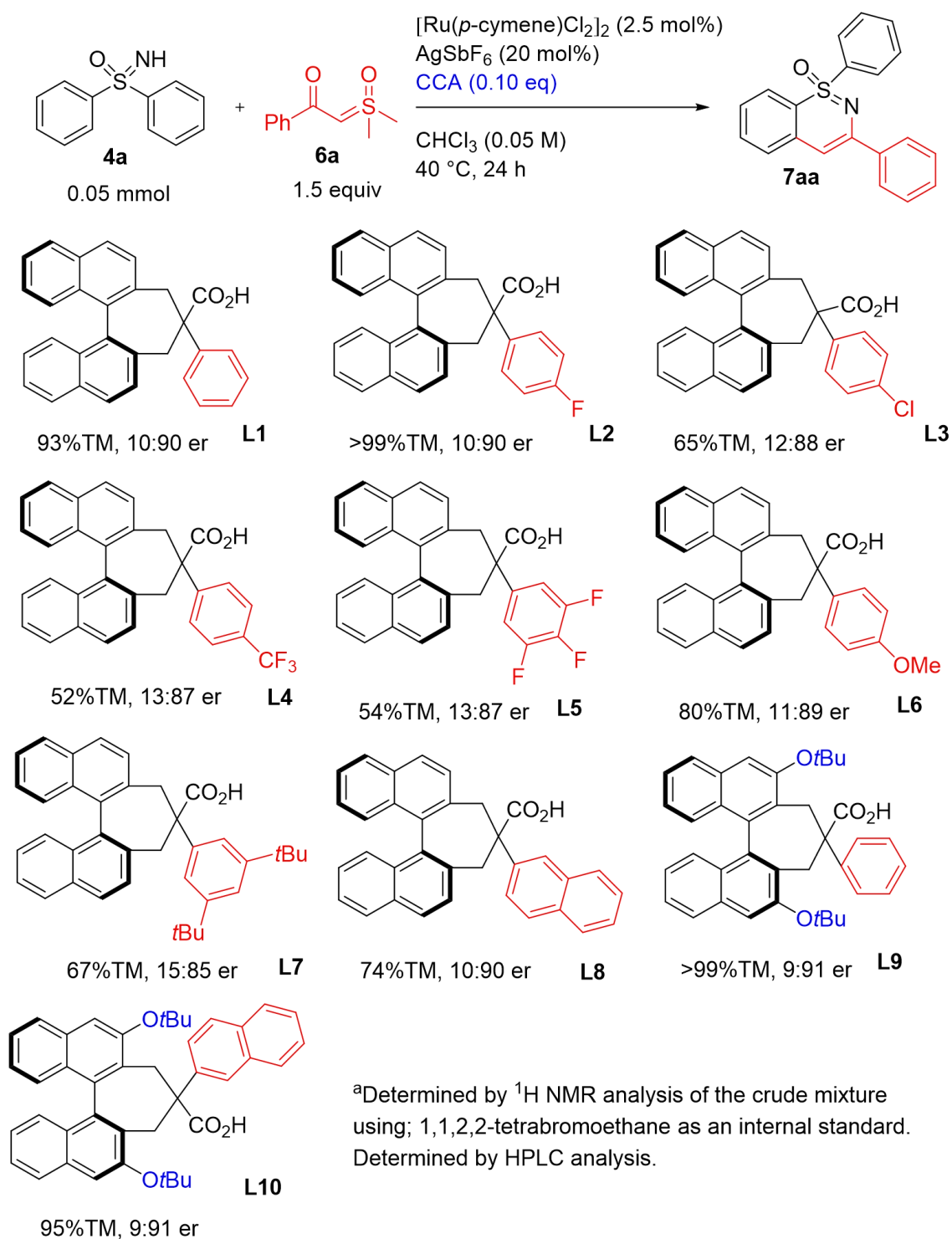


^aDetermined by ¹H NMR analysis of the crude mixture using; 1,1,2,2-tetrabromoethane as an internal standard.

^bDetermined by HPLC analysis.

8-2 Screening of CCA

After optimization studies, I started to introduce different substituent sgroup into CCA, and found L2 and L9 giving products in quant yield and good er. In addition, these results (L1/L9, L8/L10) indicated that *O*tBu group in 3 and 3' position may improve the reactivity and enantioselectivity (**Scheme 45**).

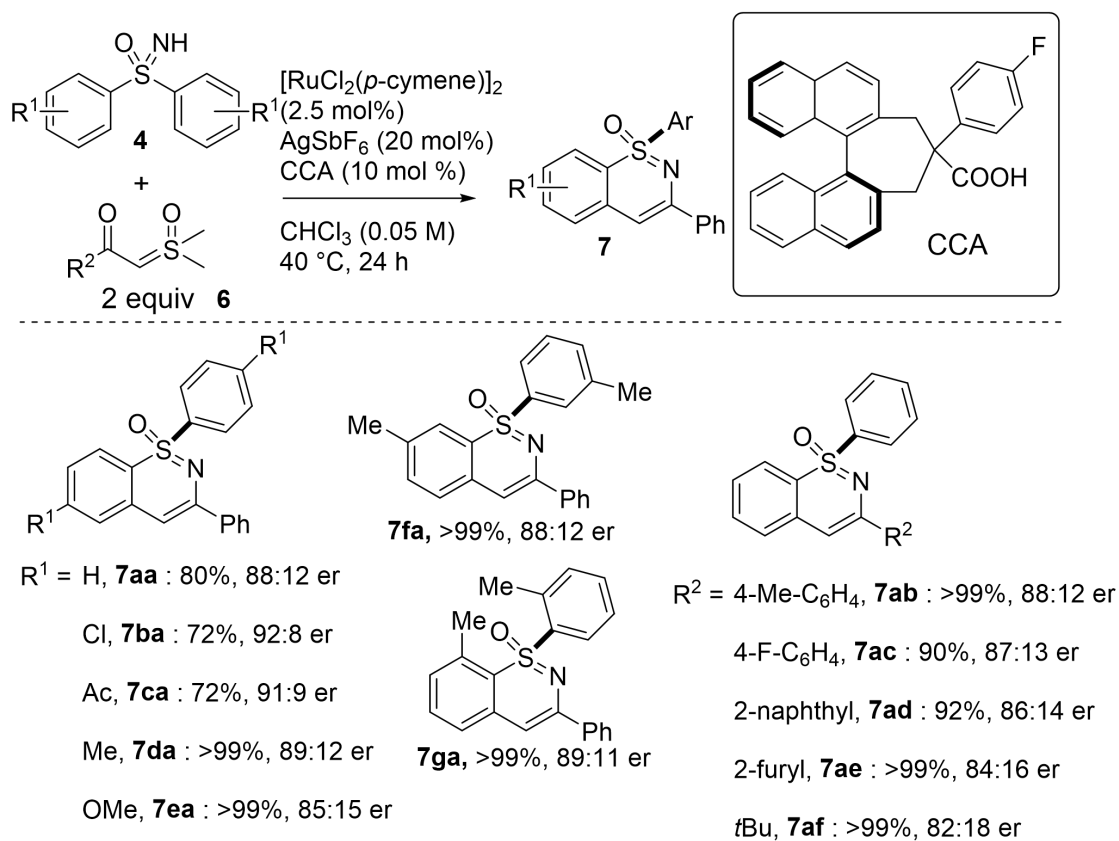


Scheme 45. Screening of CCA

8-3 Scope of Sulfoximines and Sulfoxonium Ylides

With the best conditions in hand, I next explored other various sulfoximines **4** and sulfoxonium ylides **6** (Scheme 46). Sulfoximines with *p*-, *m*-, and *o*-substituents generally provided the corresponding products in good yield and similarly good to moderate enantioselectivity (**7aa–7ga**, 85:15–91:9 er). Especially, it is

noteworthy that sulfoximines with electron withdrawing groups on the aromatic rings gave products in higher enantioselectivity (**7ba** and **7ca**) than other substrates albeit with somewhat decreased reactivity. A sterically crowded substrate with *o*-Me group (**4g**) was also applicable under the optimal reaction conditions, and product (**7ga**) was obtained in >99% yield. I then investigated several different sulfoxonium ylides **6** with **4a** as coupling partners. Aromatic-, heteroaromatic-, and aliphatic-substituted sulfoxonium ylides all were compatible under the optimized reaction conditions, thus giving desired products in high yield and moderate to good 82:18-88:12 er. The absolute configuration of product **7aa** was determined to be (S) by comparing the optical rotation ($[\alpha]_D^{24} = +10.2$ in CHCl_3) with the previously reported value for the (*R*)-enantiomer ($[\alpha]_D^{20} = -11.3$ in CHCl_3) in the literature (See, experimental section for details).



a) Scale: 0.05 mmol Yield: Determined by ^1H NMR analysis of the crude mixture using 1,1,2,2-tetrabromoethane as an internal standard.

b) Scale: 0.2 mmol Yield: isolated yield (by silic column or GPC)

er: Determined by HPLC analysis.

Scheme 46. Scope of Sulfoximines and Sulfoxonium Ylides

8-4 Proposed Mechanism

A plausible catalytic cycle is shown in **Figure 18**. An active Ru-carboxylate catalyst (A) is generated from $[\text{RuCl}_2(p\text{-cymene})]_2$, AgSbF_6 , and CCA, which would be coordinated with substrate (B). A key enantiodetermining C–H bond cleavage step would proceed via a carboxylate-assisted mechanism, in

which the chiral carboxylate base derived from CCA should selectively deprotonate one of the enantiotopic protons of sulfoximines. Then, chiral metallacycle (C) would react with sulfoxonium ylide to afford intermediate (D), while releasing DMSO. The subsequent protonation would furnish (E) and regenerate the active catalyst (A). Finally, intramolecular dehydrative condensation between the sulfoximine unit and introduced ketone provides products. While unprotected NH sulfoximines are proposed to undergo deprotonation before the C–H activation in the previous study,⁴⁹⁾ an isolated metallacycle intermediate reported by Bolm and co-workers clearly had a remaining NH proton.³⁹⁾ In addition, my catalytic system in this chapter did not involve any efficient bases, such as metal carbonates, which may facilitate the deprotonation of sulfoximines. Therefore, I suppose that the unprotected sulfoximine moiety may work as the directing group without deprotonation, although the catalytic cycle involving the deprotonation of the NH moiety cannot be excluded completely with the current data alone.

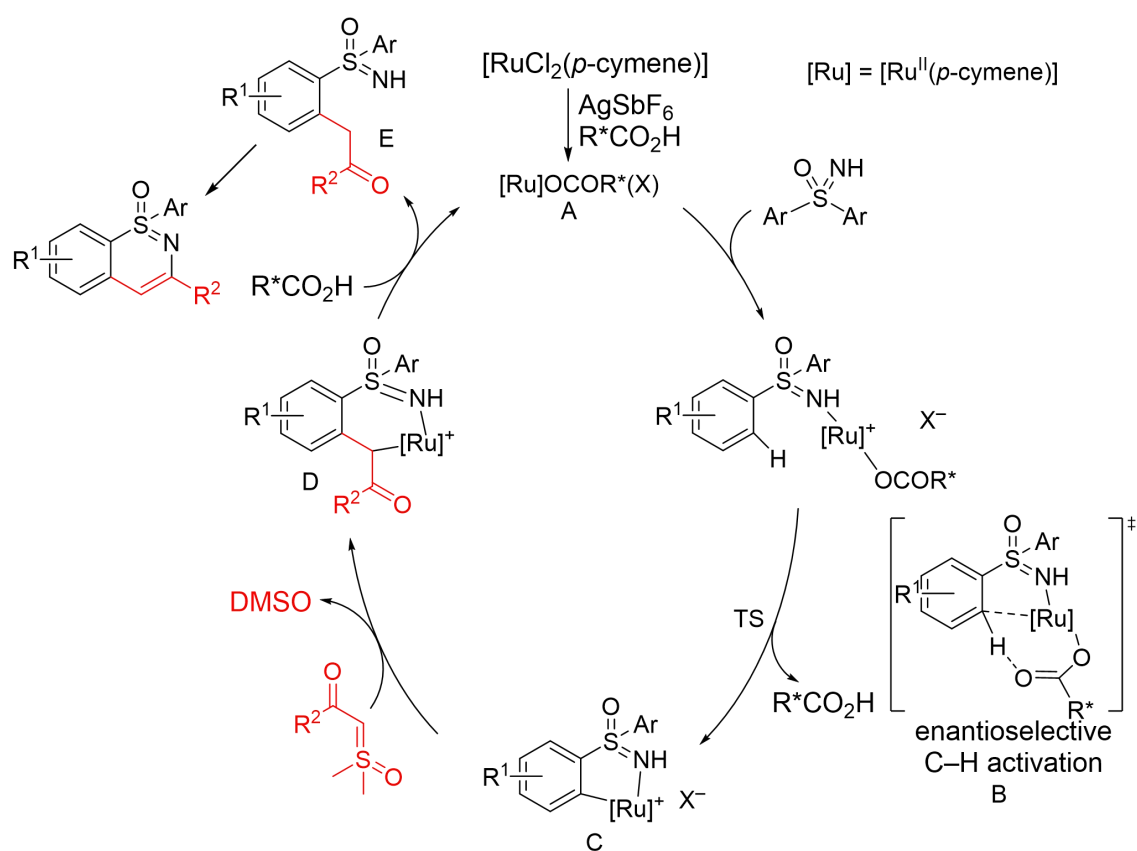


Figure 18. Proposed Mechanism

Summary

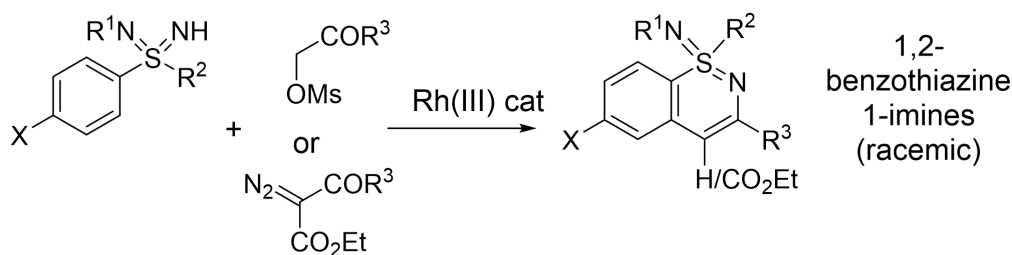
I have found that the combination of a Ru(II) catalyst and a pseudo- C_2 -symmetric binaphthyl CCA is effective and useful for enantioselective C–H functionalization of sulfoximines with sulfoxonium ylides. Although the enantioselectivities in this chapter were lower than those reported by Shi's group, I demonstrated that binaphthyl CCA in Matsunaga/Yoshino group developed originally for group 9 metals is also a suitable chiral source for Ru(II)-catalyzed C–H functionalization. Further investigation on the

combination of CCAs developed and Ru(II) catalysts are expected, and the most recent results will be discussed in next chapter, Chapter 9.

Chapter 9. Third work: Enantioselective Synthesis of 1,2-Benzothiazine 1-Imines via Ru(II)/Chiral Carboxylic Acid-Catalyzed C–H Alkylation/Cyclization⁵³⁾

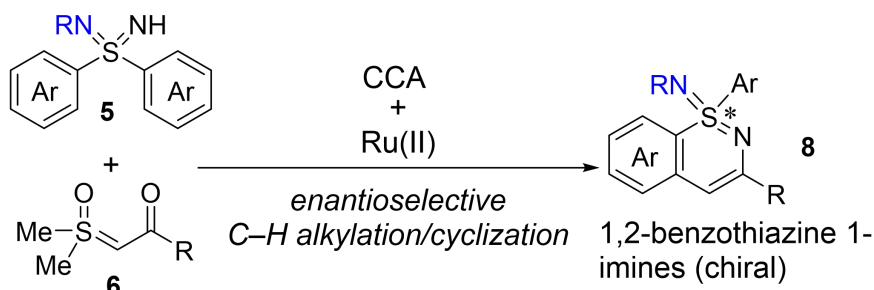
Compared to the notable advances in the synthetic chemistry of sulfoximines as described in Chapter 7 and Chapter 8, the synthesis and transformations of sulfondiimines, aza-analogues, are much less developed. The fact clearly indicates that study in the transformation of sulfondiimines should provide an unexplored promising chemical space, which will be highly useful for searching new biologically active compounds. In 2019, Bolm and co-workers reported Rh(III)-catalyzed C–H alkylation/cyclization reactions of sulfondiimines to synthesize of 1,2-benzothiazine 1-imines as unprecedented cyclic organosulfur compounds in a racemic form (Scheme 47).⁵⁰⁾ While 1,2-benzothiazine 1-imines possess S-chirality and their absolute-stereochemistry should have large influence on their biological properties, enantioselective synthesis of 1,2-benzothiazine 1-imines has not yet been reported. Thus, as the next target reaction to use Ru(II)/CCA system, I selected sulfondiimines as substrates.

First synthesis of rac-1,2-benzothiazine 1-imines by Bolm (2019)



Scheme 47. The First Synthesis of Rac-1,2-Benzothiazine 1-Imines

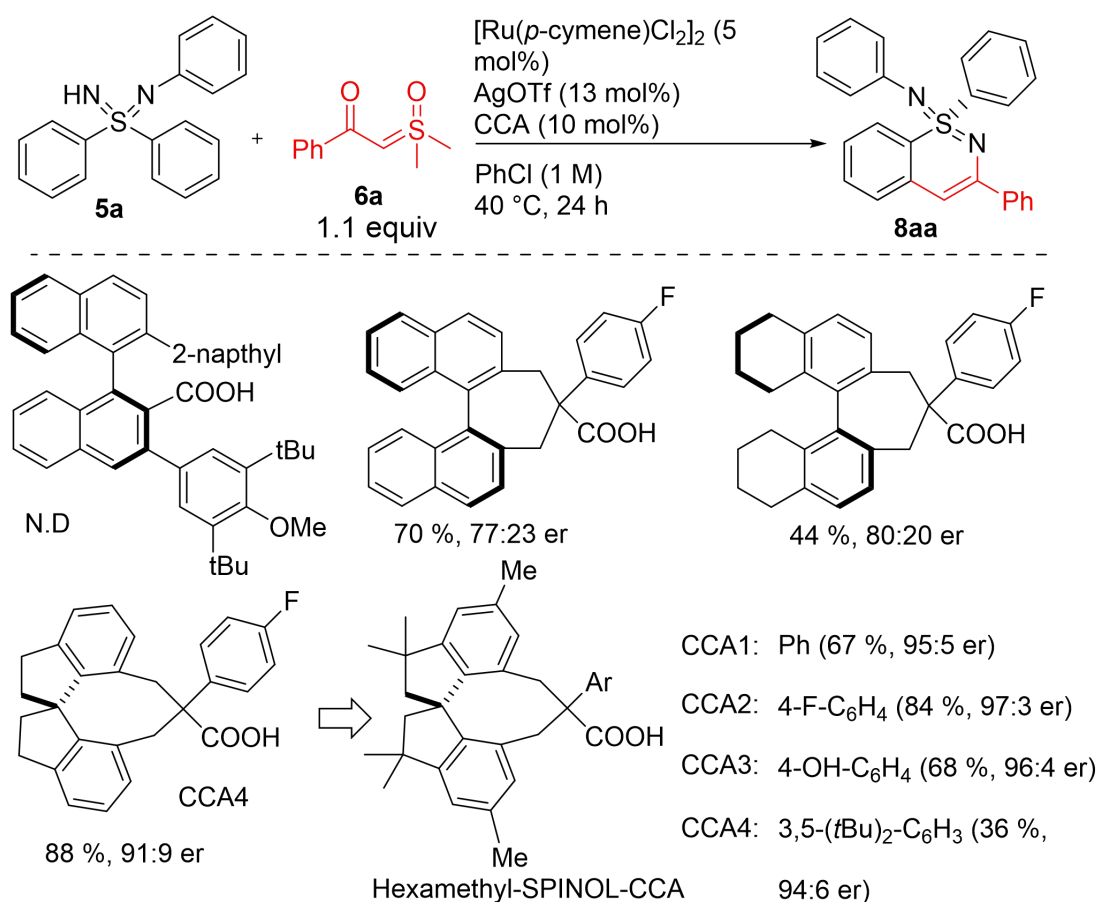
In this chapter, the enantioselective synthesis of 1,2-benzothiazine 1-imines **8** from diaryl sulfondiimines **5** and sulfoxonium ylides **6** was realized via Ru^{II}-catalyzed C–H functionalization reactions (Scheme 48).



Scheme 48. Third Work: Enantioselective Synthesis of 1,2-Benzothiazine 1-Imines via Ru(II)/Chiral Carboxylic Acid-Catalyzed C–H Alkylation/Cyclization

9-1 Screening of CCA and The Synthesis Route of New CCA

After intensive screening of the reaction conditions (**Scheme 49**), I found that the desired product was obtained in the presence of $[\text{Ru}(p\text{-cymene})\text{Cl}_2]_2$, AgOTf, and a CCA. Among the chiral acids library in Matsunaga/Yoshino group screened, the pseudo- C_2 -symmetric acids again was the most promising, and moderate enantioselectivity was observed. Despite these promising results, further improvement by minor tuning of the reaction conditions was not successful, which prompted me to develop new chiral carboxylic acids. As the chiral core structure, I selected spirochiral unit and the new CCA derived from SPINOL was investigated. The new spirochiral skeleton has much less flexibility than the binaphthyl one, thereby the spirochiral motif would lead to the construction of a much more rigid chiral environment. To my delight, the new CCA significantly improved the enantioselectivity to 91:9 er. In my further modification of spirochiral CCAs, I also tried spirochiral unit bearing hexamethyl group, which resulted in even higher er. Finally, 97:3 er was achieved with CCA bearing a 4-F-aryl unit. These results may suggest that Me in aromatic moiety would somewhat have important role for improving enantioselectivity. Possibly, the Me group is useful to adjust the position of 4-F-aryl unit and carboxylic acid unit in the enantio-determining transition state.

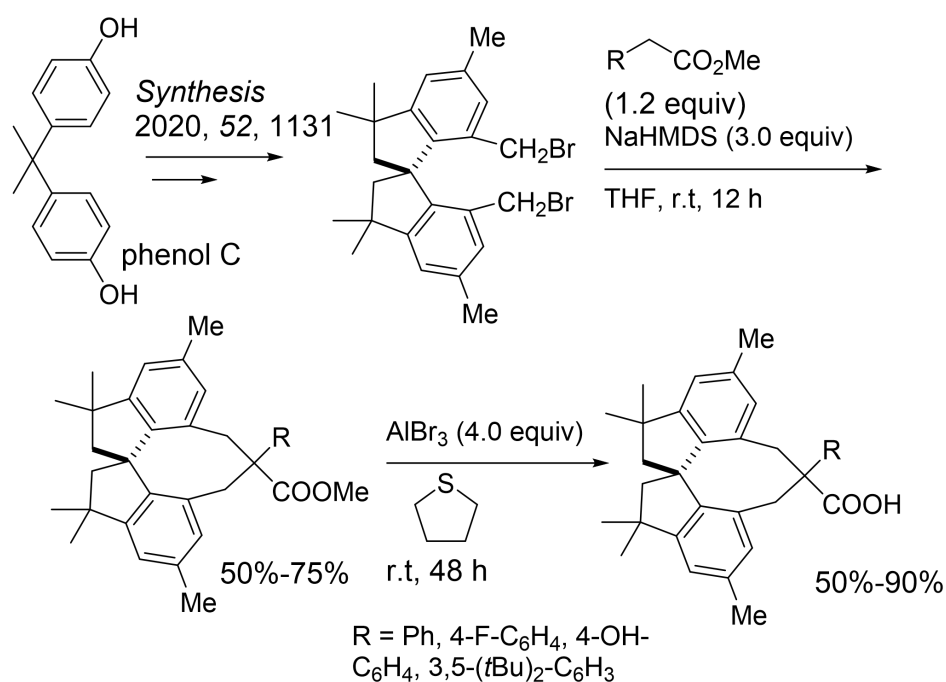


^aDetermined by ¹H NMR analysis of the crude mixture using; 1,1,2,2-tetrabromoethane as an internal standard. Determined by HPLC analysis.

Scheme 49. Screening of CCA

The synthesis of the 8-membered ring cyclic structure of the 1,1'-spirobiindane CCA was straight

forward via a double alkylation reaction of known di-Br precursor with an ester, followed by deprotection (Scheme 50).

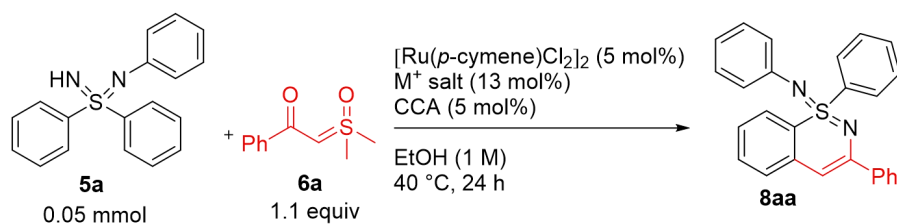


Scheme 50. The Synthesis Route of New CCA

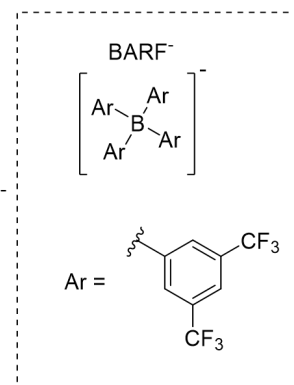
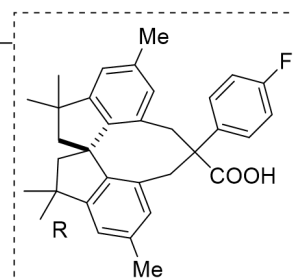
9-2 Optimization of M⁺ Salt

I also checked the influence of M⁺ salt additive on this reaction (Table 10): 1) This reaction proceeded smoothly even without M⁺ salt but resulted in somewhat lower yield. 2) M⁺ salt also has a two-direction effect on reactivity. M⁺ salt shows positive influence when used in small amount (10 mol% to 13 mol%). However, its negative effect would gradually dominate when excess M⁺ salt was used. 3) Different M⁺ salt would make different effect on the reactivity by changing the amount of M⁺ salt: Ag salt is the most affected by quantity but it still has the best reactivity; NaPF₆ is less affected when changing the ratio and has good reactivity; KPF₆ afforded low enantioselectivity in excessive amount; Zn(OTf)₂ resulted in slightly decreased enantioselectivity in small amount, and yield did not improve with increased loading. Thus, AgOTf was the best among screened. The reason may be the M⁺ could influence the balance between RCOO⁻ and ROOH by combining the RCOO⁻.

Table 10. Optimization of M⁺ Salt^a



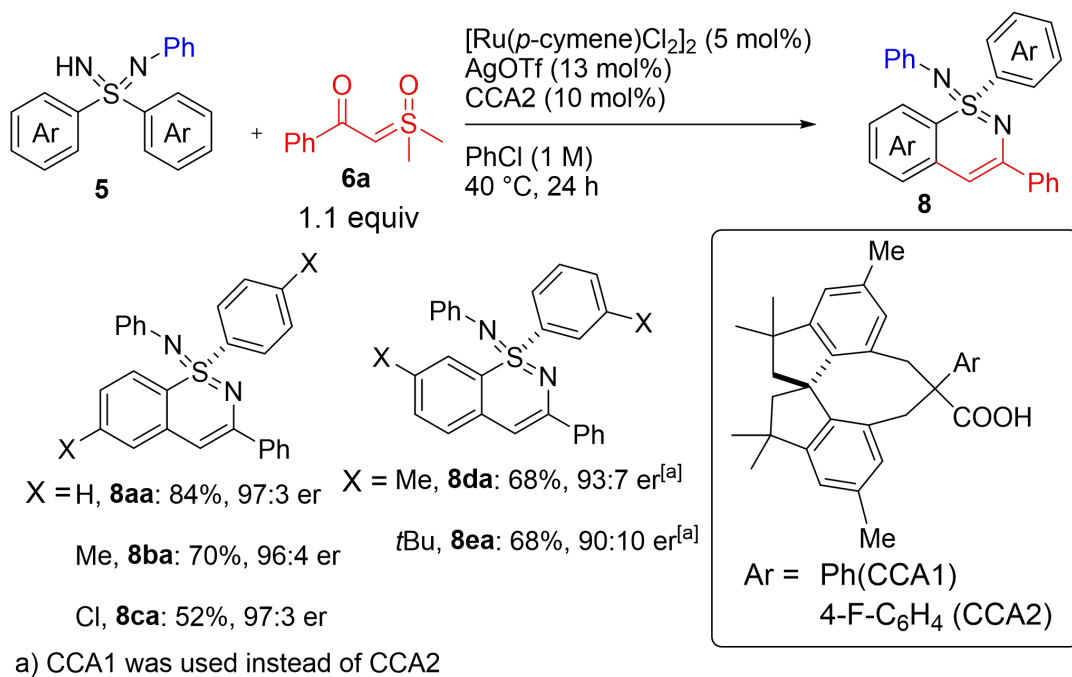
Entry	M ⁺ salt	Yield	E.r	
1	–	28%	94: 6 er	
2	AgSbF ₆	58%	96:4 er	
3	AgSbF ₆ (10 mol%)	52%		
4	AgSbF ₆ (20 mol%)	44%		
5	AgSbF ₆ (25 mol%)	26%		
6	AgPF ₆	60%		
7	AgBF ₄	62%		
8	AgNTf ₂	57%		
9	AgOTf	67%		
10	AgOTf (20 mol%)	42%		
11	NaPF ₆	66%		96:4 er
12	NaPF ₆ (20 mol%)	59%		95:5 er
13	KPF ₆	62%	96:4 er	
14	KPF ₆ (20 mol%)	62%	90:10 er	
15	NaOTf	56%	96:4 er	
16	NaBARF (20 mol%)	52%	94:6 er	
17	Zn(OTf) ₂ (20 mol%)	35%	96:4 er	
18	Zn(OTf) ₂ (10 mol%)	52%	95:5 er	
19	Zn(OTf) ₂ (6.5 mol%)	55%	94:6 er	
20	Ag ₂ CO ₃ (10 mol%)	9%	95: 5 er	



^aDetermined by ¹H NMR analysis of the crude mixture using; 1,1,2,2-tetrabromoethane as an internal standard. Determined by HPLC analysis.

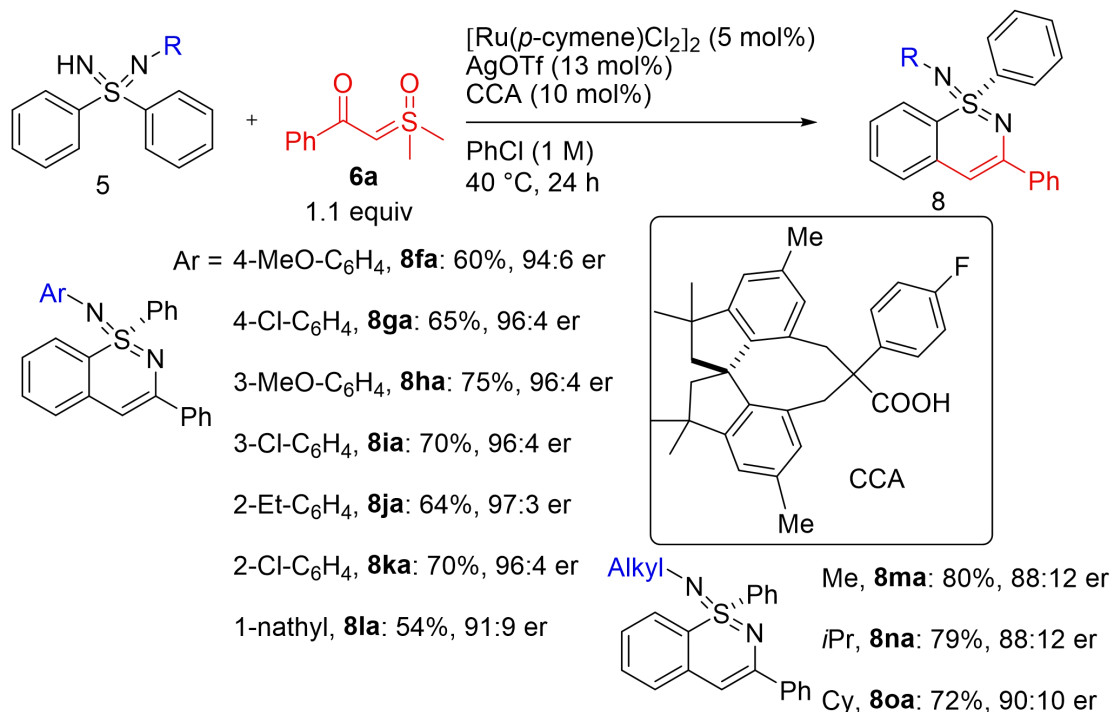
9-3 Scope of Sulfondiimines and Sulfoxonium Ylides

I then examined the scope of sulfondiimines **5** under the optimized conditions. In some cases, the use of CCA1 afforded slightly improved results. Substituents at the para and meta positions of the S-aryl groups were well tolerated to afford the product in 90:10–97:3 er (**8ba–8ea**) (Scheme 51).



Scheme 51. Scope of S-aryl substitution Sulfondiimines

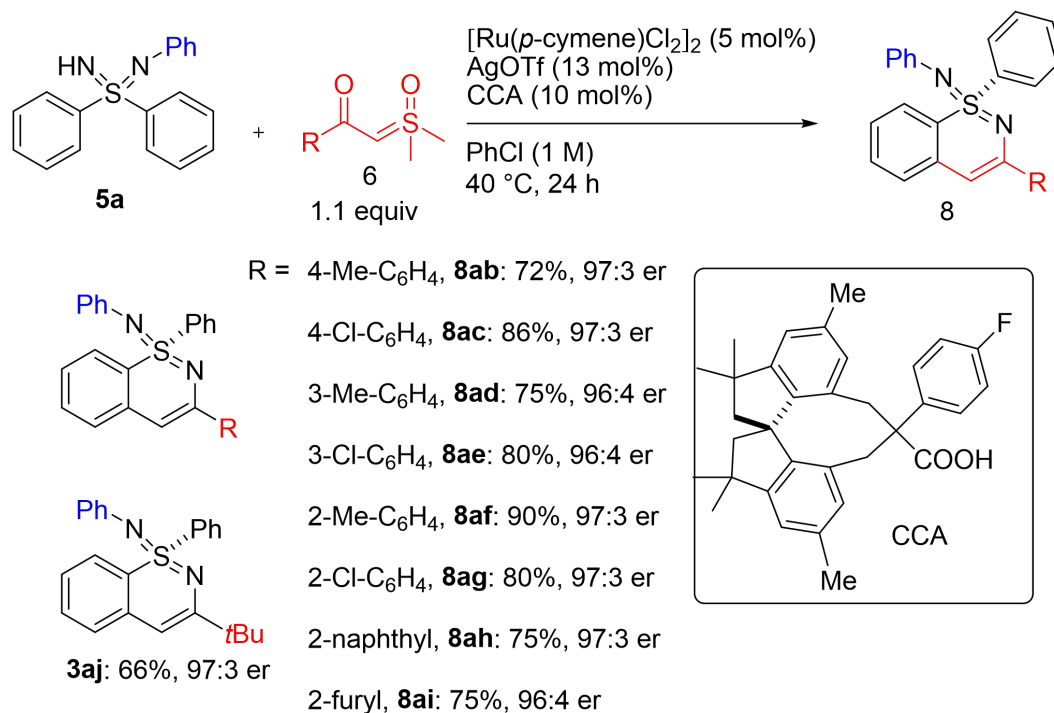
In the presence of meta-substituents, the less hindered position was selectively alkylated. As the *N*-substituent, both aryl (**8fa–8la**) and alkyl groups (**3ma–3oa**) were acceptable, although the enantioselectivity was slightly diminished for the alkyl substituent (**Scheme 52**).



Scheme 52. Scope of N-aryl/alkyl substitution Sulfondiimines

The scope of sulfoxonium ylides (**6**) was also investigated. Various substituted phenyl groups, as well as 2-naphthyl and 2-furyl groups, were successfully introduced at the 3-position of the product (**8ab–8ah**,

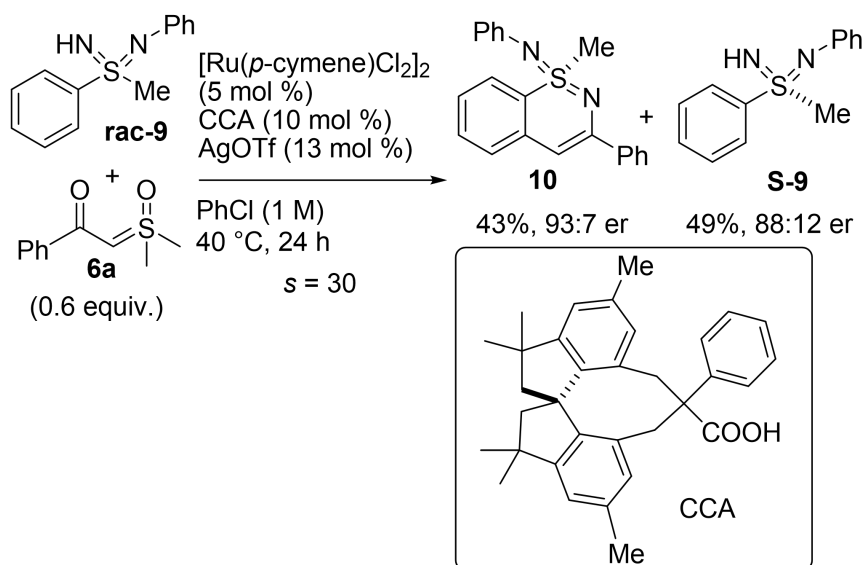
96:4–97:3 er) by employing the corresponding sulfoxonium ylides. Furthermore, *t*Bu-substituted sulfoxonium ylide also provided desired product **3aj** in excellent enantioselectivity (Scheme 53).



Scheme 53. Scope of Sulfoxonium Ylides

9-4 Kinetic Resolution of Racemic Sulfoxonium Ylide

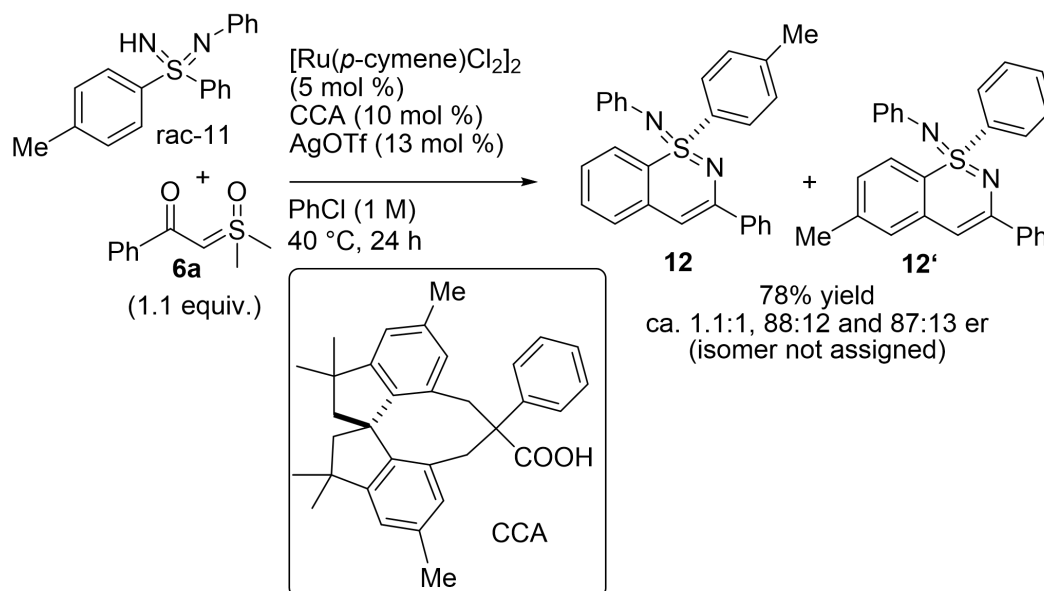
I then examined the kinetic resolution of a racemic alkyl-aryl sulfoxonium ylide, and the result is shown in Scheme 54. A reasonably good selectivity factor ($s = 30$) was observed, and product was obtained in 43% yield in 93:7 er, while recovered starting material showed 88:12 er in 49% recovery yield.



Scheme 54. Kinetic Resolution of Racemic Sulfoxonium Ylide

9-5 Parallel Kinetic Resolution

Parallel kinetic resolution of sulfondiimine bearing two different aromatic groups was also investigated as shown in **Scheme 55**. Rac-sulfondiimine with electron-donating groups (Me) on the para position gave two different products as the inseparable mixture in high yield, but in moderate ee values. The ratio of two products were nearly 1:1. The reason for the moderate enantioselectivity in this parallel kinetic resolution is not clear, but further studies to improve enantioselectivity are ongoing.

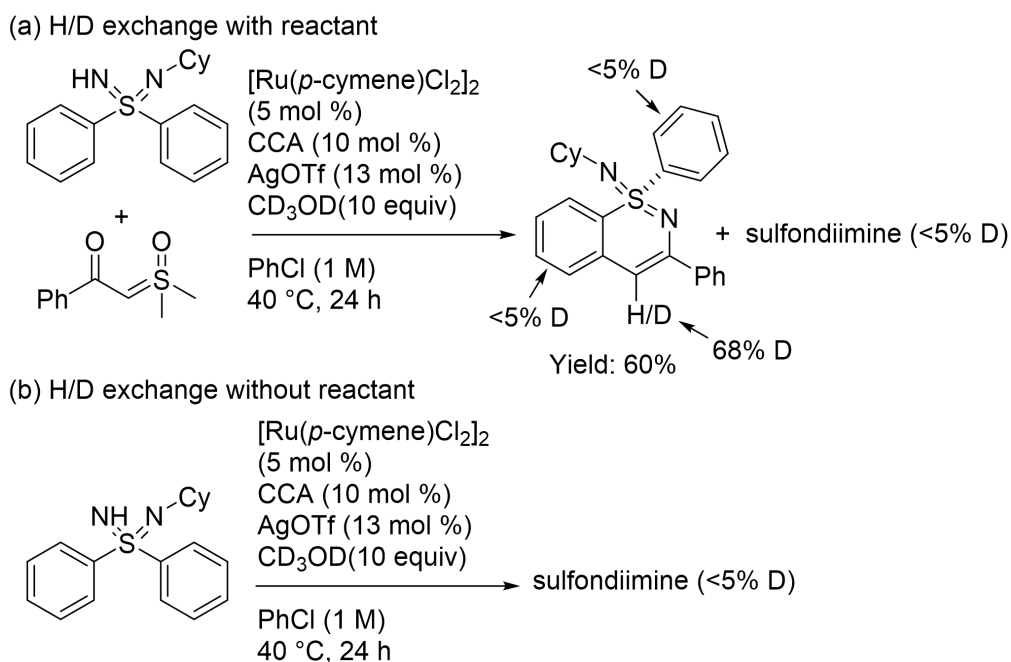


Scheme 55. Parallel Kinetic Resolution

9-6 The Experiment for Mechanism

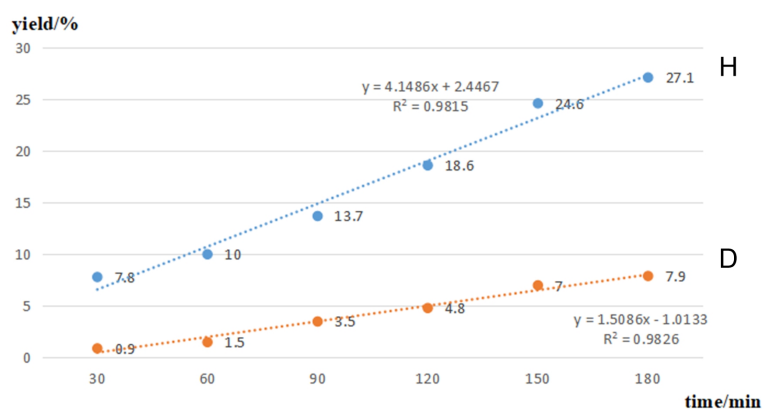
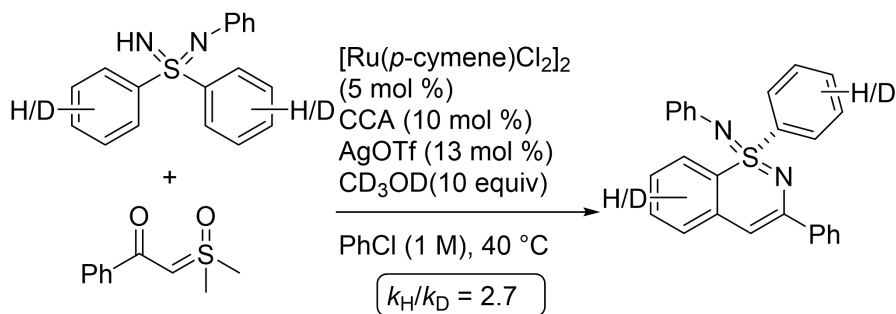
Finally, I performed several experiments to gain insight into the nature of the key enantio-determining C–H activation step. When the reaction was performed in the presence of 10 equiv of CD₃OD, deuterium incorporation was observed at the 4-position of product, but not at all at the other positions of product nor the recovered SM. The same experiment without sulfoxonium ylides also did not afford deuterium-incorporated SM (**Scheme 56**).

These results indicated that the C–H bond cleavage of SM by the Ru(II)/carboxylic acid catalyst system would be irreversible. The irreversibility may explain the independence of the enantioselectivity from the structure of starting sulfondiimines. On the other hand, the deuterium incorporation at the 4-position could be explained by the H/D exchange from reactant or the intermediate of the C–H alkylation before cyclization.



Scheme 56. H/D Exchange Experiment

I also checked the kinetic isotope effect, and a $k_{\text{H}}/k_{\text{D}} = 2.7$ was observed based on parallel two experiments (Scheme 57). The KIE experiment indicated that the C–H activation step would be involved in the rate-determining step. This is nicely in line with the experimental observation that the reactivity of this system depended on the structure of the chiral carboxylic acid. By modifying the CCAs, the reactivity changed in the optimization studies.



Scheme 57. KIE Experiment

Based on Shi's work³⁶ and my previous work (**Chapter 8**) on sulfoximine as discussed in previous chapters, I suppose that sulfondiimine basically follows a similar reaction mechanism with sulfoximine. However, the straightforward expansion to sulfondiimines is not easy, because two sterically different nitrogen atoms of sulfondiimine may work competitively as the directing group, which can potentially lead to low enantioselectivity (**Figure 19**). That is the intrinsic difficulty of enantioselective C–H bond cleavage of sulfondiimines compared with previously studied sulfoximines. At the moment, it is difficult to explain why the optimum CCA provided excellent enantioselectivity even with sulfondiimines. Preliminary DFT calculation is now ongoing by a coworker of mine, but clear explanation is still very difficult. Energy difference between two competing transition states is too small for discussion. Further intensive studies are required to understand the origin of enantioselectivity in this system.

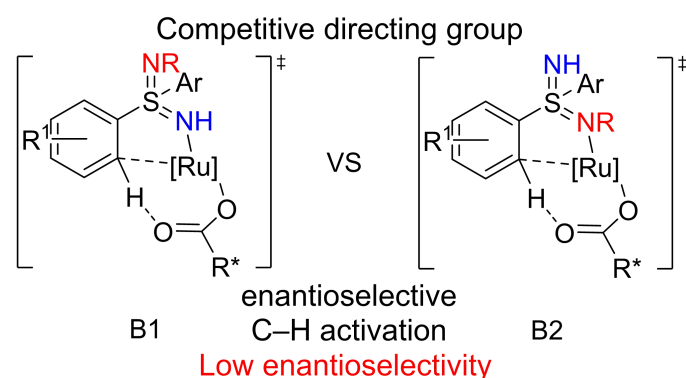


Figure 19. Competitive Directing Group

Which nitrogen works as a directing group: 1) from DFT calculation, B1 and B2 have similar energy. 2) from the structure, NH has more possibility to coordinating with Ru due to the less steric effect. However, N-alkyl and N-aryl sulfondiimine showed similar selectivity but different enantioselectivity, which may suggest that NR could play as directing group in some cases. 3) from the electron density of N atom, NR may show better or worse reactivity of directing group than NH. In a word, intermediate compound may depend on R group, B1 and B2 may exist both in my investigation.

Why are more rigid CCAs required for sulfondiimines: B1 and B2 may exist both in my reaction. Therefore, B1 and B2 may be reciprocal transformation during the reaction cycle. More rigid CCA may inhibit this transformation to afford higher selectivity.

Summary

I demonstrated that the combination of $[\text{Ru}(\text{p-cymene})\text{Cl}_2]_2$ and a newly developed chiral spiro carboxylic acid enables the enantioselective synthesis of 1,2-benzothiazine 1-imines from sulfondiimines via C–H alkylation/cyclization with a sulfoxonium ylide, thus expanding the accessible chemical space with respect to compounds with a chiral S_{V1} center. In addition, the newly developed chiral carboxylic acids based on hexamethyl-SPINOL structure will hopefully expand the applicability of the transition metal/chiral carboxylic acid catalyzed enantioselective C–H functionalization reactions.

Experimental Section

Table of contents

1. General.....	64
2. Experimental procedures: First work	
2.1. Synthesis of 8-alkylquinolines.....	65
2.2. Synthesis of enones.....	66
2.3. Rhodium(III)/chiral carboxylic acid-catalyzed enantioselective C(sp ³)-H alkylation.....	67
2.4. H/D exchange experiment.....	89
2.5. Determination of absolute configuration.....	89
3. Experimental procedures: Second work.....	92
4. Experimental procedures: Third work	
4.1. Preparation of CCA1-CCA4.....	111
4.2. Preparation of CCA5.....	116
4.3. Preparation of sulfondiimines.....	117
4.4. Ru(II)-catalyzed enantioselective C-H alkylation/cyclization.....	124
4.5. Kinetic resolution of racemic sulfondiimine.....	157
4.6. Parallel kinetic resolution of sulfondiimine.....	160
4.7. H/D exchange experiments.....	163
4.8. Kinetic isotopic effect.....	166
4.9.1 Determination of the absolute configuration.....	168
4.9.2 DFT calculation of the structures of chiral carboxylic acids.....	169
5. Reference for experimental section.....	172

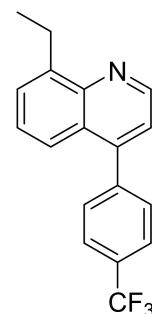
1. General

Reactions were carried out under argon atmosphere unless otherwise noted. Enantioselectivities were determined by high performance liquid chromatography (HPLC) using 4.6 nm × 25 cm Daicel Chiralpak columns. NMR spectra were recorded on JEOL JNM-ECS400 spectrometers operating at 391.78 MHz for ¹H NMR and 98.52 MHz for ¹³C NMR, JOEL JNM-ECX400 spectrometers operating at 395.88 MHz for ¹H NMR and 99.55 MHz for ¹³C NMR, and JNM-ECA500 spectrometers operating at 500.16 MHz for ¹H NMR and 125.77 MHz for ¹³C NMR. ¹H and ¹³C NMR chemical shifts are given in ppm relative to SiMe₄, with the solvent resonance used as an internal reference: CHCl₃ (7.26 ppm for ¹H NMR), CDCl₃ (77.16 ppm for ¹³C NMR), acetone-d₆ (29.84 ppm, 206.26 ppm for ¹³C NMR), methanol-d₄ (49.00 ppm for ¹³C NMR). ESI mass spectra were measured on Thermo Scientific Exactive spectrometer. Optical rotations were measured on a JASCO P-1010 polarimeter. Column chromatography was performed with silica gel Kanto Silica gel 60 N (40-50 mesh) or Yamazen YFLC AI-580 using Universal Column SiOH. Dichloromethane (CH₂Cl₂), tetrahydrofuran (THF), diethyl ether (Et₂O), and toluene were purified by Glass Contour solvent purification system before use. 1,2-Dichloroethane (DCE), N-methylprolidone (NMP), ethanol, Dimethylformamide (DMF), chloroform and acetonitrile (CH₃CN) were purchased from Kanto Chemicals (dehydrated grade) and used as received. Chlorobenzene and methanol were purchased from Aldrich (dehydrated grade) and used as received. **1a**,^[S1a] **1b-1e**, **1f**, **1h**, **1k**,^[S1b] **2b**,^[S2a] **2a**, **2c**, **2d**,^[S2b] **4a-4g**^[S3a], **6a-6f**^[S3b], **CCA**^{[S1b][S3c]} were prepared according to the literatures. All other reagents were commercially available and used as received unless otherwise noted.

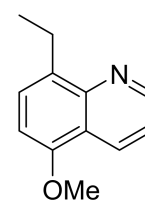
2. Experimental procedures: First Work-Cp*Rh(III)-Catalyzed Asymmetric Conjugate Addition of C(sp³)-H Bonds to α,β -Unsaturated Ketones

2.1 Synthesis of 8-alkylquinolines

4-(4-(trifluoromethyl)phenyl) 8-ethylquinoline (1g): A shield-tube was charged with 4-bromo-8-ethylquinoline **1c** (200 mg, 0.85 mmol), EtOH (1 mL), water (2 mL), toluene (4 mL), 4-(trifluoromethyl)phenyl boronic acid (243 mg, 1.28 mmol), K₂CO₃ (470 mg, 3.40 mmol, 4.0 equiv.), PPh₃ (34 mg, 0.13 mmol, 15 mol%), and Pd(OAc)₂ (10 mg, 0.43 mmol, 5 mol%). The reaction mixture was heated at 100 °C for 19 h. After cooling to room temperature, the biphasic solution was diluted with saturated NH₄Cl aq. and CH₂Cl₂. The aqueous layer was extracted with CH₂Cl₂ (x 3). The combined organic layers were dried over Na₂SO₄ and filtered. The filtrate was concentrated in vacuo and purified by silica gel column chromatography to afford **1g** as a colorless solid (240 mg, 93%). **IR** (KBr) 2960, 2936, 1589, 1562, 1502, 1413, 1322, 1282, 1126, 1108, 1072, 1022, 840, 711 cm⁻¹. **¹H NMR** (CDCl₃, 400 MHz) δ 1.43 (t, J = 7.5 Hz, 3H), 3.37 (q, J = 7.4 Hz, 2H), 7.32 (d, J = 3.2 Hz, 1H), 7.45 (t, J = 7.7 Hz, 1H), 7.60-7.65 (m, 4H), 7.79 (d, J = 8.2 Hz, 2H), 9.00 (d, J = 2.7 Hz, 1H). **¹³C NMR** (CDCl₃, 100 MHz) δ 15.1, 25.0, 121.0, 123.3, 124.1 (q, $^1J_{CF}$ = 272.2 Hz), 125.4 (q, $^3J_{CF}$ = 3.8 Hz), 126.3, 126.8, 128.1, 129.6, 129.9, 130.4 (q, $^2J_{CF}$ = 33.8 Hz), 142.2, 143.4, 147.0, 147.1, 148.6. **¹⁹F NMR** (CDCl₃, 470 MHz) δ -62.8. **HRMS** (ESI): m/z calculated for C₁₈H₁₅NF⁺ [M+H]⁺: 302.1152, found: 302.1152. **Rf** 0.75 (hexane/AcOEt = 2:1).

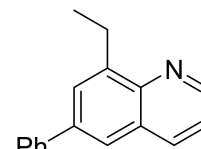


5-methoxy-8-ethylquinoline (1i): A shield-tube was charged with 5-bromo-8-ethylquinoline **1h** (55 mg, 0.22 mmol), DMF (0.6 mL), MeOH (1.5 mL), sodium methoxide (138 mg, 0.22 mmol), and CuBr (18 mg, 0.11 mmol, 0.5 equiv.). The reaction mixture was heated at 90 °C for 16 h. After cooling to room temperature, the solution was diluted with H₂O. The aqueous layer was extracted with ether (x 3). The combined organic layers were dried over Na₂SO₄ and filtered. The filtrate was concentrated in vacuo and purified by silica gel column chromatography to afford **1i** as a yellow oil (25 mg, 60%). **IR** (neat) 2961, 2933, 1615, 1591, 1473, 1402, 1369, 1268, 1206, 1158, 1090, 819, 792 cm⁻¹. **¹H NMR** (CDCl₃, 500 MHz) δ 1.36 (t, J = 7.4 Hz, 3H), 3.21 (q, J = 7.6 Hz, 2H), 3.97 (s, 3H), 6.78 (d, J = 8.0 Hz, 1H), 7.36 (dd, J = 8.6, 4.0 Hz, 1H), 7.44 (d, J = 7.4 Hz, 1H), 8.57 (dd, J = 8.3, 2.0 Hz, 1H), 8.93 (dd, J = 4.3, 2.0 Hz, 1H). **¹³C NMR** (CDCl₃, 100 MHz) δ 15.1,



24.1, 55.5, 103.9, 119.8, 120.8, 127.3, 130.8, 134.4, 147.0, 149.4, 153.3. **HRMS** (ESI): m/z calculated for $C_{13}H_{14}NO^+$ $[M+H]^+$: 188.1070, found: 188.1070. **Rf** 0.70 (hexane/AcOEt = 2:1).

6-phenyl-8-ethylquinoline (11): A shield-tube was charged with 6-bromo-8-ethylquinoline **1j** (200 mg, 0.85 mmol), EtOH (1 mL), water (2 mL), toluene (4 mL), phenyl boronic acid (160 mg, 1.28 mmol), K_2CO_3 (470 mg, 3.40 mmol, 4.0 equiv.), PPh_3 (34 mg, 0.13 mmol, 15 mol%), and $Pd(OAc)_2$ (10 mg, 0.43 mmol, 5 mol%). The reaction mixture was heated at 100 °C for 24 h. After cooling to room temperature, the biphasic solution was diluted with saturated NH_4Cl aq. and CH_2Cl_2 . The aqueous layer was extracted with CH_2Cl_2 (x 3). The combined organic layers were dried over Na_2SO_4 and filtered. The filtrate was concentrated in vacuo and purified by silica gel column chromatography to afford **11** as a colorless solid (210 mg, 90%). **IR** (KBr) 2960, 2936, 1590, 1489, 1439, 1377, 881, 793, 764, 699 cm^{-1} . **1H NMR** ($CDCl_3$, 400 MHz) δ 1.44 (d, $J = 7.4$ Hz, 3H), 3.37 (q, $J = 7.5$ Hz, 2H), 7.36-7.40 (m, 2H), 7.46-7.49 (m, 2H), 7.71 (d, $J = 6.3$ Hz, 2H), 7.82 (d, $J = 7.2$ Hz, 2H), 8.14 (d, $J = 8.5$ Hz, 1H), 8.92 (dd, $J = 3.6, 1.8$ Hz, 1H). **^{13}C NMR** ($CDCl_3$, 100 MHz) δ 15.0, 24.7, 121.1, 123.4, 127.3, 127.5, 127.7, 128.5, 128.8, 136.5, 138.9, 140.6, 143.2, 146.0, 149.1. **HRMS** (ESI): m/z calculated for $C_{17}H_{16}N^+$ $[M+H]^+$: 234.1278, found: 234.1281. **Rf** 0.68 (hexane/AcOEt = 2:1).



2.2 Synthesis of enones

Enones **2a**, **2c**, and **2d** were prepared according to the literature.^[S2b] Vinyl magnesium bromide (1 equiv., 1 M in THF) was added to the corresponding aldehyde in THF (0.2 M) at 0 °C. After 15 min, the reaction mixture was allowed to warm up to room temperature and stirred for 3 h. The reaction was quenched by the addition of saturated NH_4Cl aq. and extracted with ether. The organic layer was washed with brine, dried over magnesium sulfate and filtered. The solvent was removed under reduced pressure to provide the corresponding allylic alcohol. To a solution of the allylic alcohol (1.0 equiv.) in CH_2Cl_2 (100 mg/mL) were added iodobenzene diacetate (BAIB, 1.1 equiv.) and (2,2,6,6-tetramethylpiperidin-1-yl) oxidanyl (0.1 equiv.). The mixture was stirred at room temperature for 3 h. The reaction was quenched by saturated $Na_2S_2O_3$ aq. The aqueous layer was extracted twice with CH_2Cl_2 . The combined organic layers were washed with saturated $NaHCO_3$ aq. and brine, dried over magnesium sulfate, filtered and the solvent was removed. Purification by silica gel column chromatography afforded the corresponding vinyl ketone.

2.3 Rhodium(III)/chiral carboxylic acid-catalyzed enantioselective C(sp³)-H alkylation.

General Procedure A [GP-A]

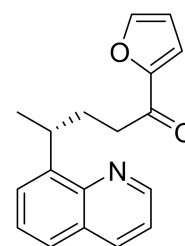
In an argon-filled glovebox, a screw-capped test tube was charged with 8-ethylquinoline **1** (0.20 mmol, 1.0 equiv), enone **2** (0.40 mmol, 2.0 equiv), chiral carboxylic acid (10.4 mg, 0.016 mmol, 8 mol %), [Cp*RhCl₂]₂ (4.9 mg, 0.008 mmol, 4 mol %), AgPF₆ (8.0 mg, 0.032 mmol, 16 mol %), and Ag₂CO₃ (15.4 mg, 0.056 mmol, 28 mol %). Chlorobenzene (2 mL) was added. The test tube was capped and brought out of the glovebox. The reaction mixture was heated to 30 °C. After stirring at the same temperature for 24 h, the reaction mixture was directly purified by silica gel column chromatography (hexane/AcOEt) to afford **3**.

General Procedure B [GP-B]

In an argon-filled glovebox, a screw-capped test tube was charged with 8-ethylquinoline **1** (0.200 mmol, 1.0 equiv), enone **2** (0.600 mmol, 3.0 equiv), chiral carboxylic acid (10.4 mg, 0.016 mmol, 8 mol %), [Cp*RhCl₂]₂ (4.9 mg, 0.008 mmol, 4 mol %), AgPF₆ (8.0 mg, 0.032 mmol, 16 mol %), and Ag₂CO₃ (15.4 mg, 0.056 mmol, 28 mol %). , and then chlorobenzene (2 mL) was added The test tube was capped and brought out of the glovebox. The reaction mixture was heated to 5 °C. After stirring at the same temperature for 48 h, the reaction mixture was directly purified by silica gel column chromatography (hexane/AcOEt) to afford **3**.

(R)-1-(furan-2-yl)-4-(quinolin-8-yl)pentan-1-one (3ab): Prepared according to **GP-A**

using 8-ethylquinoline **1a** (0.20 mmol, 31.4 mg) and 2-furyl vinyl ketone **2b** (0.40 mmol, 48.0 mg). **3ab** was isolated as a yellow oil (45.0 mg, 80%). **IR** (neat) 2961, 1674, 1567, 1497, 1468, 1393, 1013, 1013, 797 cm⁻¹. **¹H NMR** (CDCl₃, 400 MHz) δ 1.43 (d, *J* = 6.8 Hz, 3H), 2.21(q, *J* = 7.7 Hz, 2H), 2.63-2.75 (m, 1H), 2.81-2.92 (m, 1H), 4.42-4.31 (m,

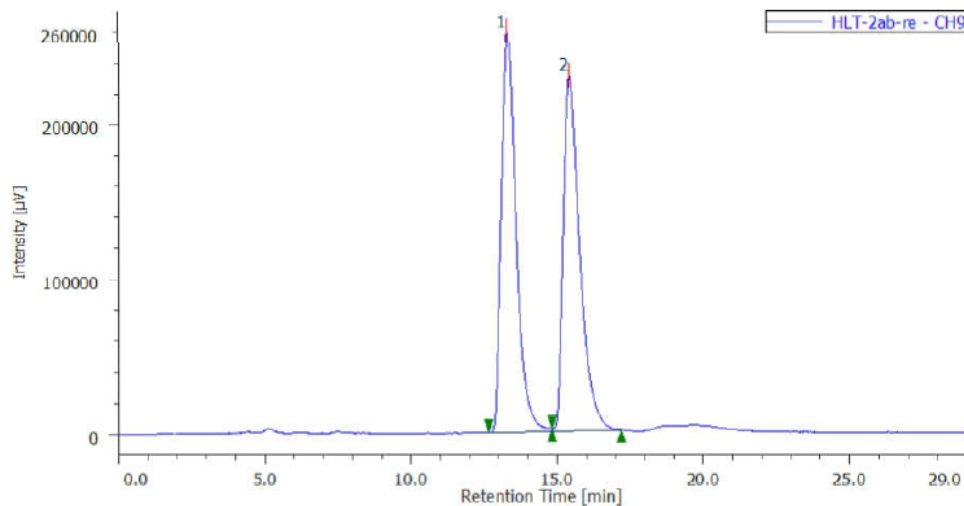


1H), 6.64 (dd, *J* = 3.4, 1.6 Hz, 1H), 7.01 (d, *J* = 3.6, 1H), 7.40 (dd, *J* = 7.9, 3.9 Hz, 1H), 7.48 (s, 1H), 7.54 (t, *J* = 7.5 Hz, 1H), 7.66 (dd, *J* = 15.4, 7.7 Hz, 2H), 8.16 (d, *J* = 8.2 Hz, 1H), 8.90 (d, *J* = 4.1 Hz, 1H).

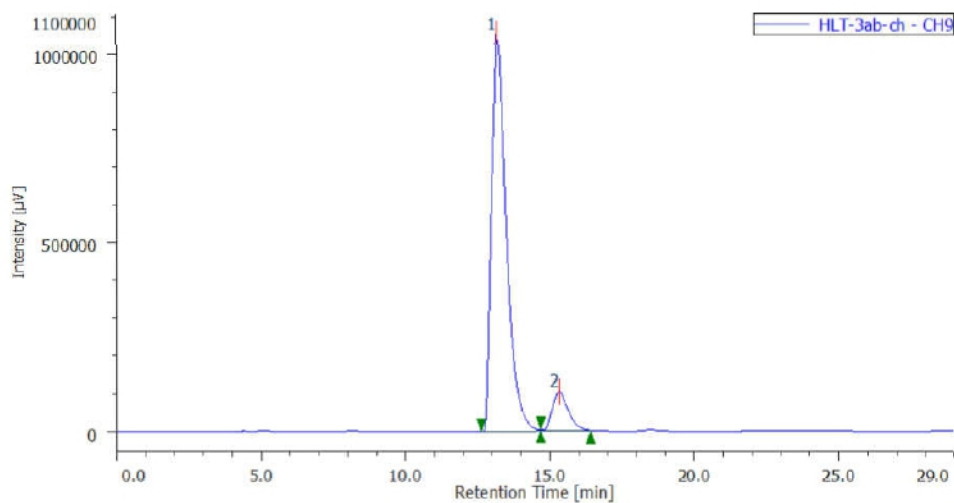
¹³C NMR (CDCl₃, 125 MHz) δ 21.9, 31.7, 31.9, 36.8, 111.9, 116.6, 122.7, 125.8, 125.9, 126.4, 128.2, 136.3, 145.0, 145.9, 146.2, 149.0, 152.5, 189.6. **HPLC** (chiral column: DAICEL CHIRALPAK IA; solvent: hexane/2-propanol = 49/1; flow rate: 1.0 mL/min; detection: at 285 nm): *t*_R = 13.2 min (major) and 15.3

min (minor). **HRMS** (ESI): m/z calculated for $C_{18}H_{17}O_2NNa^+$ $[M+Na]^+$: 302.1152, found: 302.1150.

$[\alpha]_D^{22.5} = +43.5$ ($c = 0.50$, $CHCl_3$). **Rf** 0.38 (hexane/AcOEt = 2:1).

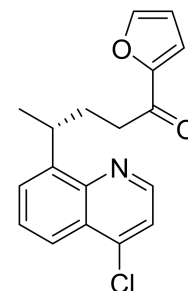


#	ピーク名	CH	tR [min]	面積%
1	Unknown	9	13.313	50.344
2	Unknown	9	15.410	49.656

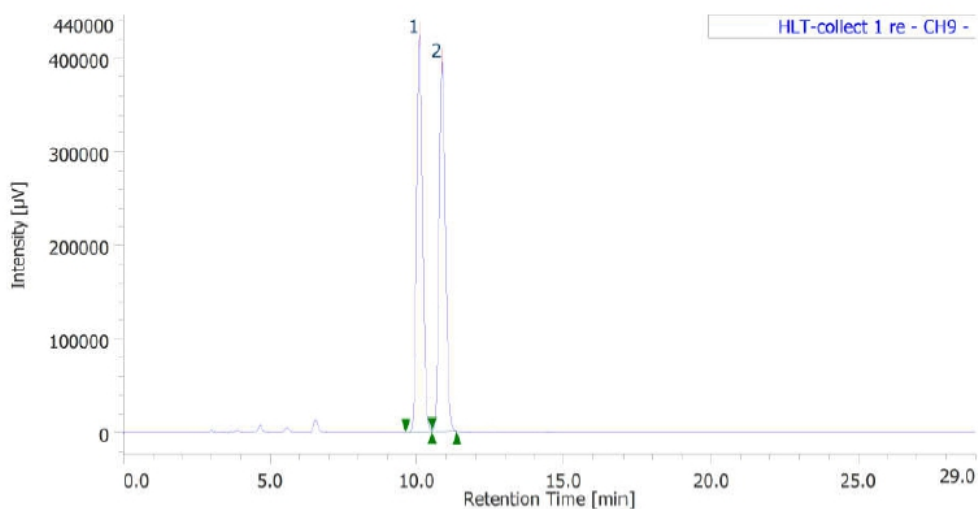


#	ピーク名	CH	tR [min]	面積%
1	Unknown	9	13.183	90.404
2	Unknown	9	15.313	9.596

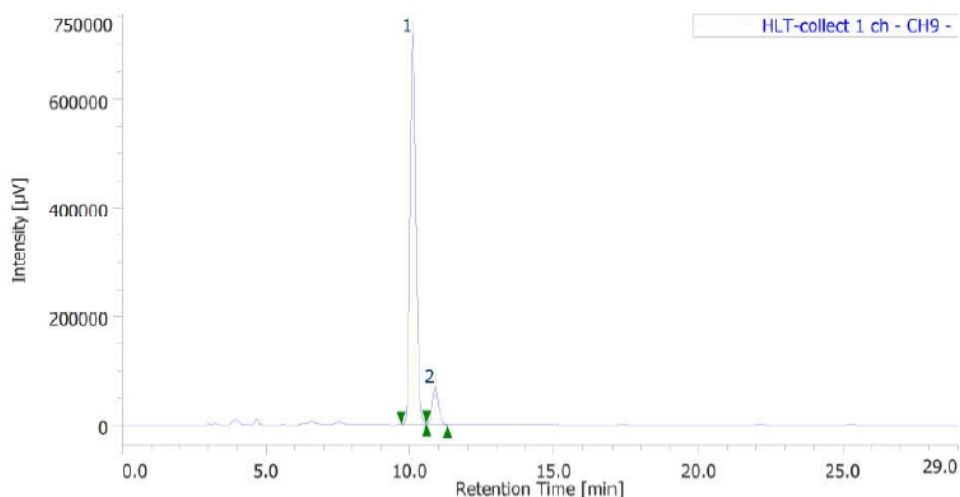
(R)-4-(4-chloroquinolin-8-yl)-1-(furan-2-yl)pentan-1-one (3bb): Prepared according to GP-A using 4-chloro-8-ethylquinoline **1b** (0.20 mmol, 38.2 mg) and 2-furyl vinyl ketone **2b** (0.40 mmol, 48.0 mg). **3bb** was isolated as a yellow oil (52.0 mg, 83%). **IR** (neat) 2961, 1674, 1585, 1567, 1488, 1468, 1390, 1013, 764 cm^{-1} . **1H NMR** ($CDCl_3$, 500 MHz) δ 1.41 (d, $J = 6.9$ Hz, 3H), 2.20 (q, $J = 7.6$, 2H), 2.63-2.69 (m, 1H), 2.78-2.89



(m, 1H), 4.31-4.40 (m, 1H), 6.63 (dd, $J = 3.4, 1.1$ Hz, 1H), 7.01 (d, $J = 3.4$, 1H), 7.46-7.49 (m, 2H), 7.63 (t, $J = 7.7$ Hz, 1H), 7.69 (d, $J = 6.3$ Hz, 1H), 8.12 (d, $J = 8.6$ Hz, 1H), 8.73 (d, $J = 4.6$ Hz, 1H). ^{13}C NMR (acetone- d_6 , 125 MHz) δ 22.0, 32.4, 32.8, 37.1, 112.7, 117.2, 122.0, 122.5, 126.9, 128.0, 128.6, 142.8, 146.8, 147.2, 148.1, 149.6, 153.6, 188.9. **HPLC** (chiral column: DAICEL CHIRALPAK IG; solvent: hexane/2-propanol = 9/1; flow rate: 1.0 mL/min; detection: at 285 nm): $t_R = 10.1$ min (major) and 10.8 min (minor). **HRMS** (ESI): m/z calculated for $\text{C}_{18}\text{H}_{16}\text{O}_2\text{NClNa}^+ [\text{M}+\text{Na}]^+$: 336.0762, found: 336.0760. $[\alpha]_D^{20.1} = +22.3$ ($c = 0.50$, CHCl_3). **Rf** 0.53 (hexane/AcOEt = 2:1).



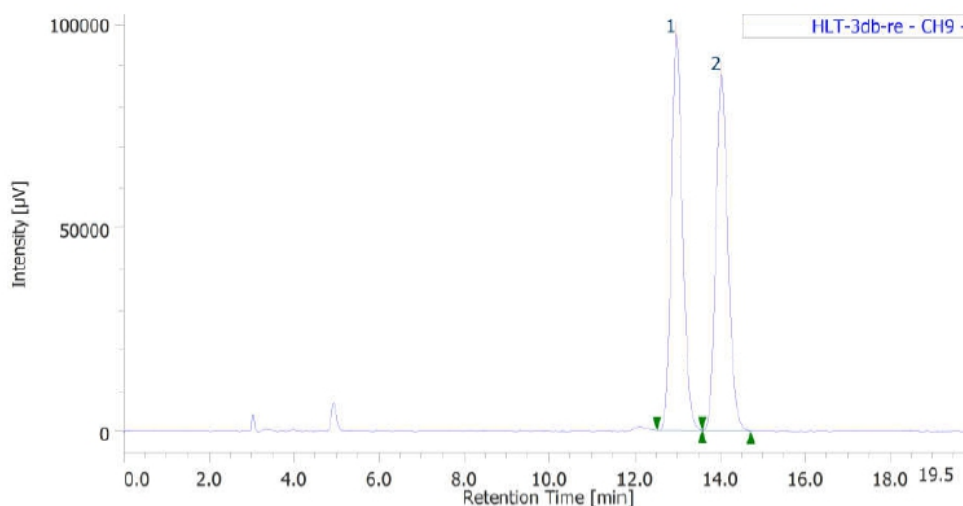
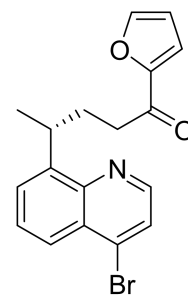
#	ピーク名	CH	tR [min]	面積%	警告
1	Unknown	9	10.090	49.980	
2	Unknown	9	10.860	50.020	



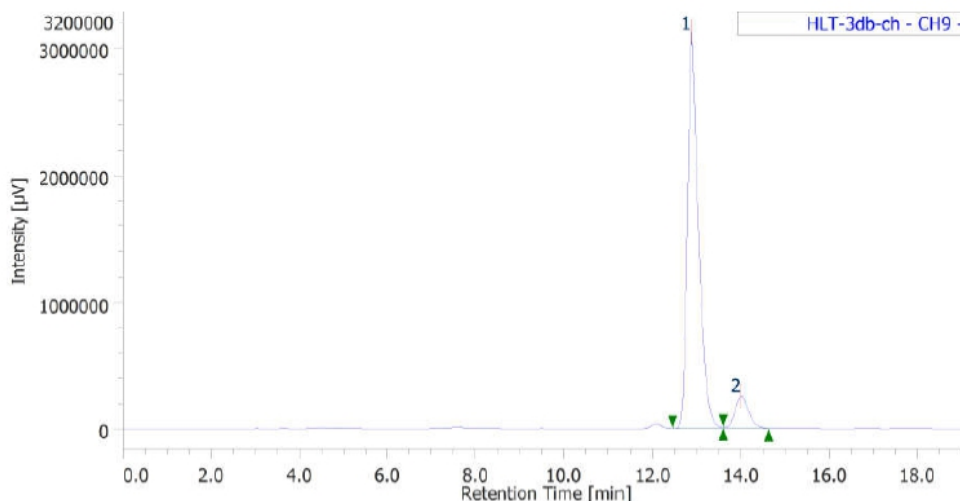
#	ピーク名	CH	tR [min]	面積%	警告
1	Unknown	9	10.100	90.405	
2	Unknown	9	10.883	9.595	

(R)-4-(4-bromoquinolin-8-yl)-1-(furan-2-yl)pentan-1-one (3cb) : Prepared according to **GP-A** using

4-bromo-8-ethylquinoline **1c** (0.20 mmol, 47.0 mg) and 2-furyl vinyl ketone **2b** (0.40 mmol, 48.0 mg). **3cb** was isolated as a yellow oil (59.0 mg, 83%). **IR** (neat) 2961, 1674, 1566, 1482, 1467, 1387, 761 cm^{-1} . **^1H NMR** (CDCl_3 , 500 MHz) δ 1.41 (d, $J = 6.9$ Hz, 3H), 2.20 (dd, $J = 14.9, 7.4$ Hz, 2H), 2.61-2.70 (m, 1H), 2.79-2.87 (m, 1H), 4.31-4.40 (m, 1H), 6.42 (dd, $J = 3.4, 1.7$ Hz, 1H), 7.00 (d, $J = 3.4$ Hz, 1H), 7.46 (d, $J = 1.1$ Hz, 1H), 7.61 (t, $J = 7.7$ Hz, 3H), 7.68-7.66 (m, 3H), 8.06 (dd, $J = 8.3, 1.4$ Hz, 1H), 8.61 (d, $J = 4.6$ Hz, 1H). **^{13}C NMR** (acetone- d_6 , 125 MHz) δ 22.0, 32.4, 32.8, 37.1, 112.7, 117.2, 125.2, 125.9, 128.0, 128.3, 128.8, 134.4, 146.8, 147.2, 147.9, 149.6, 153.5, 188.9. **HPLC** (chiral column: DAICEL CHIRALPAK IG; solvent: hexane/2-propanol = 93/7; flow rate: 1.0 mL/min; detection: at 285 nm): $t_R = 12.8$ min (major) and 14.0 min (minor). **HRMS** (ESI): m/z calculated for $\text{C}_{18}\text{H}_{16}\text{O}_2\text{NBrNa}^+$ [$\text{M}+\text{Na}$] $^+$: 380.0257, found: 380.0256. $[\alpha]_D^{22.8} = +13.2$ ($c = 0.50$, CHCl_3). **Rf** 0.50 (hexane/AcOEt = 2:1).

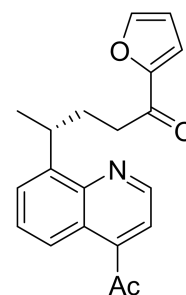


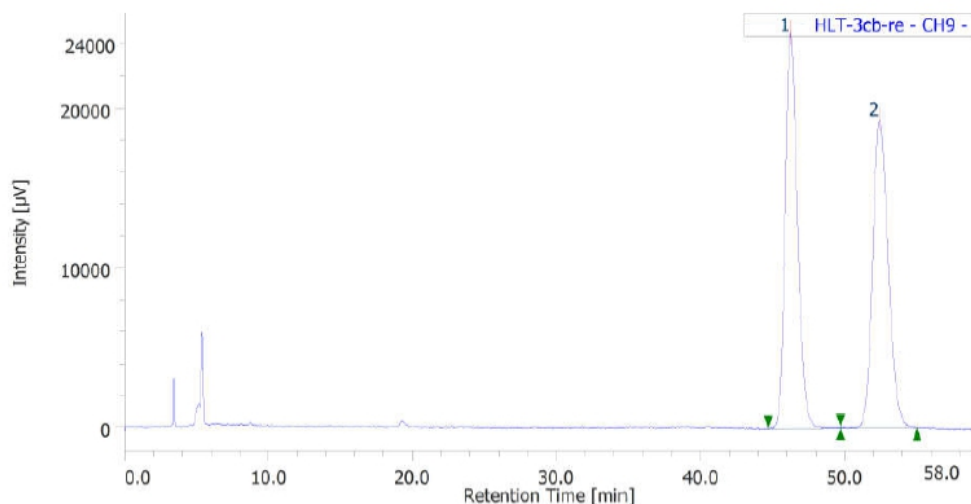
#	ピーク名	CH	tR [min]	面積%	警告
1	Unknown	9	12.970	50.739	
2	Unknown	9	14.027	49.261	



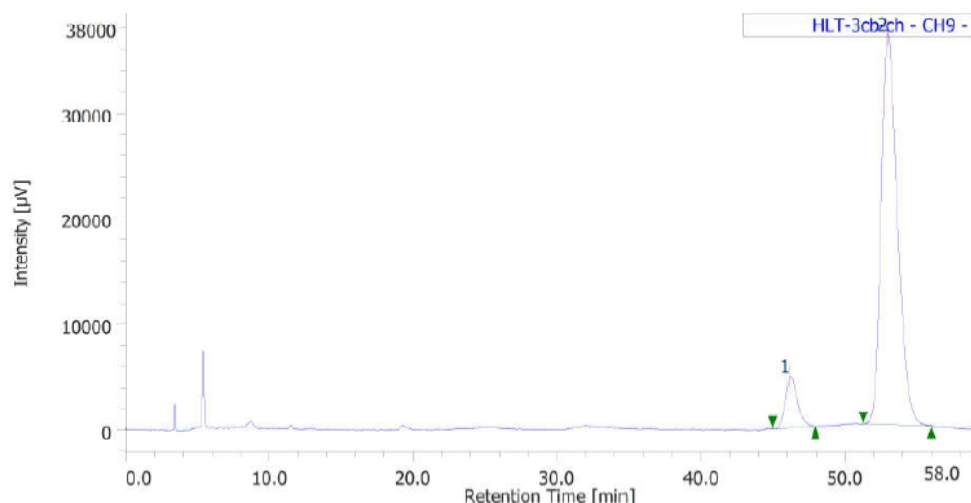
#	ピーク名	CH	tR [min]	面積%	警告
1	Unknown	9	12.873	90.830	
2	Unknown	9	14.003	9.170	

(R)-4-(4-acetylquinolin-8-yl)-1-(furan-2-yl)pentan-1-one (**3db**) : Prepared according to **GP-A** using 4-acetyl-8-ethylquinoline **1d** (0.20 mmol, 40.0 mg) and 2-furyl vinyl ketone **2b** (0.40 mmol, 48.0 mg). **3db** was isolated as a yellow oil (57.0 mg, 89%). **IR** (neat) 2962, 2930, 1691, 1673, 1567, 1354, 1262, 1242, 827, 767 cm^{-1} . **^1H NMR** (CDCl_3 , 500 MHz) δ 1.41 (d, $J = 6.9$ Hz, 3H), 2.21 (dd, $J = 15.2, 7.2$ Hz, 2H), 2.63-2.70 (m, 1H), 2.74 (s, 3H), 2.79-2.86 (m, 1H), 4.42-4.33 (m, 1H), 6.43 (dd, $J = 3.4, 1.7$ Hz, 1H), 7.01 (d, $J = 3.4$ Hz, 1H), 7.48 (d, $J = 1.7$ Hz, 1H), 7.56 (d, $J = 4.6$ Hz, 1H), 7.61 (t, $J = 7.7$ Hz, 1H), 7.68 (dd, $J = 6.9, 1.1$ Hz, 1H), 8.23 (dd, $J = 8.3, 1.4$ Hz, 1H), 8.97 (d, $J = 4.6$ Hz, 1H). **^{13}C NMR** (CDCl_3 , 125 MHz) δ 21.8, 30.2, 31.8, 32.0, 36.7, 111.8, 116.6, 119.0, 123.1, 123.4, 126.4, 128.0, 143.5, 145.5, 145.9, 147.1, 148.3, 152.5, 189.5, 201.8. **HPLC** (chiral column: DAICEL CHIRALPAK OJ-H; solvent: hexane/2-propanol = 19/1; flow rate: 1.0 mL/min; detection: at 285 nm): $t_R = 46.2$ min (minor) and 52.9 min (major). **HRMS** (ESI): m/z calculated for $\text{C}_{20}\text{H}_{19}\text{O}_3\text{NNa}^+$ $[\text{M}+\text{Na}]^+$: 344.1258, found: 344.1255. $[\alpha]_D^{21.8} = +24.4$ ($c = 0.50, \text{CHCl}_3$). **Rf** 0.23 (hexane/AcOEt = 2:1).





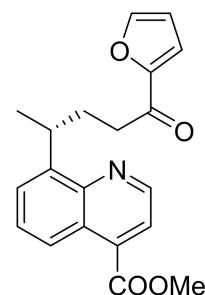
#	ピーク名	CH	tR [min]	面積%	警告
1	Unknown	9	46.233	50.253	
2	Unknown	9	52.423	49.747	



#	ピーク名	CH	tR [min]	面積%	警告
1	Unknown	9	46.207	8.868	
2	Unknown	9	52.987	91.132	

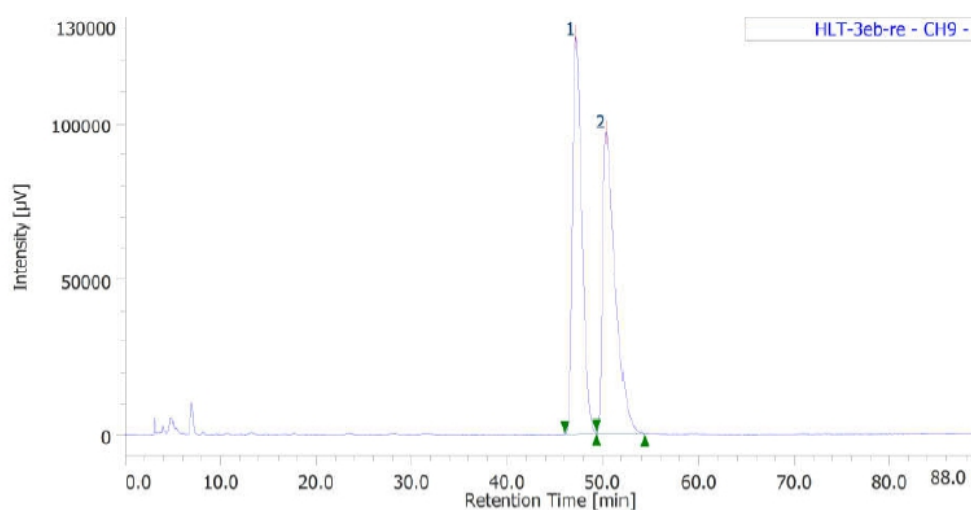
(R)-methyl 8-(5-(furan-2-yl)-5-oxopentan-2-yl)quinoline-4-carboxylate (3eb):

Prepared according to **GP-A** using methyl 8-ethylquinoline-4-carboxylate **1e** (0.20 mmol, 46.2 mg) and 2-furyl vinyl ketone **2b** (0.40 mmol, 48.0 mg). **3eb** was isolated as a yellow oil (54.0 mg, 80%). IR (neat) 2957, 1726, 1675, 1568, 1468, 1271, 1248, 1200, 778 cm^{-1} . ^1H NMR (CDCl_3 , 500 MHz) δ 1.42 (d, $J = 6.9$ Hz, 3H), 2.18-2.23 (m, 2H), 2.63-2.69 (m, 1H), 2.79-2.86 (m, 1H), 4.03 (s, 3H), 4.43-4.35 (m, 1H), 6.42

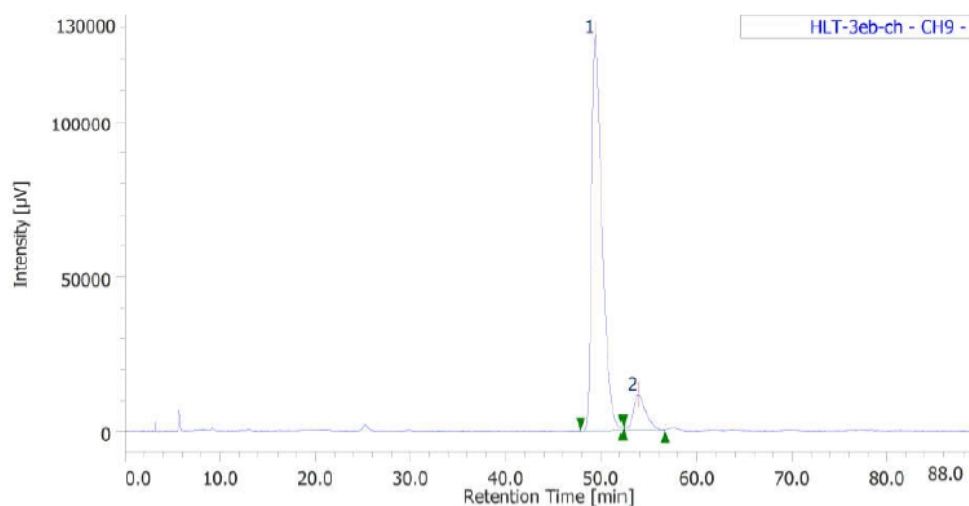


(dd, $J = 3.4, 1.7$ Hz, 1H), 7.00 (d, $J = 3.4$ Hz, 1H), 7.46 (d, $J = 1.7$ Hz, 1H), 7.63 (t, $J = 8.0$ Hz, 1H), 7.68 (dd, $J = 7.2, 1.4$ Hz, 1H), 7.84 (d, $J = 4.0$ Hz, 1H), 8.57 (dd, $J = 8.3, 1.4$ Hz, 1H), 8.96 (d, $J = 4.6$ Hz, 1H).

^{13}C NMR (CDCl_3 , 125 MHz) δ 21.8, 31.9, 32.0, 36.7, 52.6, 111.8, 116.6, 121.6, 123.3, 124.9, 126.3, 127.9, 135.2, 145.5, 145.9, 147.0, 148.2, 152.5, 166.8, 189.5. **HPLC** (chiral column: DAICEL CHIRALPAK IG; solvent: hexane/2-propanol = 97/3; flow rate: 1.0 mL/min; detection: at 285 nm): t_R = 49.4 min (major) and 53.8 min (minor). **HRMS** (ESI): m/z calculated for $\text{C}_{20}\text{H}_{19}\text{O}_4\text{NNa}^+$ $[\text{M}+\text{Na}]^+$: 360.1207, found: 360.1209,. $[\alpha]_D^{25.3} = +19.6$ ($c = 0.50$, CHCl_3). **Rf** 0.38 (hexane/AcOEt = 2:1).



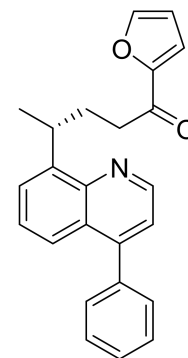
#	ピーク名	CH	tR [min]	面積%	警告
1	Unknown	9	47.227	50.101	
2	Unknown	9	50.400	49.899	



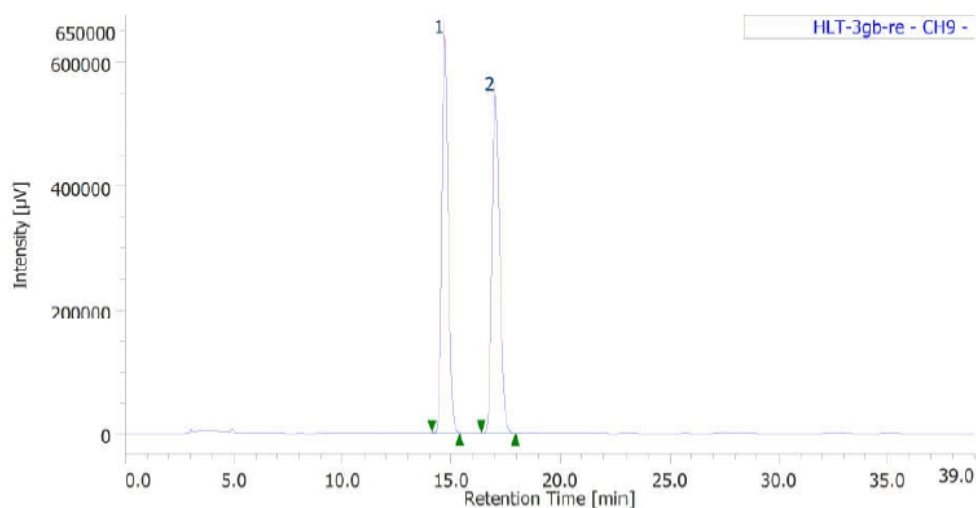
#	ピーク名	CH	tR [min]	面積%	警告
1	Unknown	9	49.423	90.256	
2	Unknown	9	53.817	9.744	

(R)-1-(furan-2-yl)-4-(4-phenylquinolin-8-yl)pentan-1-one (3fb): Prepared according to **GP-A** using 4-phenyl-8-ethylquinoline **1f** (0.20 mmol, 46.6 mg) and 2-furyl vinyl ketone **2b** (0.40 mmol, 48.0 mg). **3fb** was isolated as a yellow oil (50.0 mg, 70%). **IR** (neat) 2960, 1674, 1566, 1489, 1467, 1395, 1165, 764, 701

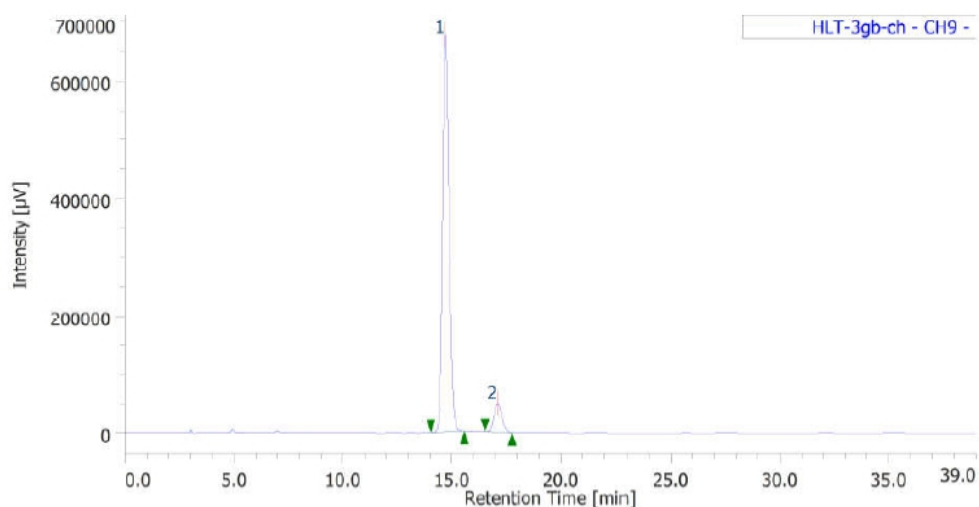
cm⁻¹. ¹H NMR (CDCl₃, 500 MHz) δ 1.45 (d, *J* = 7.4 Hz, 3H), 2.20-2.29 (m, 2H), 2.70-2.76 (m, 1H), 2.85-2.93 (m, 1H), 4.41-4.50 (m, 1H), 6.43 (dd, *J* = 3.4, 1.7 Hz, 1H), 7.03 (d, *J* = 3.4 Hz, 1H), 7.30 (d, *J* = 4.0 Hz, 1H), 7.45-7.53 (m, 7H), 7.64 (d, *J* = 6.9 Hz, 1H), 7.76 (d, *J* = 8.6 Hz, 1H), 8.91 (d, *J* = 4.6 Hz, 1H). ¹³C NMR (CD₃OD, 125 MHz) δ 22.3, 33.0, 33.2, 37.4, 113.2, 118.6, 122.3, 124.9, 127.3, 127.6, 128.0, 129.4, 129.5, 130.5, 139.4, 146.2, 147.6, 148.1, 149.6, 150.4, 153.7, 191.3. **HPLC** (chiral column:



DAICEL CHIRALPAK IG; solvent: hexane/2-propanol = 93/7; flow rate: 1.0 mL/min; detection: at 285 nm): *t_R* = 14.7 min (major) and 17.1 min (minor). **HRMS** (ESI): *m/z* calculated for C₂₄H₂₂O₂N⁺ [M+H]⁺: 356.1646, found: 356.1646. [α]_D^{25.6} = -8.5 (*c* = 0.50, CHCl₃). **R_f** 0.5 (hexane/AcOEt = 2:1).



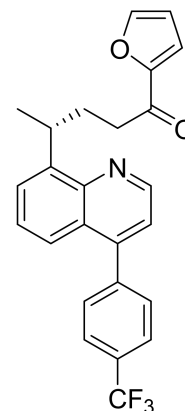
#	ピーク名	CH	tR [min]	面積%	警告
1	Unknown	9	14.690	49.918	
2	Unknown	9	17.020	50.082	



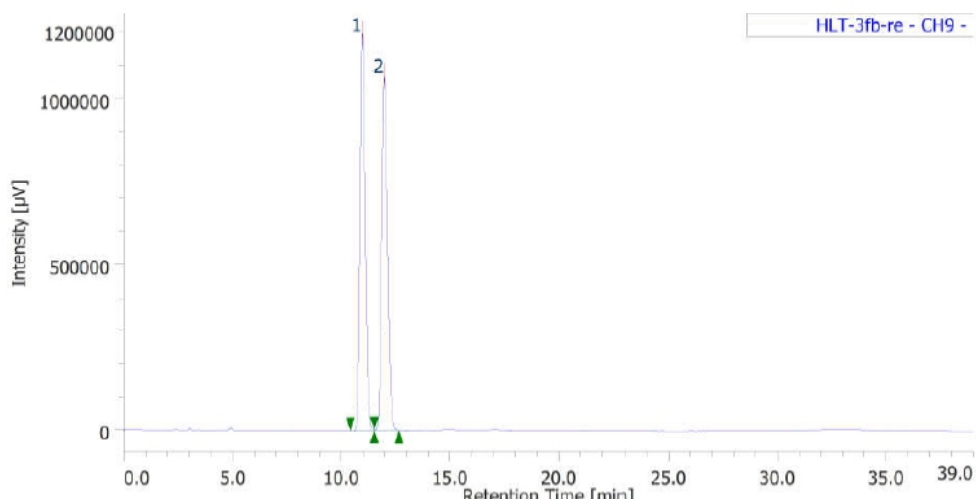
#	ピーク名	CH	tR [min]	面積%	警告
1	Unknown	9	14.707	92.146	
2	Unknown	9	17.107	7.854	

(R)-1-(furan-2-yl)-4-(4-(4-(trifluoromethyl)phenyl)quinolin-8-yl)pentan-1-one

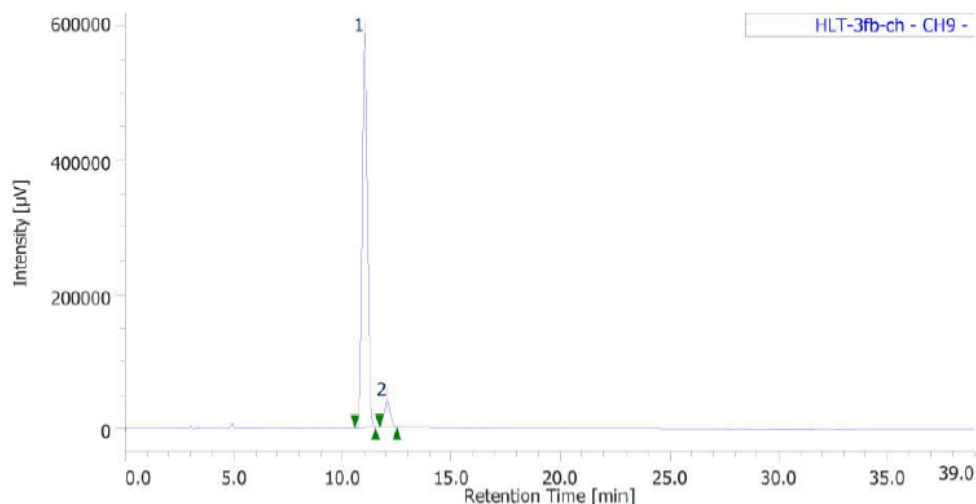
(3gb): Prepared according to **GP-A** using 4-(4-(trifluoromethyl)phenyl) 8-ethylquinoline **1g** (0.20 mmol, 60.0 mg) and 2-furyl vinyl ketone **2b** (0.40 mmol, 48.0 mg). **3gb** was isolated as a yellow oil (60.0 mg, 71%). **IR** (neat) 2962, 1675, 1467, 1324 1165, 1126, 1067, 839, 765 cm^{-1} . **$^1\text{H NMR}$** (CDCl_3 , 500 MHz) δ 1.45 (d, $J = 6.9$ Hz, 3H), 2.22-2.27 (m, 2H), 2.70-2.77 (m, 1H), 2.86-2.93 (m, 1H), 4.41-4.50 (m, 1H), 6.45 (dd, $J = 3.4, 1.7$ Hz, 1H), 7.05 (d, $J = 2.9$ Hz, 1H), 7.31 (d, $J = 4.6$ Hz, 1H), 7.48-7.52 (m, 2H), 7.61 (d, $J = 8.0$ Hz, 2H), 7.65-7.68 (m, 2H), 7.79 (d, $J = 8.6$ Hz, 2H), 8.94 (d



$J = 4.0$ Hz, 1H). **$^{13}\text{C NMR}$** (CDCl_3 , 100 MHz) δ 22.0, 32.0, 32.1, 36.9, 121.0, 123.3, 124.0 (q, $^1J_{\text{CF}} = 272.1$ Hz), 125.5 (q, $^3J_{\text{CF}} = 3.4$ Hz), 126.2, 126.4, 126.9, 129.9, 130 (q, $^2J_{\text{CF}} = 34.8\text{Hz}$), 142.1, 145.7, 146.0, 146.6, 147.2, 148.5, 152.7, 189.7. **$^{19}\text{F NMR}$** (CDCl_3 , 470 MHz) δ -62.8. **HPLC** (chiral column: DAICEL CHIRALPAK IG; solvent: hexane/2-propanol = 93/7; flow rate: 1.0 mL/min; detection: at 285 nm): $t_{\text{R}} = 11.0$ min (major) and 12.0 min (minor). **HRMS** (ESI): m/z calculated for $\text{C}_{25}\text{H}_{21}\text{O}_2\text{NF}_3^+$ $[\text{M}+\text{H}]^+$: 424.1524, found: 424.1524. $[\alpha]_{\text{D}}^{25.0} = -5.6$ ($c = 0.50, \text{CHCl}_3$). **Rf** 0.53 (hexane/AcOEt = 2:1).

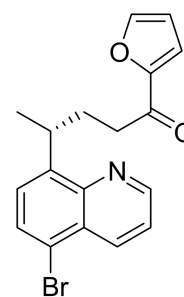


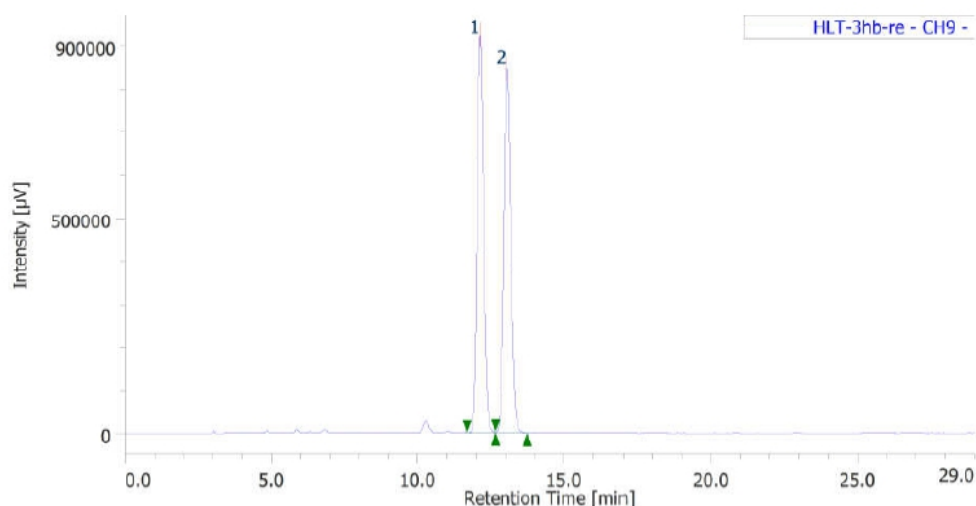
#	ピーク名	CH	tR [min]	面積%	警告
1	Unknown	9	10.963	49.930	
2	Unknown	9	11.977	50.070	



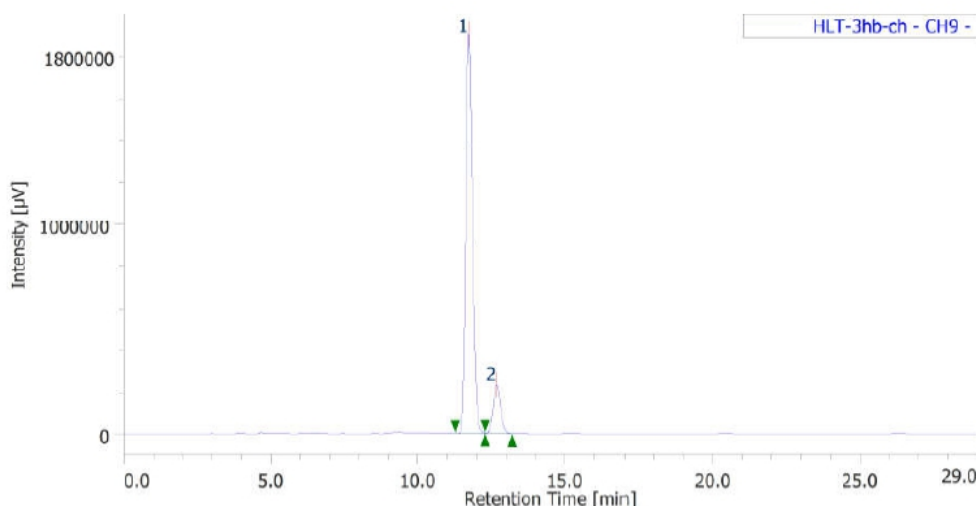
#	ピーク名	CH	tR [min]	面積%	警告
1	Unknown	9	11.010	92.755	
2	Unknown	9	12.050	7.245	

(R)-4-(5-bromoquinolin-8-yl)-1-(furan-2-yl)pentan-1-one (3hb): Prepared according to **GP-A** using 5-bromo-8-ethylquinoline **1h** (0.20 mmol, 47.0 mg) and 2-furyl vinyl ketone **2b** (0.40 mmol, 48.0 mg). **3hb** was isolated as a yellow oil (55.0 mg, 77%). **IR** (neat) 2965, 2911, 1669, 1466, 1386, 1265, 1163, 1031, 835, 793, 766 cm^{-1} . **^1H NMR** (CDCl_3 , 500 MHz) δ 1.40 (d, $J = 6.9$ Hz, 3H), 2.20 (dd, $J = 14.3, 8.6$ Hz, 2H), 2.63-2.71 (m, 1H), 2.79-2.87 (m, 1H), 4.29-4.38 (m, 1H), 6.42 (dd, $J = 3.4, 1.7$ Hz, 1H), 7.01 (d, $J = 3.4$ Hz, 1H), 7.45-7.49 (m, 3H), 7.79 (d, $J = 7.4$ Hz, 1H), 8.52 (dd, $J = 8.6, 1.7$ Hz, 1H), 8.88 (dd, $J = 4.0, 1.7$ Hz, 1H). **^{13}C NMR** (CDCl_3 , 125 MHz) δ 21.7, 31.6, 31.7, 36.6, 111.8, 116.6, 119.4, 121.8, 126.4, 127.4, 130.1, 135.6, 145.3, 145.9, 147.0, 149.6, 152.5, 189.4. **HPLC** (chiral column: DAICEL CHIRALPAK IG; solvent: hexane/2-propanol = 9/1; flow rate: 1.0 mL/min; detection: at 285 nm): $t_R = 11.7$ min (major) and 12.6 min (minor). **HRMS** (ESI): m/z calculated for $\text{C}_{18}\text{H}_{16}\text{O}_2\text{NBrNa}^+$ [$\text{M}+\text{Na}$] $^+$: 380.0257, found: 380.0258. $[\alpha]_D^{25.8} = +13.0$ ($c = 0.50, \text{CHCl}_3$). **Rf** 0.53 (hexane/AcOEt = 2:1).



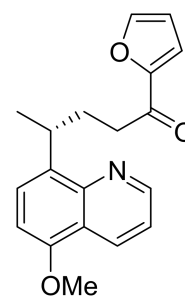


#	ピーク名	CH	tR [min]	面積%	警告
1	Unknown	9	12.137	49.920	
2	Unknown	9	13.057	50.080	

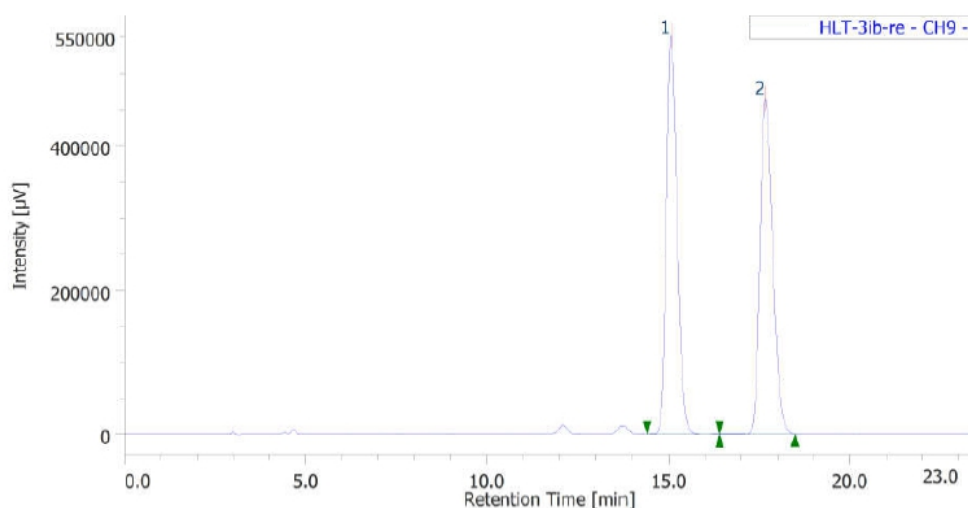


#	ピーク名	CH	tR [min]	面積%	警告
1	Unknown	9	11.733	88.006	
2	Unknown	9	12.683	11.994	

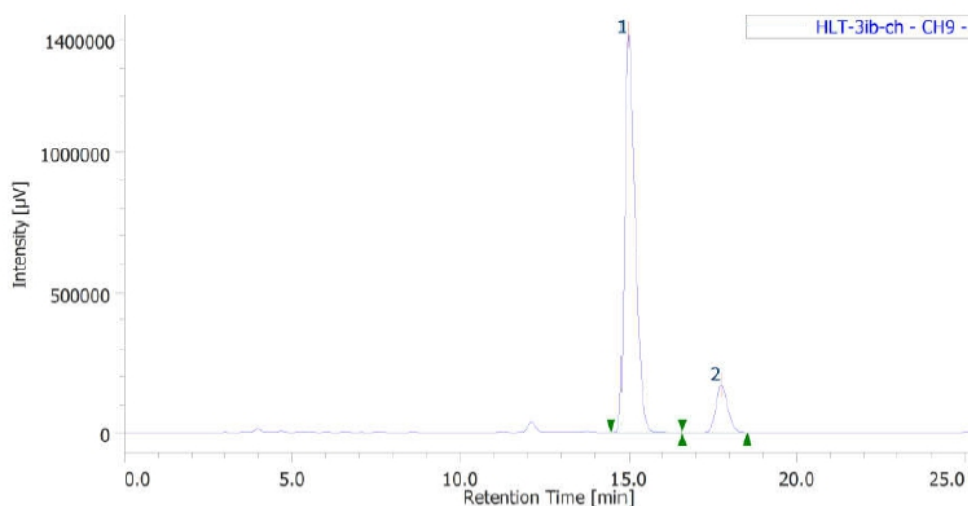
(R)-1-(furan-2-yl)-4-(5-methoxyquinolin-8-yl)pentan-1-one (3ib): Prepared according to **GP-A** using 5-methoxy-8-ethylquinoline **1i** (0.20 mmol, 37.4 mg) and 2-furyl vinyl ketone **2b** (0.40 mmol, 48.0 mg). **3ib** was isolated as a yellow solid (39.0 mg, 63%). **MP** 78-80 °C. **IR** (KBr) 3125, 2959, 1672, 1631, 1468, 1386, 1270, 1161, 1031, 821, 796, 765 cm⁻¹. **¹H NMR** (CDCl₃, 500 MHz) δ 1.39 (d, *J* = 7.0 Hz, 3H), 2.19 (q, *J* = 7.8 Hz, 2H), 2.64-2.70 (m, 1H), 2.81-2.87 (m, 1H), 3.98 (s, 3H), 4.18-4.27 (m, 1H), 6.41 (dd, *J* = 3.4, 1.7 Hz, 1H), 6.84 (d, *J* = 8.6 Hz, 1H), 6.99 (d, *J* = 3.4 Hz, 1H), 7.35 (dd, *J* = 8.0, 4.0 Hz, 1H), 7.46 (s, 2H), 7.50 (d, *J* = 8.0 Hz, 2H), 8.57 (dd, *J* = 8.3, 2.0 Hz, 1H), 8.88 (dd, *J* = 4.0, 2.3 Hz, 1H).



^{13}C NMR (CDCl_3 , 125 MHz) δ 22.0, 31.4, 32.0, 36.9, 55.5, 104.0, 111.8, 116.6, 119.8, 120.6, 125.7, 130.8, 136.6, 145.9, 146.8, 149.3, 152.5, 153.2, 189.8. **HPLC** (chiral column: DAICEL CHIRALPAK IG; solvent: hexane/2-propanol = 9/1; flow rate: 1.0 mL/min; detection: at 285 nm): t_R = 14.9 min (major) and 17.7 min (minor). **HRMS** (ESI): m/z calculated for $\text{C}_{19}\text{H}_{20}\text{O}_3\text{N}^+$ $[\text{M}+\text{H}]^+$: 310.1438, found: 310.1437. $[\alpha]_D^{26.4} = +15.9$ ($c = 0.50$, CHCl_3). **Rf** 0.40 (hexane/AcOEt = 2:1).

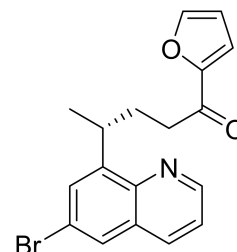


#	ピーク名	CH	tR [min]	面積%	警告
1	Unknown	9	15.057	50.022	
2	Unknown	9	17.663	49.978	

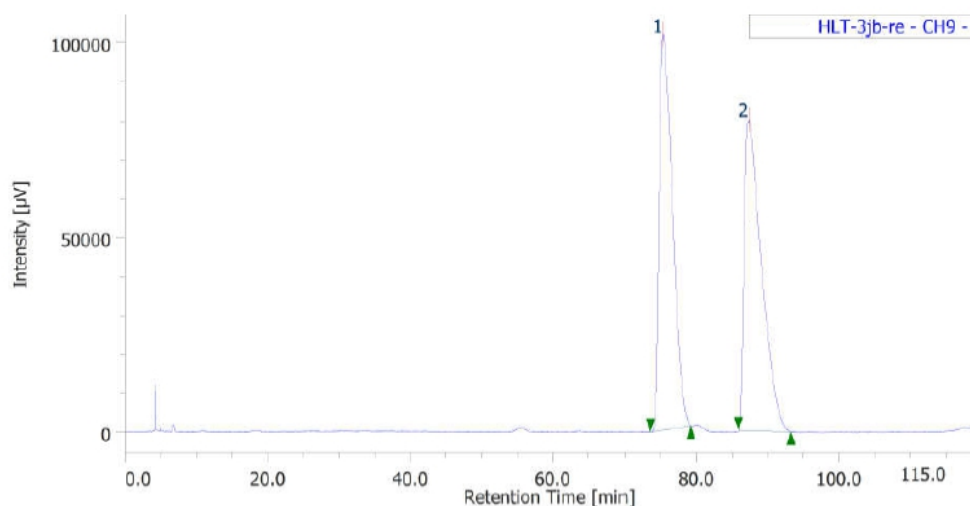


#	ピーク名	CH	tR [min]	面積%	警告
1	Unknown	9	14.983	87.945	
2	Unknown	9	17.743	12.055	

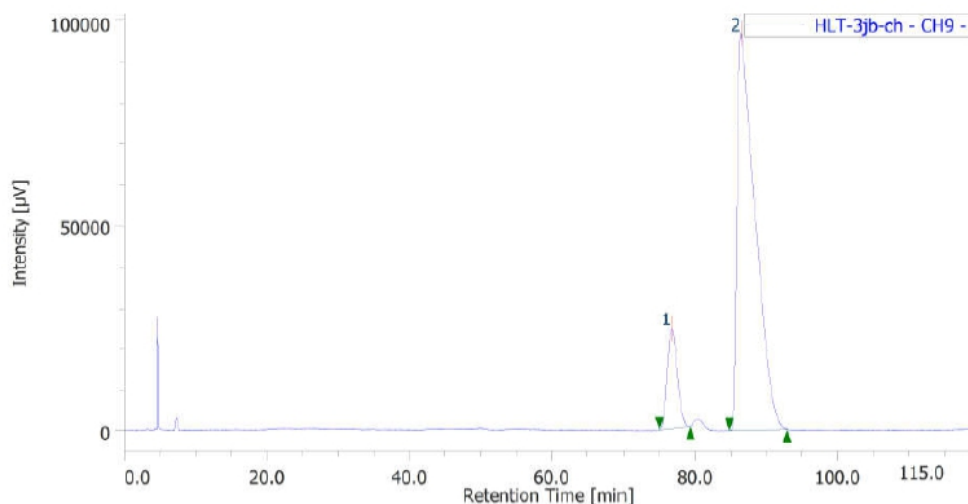
(R)-4-(6-bromoquinolin-8-yl)-1-(furan-2-yl)pentan-1-one (3jb): Prepared according to **GP-A** using 6-bromo-8-ethylquinoline **1j** (0.20 mmol, 47.0 mg) and 2-furyl vinyl ketone **2b** (0.40 mmol, 48.0 mg). **3jb** was isolated as a yellow solid



(66.0 mg, 93%). **MP** 68-70 °C. **IR** (KBr) 3124, 2961, 2868, 1672, 1488, 1394, 1196, 1024, 1031, 869, 790, 767 cm^{-1} . **$^1\text{H NMR}$** (CDCl_3 , 500 MHz) δ 1.41 (d, $J = 6.9$ Hz, 3H), 2.15-2.23 (m, 2H), 2.67-2.73 (m, 1H), 2.82-2.88 (m, 1H), 4.28-4.37 (m, 1H), 6.45 (dd, $J = 3.4, 1.7$ Hz, 1H), 7.04 (d, $J = 3.4$ Hz, 1H), 7.38 (dd, $J = 8.0, 4.0$ Hz, 1H), 7.49 (d, $J = 1.1$ Hz, 1H), 7.68 (d, $J = 2.3$ Hz, 1H), 7.82 (d, $J = 2.3$ Hz, 1H), 8.03 (dd, $J = 8.0, 1.7$ Hz, 1H), 8.86 (dd, $J = 4.6, 1.7$ Hz, 1H). **$^{13}\text{C NMR}$** (CDCl_3 , 125 MHz) δ 21.5, 31.7, 31.8, 36.6, 111.9, 116.6, 120.5, 121.6, 127.7, 129.4, 129.5, 135.3, 144.8, 145.9, 147.7, 149.3, 152.5, 189.3. **HPLC** (chiral column: DAICEL CHIRALPAK IG; solvent: hexane/2-propanol = 99/1; flow rate: 1.0 mL/min; detection: at 285 nm): $t_R = 76.6$ min (minor) and 86.4 min (major). **HRMS** (ESI): m/z calculated for $\text{C}_{18}\text{H}_{16}\text{O}_2\text{NBrNa}^+$ $[\text{M}+\text{Na}]^+$: 380.0257, found: 380.0256. $[\alpha]_D^{25.2} = -2.5$ ($c = 0.50$, CHCl_3). **Rf** 0.43 (hexane/AcOEt = 2:1).



#	ピーク名	CH	tR [min]	面積%	警告
1	Unknown	9	75.313	49.649	
2	Unknown	9	87.353	50.351	



#	ピーク名	CH	tR [min]	面積%	警告
1	Unknown	9	76.670	12.439	
2	Unknown	9	86.430	87.561	

(R)-1-(furan-2-yl)-4-(6-methoxyquinolin-8-yl)pentan-1-one (3kb): Prepared

according to **GP-A** using 6-methoxy-8-ethylquinoline **1k** (0.20 mmol, 37.4 mg) and 2-furyl vinyl ketone **2b** (0.40 mmol, 48.0 mg). **3kb** was isolated as a yellow

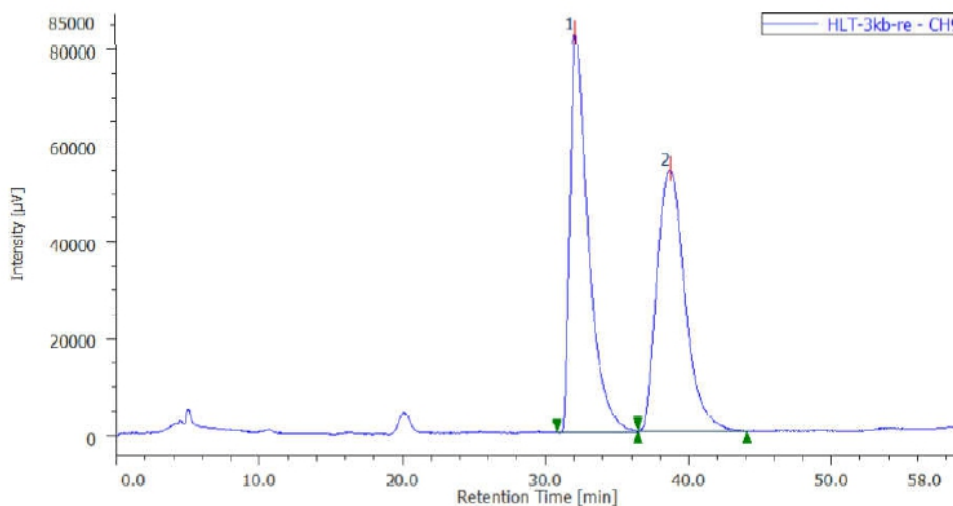
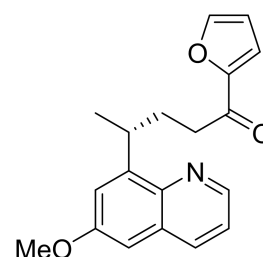
oil (34.0 mg, 55%). **IR** (neat) 2960, 1672, 1616, 1567, 1469, 1375, 1215, 1159, 1027, 760 cm^{-1} . **^1H NMR** (CDCl_3 , 500 MHz) δ 1.40 (d, $J = 7.4$ Hz, 3H),

2.19 (q, $J = 7.6$ Hz, 2H), 2.66-2.72 (m, 1H), 2.82-2.88 (m, 1H), 3.92 (s, 3H), 4.26-4.35 (m, 1H), 6.43 (dd, $J = 4.0, 1.7$ Hz, 1H), 6.93 (d, $J = 2.9$ Hz, 1H), 7.02 (d, $J = 3.4$ Hz, 1H), 7.28 (d, $J = 2.3$ Hz, 1H), 7.33 (dd, $J =$

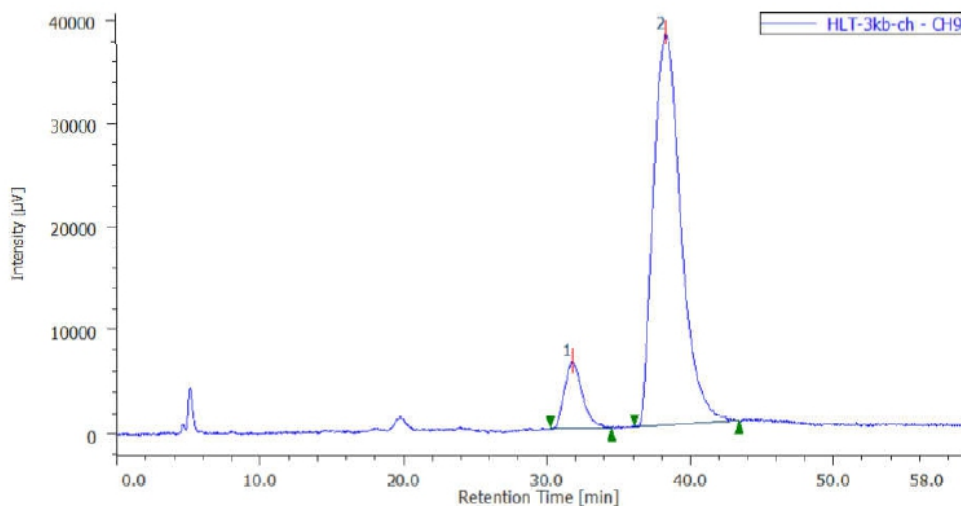
8.3, 4.3 Hz, 1H), 7.48 (s, 1H), 8.03 (dd, $J = 8.0, 1.7$ Hz, 1H), 8.73 (dd, $J = 4.0, 1.7$ Hz, 1H). **^{13}C NMR** (CDCl_3 , 125 MHz) δ 21.7, 31.7, 31.7, 36.7, 55.2, 103.0, 111.8, 116.6, 118.8, 121.1, 129.6, 135.1, 142.5,

145.9, 146.6, 146.6, 146.9, 152.5, 157.5, 189.5. **HPLC** (chiral column: DAICEL CHIRALPAK IA; solvent: hexane/2-propanol = 99/1; flow rate: 1.0 mL/min; detection: at 285 nm): $t_R = 31.7$ min (minor) and 38.2

min (major). **HRMS** (ESI): m/z calculated for $\text{C}_{19}\text{H}_{20}\text{O}_3\text{N}^+$ $[\text{M}+\text{H}]^+$: 310.1438, found: 310.1439. $[\alpha]_D^{25.4} = +18.0$ ($c = 0.50$, CHCl_3). **Rf** 0.33 (hexane/AcOEt = 2:1).

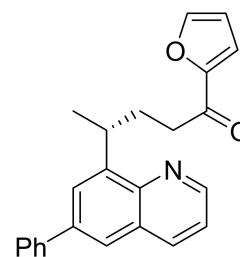


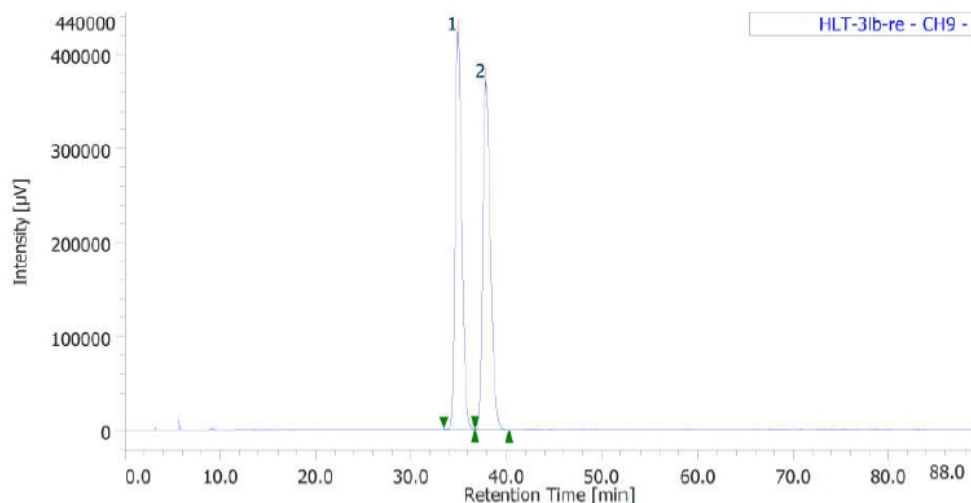
#	ピーク名	CH	tR [min]	面積%	警告
1	Unknown	9	32.117	49.978	
2	Unknown	9	38.730	50.022	



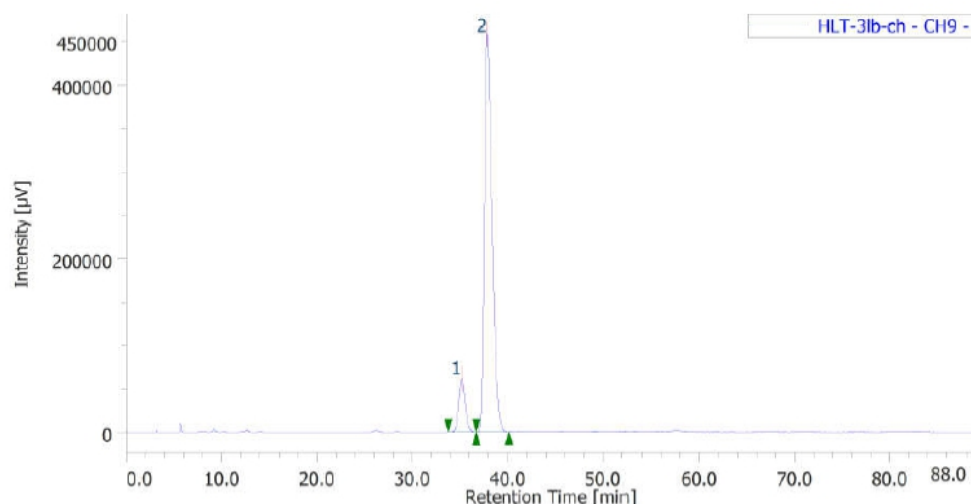
#	ピーク名	CH	tR [min]	面積%	警告
1	Unknown	9	31.750	9.917	
2	Unknown	9	38.287	90.083	

(R)-1-(furan-2-yl)-4-(6-phenylquinolin-8-yl)pentan-1-one (31b): Prepared according to GP-A using 6-phenyl-8-ethylquinoline **11** (0.20 mmol, 46.6 mg) and 2-furyl vinyl ketone **2b** (0.40 mmol, 48.0 mg). **31b** was isolated as a yellow oil (59.0 mg, 83%). IR (neat) 2960, 1673, 1567, 1468, 882, 760, 698 cm⁻¹. ¹H NMR (CDCl₃, 400 MHz) δ 1.48 (d, *J* = 6.8 Hz, 3H), 2.21-2.34 (m, 2H), 2.68-2.81 (m, 1H), 2.83-2.95 (m, 1H), 4.35-4.46 (m, 1H), 6.42 (dd, *J* = 3.4, 1.6 Hz, 1H), 7.03 (d, *J* = 3.2 Hz, 1H), 7.36-7.56 (m, 6H), 7.69-7.74 (m, 3H), 7.88 (d, *J* = 11.8 Hz, 2H), 8.22 (d, *J* = 7.7 Hz, 1H), 8.90 (d, *J* = 2.7 Hz, 1H). ¹³C NMR (CDCl₃, 125 MHz) δ 21.9, 31.9, 32.0, 36.8, 111.8, 121.1, 123.5, 125.7, 127.3, 127.5, 128.5, 128.5, 128.8, 136.5, 138.9, 140.5, 145.5, 145.6, 145.9, 149.0, 152.5, 189.6. HPLC (chiral column: DAICEL CHIRALPAK IG; solvent: hexane/2-propanol = 97/3; flow rate: 1.0 mL/min; detection: at 285 nm): t_R = 35.1 min (minor) and 37.8 min (major). HRMS (ESI): *m/z* calculated for C₂₄H₂₂O₂N⁺ [M+H]⁺: 356.1646, found: 356.1643. [α]_D^{25.7} = -23.0 (*c* = 0.50, CHCl₃). R_f 0.40 (hexane/AcOEt = 2:1).



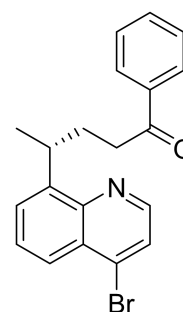


#	ピーク名	CH	tR [min]	面積%	警告
1	Unknown	9	34.900	49.971	
2	Unknown	9	37.837	50.029	

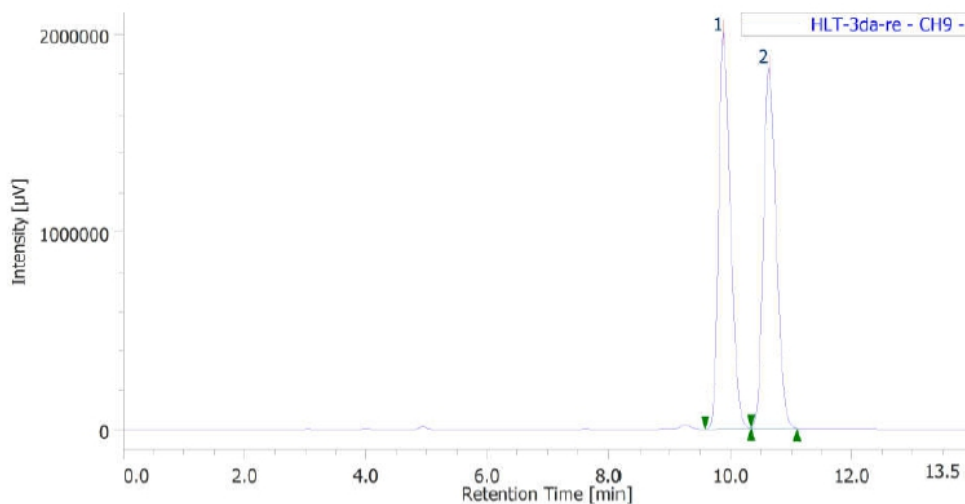


#	ピーク名	CH	tR [min]	面積%	警告
1	Unknown	9	35.190	10.227	
2	Unknown	9	37.860	89.773	

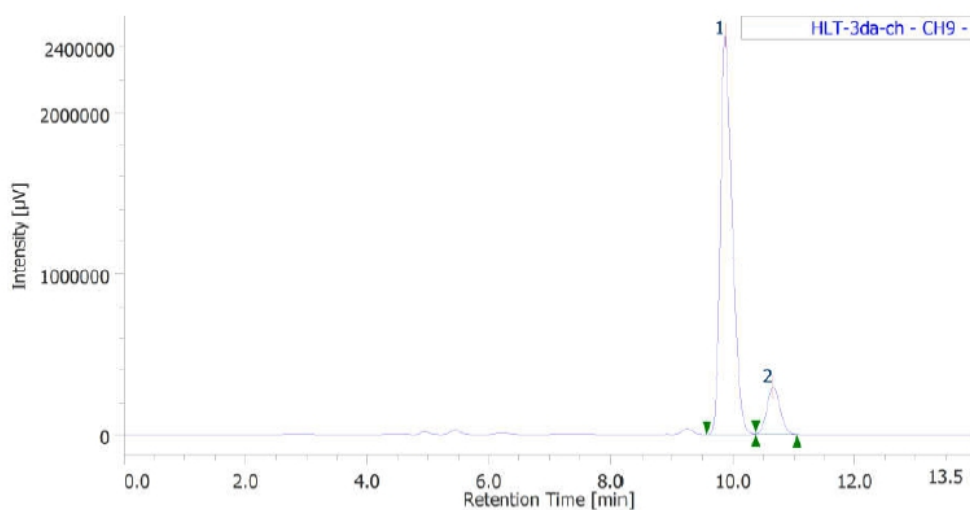
(R)-4-(4-bromoquinolin-8-yl)-1-phenylpentan-1-one (3ca): Prepared according to GP-A using 4-bromo-8-ethylquinoline **1c** (0.20 mmol, 47.0 mg) and phenyl vinyl ketone **2a** (0.40 mmol, 53.0 mg). **3ca** was isolated as a yellow oil (54.0 mg, 73%). IR (neat) 2960, 2929, 1682, 1580, 1482, 1448, 1386, 762, 737, 690 cm⁻¹. ¹H NMR (CDCl₃, 400 MHz) δ 1.42 (d, *J* = 6.7 Hz, 3H), 2.23 (q, *J* = 7.0 Hz, 2H), 2.77-2.84 (m, 1H), 2.95-3.03 (m, 1H), 4.33-4.44 (m, 1H), 7.36 (t, *J* = 6.5 Hz, 2H), 7.48 (t, *J* = 7.4 Hz, 1H), 7.58-7.71 (m, 3H), 7.80 (d, *J* = 6.7 Hz, 2H), 8.07 (dd, *J* = 8.5, 1.3 Hz, 1H), 8.60 (dd, *J* = 4.5, 3.1 Hz, 1H). ¹³C NMR (CDCl₃, 100 MHz) δ 22.0, 32.0, 32.1, 36.8, 124.8, 124.8, 126.9, 127.7, 127.8, 127.8, 128.3,



132.6, 134.4, 136.8, 145.8, 147.1, 148.3, 200.3. **HPLC** (chiral column: DAICEL CHIRALPAK IG; solvent: hexane/2-propanol = 93/7; flow rate: 1.0 mL/min; detection: at 285 nm): t_R = 9.8 min (major) and 10.6 min (minor). **HRMS** (ESI): m/z calculated for $C_{20}H_{18}ONBrNa^+$ $[M+Na]^+$: 390.0464, found: 390.0466. $[\alpha]_D^{26.1} = +2.4$ ($c = 0.50$, $CHCl_3$). **Rf** 0.68 (hexane/AcOEt = 2:1).



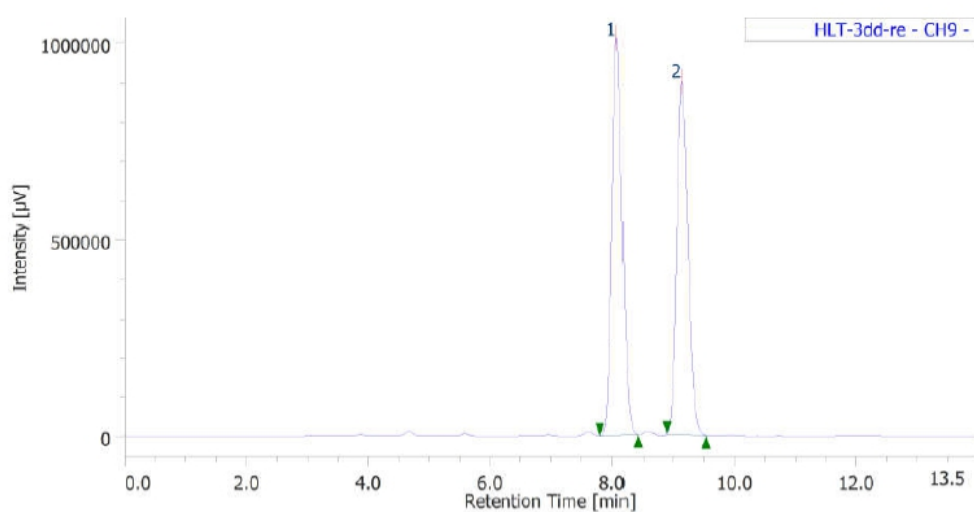
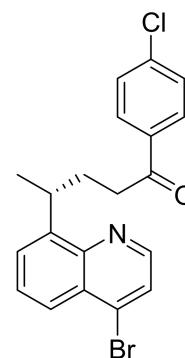
#	ピーク名	CH	tR [min]	面積%	警告
1	Unknown	9	9.880	50.237	
2	Unknown	9	10.630	49.763	



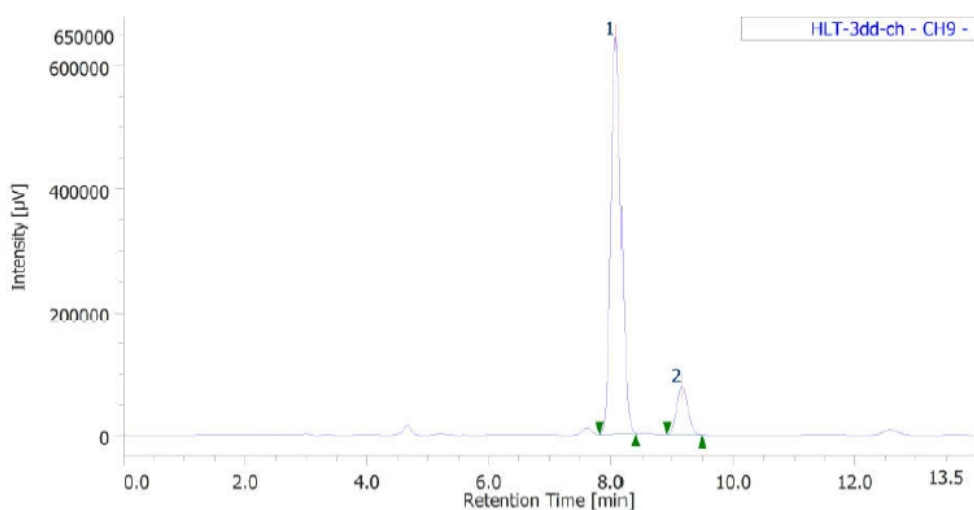
#	ピーク名	CH	tR [min]	面積%	警告
1	Unknown	9	9.867	88.278	
2	Unknown	9	10.657	11.722	

(R)-4-(4-bromoquinolin-8-yl)-1-(4-chlorophenyl)pentan-1-one (3cc): Prepared according to **GP-A** using 4-bromo-8-ethylquinoline **1c** (0.20 mmol, 47.0 mg) and 4-chlorophenyl vinyl ketone **2c** (0.40 mmol, 66.0 mg). **3cc** was isolated as a yellow solid (55.0 mg, 69%). **MP** 65-68 °C. **IR** (KBr) 2961, 2928, 1685, 1538, 1400, 1386, 1205, 1091, 1011, 835, 819, 763, 742 cm^{-1} . **1H NMR** ($CDCl_3$, 400 MHz) δ 1.42 (d, $J = 6.8$ Hz,

3H), 2.21 (q, $J = 7.2$ Hz, 2H), 2.70-2.83 (m, 1H), 2.88-2.99 (m, 1H), 4.31-4.42 (m, 1H), 7.33 (d, $J = 8.2$ Hz, 2H), 7.59-7.75 (m, 5H), 8.08 (d, $J = 8.2$ Hz, 1H), 8.61 (d, $J = 4.5$ Hz, 1H). ^{13}C NMR (acetone- d_6 , 100 MHz) δ 21.9, 32.7, 32.8, 37.2, 125.2, 125.9, 128.0, 128.3, 128.8, 129.3, 130.3, 134.4, 136.4, 139.0, 146.9, 147.9, 149.6, 198.9. **HPLC** (chiral column: DAICEL CHIRALPAK IG; solvent: hexane/2-propanol = 9/1; flow rate: 1.0 mL/min; detection: at 285 nm): $t_R = 8.0$ min (major) and 9.1 min (minor). **HRMS** (ESI): m/z calculated for $\text{C}_{20}\text{H}_{17}\text{ONClBrNa}^+ [\text{M}+\text{Na}]^+$: 424.0075, found: 424.0082. $[\alpha]_D^{26.3} = -1.6$ ($c = 0.50$, CHCl_3). **Rf** 0.73 (hexane/AcOEt = 2:1).



#	ピーク名	CH	tR [min]	面積%	警告
1	Unknown	9	8.077	50.096	
2	Unknown	9	9.130	49.904	



#	ピーク名	CH	tR [min]	面積%	警告
1	Unknown	9	8.080	87.892	
2	Unknown	9	9.157	12.108	

(R)-4-(4-bromoquinolin-8-yl)-1-(thiophen-2-yl)pentan-1-one (3cd): Prepared

according to **GP-A** using 4-bromo-8-ethylquinoline **1c** (0.20 mmol, 47.0 mg) and 4-chlorophenyl vinyl ketone **2d** (0.40 mmol, 56.0 mg). **3cd** was isolated as a yellow oil

(52.0 mg, 70%). **IR** (neat) 2960, 2928, 1660, 1482, 1415, 1386, 763, 723 cm^{-1} . **^1H**

NMR (CDCl_3 , 400 MHz) δ 1.42 (d, $J = 7.2$ Hz, 3H), 2.23 (q, $J = 7.4$ Hz, 2H), 2.67-2.80 (m, 1H), 2.84-2.96 (m, 1H), 4.31-4.42 (m, 1H), 7.01 (t, $J = 3.9$ Hz, 1H), 7.47 (d, $J = 3.2$

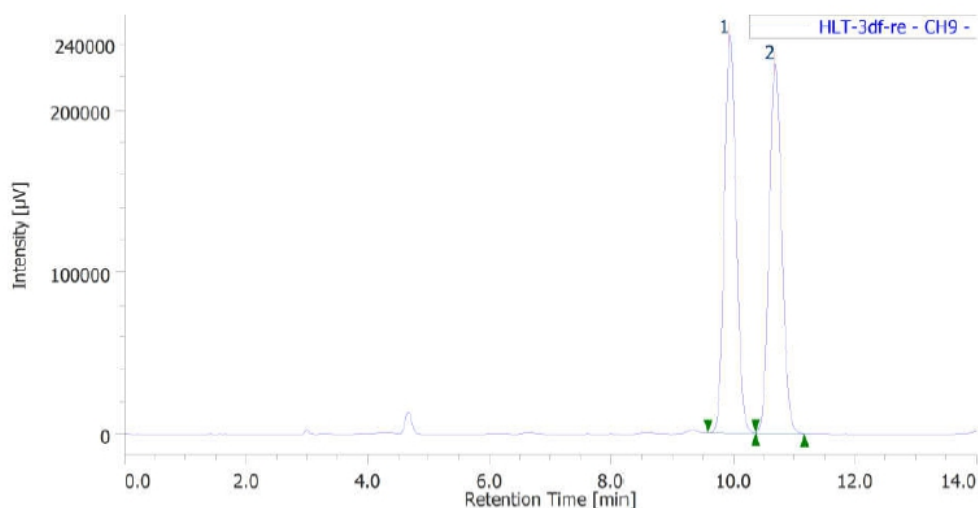
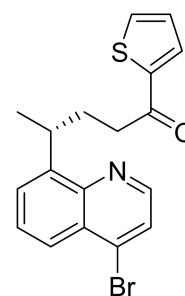
Hz, 1H), 7.55 (d, $J = 5.0$ Hz, 1H), 7.59-7.72 (m, 3H), 8.08 (d, $J = 8.2$ Hz, 1H), 8.62 (d, $J = 3.2$ Hz, 1H). **^{13}C**

NMR (acetone- d_6 , 100 MHz) δ 21.9, 32.8, 33.0, 37.8, 125.2, 125.9, 128.0, 128.3, 128.8, 128.9, 132.7, 134.1, 134.4, 145.2, 146.9, 147.9, 149.6, 193.2. **HPLC** (chiral column: DAICEL CHIRALPAK IG; solvent:

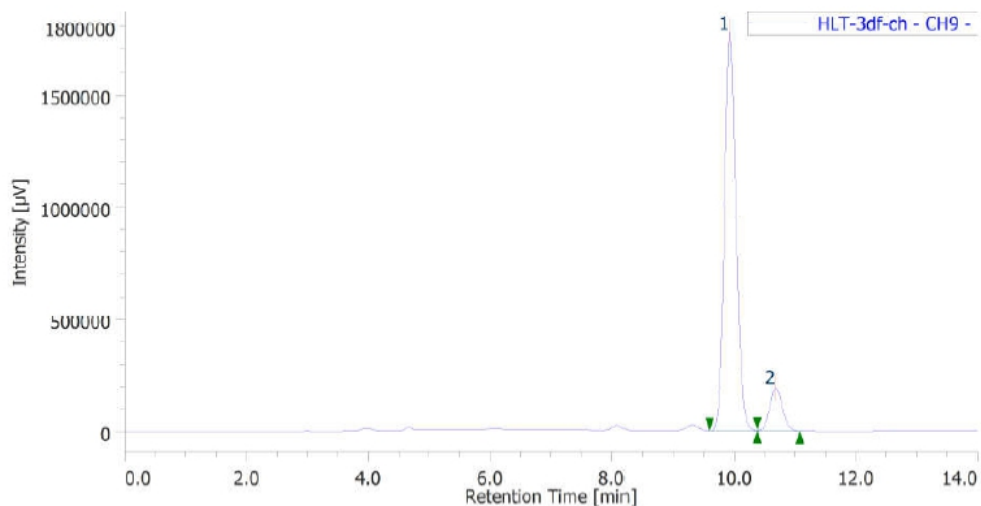
hexane/2-propanol = 9/1; flow rate: 1.0 mL/min; detection: at 285 nm): $t_R = 9.9$ min (major) and 10.6 min

(minor). **HRMS** (ESI): m/z calculated for $\text{C}_{18}\text{H}_{16}\text{ONSBrNa}^+$ $[\text{M}+\text{Na}]^+$: 396.0029, found: 396.0032. $[\alpha]_D^{26.5}$

= +20.8 ($c = 0.50$, CHCl_3). **Rf** 0.60 (hexane/AcOEt = 2:1).

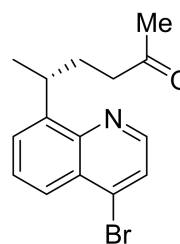


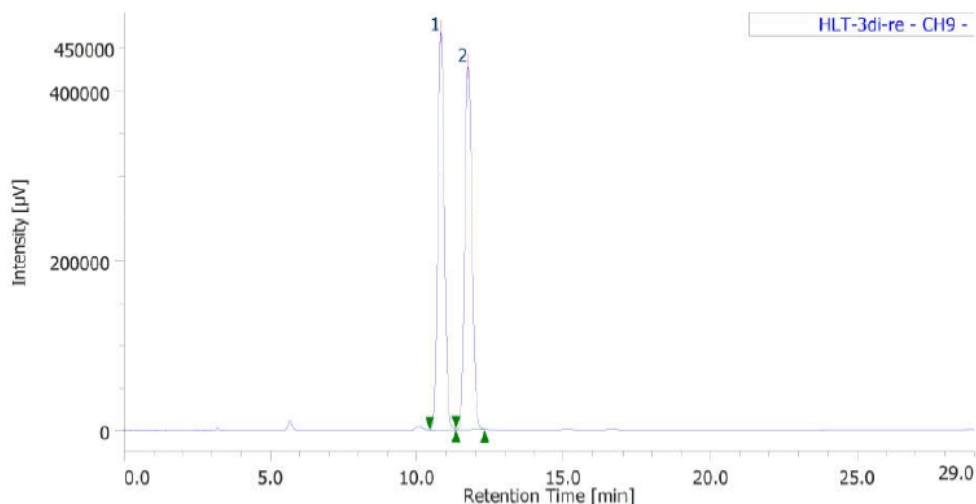
#	ピーク名	CH	tR [min]	面積%	警告
1	Unknown	9	9.940	50.270	
2	Unknown	9	10.687	49.730	



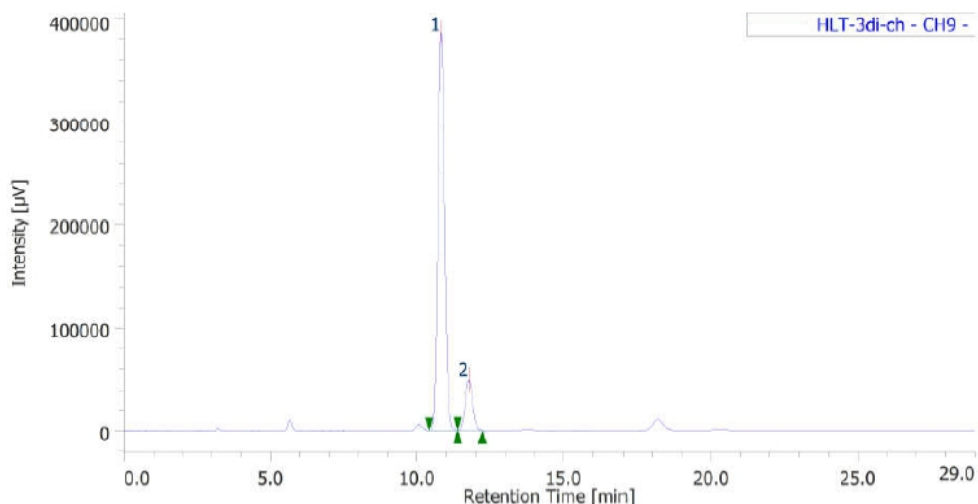
#	ピーク名	CH	tR [min]	面積%	警告
1	Unknown	9	9.923	89.366	
2	Unknown	9	10.680	10.634	

(R)-5-(4-bromoquinolin-8-yl)hexan-2-one (3ce): Prepared according to **GP-A** using 4-bromo-8-ethylquinoline **1c** (0.20 mmol, 47.0 mg) and methyl vinyl ketone **2e** (0.40 mmol, 28.0 mg). **3ce** was isolated as a yellow oil (35.0 mg, 58%). **IR** (neat) 2960, 2927 1714, 1482, 1415, 1386, 763 cm^{-1} . **^1H NMR** (CDCl_3 , 400 MHz) δ 1.37 (d, $J = 7.2$ Hz, 3H), 2.00-2.10 (m, 5H), 2.22-2.34 (m, 1H), 2.37-2.49 (m, 1H), 4.22-4.33 (m, 1H), 7.61-7.64 (m, 2H), 7.70 (t, $J = 3.8$ Hz, 1H), 8.08 (dd, $J = 7.2, 2.7$ Hz, 1H), 8.67 (t, $J = 4.0$ Hz, 1H). **^{13}C NMR** (CDCl_3 , 100 MHz) δ 21.8, 29.8, 31.6, 31.7, 41.9, 124.8, 124.9, 126.9, 127.7, 127.8, 134.4, 145.8, 147.0, 148.4, 209.1. **HPLC** (chiral column: DAICEL CHIRALPAK IG; solvent: hexane/2-propanol = 97/3; flow rate: 1.0 mL/min; detection: at 285 nm): $t_R = 10.8$ min (major) and 11.7 min (minor). **HRMS** (ESI): m/z calculated for $\text{C}_{15}\text{H}_{16}\text{ONBrNa}^+$ [$\text{M}+\text{Na}$] $^+$: 328.0308, found: 328.0310. **$[\alpha]_D^{26.7} = +13.1$** ($c = 0.50$, CHCl_3). **Rf** 0.50 (hexane/AcOEt = 2:1).



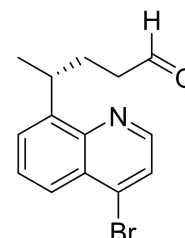


#	ピーク名	CH	tR [min]	面積%	警告
1	Unknown	9	10.817	50.272	
2	Unknown	9	11.750	49.728	

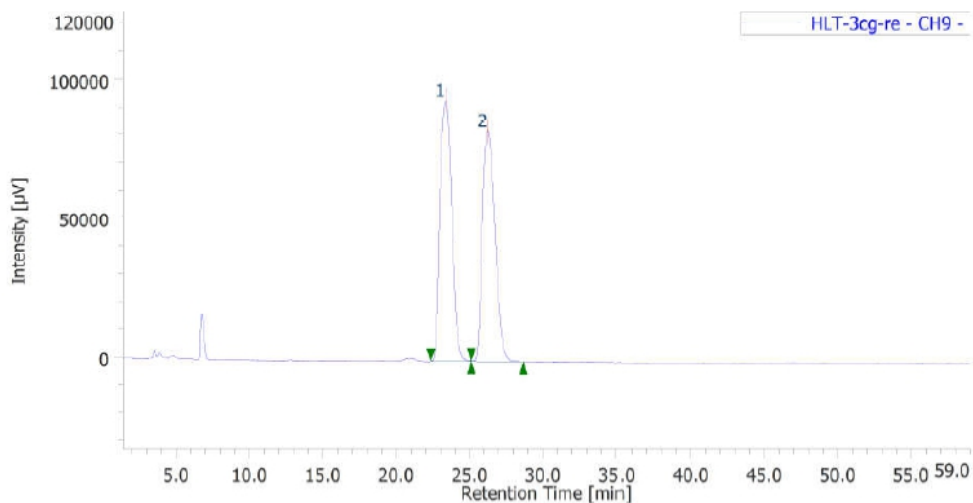


#	ピーク名	CH	tR [min]	面積%	警告
1	Unknown	9	10.817	87.963	
2	Unknown	9	11.767	12.037	

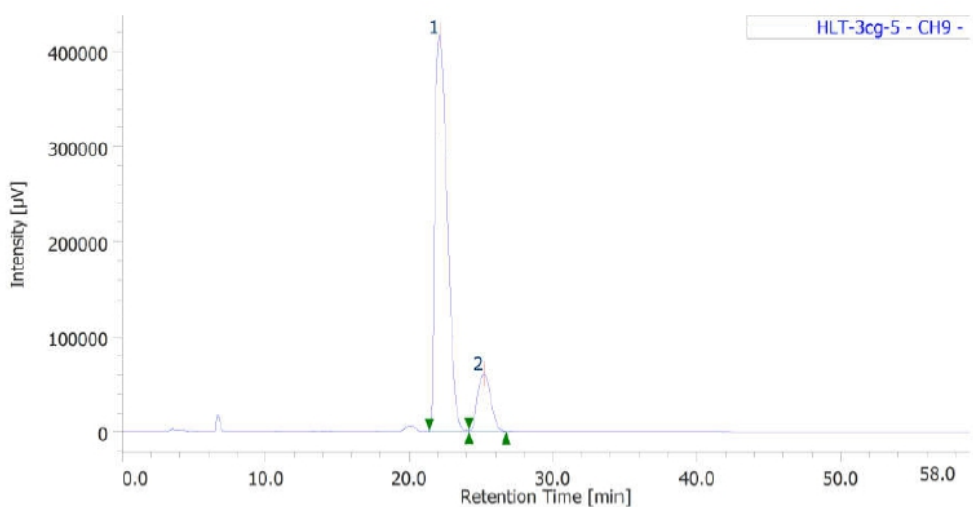
(R)-4-(4-bromoquinolin-8-yl)pentanal (3cf): Prepared according to **GP-B** using 4-bromo-8-ethylquinoline **1c** (0.20 mmol, 47.0 mg) and acrolein **2f** (0.60 mmol, 22.4 mg). **3cf** was isolated as a pale yellow oil (32.0 mg, 55%). IR (neat) 2960, 2930, 1722, 1380, 768 cm^{-1} . $^1\text{H NMR}$ (CDCl_3 , 400 MHz) δ 1.39 (d, $J = 6.9$ Hz, 3H), 2.10 (dd, $J = 14.6, 7.0$ Hz, 2H), 2.25-2.35 (m, 1H), 2.37-2.47 (m, 1H), 4.26-4.37 (m, 1H), 7.60-7.67 (m, 2H), 7.70 (d, $J = 4.5$ Hz, 1H), 8.09 (dd, $J = 7.2, 2.2$ Hz, 1H), 8.66 (d $J = 4.9$ Hz, 1H) 9.70 (t $J = 1.6$ Hz, 1H). $^{13}\text{C NMR}$ (CDCl_3 , 100 MHz) δ 21.6, 30.0, 31.8, 42.2, 124.9, 125.0, 126.9, 127.7, 127.9, 134.5, 145.5, 147.0, 148.5, 202.7. For the HPLC analysis to determine the enantiomeric ratio, **3cf**



was reduced to the corresponding alcohol with NaBH₄. **HPLC** (chiral column: DAICEL CHIRALPAK IH; solvent: hexane/2-propanol = 99/1; flow rate: 1.0 mL/min; detection: at 285 nm): t_R = 22.8 min (major) and 26.0 min (minor). **HRMS** (ESI): m/z calculated for C₁₄H₁₅ONBr⁺ [M+H]⁺: 292.0332, found: 292.0331. **[α]_D^{22.7}** = +14.7 (c = 0.50, CHCl₃). **Rf** 0.50 (hexane/AcOEt = 2:1).

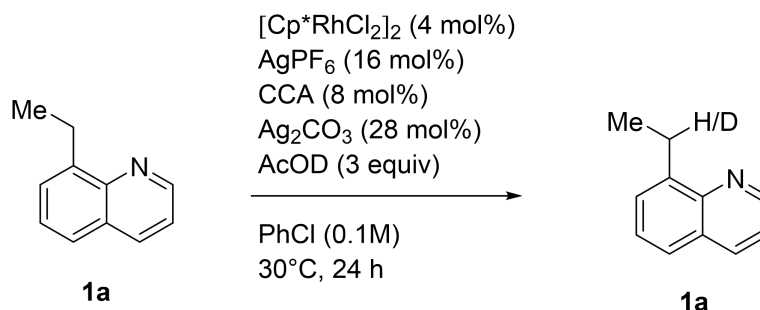


#	ピーク名	CH	tR [min]	面積%	警告
1	Unknown	9	23.373	51.322	
2	Unknown	9	26.247	48.678	

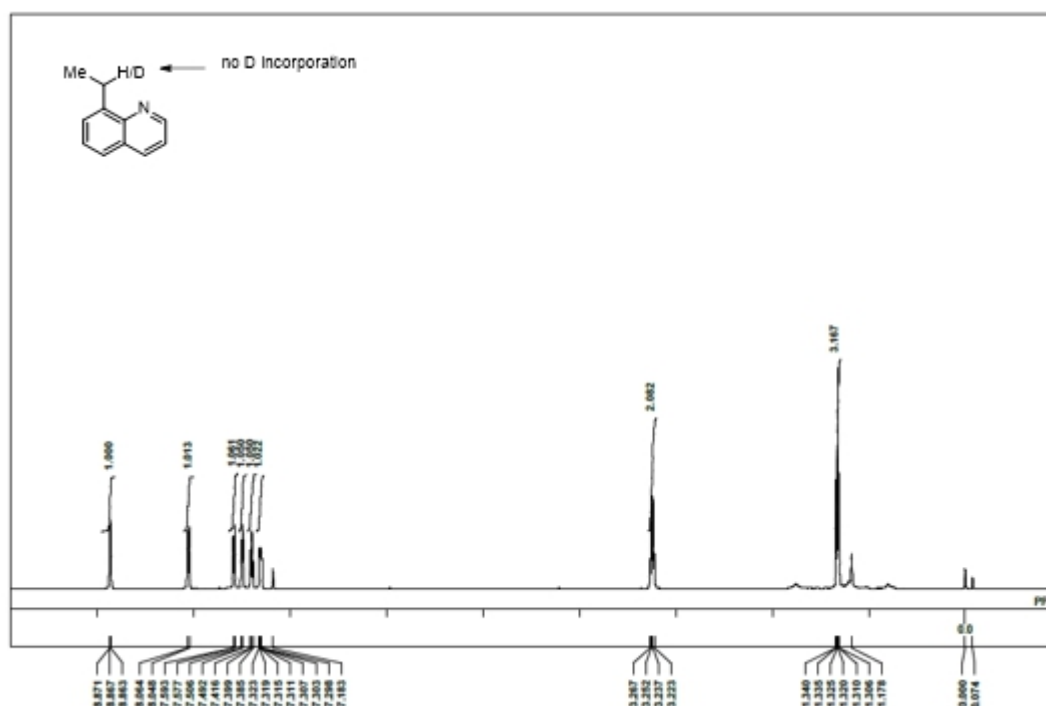


#	ピーク名	CH	tR [min]	面積%	警告
1	Unknown	9	22.123	86.459	
2	Unknown	9	25.220	13.541	

2.4 H/D exchange experiment



To a screw-cap vial were added chiral carboxylic acid (5.1 mg, 0.08 mmol) and AcOD (ca. 0.2 mL), and the mixture was stirred for 30 min at room temperature. The reaction mixture was concentrated in vacuo, and AcOD (3 equiv) was added to the residue, and the vial was moved into an argon-filled glovebox. The vial was charged with **1a** (15.7 mg, 0.10 mmol), [Cp*RhCl₂]₂ (2.4 mg, 0.04 mmol), AgPF₆ (4.0 mg, 0.016 mmol), Ag₂CO₃ (7.7 mg, 0.028 mmol), and chlorobenzene (1 mL). The vial was capped, and then brought out of the glovebox. The reaction mixture was stirred at 30 °C for 24 h. The reaction mixture was directly subjected to silica gel column chromatography (hexane/AcOEt) to afford **1a** (13.0 mg, 85%). The ¹H NMR analysis of the recovered **1a** indicated no H/D exchange.



2.5 Preparative scale reaction

In an argon-filled glovebox, a test tube was charged with 8-ethylquinoline **1a** (1.00 mmol, 1.0 equiv), enone **2b** (2.00 mmol, 2.0 equiv), chiral carboxylic acid (51.2 mg, 0.08 mmol, 8 mol %), [Cp*RhCl₂]₂ (24.7 mg, 0.04 mmol, 4 mol %), AgPF₆ (40.0 mg, 0.16 mmol, 16 mol %), and Ag₂CO₃ (77.0 mg, 0.28 mmol, 28 mol %). Chlorobenzene (10 mL) was added. beforeT the test tube was capped and brought out of the glovebox. The reaction mixture was heated to 30 °C. After stirring at the same temperature for 24 h, the reaction mixture was directly purified by silica gel column chromatography (hexane/AcOEt) to afford **3aa** (212.0 mg, 76%), 90: 10 er.

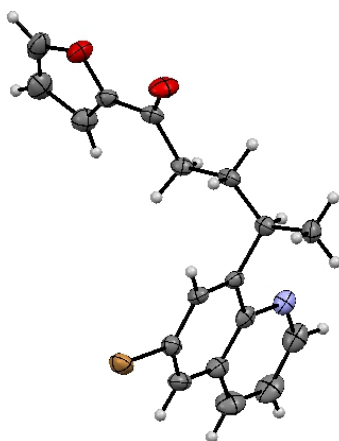
2.6 Determination of absolute configuration

A single crystal of **3jb** suitable for X-ray crystallography was grown by slow vapor diffusion of pentane to a solution of **3jb** in THF.

Table. S1 Crystal data and structure refinement for **3jb**.

Identification code	product	
Empirical formula	C ₁₈ H ₁₆ Br N O ₂	
Formula weight	358.23	
Temperature	133(2) K	
Wavelength	0.71075 Å	
Crystal system	Monoclinic	
Space group	P 1 21 1	
Unit cell dimensions	a = 5.6584(3) Å	= 90°.
	b = 9.9080(6) Å	= 93.242(6)°.
	c = 14.1490(7) Å	= 90°.
Volume	791.97(7) Å ³	
Z	2	
Density (calculated)	1.502 Mg/m ³	
Absorption coefficient	2.602 mm ⁻¹	
F(000)	364	
Crystal size	0.390 x 0.190 x 0.100 mm ³	
Theta range for data collection	2.511 to 25.346°.	
Index ranges	-6<=h<=6, -11<=k<=11, -17<=l<=16	
Reflections collected	6167	
Independent reflections	2826 [R(int) = 0.0260]	
Completeness to theta = 25.242°	99.8 %	
Absorption correction	Semi-empirical from equivalents	

Max. and min. transmission	0.9904 and 0.6533
Refinement method	Full-matrix least-squares on F^2
Data / restraints / parameters	2826 / 1 / 200
Goodness-of-fit on F^2	1.083
Final R indices [$I > 2\sigma(I)$]	R1 = 0.0282, wR2 = 0.0623
R indices (all data)	R1 = 0.0313, wR2 = 0.0633
Absolute structure parameter	0.030(7)
Extinction coefficient	n/a
Largest diff. peak and hole	0.320 and -0.720 e. \AA^{-3}



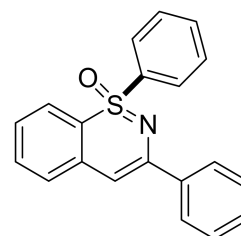
3. Experimental procedures: Second work-Ru(II)/Chiral Carboxylic Acid-Catalyzed Enantioselective C–H Functionalization of Sulfoximines

General Procedure C [GP-C]

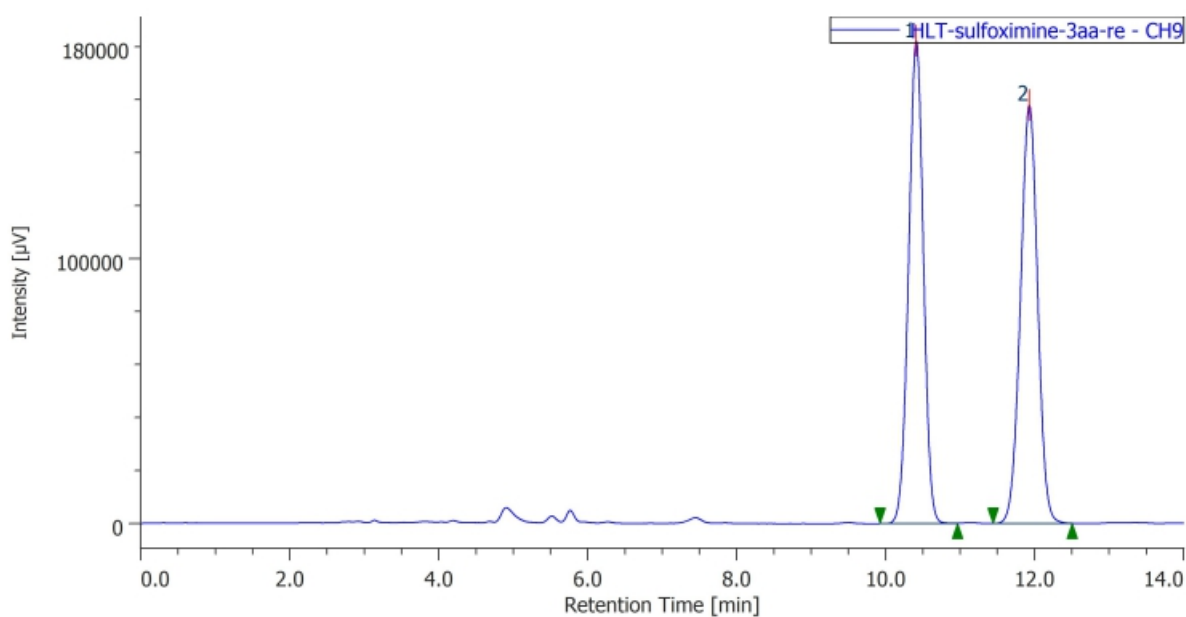
In an argon-filled glovebox, a screw-capped test tube was charged with sulfoximine **4** (0.20 mmol, 1.0 equiv), sulfoxonium ylide **6** (0.3 mmol, 1.5 equiv), chiral carboxylic acid (0.02 mmol, 8.4 mg), AgSbF₆ (13.6 mg, 20 mol%), [RuCl₂(p-cymene)]₂ (3.0 mg, 2.5 mol%), and CHCl₃ (4.0 mL). Then the reaction mixture was stirred at 40 °C for 24 h. The resulting mixture was directly purified by silica gel column chromatography (hexane/AcOEt) to afford **7**.

(S)-1,3-diphenylbenzo[e][1,2]thiazine 1-oxide (7aa): Prepared according to

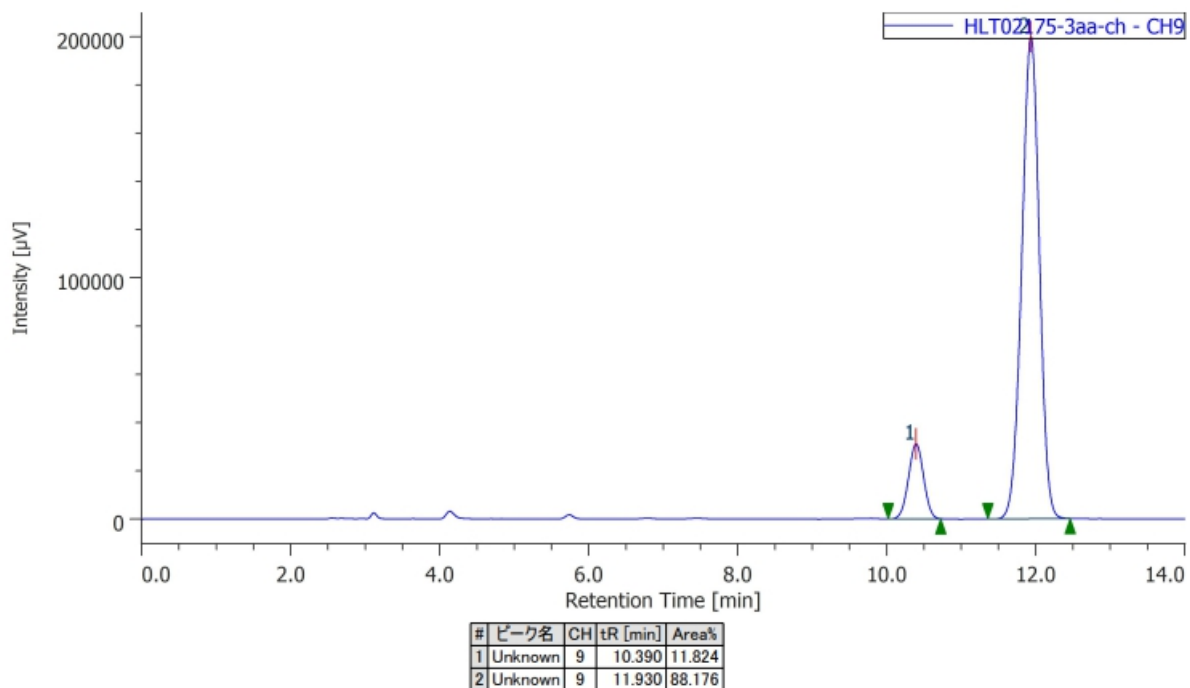
GP-C using sulfoximine **4a** (0.20 mmol, 43.4 mg) and sulfoxonium ylide **6a** (0.30 mmol, 59.1 mg) afforded **7aa** as a yellow foam (51.0 mg, 80%). ¹H NMR (CDCl₃, 400 MHz) δ 8.03–7.97 (m, 4H), 7.66–7.53 (m, 3H), 7.51–7.30 (m, 6H), 7.25–7.19 (m, 1H), 6.81 (s, 1H). ¹³C NMR (CDCl₃, 100 MHz) δ 147.2, 140.5, 138.7, 136.5,



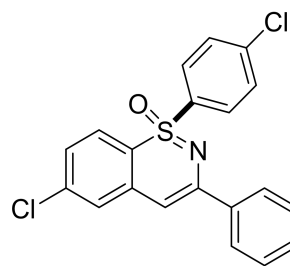
133.3, 132.1, 129.3, 129.0, 128.8, 128.3, 126.9, 126.6, 126.2, 124.9, 119.6, 98.1. **HPLC** (chiral column: DAICEL CHIRALPAK AD-H; solvent: hexane/2-propanol = 4/1; flow rate: 1.2 mL/min; detection: at 254 nm): t_R = 10.4 min (minor) and 11.9 min (major). [α]_D²⁴ = +10.2 (c = 1.0, CHCl₃). **Rf** 0.40 (hexane/AcOEt = 6:1). The NMR spectra of the obtained product were consistent with the reported data.^[S4]

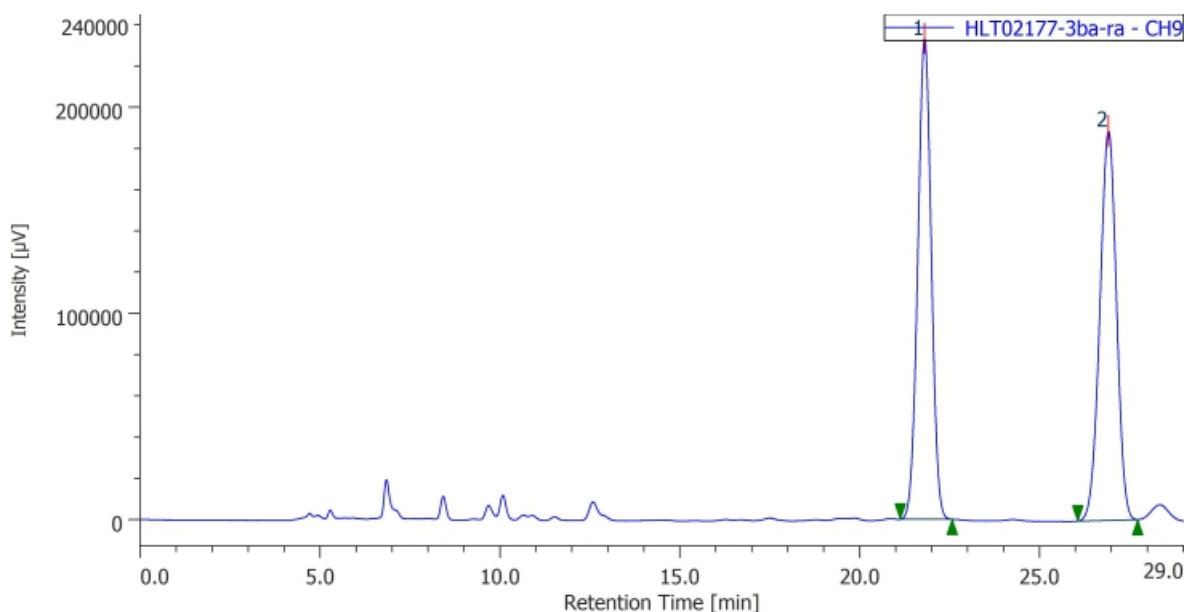


#	ピーク名	CH	tR [min]	Area%
1	Unknown	9	10.407	49.807
2	Unknown	9	11.923	50.193

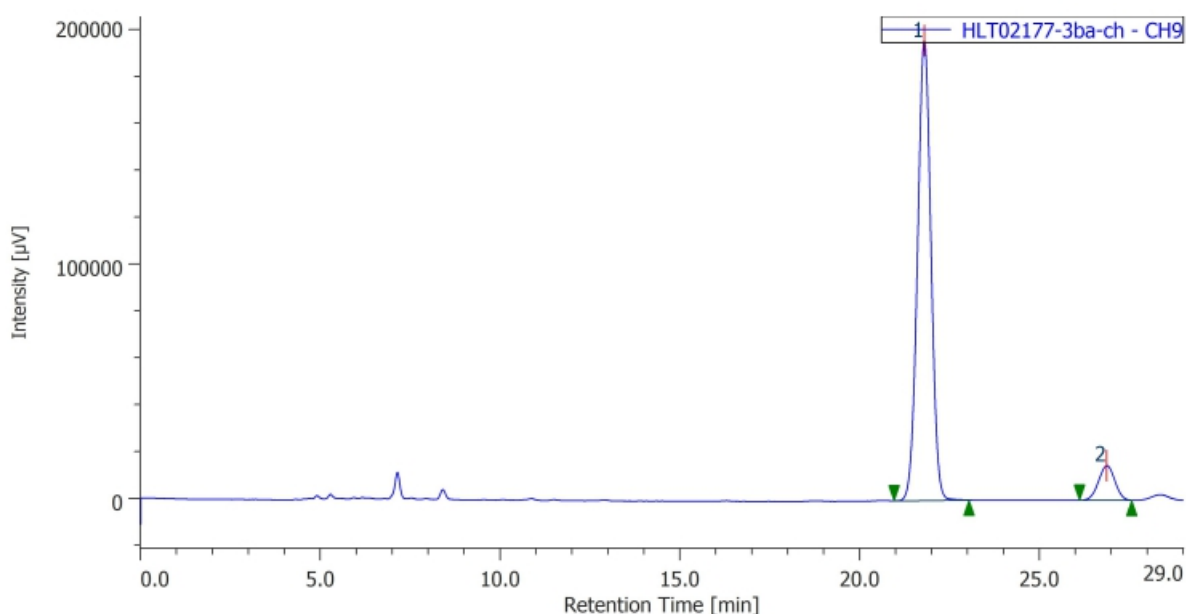


(S)-6-chloro-1-(4-chlorophenyl)-3-phenylbenzo[e][1,2]thiazine-1-oxide (7ba): Prepared according to GP-C using sulfoximine **4b** (0.20 mmol, 56.8 mg) and sulfoxonium ylide **6a** (0.30 mmol, 59.1 mg) afforded **7ba** as a yellow foam (55.0 mg, 72%). ¹H NMR (CDCl₃, 400 MHz) δ 7.97 (d, *J* = 6.7 Hz, 2H), 7.90 (d, *J* = 8.5 Hz, 2H), 7.56 (d, *J* = 8.5 Hz, 2H), 7.46-7.35 (m, 4H), 7.28-7.22 (m, 1H), 7.21-7.15 (m, 1H), 6.74 (s, 1H). ¹³C NMR (CDCl₃, 100 MHz) δ 148.6, 140.6, 138.8, 138.6, 138.1, 138.1, 130.6, 129.4, 129.3, 128.4, 126.7, 126.7, 126.5, 126.1, 117.3, 97.4. HPLC (chiral column: DAICEL CHIRALPAK AD-H; solvent: hexane/2-propanol = 4/1; flow rate: 0.7 mL/min; detection: at 254 nm): t_R = 21.8 min (major) and 26.9 min (minor). R_f 0.40 (hexane/AcOEt = 3:1). The NMR spectra of the obtained product were consistent with the reported data.^[S4]





#	ピーク名	CH	tR [min]	Area%
1	Unknown	9	21.797	50.096
2	Unknown	9	26.910	49.904



#	ピーク名	CH	tR [min]	Area%
1	Unknown	9	21.793	91.614
2	Unknown	9	26.863	8.386

(S)-1-(4-(6-acetyl-1-oxido-3-phenyl-1H-benzo[e][1,2]thiazin-1-yl)phenyl)ethan-1-one (7ca): Prepared

according to GP-C using sulfoximine **4c** (0.20 mmol, 60.2 mg) and

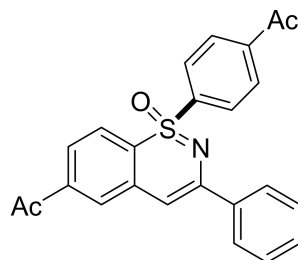
sulfoxonium ylide **6a** (0.30 mmol, 59.1 mg) afforded **7ca** as a yellow foam

(58.0 mg, 72%). $^1\text{H NMR}$ (CDCl_3 , 400 MHz) δ 8.14 (d, $J = 9.0$ Hz, 2H), 8.09

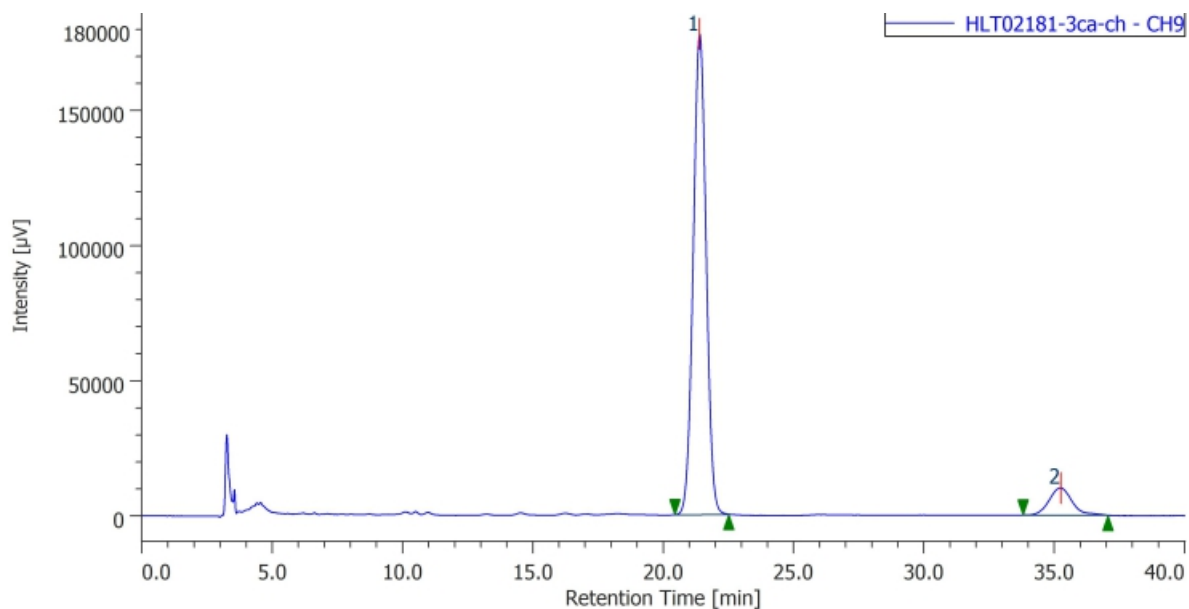
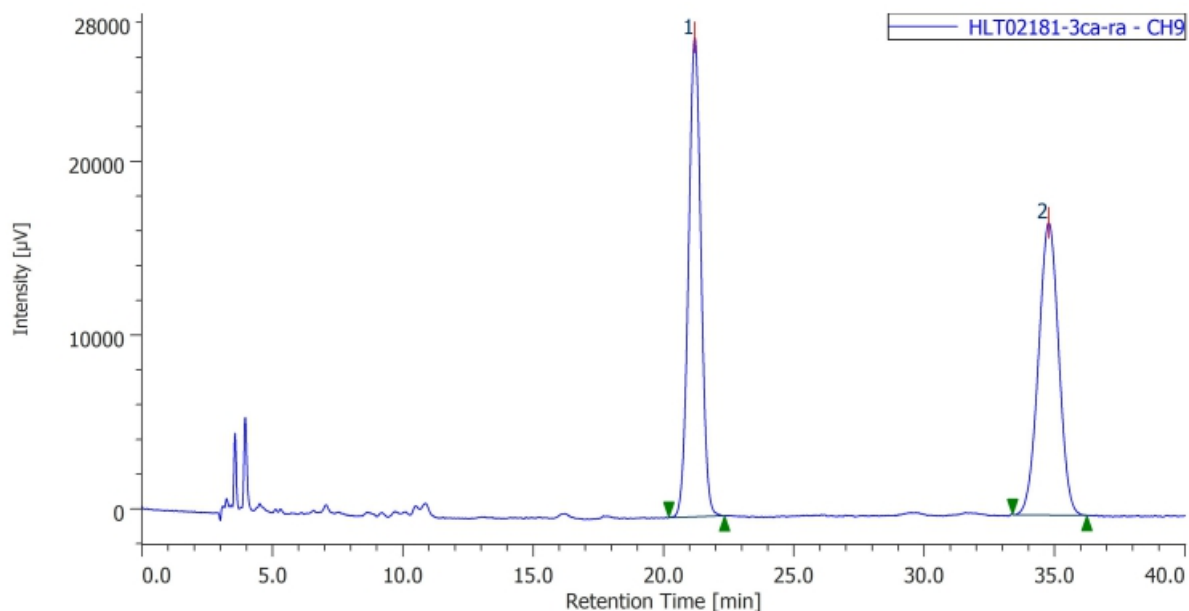
(d, $J = 8.5$ Hz, 3H), 8.04-7.97 (m, 3H), 7.75 (dd, $J = 8.5, 1.8$ Hz, 1H),

7.47-7.37 (m, 4H), 6.95 (s, 1H), 2.67 (s, 3H), 2.66 (s, 3H). $^{13}\text{C NMR}$ (CDCl_3 ,

100 MHz) δ 197.0, 196.6, 148.2, 143.6, 140.8, 139.7, 138.0, 136.8, 129.7, 129.3, 128.8, 128.5, 127.9, 126.7,

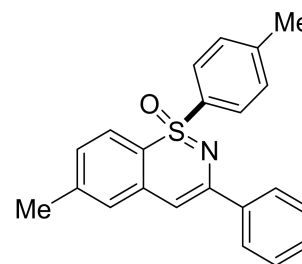


125.4, 124.9, 121.1, 98.6, 27.0, 26.8. **HPLC** (chiral column: DAICEL CHIRALPAK AD-H; solvent: hexane/2-propanol = 2/1; flow rate: 1.0 mL/min; detection: at 254 nm): t_R = 21.4 min (major) and 35.2 min (minor). **Rf** 0.30 (hexane/AcOEt = 1:1). The NMR spectra of the obtained product were consistent with the reported data.^[S4]



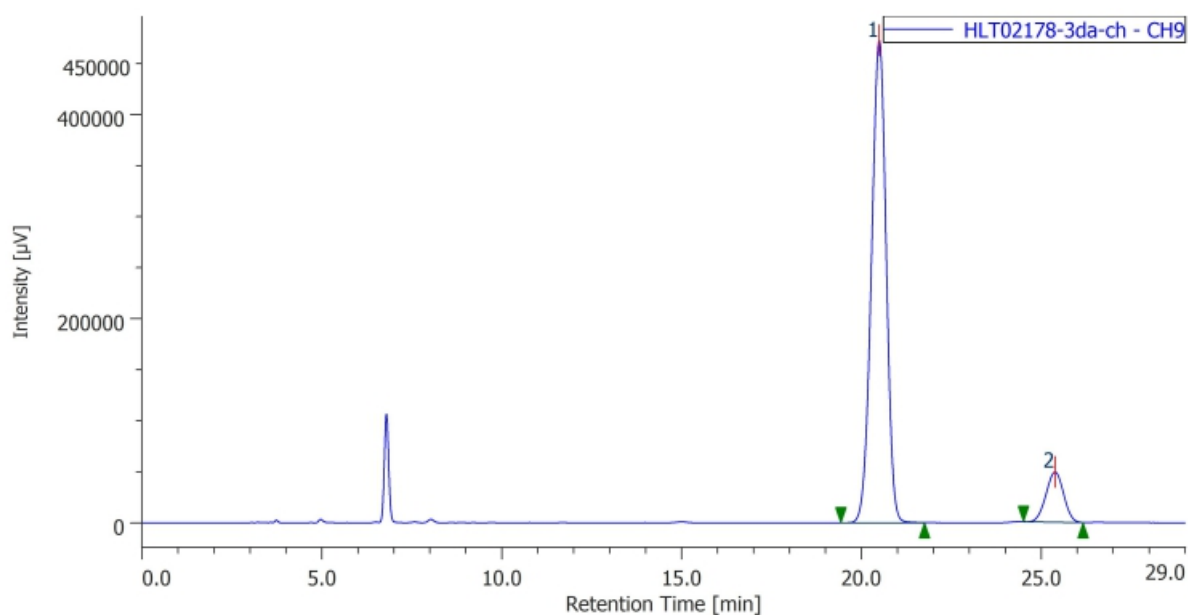
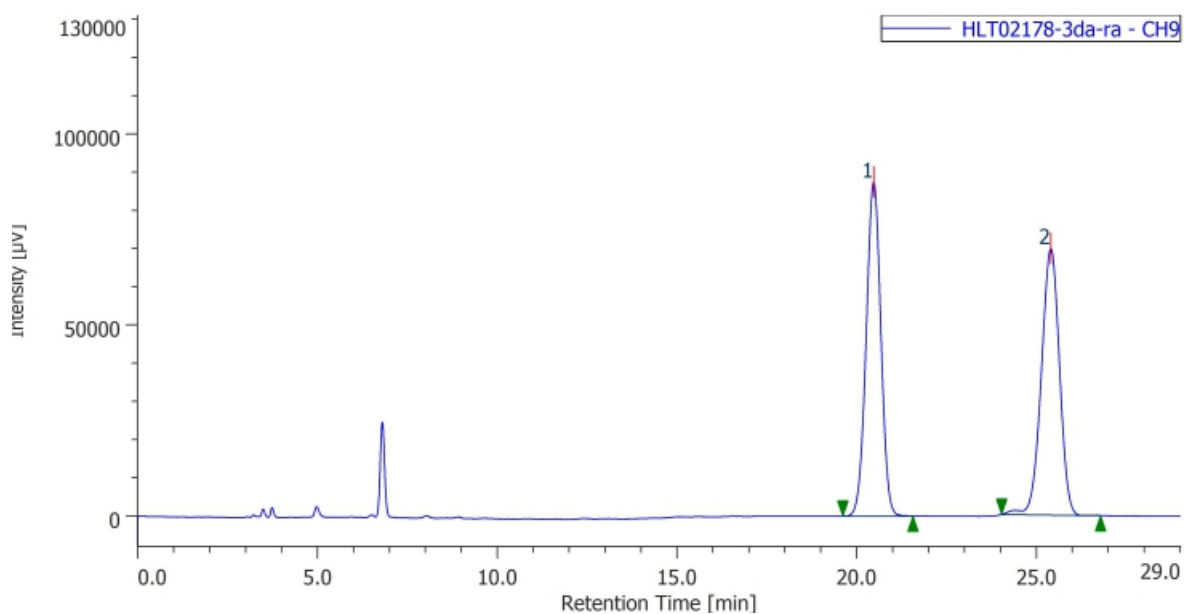
(S)-6-methyl-3-phenyl-1-(p-tolyl)benzo[e][1,2]thiazine-1-oxide (7da): Prepared according to **GP-C** using sulfoximine **4d** (0.20 mmol, 49.0 mg) and sulfoxonium ylide **6a** (0.30 mmol, 59.1 mg) afforded **7da** as a yellow foam (70.0 mg, >99%). ¹H NMR (CDCl₃, 400 MHz) δ 7.99 (d, J = 7.2 Hz, 2H), 7.85 (d, J = 8.5

Hz, 2H), 7.43-7.32 (m, 5H), 7.26-7.20 (m, 2H), 7.03 (d, $J = 9.0$ Hz, 1H), 6.73 (s, 1H), 2.44 (s, 3H), 2.39 (s, 3H). ^{13}C NMR (CDCl_3 , 100 MHz) δ 147.1, 144.2, 142.5, 138.9, 137.9, 136.6, 129.6, 129.2, 128.6, 128.3, 127.6, 126.6, 126.5, 124.8, 117.5, 97.9, 21.7, 21.5. HPLC (chiral column: DAICEL CHIRALPAK AD-H; solvent: hexane/2-propanol = 4/1; flow rate: 1.0

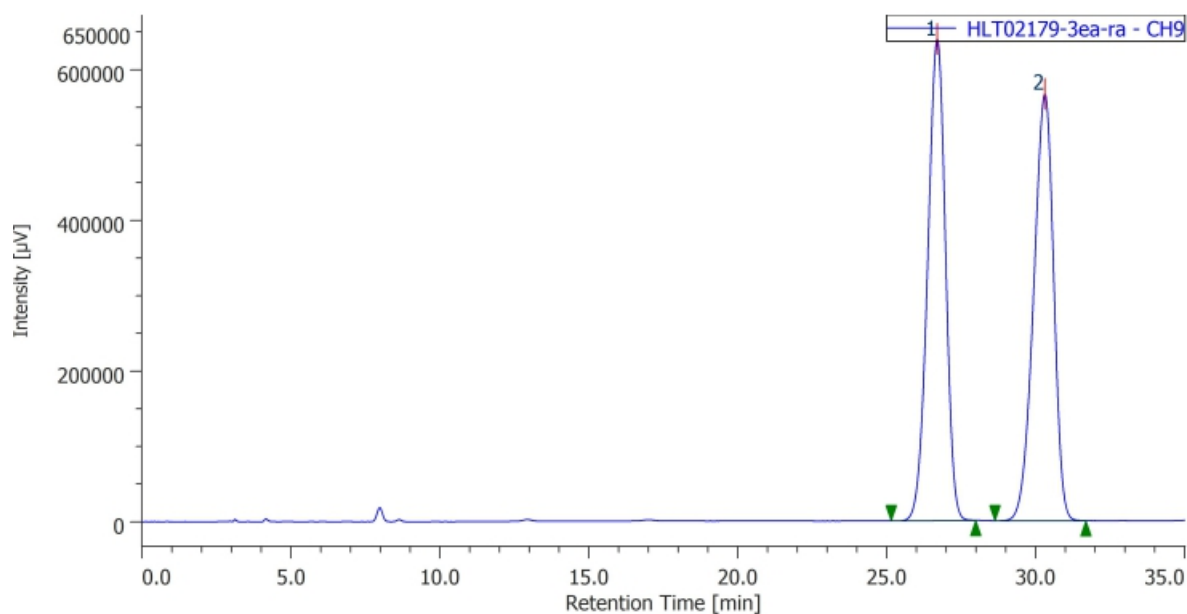
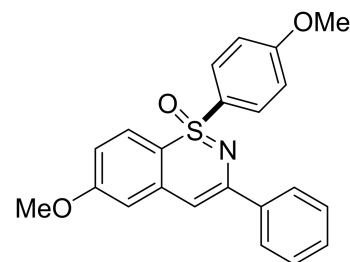


mL/min; detection: at 254 nm): $t_R = 20.5$ min (major) and 25.4 min (minor). **Rf** 0.50 (hexane/AcOEt = 4:1).

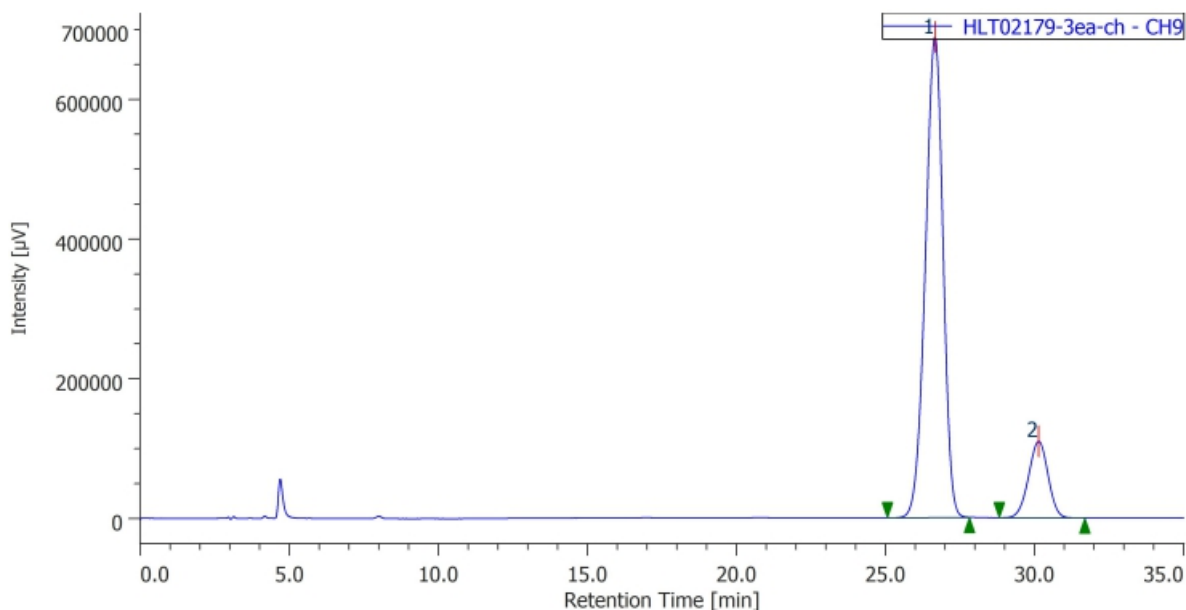
The NMR spectra of the obtained product were consistent with the reported data.^[S4]



(S)-6-methoxy-1-(4-methoxyphenyl)-3-phenylbenzo[e][1,2]thiazine 1-oxide (7ea): Prepared according to GP-C using sulfoximine **4e** (0.20 mmol, 55.4 mg) and sulfoxonium ylide **6a** (0.30 mmol, 59.1 mg) afforded **7ea** as a yellow foam (75.0 mg, >99%). ¹H NMR (CDCl₃, 400 MHz) δ 7.99 (d, *J* = 7.2 Hz, 2H), 7.89-7.86 (m, 2H), 7.44-7.33 (m, 3H), 7.28-7.24 (m, 1H), 7.03-6.99 (m, 3H), 6.82-6.77 (m, 2H), 6.71 (s, 1H), 3.89-3.86 (m, 6H). ¹³C NMR (CDCl₃, 100 MHz) δ 163.4, 162.0, 147.8, 138.9, 138.7, 132.6, 131.1, 128.7, 128.3, 126.9, 126.6, 115.8, 114.1, 113.3, 107.4, 98.0, 55.7, 55.5. HPLC (chiral column: DAICEL CHIRALPAK AD-H; solvent: hexane/2-propanol = 4/1; flow rate: 1.2 mL/min; detection: at 254 nm): t_R = 26.7 min (major) and 30.1 min (minor). R_f 0.50 (hexane/AcOEt = 4:1). The NMR spectra of the obtained product were consistent with the reported data.^[S4]

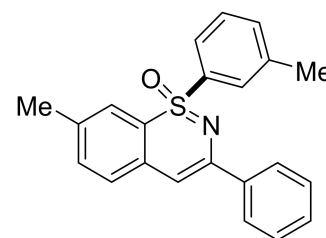


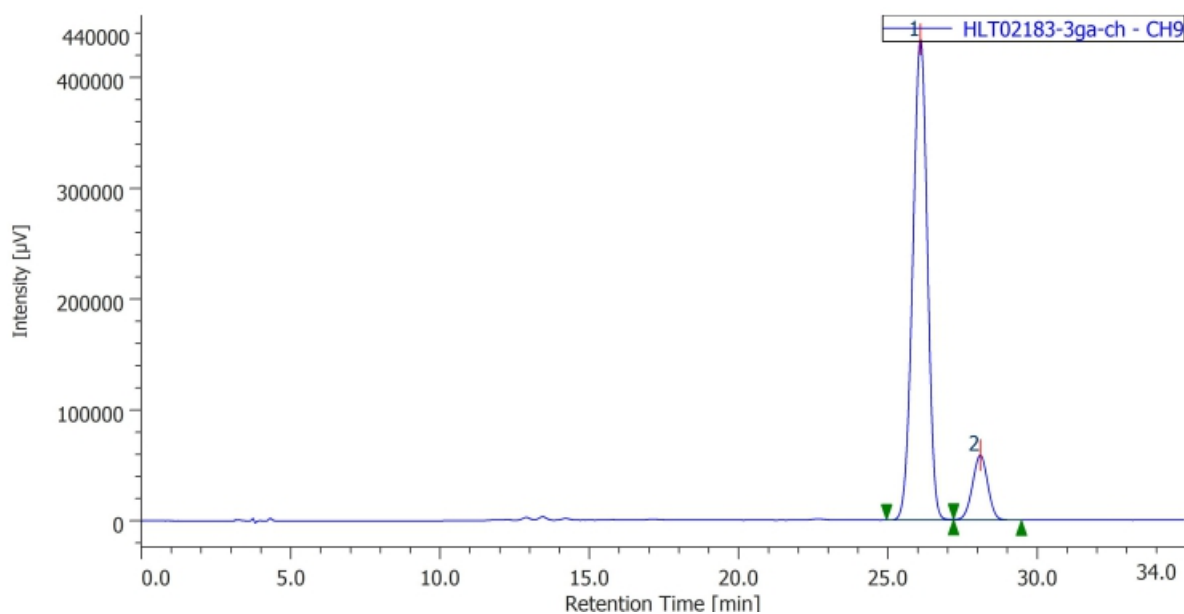
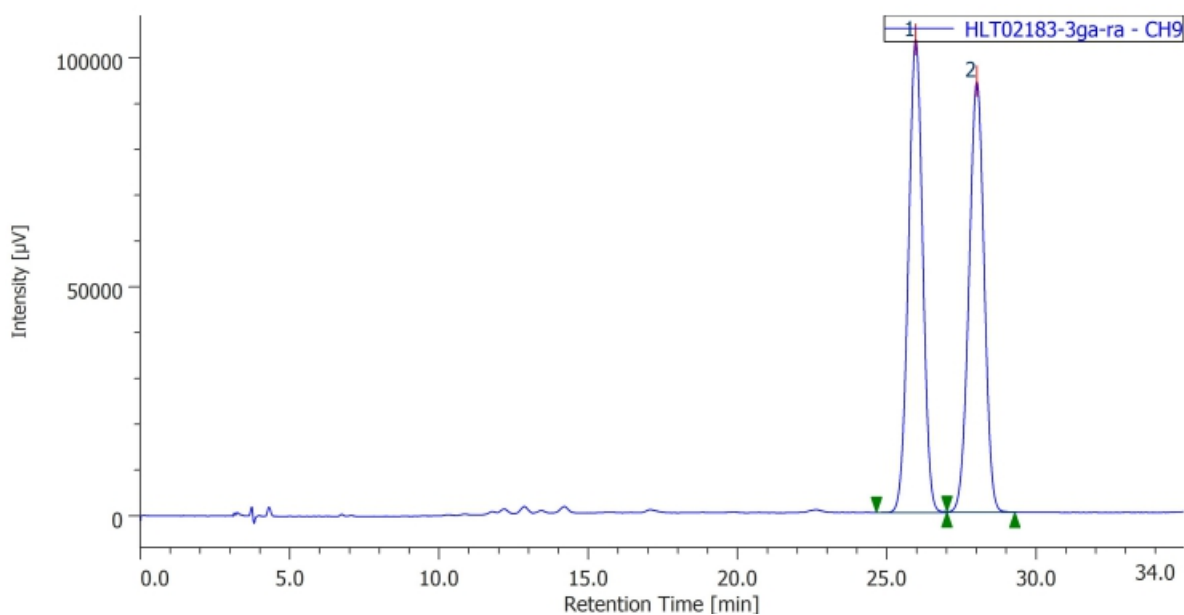
#	ピーク名	CH	tR [min]	Area%
1	Unknown	9	26.687	50.101
2	Unknown	9	30.300	49.899



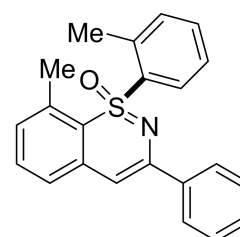
#	ピーク名	CH	tR [min]	Area%
1	Unknown	9	26.650	85.045
2	Unknown	9	30.127	14.955

(S)-7-methyl-3-phenyl-1-(m-tolyl)benzo[e][1,2]thiazine-1-oxide (7fa): Prepared according to **GP-C** using sulfoximine **4f** (0.20 mmol, 49.0 mg) and sulfoxonium ylide **6a** (0.30 mmol, 59.1 mg) afforded **7fa** as a yellow foam (69.0 mg, >99%). $^1\text{H NMR}$ (CDCl_3 , 400 MHz) δ 7.99 (dd, $J = 7.2, 1.6$ Hz, 2H), 7.81 (d, $J = 7.2$ Hz, 1H), 7.77 (s, 1H), 7.49-7.28 (m, 7H), 7.11 (s, 1H), 6.78 (s, 1H), 2.43 (s, 3H), 2.30 (s, 3H). $^{13}\text{C NMR}$ (CDCl_3 , 100 MHz) δ 146.1, 140.4, 139.2, 138.9, 136.5, 134.1, 134.1, 133.6, 129.6, 128.8, 128.5, 128.3, 126.8, 126.5, 124.2, 119.6, 98.0, 21.3, 21.3. **HPLC** (chiral column: DAICEL CHIRALPAK AD-H; solvent: hexane/2-propanol = 19/1; flow rate: 1.0 mL/min; detection: at 254 nm): $t_R = 26.1$ min (major) and 28.1 min (minor). **Rf** 0.40 (hexane/AcOEt = 4:1). The NMR spectra of the obtained product were consistent with the reported data.^[S4]

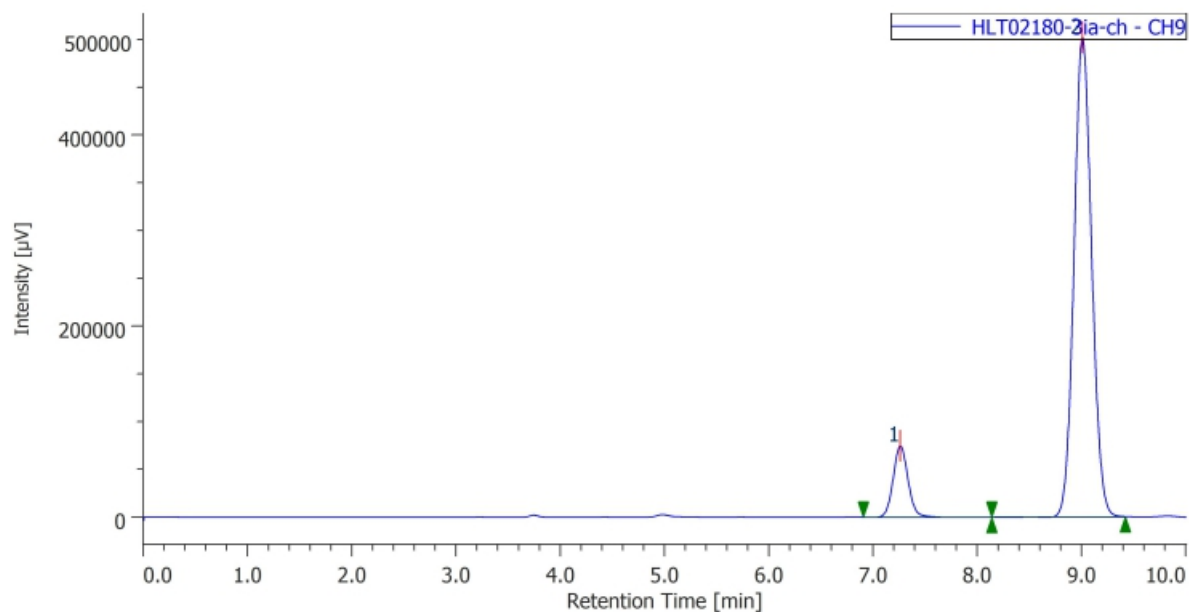
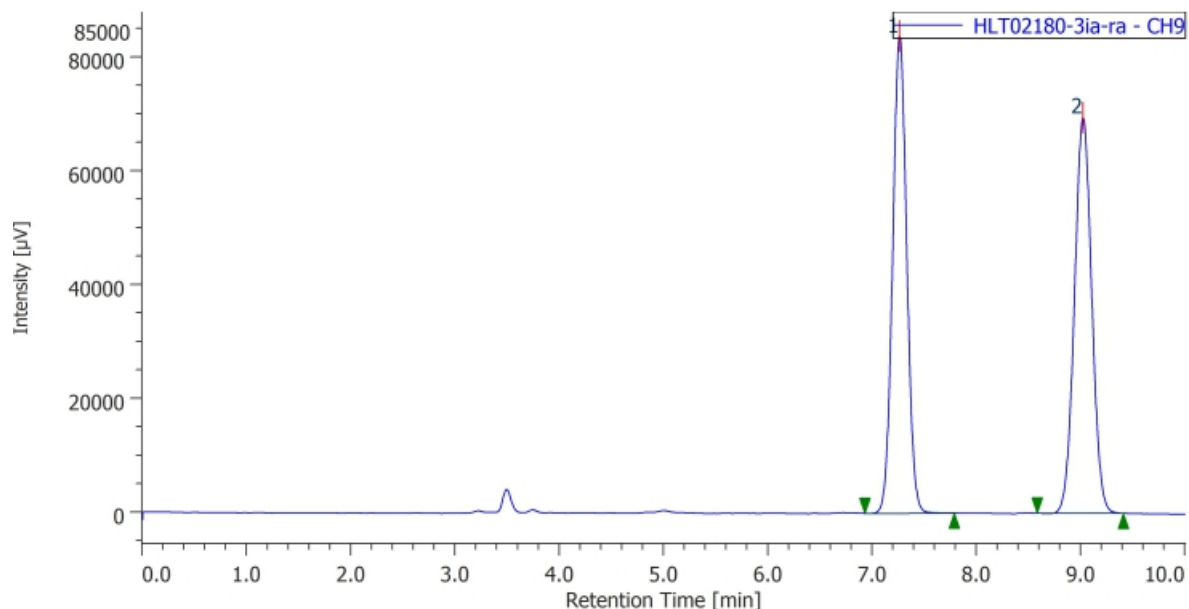




(S)-8-methyl-3-phenyl-1-(o-tolyl)benzo[e][1,2]thiazine-1-oxide (7ga): Prepared according to GP-C using sulfoximine **4g** (0.20 mmol, 49.0 mg) and sulfoxonium ylide **6a** (0.30 mmol, 59.1 mg) afforded **7ga** as a yellow foam (70.0 mg, >99%). ¹H NMR (CDCl₃, 400 MHz) δ 8.44-8.38 (m, 1H), 7.97-7.91 (m, 2H), 7.52-7.47 (m, 2H), 7.45-7.28 (m, 5H), 7.24-7.18 (m, 1H), 7.02 (d, *J* = 7.6 Hz, 1H), 6.76 (s, 1H), 2.08 (s, 3H), 1.73 (s, 3H). ¹³C NMR (CDCl₃, 100 MHz) δ 146.2, 140.5, 140.0, 138.5, 135.4, 133.4, 132.8, 132.3, 129.2, 128.7, 128.6, 128.3, 126.4, 126.2, 125.5, 117.0, 97.8, 20.1, 19.1. One aromatic signal was



missing probably due to overlapping. **HPLC** (chiral column: DAICEL CHIRALPAK AD-H; solvent: hexane/2-propanol = 4/1; flow rate: 1.0 mL/min; detection: at 254 nm): t_R = 7.3 min (minor) and 9.0 min (major). **Rf** 0.50 (hexane/AcOEt = 4:1). The NMR spectra of the obtained product were consistent with the reported data.^[S4]



(S)-1-phenyl-3-(p-tolyl)benzo[e][1,2]thiazine-1-oxide (7ab): Prepared according to **GP-C** using sulfoximine **4a** (0.20 mmol, 43.4 mg) and sulfoxonium ylide **6b** (0.30 mmol, 63.3 mg) afforded **7ab** as a yellow foam (66.0 mg, >99%). ¹H NMR (CDCl₃, 400 MHz) δ 7.99 (d, J = 7.2 Hz, 2H), 7.90 (d, J = 8.5 Hz,

2H), 7.63 (t, $J = 7.2$ Hz, 1H), 7.56 (t, $J = 7.2$ Hz, 2H), 7.47 (t, $J = 7.4$ Hz, 1H).

7.42 (d, $J = 7.2$ Hz, 1H), 7.32 (d, $J = 7.6$ Hz, 1H), 7.26-7.17 (m, 3H), 6.78 (s,

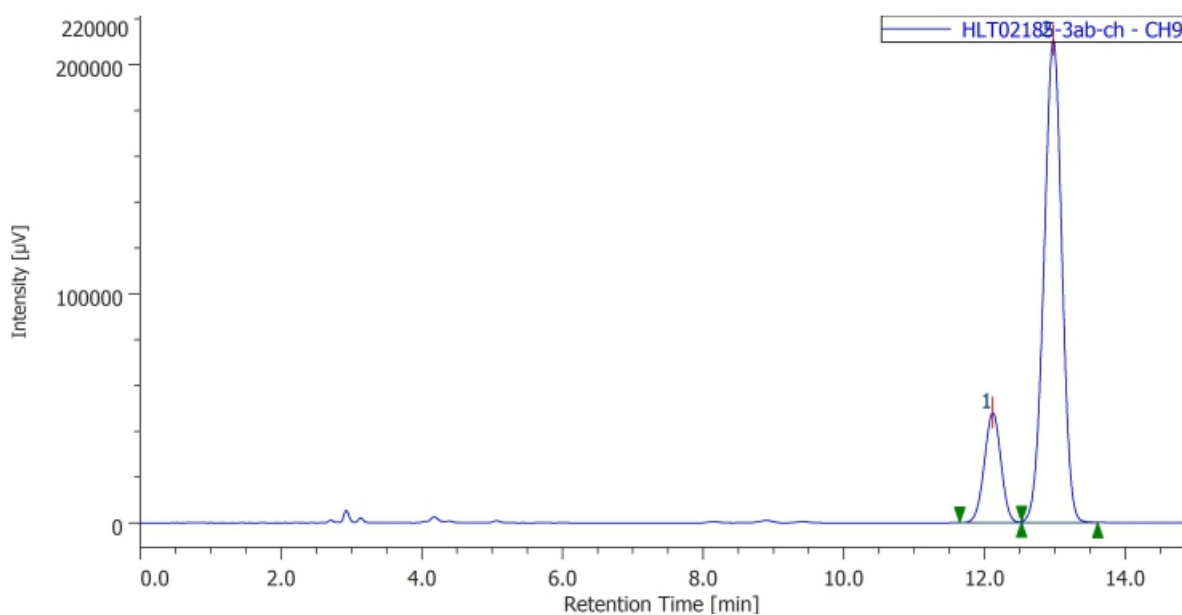
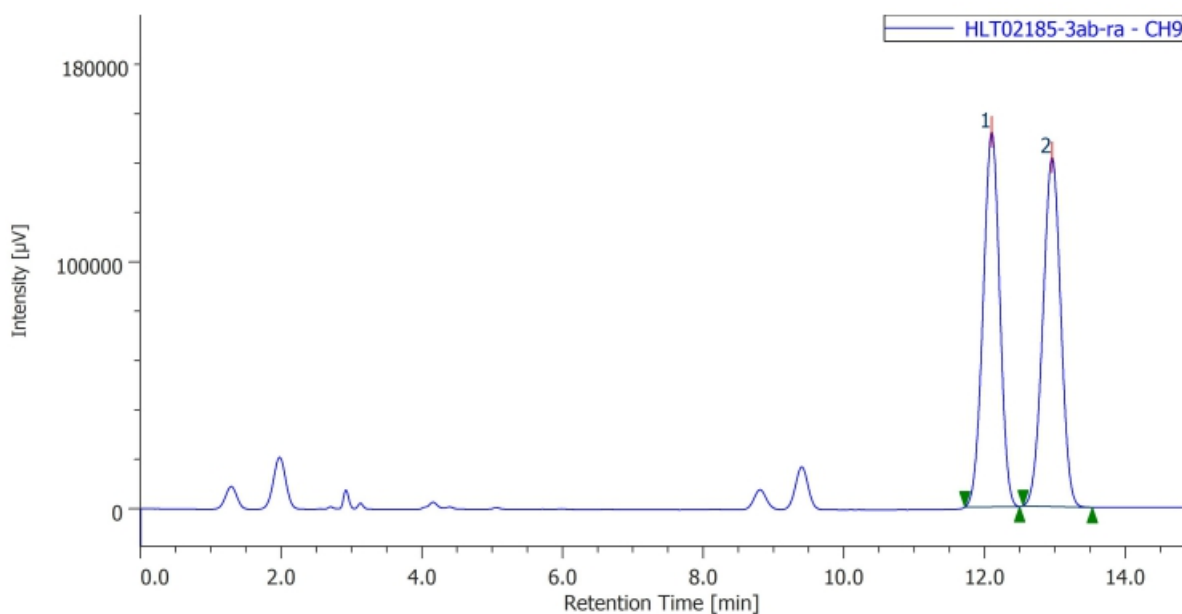
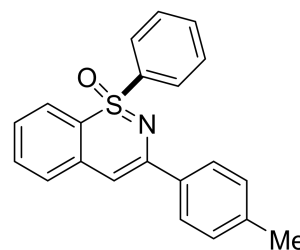
1H), 2.38 (s, 3H). ^{13}C NMR (CDCl_3 , 100 MHz) δ 147.2, 140.4, 138.8, 136.6,

135.9, 133.3, 132.0, 129.3, 129.0, 128.9, 126.7, 126.5, 126.0, 124.9, 119.4,

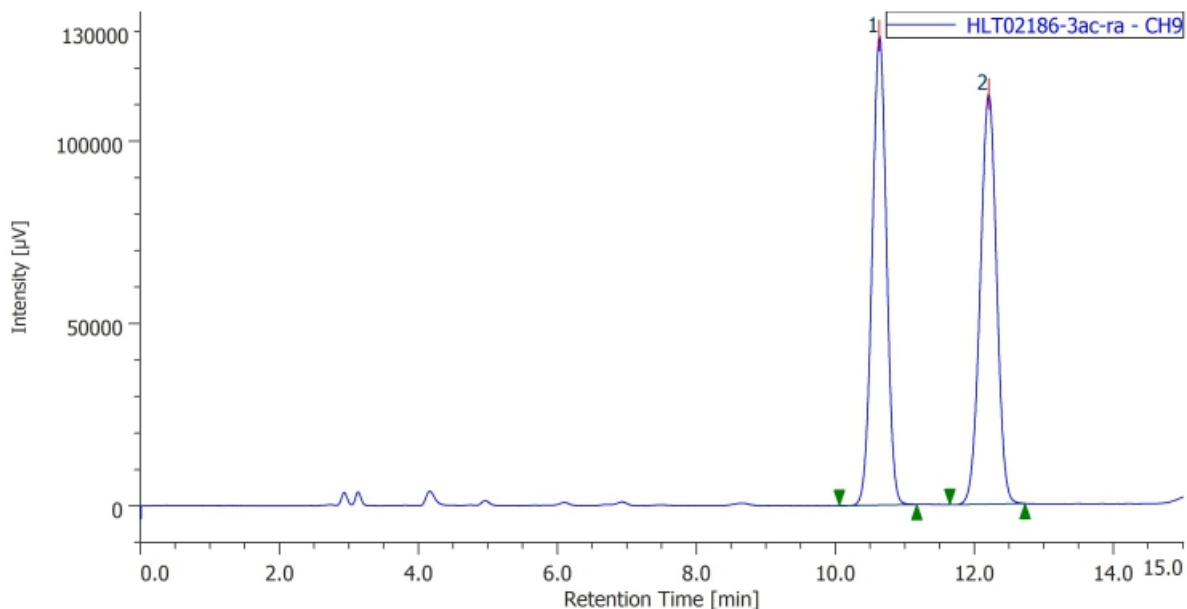
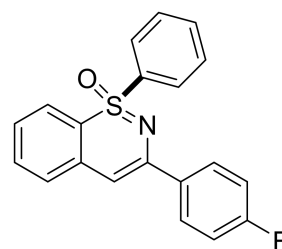
97.5, 21.3. **HPLC** (chiral column: DAICEL CHIRALPAK AD-H; solvent: hexane/2-propanol = 4/1; flow

rate: 1.2 mL/min; detection: at 254 nm): $t_R = 12.1$ min (minor) and 13.0 min (major). **Rf** 0.50

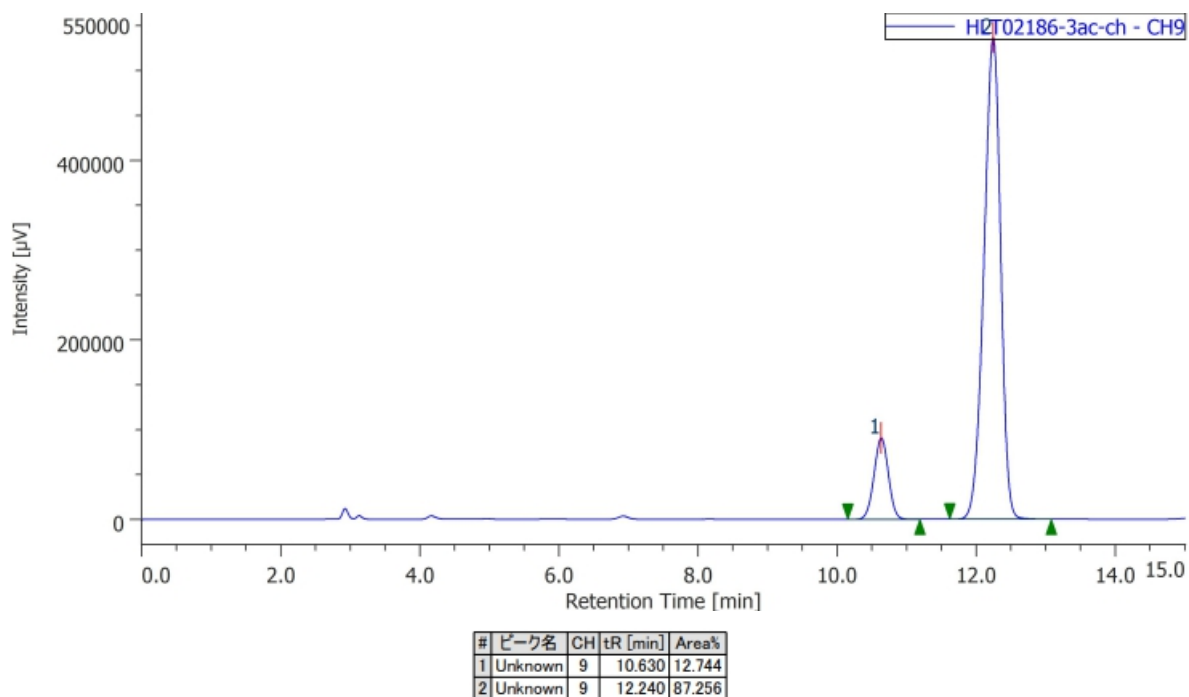
(hexane/AcOEt = 5:1). The NMR spectra of the obtained product were consistent with the reported data.^[S4]



(S)-3-(4-fluorophenyl)-1-phenylbenzo[e][1,2]thiazine 1-oxide (7ac): Prepared according to **GP-C** using sulfoximine **4a** (0.20 mmol, 43.4 mg) and sulfoxonium ylide **6c** (0.30 mmol, 64.2 mg) afforded **7ac** as a yellow foam (60.0 mg, 90%). ¹H NMR (CDCl₃, 400 MHz) δ 7.97-7.88 (m, 4H), 7.61-7.56 (m, 1H), 7.54-7.49 (m, 2H), 7.45-7.40 (m, 1H), 7.36 (d, *J* = 7.6 Hz, 1H), 7.25 (d, *J* = 8.1 Hz, 1H), 7.19-7.13 (m, 1H), 7.05-6.99 (m, 2H), 6.68 (s, 1H). ¹³C NMR (CDCl₃, 100 MHz) δ 163.3(d, ¹*J*_{C-F} = 248.0 Hz), 146.1, 140.1, 136.3, 134.9(d, ⁴*J*_{C-F} = 2.8 Hz), 133.4, 132.1, 129.3, 129.0, 128.4 (d, ³*J*_{C-F} = 8.5 Hz), 126.8, 126.3, 124.9, 119.4, 115.2 (d, ²*J*_{C-F} = 21.6 Hz), 97.9. **HPLC** (chiral column: DAICEL CHIRALPAK AD-H; solvent: hexane/2-propanol = 4/1; flow rate: 1.2 mL/min; detection: at 254 nm): *t*_R = 10.6 min (minor) and 12.2 min (major). **Rf** 0.30 (hexane/AcOEt = 5:1). The NMR spectra of the obtained product were consistent with the reported data.^[S4]

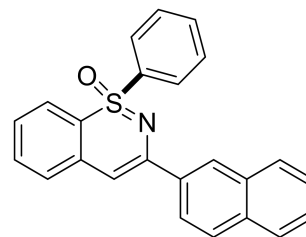


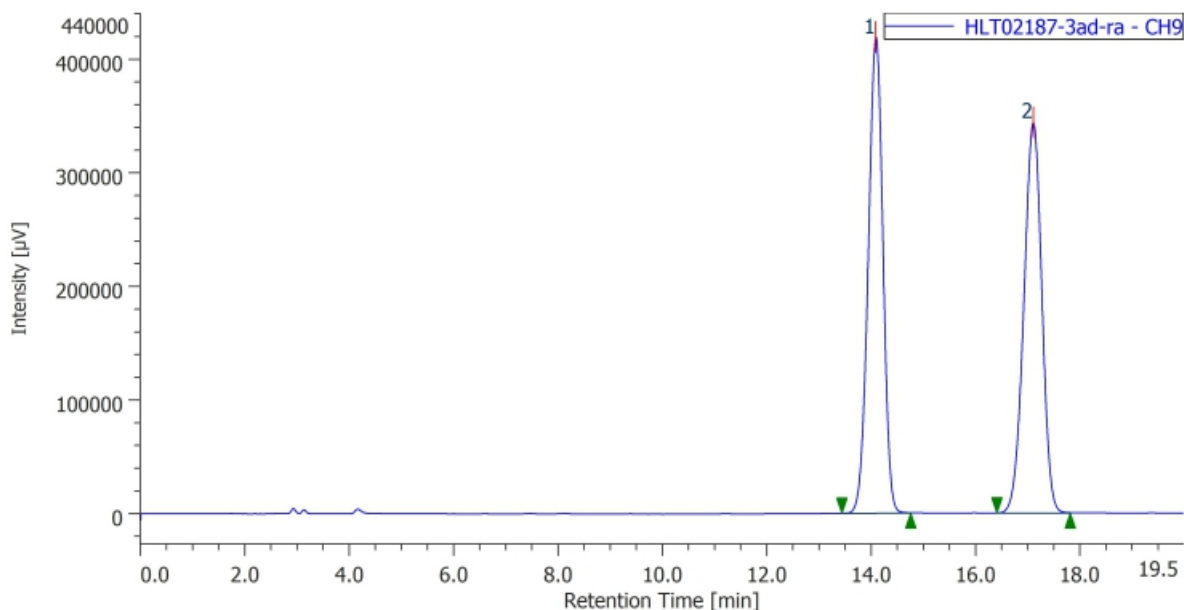
#	ピーク名	CH	tR [min]	Area%
1	Unknown	9	10.630	49.972
2	Unknown	9	12.203	50.028



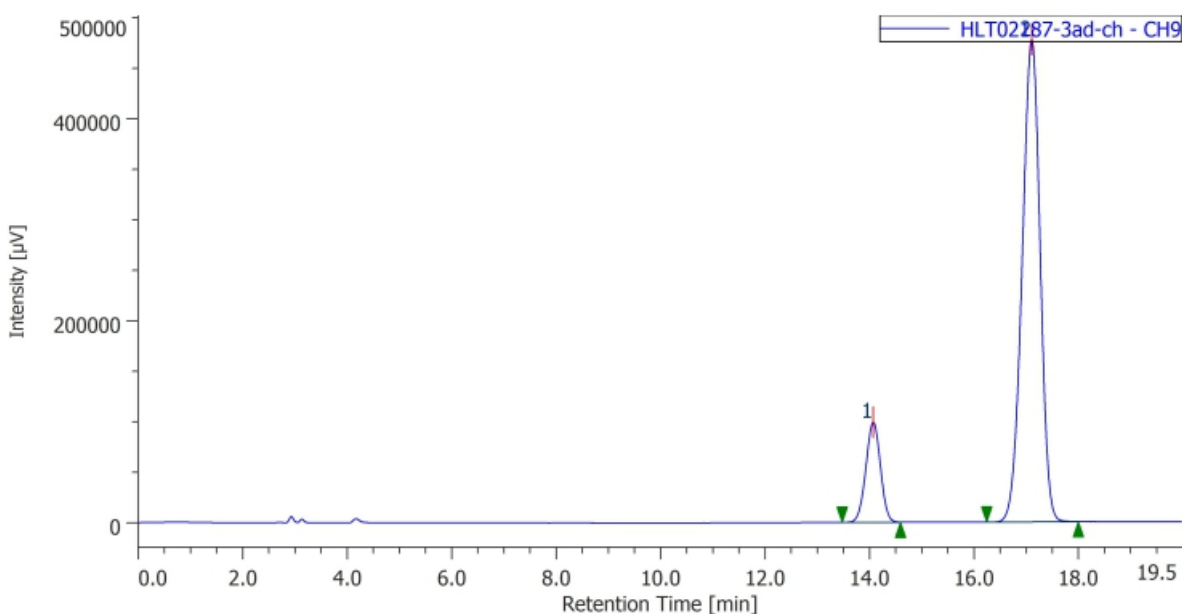
(S)-3-(naphthalen-2-yl)-1-phenylbenzo[e][1,2]thiazine-1-oxide (7ad): Prepared according to GP-C using sulfoximine **4a** (0.20 mmol, 43.4 mg) and sulfoxonium ylide **6d** (0.30 mmol, 73.8 mg) afforded **7ad** as a yellow foam (68.0 mg, 92%). ¹H NMR (CDCl₃, 400 MHz) δ 8.55 (s, 1H), 8.10-8.01 (m, 3H), 7.91-7.80 (m, 3H), 7.67-7.55 (m, 3H), 7.51-7.44 (m, 4H), 7.34 (d, *J* = 7.6 Hz, 1H), 7.26- 7.19 (m, 1H), 6.96 (s, 1H). ¹³C NMR (CDCl₃, 100 MHz) δ 146.9, 140.4, 136.4, 135.9, 133.6, 133.4, 133.4, 132.1, 129.4, 129.0, 128.8, 127.8, 127.5, 127.0, 126.4, 126.4, 126.3, 126.1, 125.0, 124.0, 119.8, 98.7.

HPLC (chiral column: DAICEL CHIRALPAK AD-H; solvent: hexane/2-propanol = 4/1; flow rate: 1.2 mL/min; detection: at 254 nm): t_R = 14.1 min (minor) and 17.1 min (major). **Rf** 0.60 (hexane/AcOEt = 8:1). The NMR spectra of the obtained product were consistent with the reported data.^[S4]



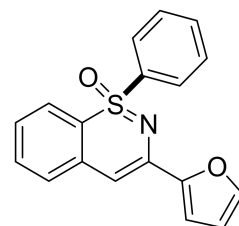


#	ピーク名	CH	tR [min]	Area%
1	Unknown	9	14.087	49.947
2	Unknown	9	17.103	50.053

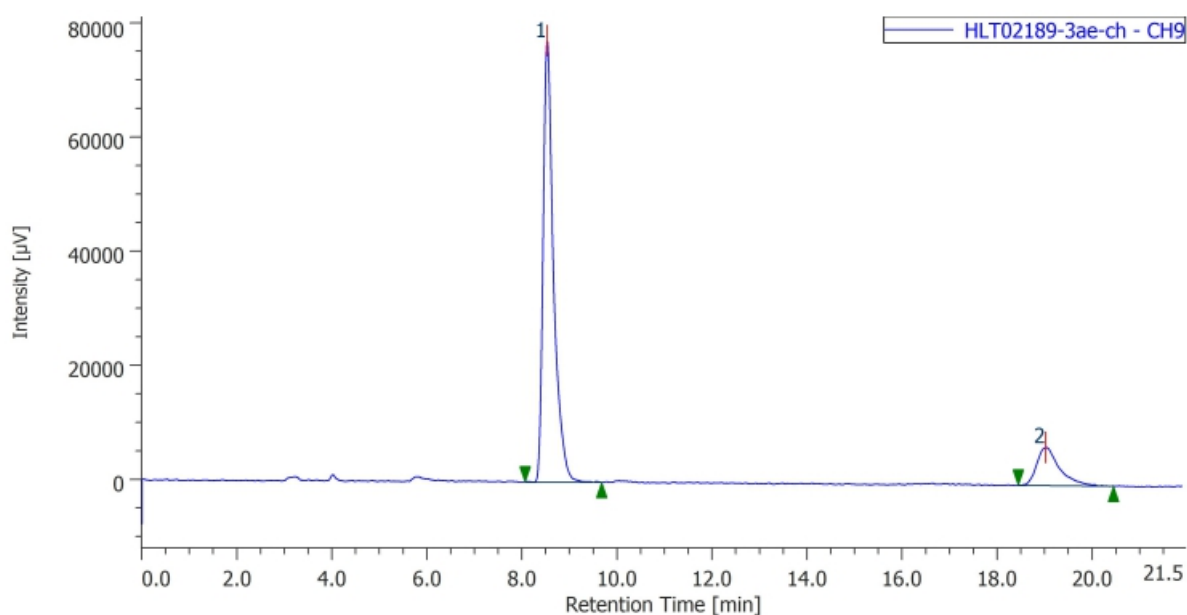
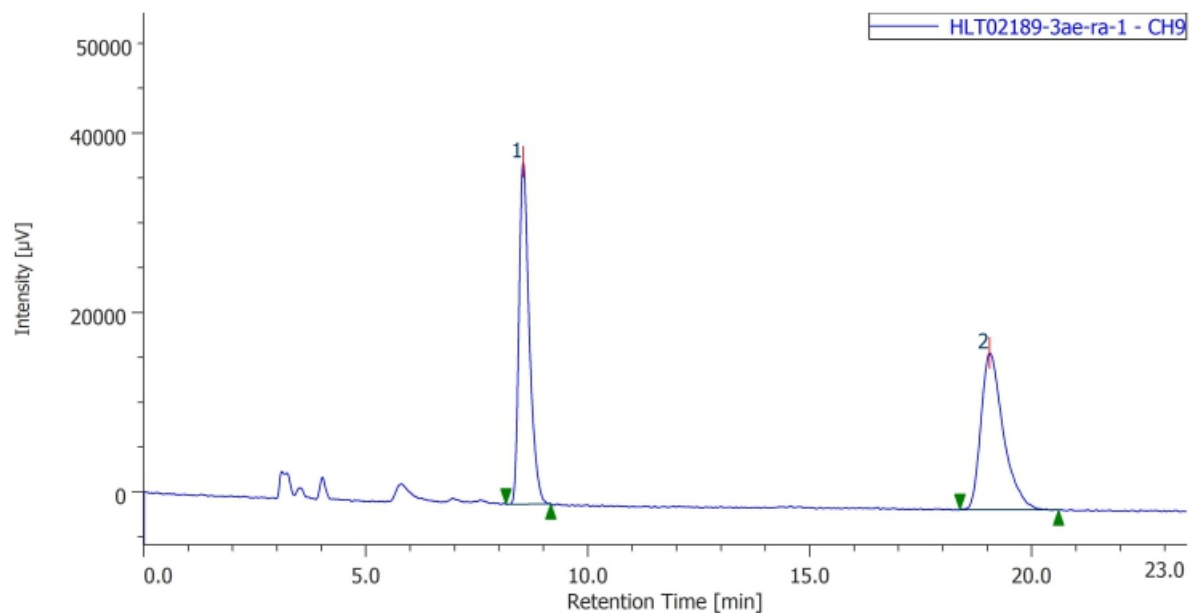


#	ピーク名	CH	tR [min]	Area%
1	Unknown	9	14.067	14.429
2	Unknown	9	17.100	85.571

(S)-3-(furan-2-yl)-1-phenylbenzo[e][1,2]thiazine-1-oxide (7ae): Prepared according to GP-C using sulfoximine **4a** (0.20 mmol, 43.4 mg) and sulfoxonium ylide **6e** (0.30 mmol, 54.9 mg) afforded **7ae** as a brown foam (62.0 mg, >99%). ^1H NMR (CDCl_3 , 400 MHz) δ 7.94-7.88 (m, 2H), 7.59-7.54 (m, 1H), 7.53-7.47 (m, 2H), 7.42-7.32 (m, 3H), 7.21 (d, J = 7.6, 1H), 7.14-7.10 (m, 1H), 6.83 (d, J = 3.6 Hz, 1H), 6.73 (s, 1H), 6.40 (dd, J = 3.6, 1.8, 1H). ^{13}C NMR (CDCl_3 , 100 MHz) δ 153.3, 143.0, 140.0, 138.5, 136.1, 133.4, 132.1, 129.4, 129.0, 126.8, 126.1, 125.0, 120.1, 111.8, 109.4, 96.4. HPLC (chiral column: DAICEL

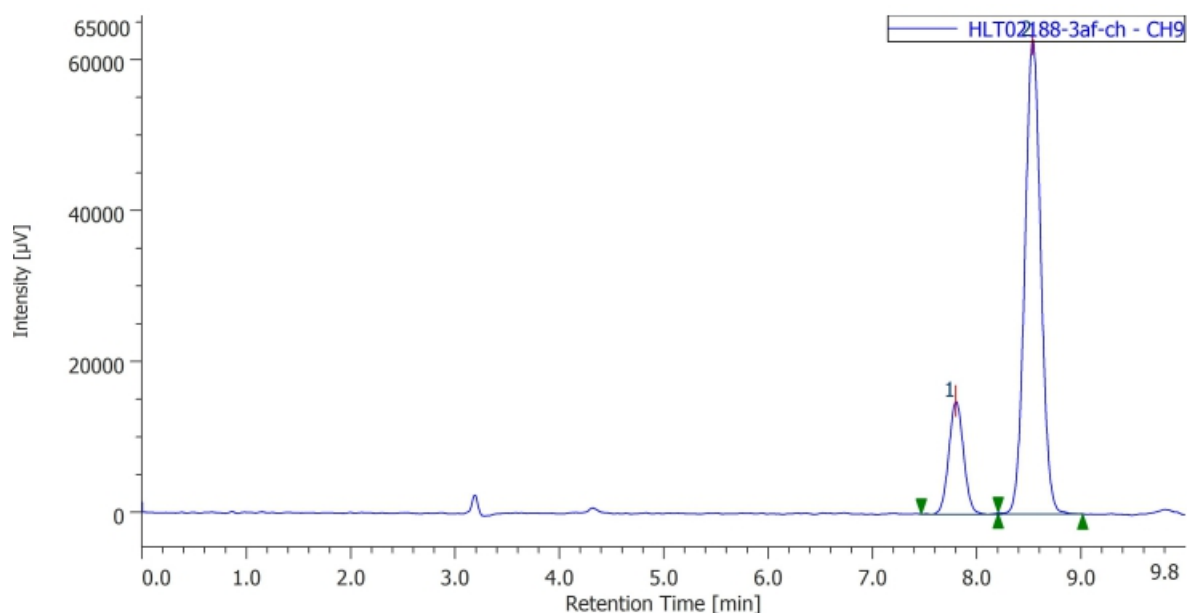
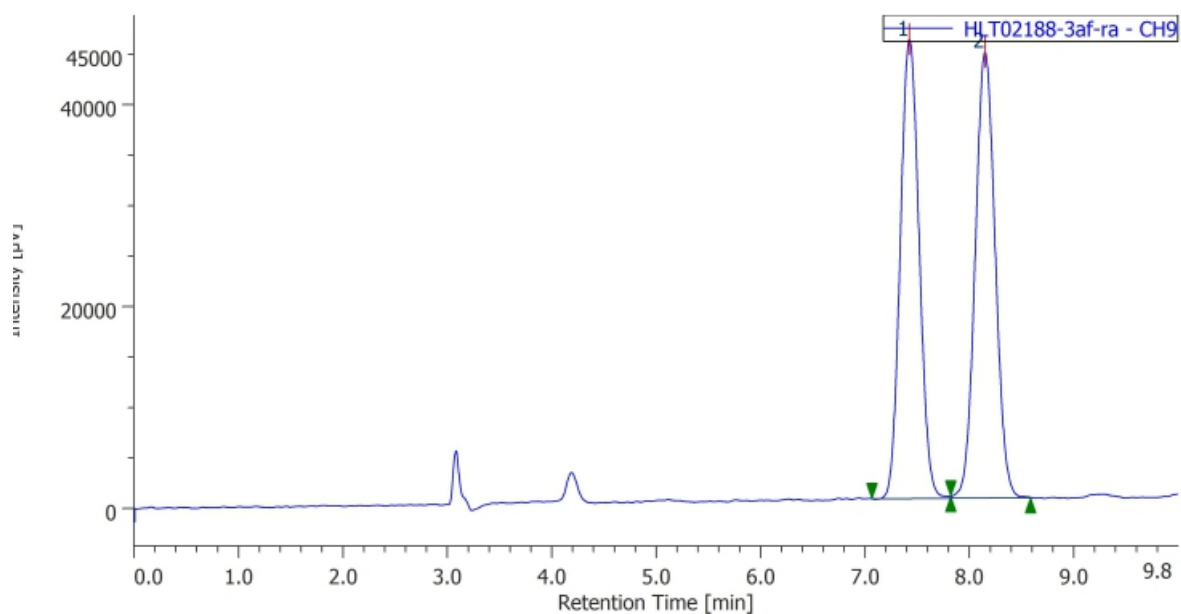
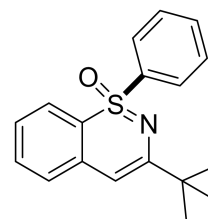


CHIRALPAK IB; solvent: hexane/2-propanol = 4/1; flow rate: 1.0 mL/min; detection: at 254 nm): t_R = 8.5 min (major) and 19.1 min (minor). **Rf** 0.60 (hexane/AcOEt = 1:1). The NMR spectra of the obtained product were consistent with the reported data.^[S4]



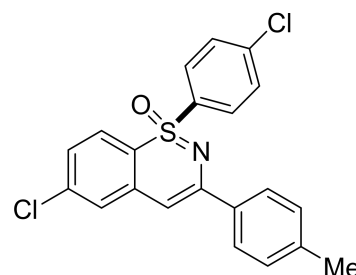
(S)-3-(tert-butyl)-1-phenylbenzo[e][1,2]thiazine-1-oxide (7af): Prepared according to GP-C using sulfoximine **4a** (0.20 mmol, 43.4 mg) and sulfoxonium ylide **6f** (0.30 mmol, 52.8 mg) afforded **7af** as a yellow foam (60.0 mg, >99%). ¹H NMR (CDCl₃, 400 MHz) δ 7.89-7.81 (m, 2H), 7.56-7.45 (m, 3H), 7.36-7.31 (m, 1H), 7.25-7.17 (m, 2H), 7.11-7.06 (m, 1H), 6.12 (s, 1H), 1.27 (s, 9H). ¹³C NMR (CDCl₃, 100

MHz) δ 159.7, 141.0, 136.6, 133.0, 131.7, 129.1, 128.8, 126.5, 125.6, 124.7, 118.6, 95.0, 37.5, 28.9. **HPLC** (chiral column: DAICEL CHIRALPAK IF; solvent: hexane/2-propanol = 19/1; flow rate: 1.0 mL/min; detection: at 254 nm): t_R = 7.8 min (minor) and 8.5 min (major). **Rf** 0.50 (hexane/AcOEt = 6:1). The NMR spectra of the obtained product were consistent with the reported data.^[S4]

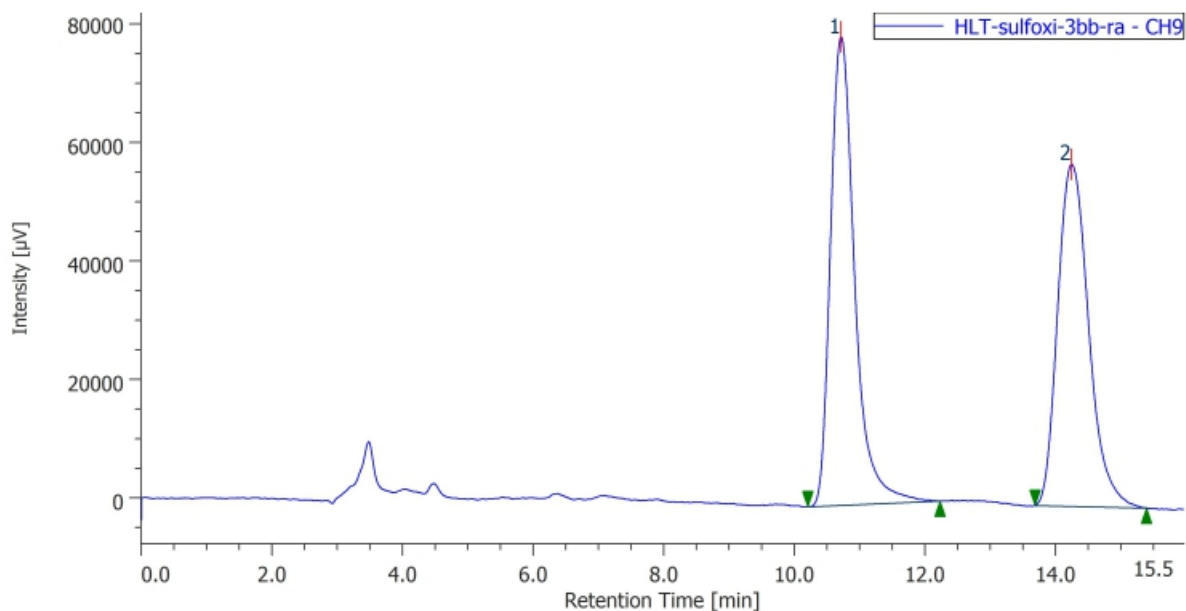


(S)-6-chloro-1-(4-chlorophenyl)-3-(p-tolyl)benzo[e][1,2]thiazine-1-oxide (7bb): Prepared according to GP-C using sulfoximine **4b** (0.20 mmol, 56.8 mg) and sulfoxonium ylide **6b** (0.30 mmol, 63.3 mg)

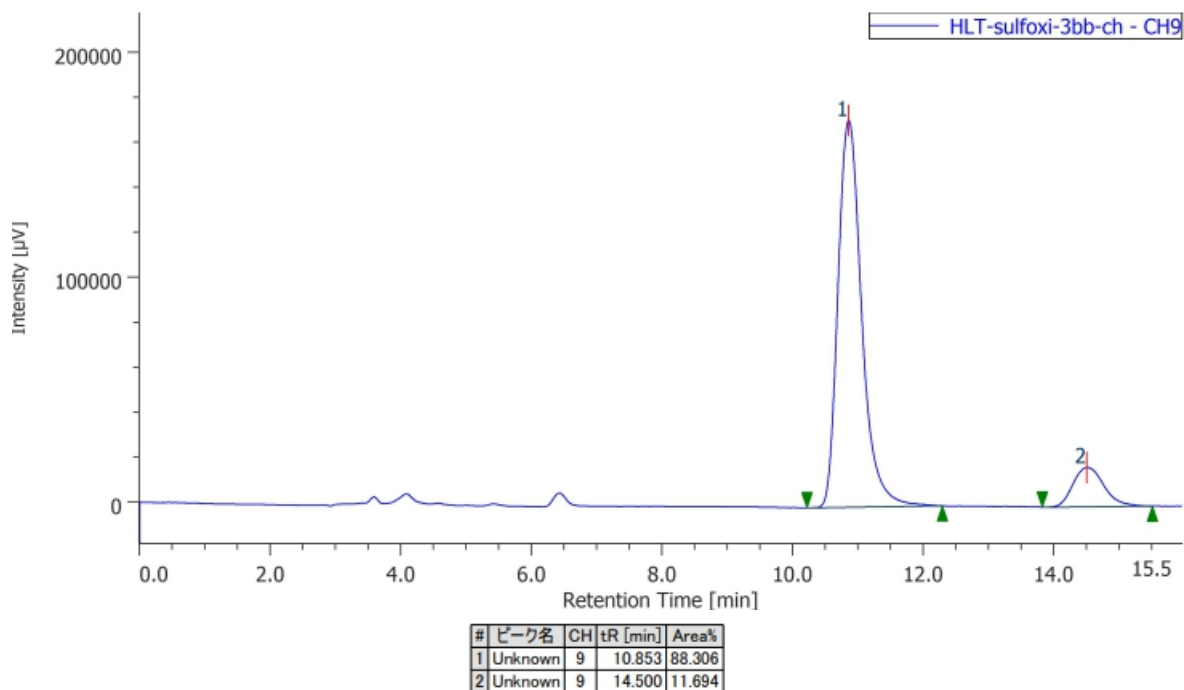
afforded **7bb** as a yellow solid (54.0 mg, 68%). **¹H NMR** (CDCl₃, 400 MHz) δ 7.83-7.78 (m, 4H), 7.50-7.46 (m, 2H), 7.34 (d, *J* = 1.8 Hz, 1H), 7.17 (t, *J* = 8.0 Hz, 3H), 7.09 (dd, *J* = 8.0, 1.8 Hz, 1H), 6.63 (s, 1H), 2.32 (s, 3H). **¹³C NMR** (CDCl₃, 100 MHz) δ 148.6, 140.5, 139.4, 138.9, 138.5, 138.2, 135.3, 130.5, 129.4, 129.2, 126.6, 126.5, 126.4, 125.9, 117.1, 96.8, 21.3. **HPLC** (chiral column: DAICEL CHIRALPAK IA;



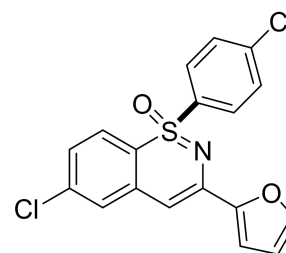
solvent: hexane/2-propanol = 2/1; flow rate: 1.0 mL/min; detection: at 254 nm): *t_R* = 10.8 min (major) and 14.4 min (minor). **HRMS** (ESI): *m/z* calculated for C₂₁H₁₅Cl₂NOSNa⁺ [M+Na]⁺: 422.0144, found: 422.0137. [α]_D²⁴ = +160.4 (*c* = 0.50, CHCl₃). **R_f** 0.50 (hexane/AcOEt = 6:1).

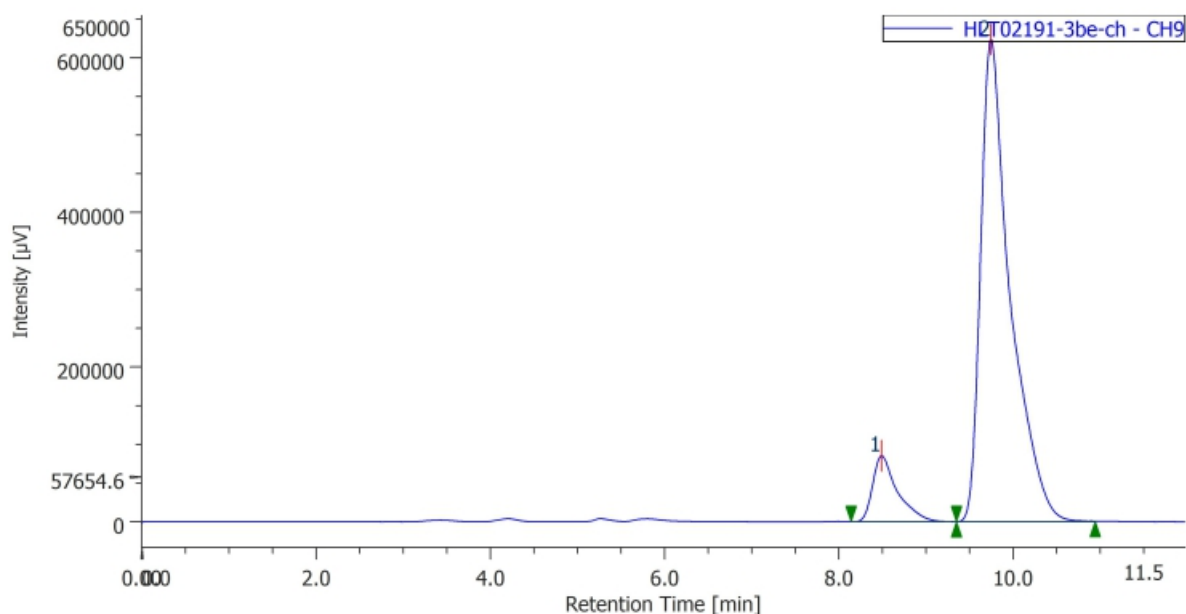
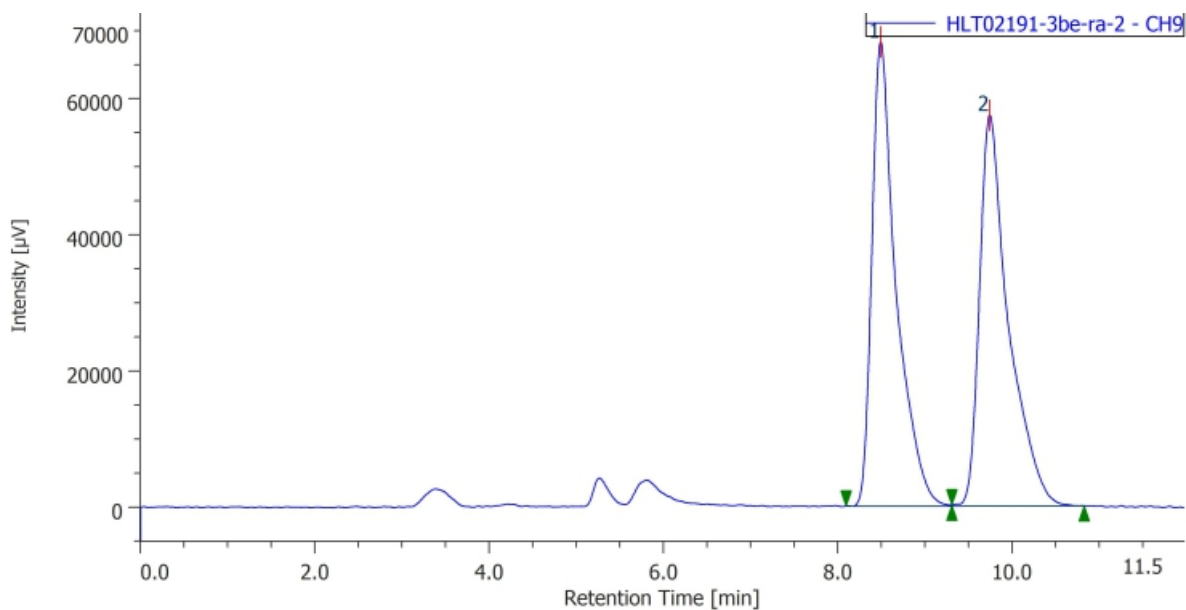


#	ピーク名	CH	tR [min]	Area%
1	Unknown	9	10.713	51.692
2	Unknown	9	14.240	48.308

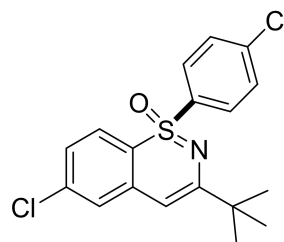


(S)-6-chloro-1-(4-chlorophenyl)-3-(furan-2-yl)benzo[e][1,2]thiazine-1-oxide (7be): Prepared according to **GP-C** using sulfoximine **4b** (0.20 mmol, 56.8 mg) and sulfoxonium ylide **6e** (0.30 mmol, 54.9 mg) afforded **7be** as a yellow solid (74.0 mg, >99%). ¹H NMR (CDCl₃, 400 MHz) δ 7.81 (d, *J* = 8.5 Hz, 2H), 7.48 (d, *J* = 8.5 Hz, 2H), 7.43 (s, 1H), 7.32 (s, 1H), 7.14 (d, *J* = 8.5 Hz, 1H), 7.08 (d, *J* = 9.0 Hz, 1H), 6.83 (d, *J* = 3.1 Hz, 1H), 6.65 (s, 1H), 6.42 (dd, *J* = 2.9, 1.6 Hz, 1H). ¹³C NMR (CDCl₃, 100 MHz) δ 152.7, 143.5, 140.7, 139.7, 138.7, 138.6, 137.8, 130.6, 129.4, 126.6, 126.5, 125.9, 117.8, 112.0, 110.3, 95.6. **HPLC** (chiral column: DAICEL CHIRALPAK IC; solvent: hexane/2-propanol = 4/1; flow rate: 1.0 mL/min; detection: at 254 nm): *t*_R = 8.5 min (minor) and 9.7 min (major). **HRMS** (ESI): *m/z* calculated for C₁₈H₁₁Cl₂NO₂SNa⁺ [M+Na]⁺: 397.9780, found: 397.9775. [α]_D²⁴ = +203.2 (*c* = 0.50, CHCl₃). **Rf** 0.40 (hexane/AcOEt = 3:1).

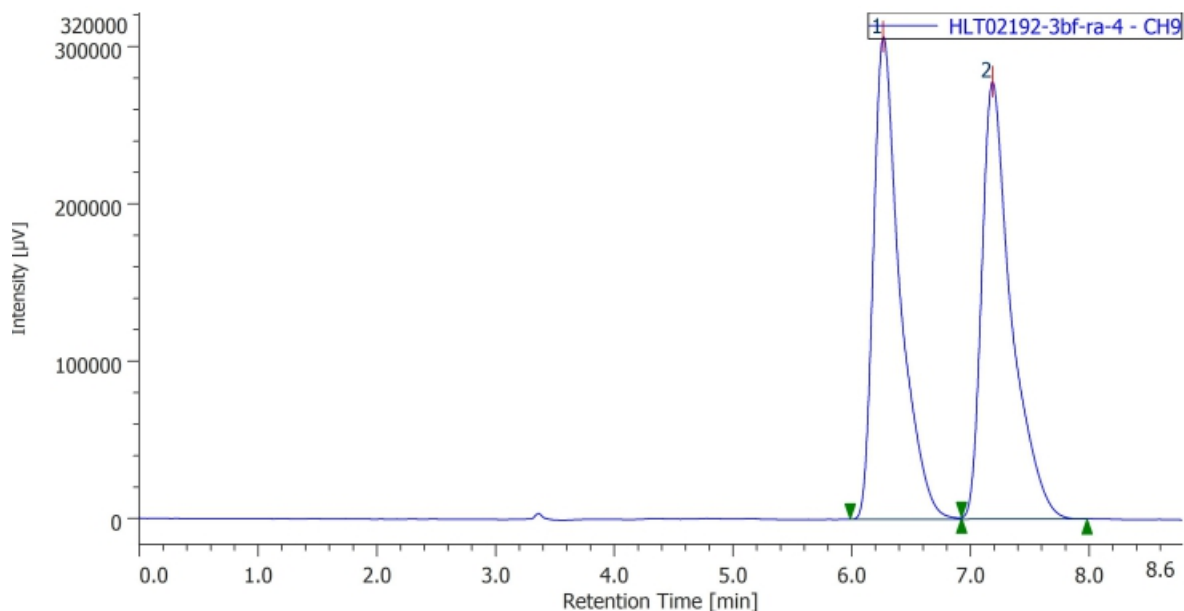




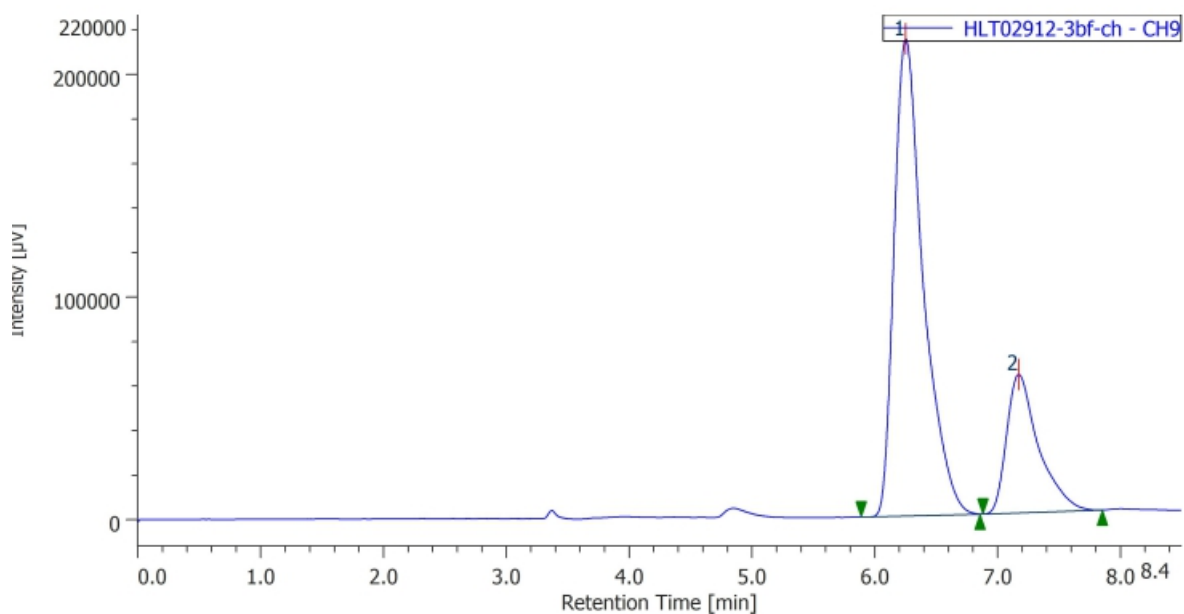
(S)-3-(tert-butyl)-6-chloro-1-(4-chlorophenyl)benzo[e][1,2]thiazine 1-oxide (7bf): Prepared according to GP-C using sulfoximine **4b** (0.20 mmol, 56.8 mg) and sulfoxonium ylide **6f** (0.30 mmol, 52.8 mg) afforded **7bf** as a yellow oil (70.0 mg, 95%). ¹H NMR (CDCl₃, 400 MHz) δ 7.74 (d, *J* = 9.0 Hz, 2H), 7.47 (d, *J* = 8.5 Hz, 2H), 7.24 (d, *J* = 2.2 Hz, 1H), 7.13 (d, *J* = 8.5 Hz, 1H), 7.05 (dd, *J* = 8.5, 2.2 Hz, 1H), 6.05 (s, 1H), 1.24 (s, 9H). ¹³C NMR (CDCl₃, 100 MHz) δ 161.4, 140.2, 139.4, 138.2, 138.2, 130.3, 129.3, 126.3, 126.2, 125.8, 116.3, 94.6, 37.7, 28.8. HPLC (chiral column: DAICEL



CHIRALPAK IC; solvent: hexane/2-propanol = 19/1; flow rate: 1.0 mL/min; detection: at 254 nm): $t_R = 6.3$ min (major) and 7.2 min (minor). **HRMS** (ESI): m/z calculated for $C_{18}H_{17}Cl_2NOSNa^+ [M+Na]^+$: 388.0301, found: 388.0294. $[\alpha]_D^{24} = +54.6$ ($c = 0.50$, $CHCl_3$). **Rf** 0.60 (hexane/AcOEt = 6:1).



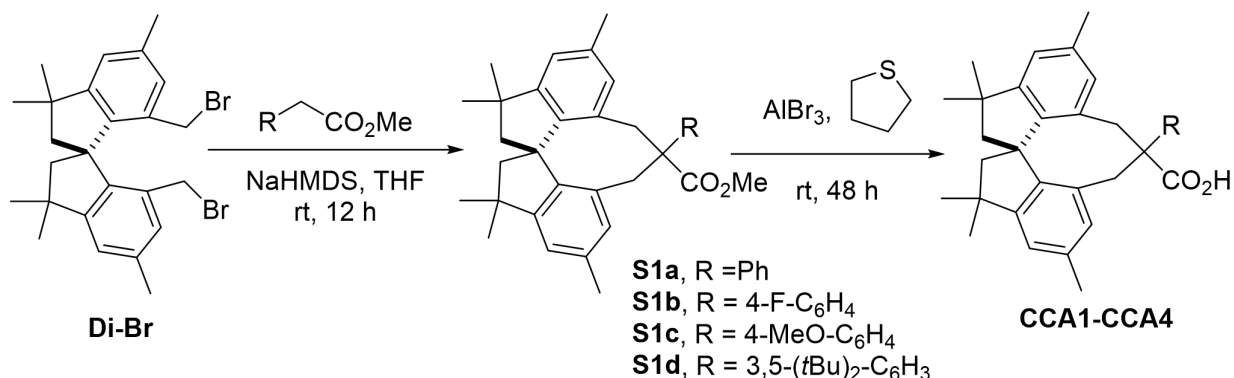
#	ピーク名	CH	tR [min]	Area%
1	Unknown	9	6.263	49.897
2	Unknown	9	7.183	50.103



#	ピーク名	CH	tR [min]	Area%
1	Unknown	9	6.250	75.955
2	Unknown	9	7.170	24.045

4. Experimental procedures: third work-Enantioselective Synthesis of 1,2-Benzothiazine 1-Imines via RuII/Chiral Carboxylic Acid-Catalyzed C–H Alkylation/Cyclization

4.1. Preparation of New Spiro CCA



General Procedure D for S1a–S1d

To a solution of compound **Di-Br** (100 mg, 1.0 equiv.) in THF (4 mL) was added NaHMDS (1 M in THF, 0.31 mL, 1.5 equiv.) dropwise at $-78\text{ }^\circ\text{C}$, and then corresponding methyl- α -arylacrylate (1.1 equiv.) in THF (2 mL) was added at $-78\text{ }^\circ\text{C}$. The reaction mixture was stirred for 1 h at $-78\text{ }^\circ\text{C}$ and then stirred for 1 h at $0\text{ }^\circ\text{C}$. The reaction mixture was cooled to $-78\text{ }^\circ\text{C}$ again and stirred for 30 min. To the reaction mixture was added NaHMDS (1 M in THF, 0.31 mL, 1.5 equiv.) dropwise at $-78\text{ }^\circ\text{C}$ and then stirred for 12 h at room temperature. The reaction was quenched by adding water at $0\text{ }^\circ\text{C}$, and extracted with AcOEt three times. The combined organic layers were washed with brine, dried over Na₂SO₄, filtered, and evaporated under vacuum. The residue was purified by silica gel column chromatography (hexane/AcOEt) to give **S1a–S1d**.

General Procedure E for CCA1-CCA4

To a solution of compound **S1a–S1d** (1.0 equiv.) in tetrahydrothiophene (2 mL) was added AlBr₃ (4.0 equiv.) and the reaction mixture was stirred for 48 h at room temperature. The reaction was quenched by adding water at $0\text{ }^\circ\text{C}$, and extracted with CH₂Cl₂ three times. The combined organic layers were washed with brine, dried over Na₂SO₄, filtered, and evaporated under vacuum. The residue was purified by silica gel column chromatography (hexane/AcOEt) to give **CCA1-CCA4**.

Methyl

2,4,4,7,7,9-hexamethyl-12-phenyl-4,5,6,7,12,13-hexahydro-11H-cycloocta[1,2,3-cd:1,8,7-c'-d']diindene-

12-carboxylate (S1a): Prepared according to **GP-D** using compound **Di-Br**

(0.21 mmol, 100 mg, 1.0 equiv.), methyl- α -phenylacetate (0.23 mmol, 35 mg, 1.1 equiv.), NaHMDS (1 M in THF, 0.31 mmol, 0.31 mL, 1.5 equiv. x

2). **S1a** was isolated as a colorless solid (70 mg, 70%). **IR** (KBr) 2959, 2949, 2916, 2857, 1731, 1446, 1220, 1174, 1048, 860, 696 cm^{-1} . **^1H NMR** (CDCl_3 ,

400 MHz) δ 7.21-7.19 (m, 3H), 6.87 (s, 1H), 6.81-6.77 (m, 2H), 6.74 (s, 1H), 6.64 (s, 1H), 5.48 (s, 1H),

3.63 (s, 3H), 3.28 (d, $J = 13.3$ Hz, 1H), 3.21 (d, $J = 12.6$ Hz, 1H), 2.97 (d, $J = 12.5$ Hz, 1H), 2.63 (d, $J =$

13.3 Hz, 1H), 2.40 (d, $J = 12.7$ Hz, 1H), 2.37 (d, $J = 12.7$ Hz, 1H), 2.31 (s, 3H), 2.00 (d, $J = 8.9$ Hz, 1H),

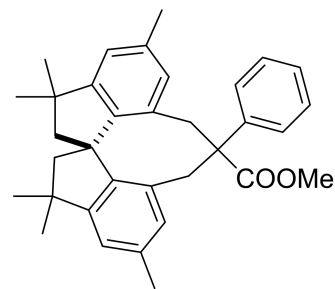
1.97 (d, $J = 8.9$ Hz, 1H), 1.92 (s, 3H), 1.49 (s, 3H), 1.46 (s, 3H), 1.29 (s, 3H), 1.27 (s, 3H). **^{13}C NMR**

(CDCl_3 , 100 MHz) δ 175.3, 151.6, 151.0, 145.7, 145.3, 141.8, 136.8, 135.6, 132.2, 131.2, 130.5, 128.7,

127.8, 126.8, 126.6, 122.2, 121.4, 58.2, 57.2, 57.0, 56.7, 51.6, 42.0, 41.9, 38.9, 34.2, 32.4, 32.3, 30.4, 30.3,

21.3, 20.9. **HRMS** (ESI) m/z : $[\text{M}+\text{Na}]^+$ Calcd for $\text{C}_{34}\text{H}_{38}\text{O}_2\text{Na}^+$: 501.2764; Found 501.2757. $[\alpha]_D^{24.1} =$

-54.2 ($c = 0.50$, CHCl_3). **Rf** 0.5 (hexane/AcOEt = 10:1).



2,4,4,7,7,9-hexamethyl-12-phenyl-4,5,6,7,12,13-hexahydro-11H-cycloocta[1,2,3-cd:1,8,7-c'-d']diindene-

12-carboxylic acid (CCA1): Prepared according to **GP-E** using compound **S1a** (0.15 mmol, 70 mg, 1.0 equiv.) in tetrahydrothiophene (2 mL), AlBr_3 (0.60 mmol, 140 mg, 4.0 equiv.).

CCA1 was isolated as a colorless solid (70 mg, >99%). **IR** (KBr) 2956, 2919,

2860, 1737, 1698, 1448, 1278, 860, 696 cm^{-1} . **^1H NMR** (CDCl_3 , 400 MHz) δ

7.25-7.19 (m, 3H), 6.92-8.85 (m, 3H), 6.82 (s, 1H), 6.74 (s, 1H), 5.51 (s, 1H),

3.29-3.18 (m, 2H), 3.01 (d, $J = 12.6$ Hz, 1H), 2.66 (d, $J = 13.3$ Hz, 1H), 2.41 (d

$J = 12.5$ Hz, 1H), 2.38 (d, $J = 12.5$ Hz, 1H), 2.24 (s, 3H), 2.00 (s, 1H), 1.97 (s,

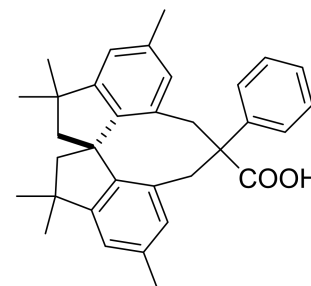
1H), 1.92 (s, 3H), 1.50 (s, 3H), 1.46 (s, 3H), 1.28 (s, 6H). **^{13}C NMR** (CDCl_3 , 100 MHz) δ 181.26, 151.5,

151.1, 145.6, 145.3, 141.3, 137.1, 135.6, 131.8, 131.0, 130.5, 129.2, 127.9, 127.0, 126.7, 122.3, 121.5, 58.2,

57.1, 57.0, 56.8, 42.0, 41.9, 38.2, 34.1, 32.5, 32.3, 30.4, 30.3, 21.3, 20.8. **HRMS** (ESI) m/z : $[\text{M}+\text{Na}]^+$ Calcd

for $\text{C}_{33}\text{H}_{36}\text{O}_2\text{Na}^+$: 487.2608; Found 487.2603. $[\alpha]_D^{23.2} = -45.5$ ($c = 0.50$, CHCl_3). **Rf** 0.34 (hexane/AcOEt =

2:1).

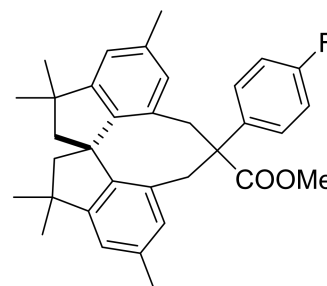


Methyl

12-(4-fluorophenyl)-2,4,4,7,7,9-hexamethyl-4,5,6,7,12,13-hexahydro

-11H-cycloocta[1,2,3-cd:1,8,7-c'-d']diindene-12-carboxylate (S1b): Prepared according to **GP-D** using

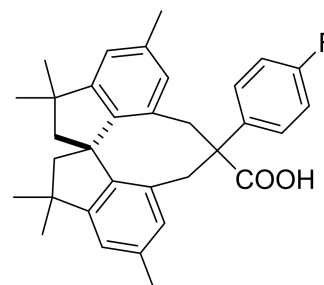
compound **Di-Br** (0.21 mmol, 100 mg, 1.0 equiv.), methyl- α -(4-fluorophenyl)acetate (0.23 mmol, 39 mg, 1.1 equiv.), NaHMDS (1 M in THF, 0.31 mmol, 0.31 mL, 1.5 equiv. x 2). **S1b** was isolated as a colorless solid (70 mg, 67%). **IR** (KBr) 2960, 2931, 2859, 1731, 1509, 1458, 1235, 1175, 1051, 858, 835, 818, 720 cm^{-1} . **^1H NMR**



(CDCl_3 , 400 MHz) δ 6.94-6.87 (m, 3H), 6.77-6.73 (m, 3H), 6.63 (s, 1H), 5.52 (s, 1H), 3.63 (s, 3H), 3.27 (d, $J = 13.4$ Hz, 1H), 3.16 (d, $J = 12.5$ Hz, 1H), 2.95 (d, $J = 12.6$, 1H), 2.59 (d, $J = 13.4$ Hz, 1H), 2.42-2.35 (m, 2H), 2.01-1.95 (m, 5H), 1.49 (s, 3H), 1.46 (s, 3H), 1.28 (s, 3H), 1.27 (s, 3H). **^{13}C NMR** (CDCl_3 , 100 MHz) δ 175.2, 161.2 (d, $J = 254.1$ Hz), 151.7, 151.2, 145.6, 145.3, 137.7 (d, $J = 2.9$ Hz), 136.9, 135.7, 131.9, 131.0, 130.4, 128.6, 128.3 (d, $J = 7.6$ Hz), 122.3, 121.5, 114.6 (d, $J = 21.0$ Hz), 58.2, 57.1, 56.7, 56.5, 51.7, 42.0, 41.9, 38.9, 34.5, 32.4, 32.3, 30.4, 30.3, 21.3, 20.9. **^{19}F NMR** (370 MHz, CDCl_3) δ : -116.1. **HRMS** (ESI) m/z : $[\text{M}+\text{Na}]^+$ Calcd for $\text{C}_{34}\text{H}_{37}\text{O}_2\text{FNa}^+$: 519.2670; Found 519.2665. $[\alpha]_D^{23.6} = -36.7$ ($c = 0.50$, CHCl_3). **Rf** 0.65 (hexane/AcOEt = 10:1).

12-(4-fluorophenyl)-2,4,4,7,7,9-hexamethyl-4,5,6,7,12,13-hexahydro-11H-cycloocta[1,2,3-cd:1,8,7-c'd'] diindene-12-carboxylic acid (CCA2): Prepared according to **GP-E** using

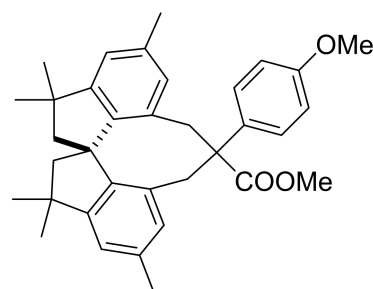
compound **S1b** (0.20 mmol, 100 mg, 1.0 equiv.) in tetrahydrothiophene (2 mL), AlBr_3 (0.80 mmol, 213 mg, 4.0 equiv.). **CCA2** was isolated as a colorless solid (80 mg, 83%). **IR** (KBr) 2955, 2918, 2864, 1708, 1509, 1459 1235, 1168, 860, 830, 732 cm^{-1} . **^1H NMR** (CDCl_3 , 400 MHz) δ 6.96-6.90



(m, 3H), 6.88-6.82 (m, 2H), 6.80 (s, 1H), 6.75 (s, 1H), 5.55 (s, 1H), 3.26 (d, $J = 13.3$ Hz, 1H), 3.19 (d, $J = 12.6$ Hz, 1H), 2.98 (d, $J = 12.6$, 1H), 2.62 (d, $J = 13.3$ Hz, 1H), 2.43-2.36 (m, 2H), 2.24 (s, 3H), 1.99-1.95 (m, 5H), 1.50 (s, 3H), 1.47 (s, 3H), 1.28 (s, 6H). **^{13}C NMR** (CDCl_3 , 100 MHz) δ 180.2, 161.7 (d, $J = 246.6$ Hz), 151.6, 151.2, 145.5, 145.3, 137.1 (d, $J = 2.9$ Hz) (one peak is overlap), 135.7, 131.5, 130.7, 130.4, 129.1, 128.4 (d, $J = 8.7$ Hz), 122.4, 121.6, 114.7 (d, $J = 22.2$ Hz), 58.2, 57.0, 56.8, 56.4, 42.0, 41.9, 38.3, 34.4, 32.5, 32.3, 30.4, 30.3, 21.3, 20.9. **^{19}F NMR** (370MHz, CDCl_3) δ : -115.1. **HRMS** (ESI) m/z : $[\text{M}+\text{Na}]^+$ Calcd for $\text{C}_{33}\text{H}_{35}\text{O}_2\text{FNa}^+$: 505.2513; Found 505.2511. $[\alpha]_D^{23.4} = -49.1$ ($c = 0.50$, CHCl_3). **Rf** 0.35 (hexane/AcOEt = 2:1).

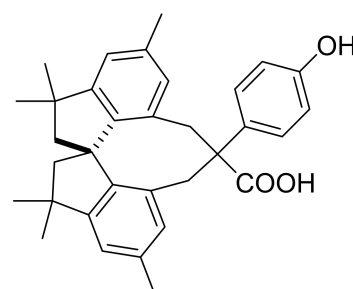
Methyl-12-(4-methoxyphenyl)-2,4,4,7,7,9-hexamethyl-4,5,6,7,12,13-hexahydro-11H-cycloocta[1,2,3-cd:

1,8,7-c'd']diindene-12-carboxylate (S1c): Prepared according to **GP-D** using compound **Di-Br** (0.21 mmol, 100 mg, 1.0 equiv.), methyl- α -(4-methoxyphenyl)acetate (0.23 mmol, 41 mg, 1.1 equiv.), NaHMDS (1 M in THF, 0.31 mmol, 0.31 mL, 1.5 equiv. x 2). **S1c** was isolated as a colorless solid (50 mg, 47%). **IR** (KBr) 2952, 2921, 2860,



1732, 1512, 1464, 1250, 1186, 1038, 860, 827 cm^{-1} . **$^1\text{H NMR}$** (CDCl_3 , 400 MHz) δ 6.86 (s, 1H), 6.76-6.68 (m, 5H), 6.63 (s, 1H), 5.55 (s, 1H), 3.78 (s, 3H), 3.63 (s, 3H), 3.25 (d, $J = 13.3$ Hz, 1H), 3.15 (d, $J = 12.6$ Hz, 1H), 2.94 (d, $J = 12.5$ Hz, 1H), 2.59 (d, $J = 13.3$, 1H), 2.42-2.35 (m, 2H), 2.31 (s, 3H), 2.01-1.94 (m, 5H), 1.49 (s, 3H), 1.46 (s, 3H), 1.28 (s, 3H), 1.26 (s, 3H). **$^{13}\text{C NMR}$** (CDCl_3 , 100 MHz) δ 175.5, 158.3, 151.6, 151.0, 145.7, 145.3, 136.8, 135.5, 133.9, 132.3, 131.4, 130.7, 128.7, 127.7, 122.1, 121.3, 113.2, 58.2, 57.2, 56.7, 56.4, 55.3, 51.6, 42.0, 41.9, 38.8, 34.4, 32.4, 32.3, 30.4, 30.3, 21.3, 20.9. **HRMS** (ESI) m/z : $[\text{M}+\text{Na}]^+$ Calcd for $\text{C}_{35}\text{H}_{40}\text{O}_3\text{Na}^+$: 531.2870; Found 531.2868. $[\alpha]_{\text{D}}^{23.4} = -78.9$ ($c = 0.50$, CHCl_3). **Rf** 0.5 (hexane/AcOEt = 10:1).

2,4,4,7,7,9-hexamethyl-12-phenyl-4,5,6,7,12,13-hexahydro-11H-cycloocta[1,2,3-cd:1,8,7-c'd']diindene-12-carboxylic acid (CCA3): Prepared according to **GP-E** using compound **S1c** (0.089 mmol, 45 mg, 1.0 equiv.) in tetrahydrothiophene (2 mL), AlBr_3 (0.354 mmol, 94 mg, 4.0 equiv.). **CCA3** was isolated as a colorless solid (43 mg, >99%). **IR** (KBr) 3400, 2956, 2919, 2861, 1701,



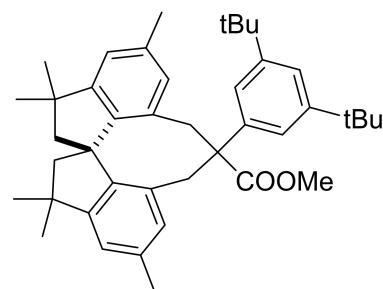
1514, 1449, 1262, 1180, 859, 827 cm^{-1} . **$^1\text{H NMR}$** (CDCl_3 , 400 MHz) δ 6.89 (s, 1H), 6.81 (s, 1H), 6.77-6.74 (m, 3H), 6.69-6.66 (m, 2H), 5.60 (s, 1H), 3.23 (d, $J = 13.3$ Hz, 1H), 3.15 (d, $J = 12.6$ Hz, 1H), 2.97 (d, $J = 12.6$ Hz, 1H), 2.62 (d, $J = 13.3$, 1H), 2.42-2.35 (m, 2H), 2.23 (s, 3H), 2.00-1.95 (m, 5H), 1.50 (s, 3H), 1.46 (s, 3H), 1.27 (s, 6H). **$^{13}\text{C NMR}$** (CDCl_3 , 100 MHz) δ 181.1, 154.4, 151.5, 151.1, 145.6, 145.2, 137.1, 135.6, 133.5, 131.8, 131.1, 130.6, 129.1, 128.0, 122.3, 121.5, 114.7, 58.2, 57.1, 56.7, 56.2, 42.0, 41.9, 38.1, 34.3, 32.5, 32.3, 30.4, 30.3, 21.3, 21.0. **HRMS** (ESI) m/z : $[\text{M}+\text{Na}]^+$ Calcd for $\text{C}_{33}\text{H}_{36}\text{O}_3\text{Na}^+$: 503.2557; Found 531.2554. $[\alpha]_{\text{D}}^{24.3} = -78.7$ ($c = 0.50$, CHCl_3). **Rf** 0.5 (hexane/AcOEt = 2:1).

Methyl-12-(3,5-di-tert-butylphenyl)-2,4,4,7,7,9-hexamethyl-4,5,6,7,12,13-hexahydro-11H-cycloocta[1,2,3-cd:1,8,7-c'd']diindene-12-carboxylate (S1d): Prepared according to **GP-D** using compound **Di-Br**

(0.21 mmol, 100 mg, 1.0 equiv.),

methyl- α -(3,5-di-tert-butylphenyl)acetate (0.23 mmol, 60 mg, 1.1 equiv.), NaHMDS (1 M in THF, 0.31 mmol, 0.31 mL, 1.5 equiv. x 2).

S1d was isolated as a colorless solid (50 mg, 47%). IR (KBr) 2960, 2947, 2918, 2859, 1731, 1596, 1449, 1360, 1172, 1051 cm^{-1} . $^1\text{H NMR}$ (CDCl_3 , 400 MHz) δ 7.24 (s, 1H), 6.87 (s, 1H), 6.68 (s, 1H), 6.66 (s,



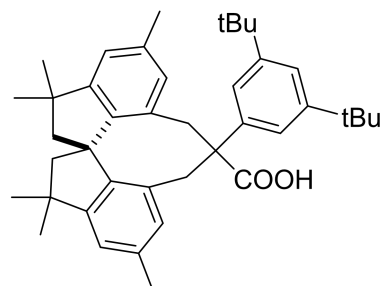
1H), 6.63 (s, 2H), 5.43 (s, 1H), 3.65 (s, 3H), 3.32 (d, $J = 12.6$ Hz, 1H), 3.21 (d, $J = 13.3$ Hz, 1H), 3.00 (d, $J = 12.5$, 1H), 2.62 (d, $J = 13.3$ Hz, 1H), 2.42-2.35 (m, 2H), 2.32 (s, 3H), 2.02 (d, $J = 12.5$ Hz, 1H), 1.94 (d, $J = 12.8$ Hz, 1H), 1.88 (s, 3H), 1.48-1.47 (m, 6H), 1.26 (s, 6H), 1.23 (s, 18H). $^{13}\text{C NMR}$ (CDCl_3 , 100 MHz) δ 175.5, 151.6, 150.8, 149.9, 145.6, 145.3, 140.5, 136.9, 135.4, 132.6, 131.2, 130.5, 128.5, 122.1, 121.2, 120.7, 120.5, 58.3, 57.1, 57.0, 56.8, 51.6, 42.0, 41.8, 39.2, 34.8, 34.1, 32.8, 32.1, 31.4, 30.4, 30.2, 21.4, 21.1. HRMS (ESI) m/z : $[\text{M}+\text{Na}]^+$ Calcd for $\text{C}_{42}\text{H}_{54}\text{O}_2\text{Na}^+$: 613.4016; Found 613.4010. $[\alpha]_D^{23.1} = -31.4$ ($c = 0.50$, CHCl_3). Rf 0.6 (hexane/AcOEt = 10:1).

12-(3,5-di-tert-butylphenyl)-2,4,4,7,7,9-hexamethyl-4,5,6,7,12,13-hexahydro-11H-cycloocta[1,2,3-cd:1,8,7-c'-d']diindene-12-carboxylic acid (CCA4): Prepared according to

GP-E using compound **S1d** (0.19 mmol, 110 mg, 1.0 equiv.) in tetrahydrothiophene (2 mL), AlBr_3 (0.8 mmol, 213 mg, 4.0 equiv.).

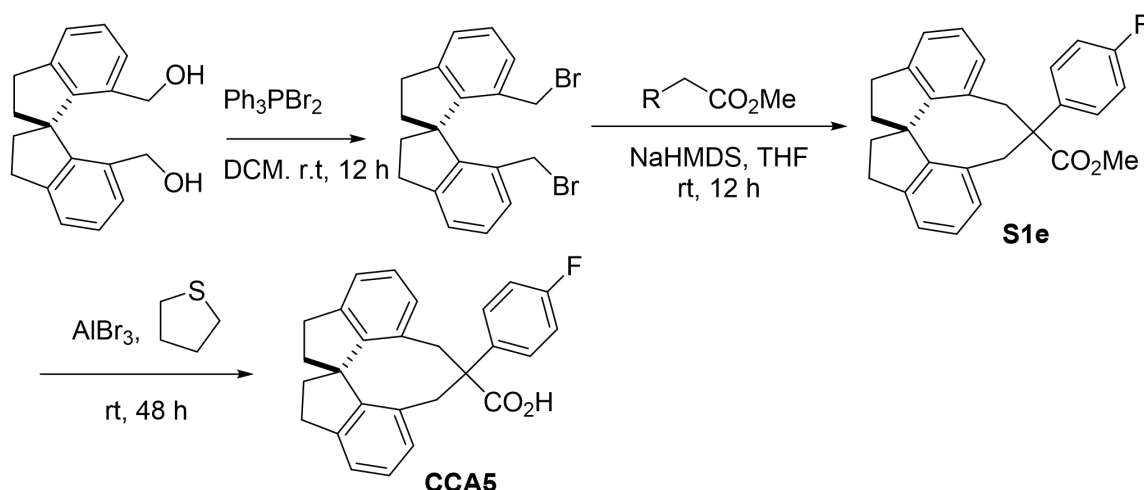
CCA4 was isolated as a colorless solid (70 mg, 64%). IR (KBr) 2960, 2955, 2920, 2863, 1700, 1598, 1465, 1448, 1361, 1248, 860, 712 cm^{-1} .

$^1\text{H NMR}$ (CDCl_3 , 400 MHz) δ 7.25 (s, 1H), 6.88 (s, 1H), 6.86 (s, 1H),



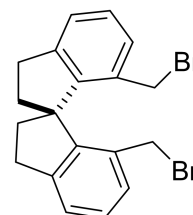
6.75 (s, 2H), 6.66 (s, 1H), 5.45 (s, 1H), 3.33 (d, $J = 12.6$ Hz, 1H), 3.20 (d, $J = 13.1$ Hz, 1H), 3.07 (d, $J = 12.6$, 1H), 2.68 (d, $J = 13.1$ Hz, 1H), 2.40 (d, $J = 12.8$ Hz, 1H), 2.34 (d, $J = 12.8$ Hz, 1H), 2.17 (s, 3H), 2.02 (d, $J = 12.7$ Hz, 1H), 1.93 (d, $J = 12.8$ Hz, 1H), 1.85 (s, 3H), 1.49 (s, 3H), 1.47 (s, 3H), 1.27 (s, 3H), 1.25 (s, 3H), 1.22 (s, 18H). $^{13}\text{C NMR}$ (CDCl_3 , 100 MHz) δ 179.8, 151.5, 150.8, 150.1, 145.4, 145.2, 139.7, 137.2, 135.4, 132.2, 130.9, 130.5, 129.0, 122.2, 121.2, 120.8, 120.6, 58.2, 57.2, 56.7, 56.6, 42.0, 41.8, 38.7, 34.8, 33.8, 32.8, 32.2, 31.4, 30.4, 30.2, 21.3, 20.9. HRMS (ESI) m/z : $[\text{M}+\text{Na}]^+$ Calcd for $\text{C}_{41}\text{H}_{52}\text{O}_2\text{Na}^+$: 599.3860; Found 599.3854. $[\alpha]_D^{23.7} = -27.4$ ($c = 0.50$, CHCl_3). Rf 0.2 (hexane/AcOEt = 6:1).

4.2. Preparation of CCA5



(*R*)-7,7'-bis(bromomethyl)-2,2',3,3'-tetrahydro-1,1'-spirobi[indene]:

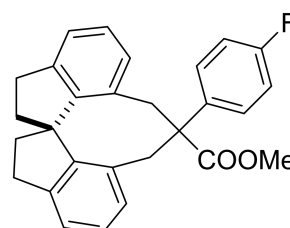
To a solution of (*R*)-(2,2',3,3'-tetrahydro-1,1'-spirobi[indene]-7,7'-diyl)dimethanol (0.36 mmol, 100 mg, 1.0 equiv.)^[S4] in DCM (5 mL) was added Ph_3PBr_2 (1.8 mmol, 760 mg, 5.0 equiv.) in several portions at room temperature. The reaction mixture was stirred for 12 h at room temperature. The reaction was quenched by adding water at 0 °C, and extracted with DCM three times. The combined organic layers were washed with brine, dried over Na_2SO_4 , filtered, and evaporated under vacuum. The residue was purified by silica gel column chromatography (hexane/AcOEt) to give (*R*)-7,7'-bis(bromomethyl)-2,2',3,3'-tetrahydro-1,1'-spirobi[indene] as a colorless solid (135 mg, 93%).



IR (KBr) 2957, 2947, 2843, 1448, 1434, 1215, 1203, 785, 752 cm^{-1} . **¹H NMR** (CDCl_3 , 400 MHz) δ 7.28-7.21 (m, 6H), 4.13 (d, $J = 10.4$ Hz, 2H), 4.05 (d, $J = 10.4$ Hz, 2H), 3.07-3.02 (m, 4H), 2.41-2.29 (m, 4H). **¹³C NMR** (CDCl_3 , 100 MHz) δ 147.0, 144.1, 133.8, 130.6, 128.2, 125.2, 61.6, 38.2, 30.7, 30.3. **HRMS** (EI) m/z : $[\text{M}]^+$ Calcd for $\text{C}_{19}\text{H}_{18}\text{Br}_2^+$: 403.9775; Found 403.9751. $[\alpha]_{\text{D}}^{22.0} = +280.9$ ($c = 0.25$, CHCl_3). **Rf** 0.7 (hexane/AcOEt = 10:1).

methyl

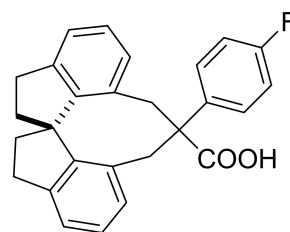
12-(4-fluorophenyl)-4,5,6,7,12,13-hexahydro-11H-cycloocta[1,2,3-cd:1,8,7-c'd']diindene-12-carboxylate (S1e): Prepared according to **GP-D** using compound (*R*)-7,7'-bis(bromomethyl)-2,2',3,3'-tetrahydro-1,1'-spirobi[indene] (0.1 mmol, 40 mg, 1.0 equiv.), methyl- α -(4-fluorophenyl)acetate (0.11 mmol, 18 mg, 1.1 equiv.), NaHMDS (1 M in THF, 0.15 mmol, 0.15 mL, 1.5 equiv. x 2). **S1e** was



isolated as a colorless solid (20 mg, 50%). **IR** (KBr) 2936, 1721, 1509, 1455, 1276, 1243, 1228, 1176, 841 cm^{-1} . **$^1\text{H NMR}$** (CDCl_3 , 400 MHz) δ 7.15 (d, $J = 7.2$ Hz, 1H), 7.10 (t, $J = 7.4$ Hz, 1H), 7.02 (d, $J = 7.2$ Hz, 1H), 6.93-6.91 (m, 4H), 6.83 (d, $J = 7.2$ Hz, 1H), 6.72 (t, $J = 7.5$ Hz, 1H), 5.80 (d, $J = 7.6$ Hz, 1H), 3.65 (s, 3H), 3.42 (d, $J = 13.5$ Hz, 1H), 3.31 (d, $J = 12.6$ Hz, 1H), 3.10-2.98 (m, 3H), 2.86-2.74 (m, 3H), 2.30-2.21 (m, 2H), 2.00-1.88 (m, 2H). **$^{13}\text{C NMR}$** (CDCl_3 , 100 MHz) δ 175.1, 161.7 (d, $J = 246.6$ Hz), 149.0, 148.8, 143.2, 142.6, 137.5 (d, $J = 2.9$ Hz), 132.2, 131.5, 129.1, 128.3 (d, $J = 8.7$ Hz), 127.7, 127.1, 125.9, 123.9, 123.1, 114.9 (d, $J = 21.2$ Hz), 61.2, 55.9, 51.9, 38.5, 38.0, 34.5, 30.4, 30.4. (one aliphatic signal was missing probably due to overlap) **$^{19}\text{F NMR}$** (370MHz, CDCl_3) δ : -114.9. **HRMS** (ESI) m/z : $[\text{M}+\text{Na}]^+$ Calcd for $\text{C}_{28}\text{H}_{25}\text{FO}_2\text{Na}^+$: 435.1731; Found 435.1718. $[\alpha]_{\text{D}}^{22.1} = -60.7$ ($c = 0.25$, CHCl_3). **Rf** 0.5 (hexane/AcOEt = 10:1).

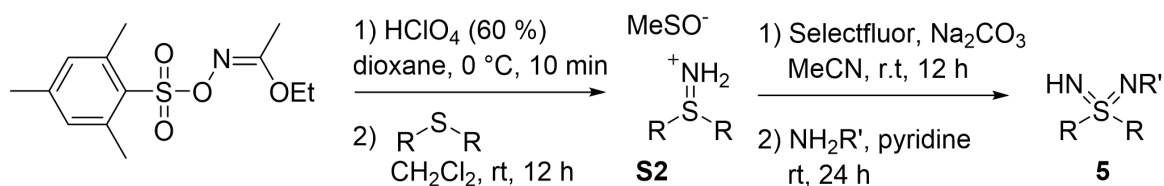
12-(4-fluorophenyl)-4,5,6,7,12,13-hexahydro-11H-cycloocta[1,2,3-cd:1,8,7-c'd']diindene-12-carboxylic acid (CCA5): Prepared according to **GP-E** using compound **S1e** (0.05 mmol,

20 mg, 1.0 equiv.) in tetrahydrothiophene (2 mL), AlBr_3 (0.2 mmol, 54 mg, 4.0 equiv.). **CCA5** was isolated as a colorless solid (10 mg, 50%). **IR** (KBr) 3068, 2942, 1705, 1510, 1456, 1085, 1240, 719 cm^{-1} . **$^1\text{H NMR}$** (CDCl_3 , 400



MHz) δ 7.23-7.20 (m, 1H), 7.14-7.10 (m, 1H), 7.03-6.94 (m, 6H), 6.74-6.69 (m, 1H), 5.82 (d, $J = 7.4$ Hz, 1H), 3.40 (d, $J = 13.4$ Hz, 1H), 3.32 (d, $J = 12.6$ Hz, 1H), 3.14-2.99 (m, 3H), 2.90-2.74 (m, 3H), 2.31-2.22 (m, 2H), 2.00-1.89 (m, 2H). **$^{13}\text{C NMR}$** (CDCl_3 , 100 MHz) δ 180.1, 161.8 (d, $J = 246.6$ Hz), 149.1, 148.8, 143.3, 142.7, 136.8 (d, $J = 2.9$ Hz), 131.9, 131.3, 129.1, 128.4 (d, $J = 7.7$ Hz), 128.1, 127.2, 126.0, 123.9, 123.2, 115.0 (d, $J = 21.2$ Hz), 61.2, 55.7, 38.4, 38.1, 37.9, 34.3, 30.5, 30.4. **$^{19}\text{F NMR}$** (370MHz, CDCl_3) δ : -114.5. **HRMS** (ESI) m/z : $[\text{M}+\text{Na}]^+$ Calcd for $\text{C}_{27}\text{H}_{23}\text{FO}_2\text{Na}^+$: 421.1574; Found 421.1559. $[\alpha]_{\text{D}}^{22.2} = -82.4$ ($c = 0.25$, CHCl_3). **Rf** 0.4 (hexane/AcOEt = 2:1).

4.3. Preparation of sulfondiimines



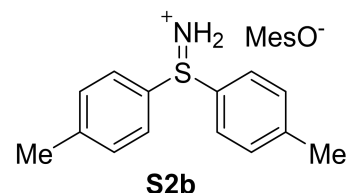
General Procedure F for 5a-5o^[S5]

To ethyl *o*-(mesitylenesulfonyl)acetohydroxamate (1.0 g, 3.51 mmol, 1 equiv.) in 1,4-dioxane (4 mL) was

added 60% perchloric acid (2.5 mL) dropwise at 0 °C. After additional vigorous stirring for 10 min at 0 °C, cold water was added and the product was extracted with CH₂Cl₂. The combined organic layers were washed with brine, dried over Na₂SO₄, filtered, and evaporated under vacuum to approximately 1 mL. This mixture was slowly added to a solution of the corresponding sulfide (3.51 mmol, 1 equiv.) in CH₂Cl₂ (4 mL) at 0 °C. The reaction mixture was stirred at room temperature for 12 h. Half of the CH₂Cl₂ was evaporated and diethyl ether (20 mL) was added. The product crystallized upon storage at -30 °C overnight and was collected by filtration and dried in high vacuum to give the corresponding sulfiliminium salt **S2**.

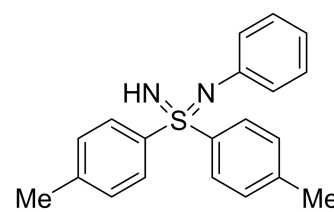
To a solution of the obtained sulfiliminium salt **S2** (1.0 equiv.) and Na₂CO₃ (5.0 equiv.) in MeCN (8 mL) was added Selectfluor® (1.0 equiv.) at 0 °C and the mixture was stirred for 12 h at room temperature. The mixture was quenched by water and extracted with CH₂Cl₂. The combined organic layers were washed with brine, dried over Na₂SO₄, filtered, and evaporated under vacuum. To the residue was added to a solution of R'NH₂ (3.0 equiv.) and pyridine (1.2 equiv.) and the mixture was stirred for 24 h at room temperature. The residue was purified by silica gel column chromatography (hexane/AcOEt) and evaporated under vacuum. The residual solid was washed by hexane and filtered to give the desired sulfondiimine **5**. When necessary, **5** was further purified by GPC.

Bis(4-methylphenyl)sulfiliminium mesitylenesulfonate (S2b): Prepared according to **GP-F** using bis(4-methylphenyl) sulfide (3.51 mmol, 750 mg, 1.0 equiv.), **S2b** was isolated as a colorless solid (1.2 g, 79%). **IR** (KBr) 3180, 3046, 2983, 2934, 1593, 1453, 1403, 1215, 1080, 1015, 809, 678



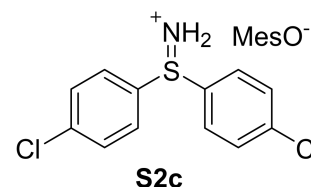
cm⁻¹. **¹H NMR** (CDCl₃, 400 MHz) δ 7.62-7.59 (m, 4H), 7.23-7.20 (m, 4H), 6.76 (s, 2H), 2.50 (s, 6H), 2.34 (s, 6H), 2.23 (s, 3H). **¹³C NMR** (CDCl₃, 100 MHz) δ 144.2, 138.8, 137.4, 130.9, 130.7, 129.8, 128.4, 22.8, 21.5, 20.8; one aromatic signal was missing probably due to overlap. **HRMS** (ESI) m/z: [M-MesO]⁺ Calcd for C₁₄H₁₆NS⁺: 230.0998; Found 230.0994.

N-phenyl-1,1-di-p-tolyl-λ⁶-sulfondiimine (5b): Prepared according to **GP-F** using compound **S2b** (2.7 mmol, 1.2 g, 1.0 equiv.), Na₂CO₃ (13.5 mmol, 1.4 g, 5.0 equiv.), Selectfluor® (2.7 mmol, 990 mg, 1.0 equiv.), aniline (8.1 mmol, 0.8 mL, 3.0 equiv.), pyridine (3.24 mmol, 0.28 mL, 1.2 equiv.). **5b** was isolated as a colorless solid (0.2 g, 23%). **IR** (KBr) 3180, 3057, 1595, 1485, 1283, 1254,



1086, 1074, 1044, 954, 946, 765, 759, 749 cm^{-1} . $^1\text{H NMR}$ (CDCl_3 , 400 MHz) δ 8.04 (d, $J = 8.3$ Hz, 4H), 7.24 (d, $J = 8.5$ Hz, 4H), 7.17-7.10 (m, 4H), 6.86-6.81 (m, 1H), 2.35 (s, 6H). $^{13}\text{C NMR}$ (CDCl_3 , 125 MHz) δ 146.0, 142.6, 140.3, 129.8, 128.8, 127.9, 123.3, 120.6, 21.4. **HRMS** (ESI) m/z : $[\text{M}+\text{H}]^+$ Calcd for $\text{C}_{20}\text{H}_{21}\text{N}_2\text{S}^+$: 321.1420; Found 321.1415. **Rf** 0.4 (hexane/AcOEt = 3:1).

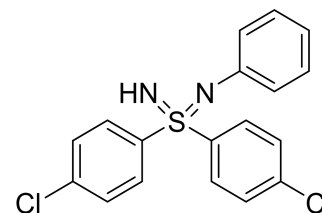
Bis(4-chlorophenyl)sulfiliminium mesitylenesulfonate (S2c): Prepared according to **GP-F** using bis(4-chlorophenyl) sulfide (3.51 mmol, 900 mg, 1.0 equiv.), **S2c** was isolated as a colorless solid (1.2 g, 72%). **IR** (KBr) 3152 3079, 2971, 2937, 1603, 1569, 1478, 1398, 1224, 1172, 1085, 1015, 818, 680



cm^{-1} . $^1\text{H NMR}$ (CDCl_3 , 400 MHz) δ 7.83 (brs, 2H), 7.72 (d, $J = 8.6$ Hz, 4H), 7.37 (d, $J = 8.6$ Hz, 4H), 6.80 (s, 2H), 2.51 (s, 6H), 2.25 (s, 3H). $^{13}\text{C NMR}$ (CDCl_3 , 100 MHz) δ 140.3, 139.5, 138.7, 137.0, 131.2, 130.8, 130.7, 129.9, 22.9, 20.8. **HRMS** (ESI) m/z : $[\text{M}-\text{MesO}]^+$ Calcd for $\text{C}_{12}\text{H}_{10}\text{NSCl}_2^+$: 269.9906; Found 269.9901.

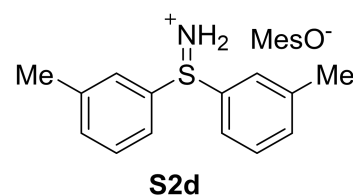
1,1-bis(4-chlorophenyl)-N-phenyl- λ^6 -sulfondiimine (5c): Prepared according to **GP-F** using compound **S2c** (2.12 mmol, 1.0 g, 1.0 equiv.), Na_2CO_3 (10.6 mmol, 1.12 g, 5.0 equiv.)

Selectfluor® (2.12 mmol, 750 mg, 1.0 equiv.), aniline (6.36 mmol, 0.6 mL, 3.0 equiv.), pyridine (2.54 mmol, 0.22 mL, 1.2 equiv.). **5c** was isolated as a colorless solid (0.42 g, 42%). **IR** (KBr) 3150, 1591, 1573, 1483, 1471,



1391, 1283, 1255, 1083, 948, 755, 749 cm^{-1} . $^1\text{H NMR}$ (CDCl_3 , 400 MHz) δ 8.10 (dd, $J = 8.8, 2.0$ Hz, 4H), 7.43 (dd, $J = 8.8, 2.0$ Hz, 4H), 7.17-7.10 (m, 4H), 6.90-6.87 (m, 1H), 2.26 (brs, 1H). $^{13}\text{C NMR}$ (CDCl_3 , 100 MHz) δ 145.0, 141.4, 138.9, 129.5, 129.5, 129.0, 123.3, 121.3. **HRMS** (ESI) m/z : $[\text{M}+\text{H}]^+$ Calcd for $\text{C}_{18}\text{H}_{15}\text{N}_2\text{SCl}_2^+$: 361.0328; Found 361.0321. **Rf** 0.6 (hexane/AcOEt = 3:1).

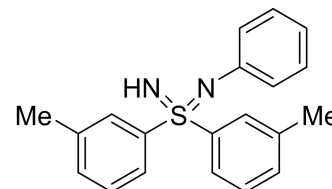
Bis(3-methylphenyl)sulfiliminium mesitylenesulfonate (S2d): Prepared according to **GP-F** using bis(3-methylphenyl) sulfide (3.5 mmol, 750 mg, 1.0 equiv.), **S2d** was isolated as a colorless solid (1.1 g, 72%). **IR** (KBr) 3174, 3041, 2968, 2959 1598, 1477, 1451, 1225, 1186, 1083, 1013, 850, 781, 669 cm^{-1} . $^1\text{H NMR}$ (CDCl_3 , 400 MHz) δ 7.60 (s, 2H), 7.53-7.50 (m, 2H), 7.34-7.30 (m, 4H),



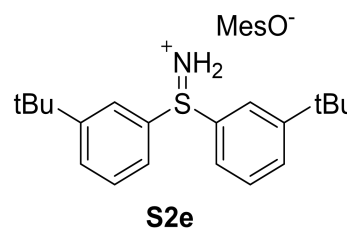
6.75 (s, 2H), 2.52 (s, 6H), 2.32 (s, 6H), 2.21 (s, 3H). $^{13}\text{C NMR}$ (CDCl_3 , 100 MHz) δ 140.9, 139.3, 138.5,

137.2, 134.0, 132.9, 130.6, 130.0, 128.5, 125.4, 22.9, 21.3, 20.8. **HRMS** (ESI) m/z : $[M-MesO]^{+}$ Calcd for $C_{14}H_{16}NS^{+}$: 230.0998; Found 230.0993.

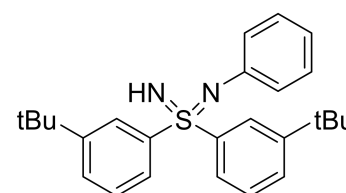
N-phenyl-1,1-di-m-tolyl- λ^6 -sulfondiimine (5d): Prepared according to **GP-F** using compound **S2d** (2.3 mmol, 1.0 g, 1.0 equiv.), Na_2CO_3 (11.6 mmol, 1.4 g, 5.0 equiv.), Selectfluor® (2.3 mmol, 820 mg, 1.0 equiv.), aniline (6.9 mmol, 0.8 mL, 3.0 equiv.), pyridine (8.3 mmol, 0.4 mL, 1.2 equiv.). **5d** was isolated as a colorless solid (0.25 g, 34%). **IR** (KBr) 3243, 3062, 1593, 1486, 1293, 1262, 1088, 933, 795, 749, 684 cm^{-1} . **1H NMR** ($CDCl_3$, 400 MHz) δ 8.00 (s, 2H), 7.96 (d, $J = 7.7$ Hz, 2H), 7.34 (t, $J = 7.7$ Hz, 2H), 7.28 (d, $J = 7.7$ Hz, 2H), 7.15-7.13 (m, 4H), 6.87-6.83 (m, 1H), 2.39 (s, 6H). **^{13}C NMR** ($CDCl_3$, 125 MHz) δ 143.0, 139.3, 132.8, 128.9, 128.8, 128.2, 125.1, 123.4, 120.7, 21.5; one aromatic signal was missing probably due to overlap. **HRMS** (ESI) m/z : $[M+Na]^{+}$ Calcd for $C_{20}H_{20}N_2SNa^{+}$: 343.1239; Found 343.1237. **Rf** 0.4 (hexane/AcOEt = 3:1).



Bis(3-tert-butylphenyl)sulfiliminium mesitylenesulfonate (S2e): Prepared according to **GP-F** using bis(2-methylphenyl) sulfide (1.0 mmol, 310 mg, 1.0 equiv.), **S2e** was isolated as a color solid (0.6 g, >99%). **IR** (KBr) 3206, 3190, 3174, 3142, 3070, 3050, 2957, 2877, 1593, 1481, 1365, 1183, 1082, 1008, 717 cm^{-1} . **1H NMR** ($CDCl_3$, 400 MHz) δ 7.68-7.62 (m, 4H), 7.59-7.54 (m, 4H), 7.43-7.37 (m, 2H), 6.75 (s, 2H), 2.54 (s, 6H), 2.22 (s, 3H), 1.26 (s, 18H). **^{13}C NMR** ($CDCl_3$, 100 MHz) δ 153.5, 139.9, 138.0, 137.0, 133.0, 130.4, 130.1, 130.1, 125.6, 125.3, 35.1, 30.9, 22.9, 20.7. **HRMS** (ESI) m/z : $[M-MesO]^{+}$ Calcd for $C_{20}H_{28}NS^{+}$: 314.1937; Found 314.1930.



1,1-bis(3-(tert-butyl)phenyl)-N-phenyl- λ^6 -sulfondiimine (5e): Prepared according to **GP-F** using compound **S2e** (1.0 mmol, 514 mg, 1.0 equiv.), Na_2CO_3 (5 mmol, 550 mg, 5.0 equiv.), Selectfluor® (1 mmol, 354 mg, 1.0 equiv.), aniline (3.0 mmol, 0.3 mL, 3.0 equiv.), pyridine (1.2 mmol, 0.1 mL, 1.2 equiv.). **5e** was isolated as a brown solid (0.12 g, 30%). **IR** (KBr) 3214, 2954, 2864, 1593, 1479, 1291, 1255, 1089, 957, 754 cm^{-1} . **1H NMR** ($CDCl_3$, 400 MHz) δ 8.22 (t, $J = 1.8$ Hz, 2H), 7.96 (d, $J = 7.7$ Hz, 2H), 7.50-7.47 (m, 2H), 7.36 (t, $J = 7.9$ Hz, 2H), 7.19-7.11 (m, 4H), 6.86-6.82 (m,

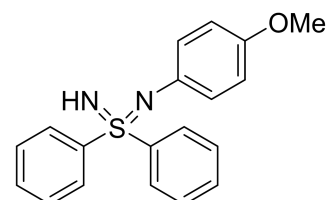


1H), 2.21 (brs, 1H), 1.30 (s, 18H). ¹³C NMR (CDCl₃, 100 MHz) δ 152.4, 146.0, 142.9, 128.9, 128.8, 128.7, 125.1, 124.8, 123.5, 120.7, 35.0, 31.1. HRMS (ESI) m/z: [M+H]⁺ Calcd for C₂₆H₃₃N₂S⁺: 405.2359; Found 405.2353. Rf 0.7 (hexane/AcOEt = 3:1).

N-(4-methoxyphenyl)-1,1-diphenyl-λ⁶-sulfondiimine (5f): Prepared according to GP-F using diphenylsulfiliminium mesitylenesulfonate (2.49 mmol, 1.0 g, 1.0 equiv.),

Na₂CO₃ (12.47 mmol, 1.3 g, 5.0 equiv.), Selectfluor® (2.49 mmol, 881 mg,

1.0 equiv.), 4-methoxyaniline (7.47 mmol, 919 mg, 3.0 equiv.), pyridine (2.97 mmol, 0.24 mL, 1.2 equiv.). **5f** was isolated by GPC as a brown solid

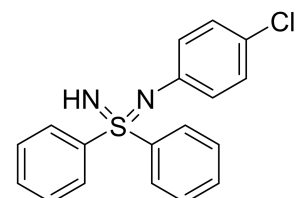


(0.27 g, 37%). IR (KBr) 3281, 1500, 1444, 1272, 1229, 1084, 1038, 958, 835, 721, 687 cm⁻¹. ¹H NMR (CDCl₃, 400 MHz) δ 8.20-8.15 (m, 4H), 7.47-7.44 (m, 6H), 7.08 (d, *J* = 9.1 Hz, 2H), 6.71 (d, *J* = 8.6, 1H), 3.71 (s, 3H), 2.17 (brs, 1H). ¹³C NMR (CDCl₃, 100 MHz) δ 154.2, 143.1, 138.6, 131.9, 129.1, 128.1, 124.3, 114.2, 55.4. HRMS (ESI) m/z: [M+H]⁺ Calcd for C₁₉H₁₉N₂SO⁺: 323.1213; Found 323.1210. Rf 0.5 (hexane/AcOEt = 2:1).

N-(4-chlorophenyl)-1,1-diphenyl-λ⁶-sulfondiimine (5g): Prepared according to GP-F using diphenylsulfiliminium mesitylenesulfonate (2.49 mmol, 1.0 g, 1.0 equiv.), Na₂CO₃ (12.47 mmol, 1.3 g, 5.0 equiv.), Selectfluor® (2.49 mmol, 881 mg, 1.0 equiv.), 4-chloroaniline (7.47

mmol, 949 mg, 3.0 equiv.), pyridine (2.97 mmol, 0.24 mL, 1.2 equiv.). **5g** was

isolated by GPC as a brown solid (0.18 g, 22%). IR (KBr) 1482, 1444, 1278, 1244, 1081, 1038, 950, 828, 718, 685 cm⁻¹. ¹H NMR (CDCl₃, 400 MHz) δ 8.16

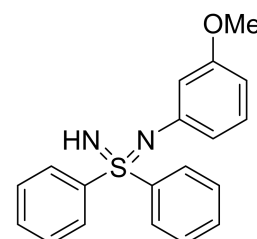


(d, *J* = 8.2 Hz, 4H), 7.52-7.43 (m, 6H), 7.11-7.05 (m, 4H), 2.21 (brs, 1H). ¹³C NMR (CDCl₃, 100 MHz) δ 144.5, 142.6, 132.2, 129.2, 128.8, 128.0, 125.8, 124.4. HRMS (ESI) m/z: [M+H]⁺ Calcd for C₁₈H₁₆N₂SCl⁺: 327.0717; Found 327.0714. Rf 0.5 (hexane/AcOEt = 3:1).

N-(3-methoxyphenyl)-1,1-diphenyl-λ⁶-sulfondiimine (5h): Prepared according to GP-F using diphenylsulfiliminium mesitylenesulfonate (2.49 mmol, 1.0 g, 1.0 equiv.), Na₂CO₃

(12.47 mmol, 1.3 g, 5.0 equiv.), Selectfluor® (2.49 mmol, 881 mg, 1.0 equiv.),

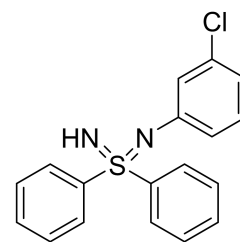
3-methoxyaniline (7.47 mmol, 0.80 mL, 3.0 equiv.), pyridine (2.97 mmol, 0.24 mL, 1.2 equiv.). **5h** was isolated as a brown solid (0.27 g, 37%). IR (KBr) 3178,



1579, 1490, 1444, 1289, 1208, 1151, 1081, 1037, 979, 884, 772, 725, 691 cm^{-1} . $^1\text{H NMR}$ (CDCl_3 , 400 MHz) δ 8.19-8.17 (m, 4H), 7.48-7.42 (m, 6H), 7.03-7.01 (m, 1H), 6.78 -6.74 (m, 2H), 6.44-6.42 (m, 1H), 3.70 (s, 3H), 2.24 (brs, 1H). $^{13}\text{C NMR}$ (CDCl_3 , 100 MHz) δ 160.1, 147.0, 143.0, 132.0, 129.3, 129.1, 128.0, 115.6, 109.0, 106.8, 55.0. **HRMS** (ESI) m/z : $[\text{M}+\text{H}]^+$ Calcd for $\text{C}_{19}\text{H}_{19}\text{N}_2\text{SO}^+$: 323.1213; Found 323.1208. **Rf** 0.5 (hexane/AcOEt = 2:1).

N-(3-chlorophenyl)-1,1-diphenyl- λ^6 -sulfondiimine (5i): Prepared according to **GP-F** using diphenylsulfiliminium mesitylenesulfonate (2.49 mmol, 1.0 g, 1.0 equiv.), Na_2CO_3

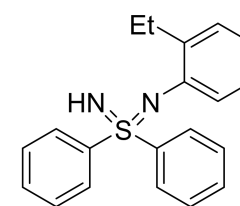
(12.47 mmol, 1.3 g, 5.0 equiv.), Selectfluor® (2.49 mmol, 881 mg, 1.0 equiv.), 3-chloroaniline (7.47 mmol, 0.72 mL, 3.0 equiv.), pyridine (2.97 mmol, 0.24 mL, 1.2 equiv.). **5i** was isolated as a brown solid (0.37 g, 50%). **IR** (KBr) 3170, 1588,



1553, 1472, 1442, 1313, 1257, 1094, 1043, 971, 786, 716, 684 cm^{-1} . $^1\text{H NMR}$ (CDCl_3 , 400 MHz) δ 8.17 (dd, $J = 7.5, 1.6$ Hz, 4H), 7.52-7.44 (m, 6H), 7.19 (s, 1H), 7.06-6.99 (m, 2H), 6.84-6.78 (m, 1H), 2.24 (brs, 1H). $^{13}\text{C NMR}$ (CDCl_3 , 100 MHz) δ 147.3, 142.6, 134.2, 132.2, 129.6, 129.2, 127.9, 123.4, 121.1, 120.8. **HRMS** (ESI) m/z : $[\text{M}+\text{H}]^+$ Calcd for $\text{C}_{18}\text{H}_{16}\text{N}_2\text{SCl}^+$: 327.0717; Found 327.0713. **Rf** 0.5 (hexane/AcOEt = 2:1).

N-(2-ethylphenyl)-1,1-diphenyl- λ^6 -sulfondiimine (5j): Prepared according to **GP-F** using diphenylsulfiliminium mesitylenesulfonate (2.49 mmol, 1.0 g, 1.0 equiv.), Na_2CO_3 (12.47 mmol, 1.3 g, 5.0 equiv.), Selectfluor® (2.49 mmol, 881 mg, 1.0 equiv.), 2-ethylaniline (7.47 mmol,

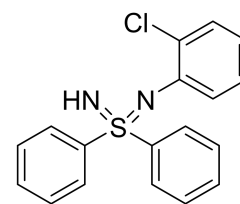
0.87 mL, 3.0 equiv.), pyridine (2.97 mmol, 0.24 mL, 1.2 equiv.). **5j** was isolated as a colorless solid (0.27 g, 37%). **IR** (KBr) 3273, 3246, 2964, 1592, 1481, 1445, 1302, 1282, 1252, 1119, 1078, 1056, 955, 757, 686 cm^{-1} . $^1\text{H NMR}$ (CDCl_3 , 400



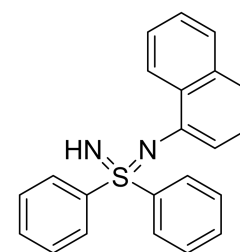
MHz) δ 8.19-8.16 (m, 4H), 7.49-7.43 (m, 6H), 7.19-7.13 (m, 2H), 6.88 (t, $J = 7.6$ Hz, 1H), 6.81 (t, $J = 7.3$ Hz, 1H), 2.94 (q, $J = 7.1$ Hz, 2H), 2.22 (brs, 1H), 1.40-1.33 (m, 3H). $^{13}\text{C NMR}$ (CDCl_3 , 100 MHz) δ 143.6, 143.4, 138.5, 131.9, 129.1, 128.6, 127.9, 126.0, 120.7, 120.6, 25.5, 14.5. **HRMS** (ESI) m/z : $[\text{M}+\text{H}]^+$ Calcd for $\text{C}_{20}\text{H}_{21}\text{N}_2\text{S}^+$: 321.1420; Found 321.1418. **Rf** 0.6 (hexane/AcOEt = 2:1).

N-(2-chlorophenyl)-1,1-diphenyl- λ^6 -sulfondiimine (5k): Prepared according to **GP-F** using diphenylsulfiliminium mesitylenesulfonate (2.49 mmol, 1.0 g, 1.0 equiv.), Na_2CO_3 (12.47 mmol, 1.3 g, 5.0

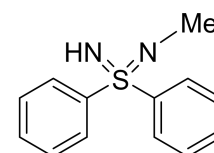
equiv.), Selectfluor® (2.49 mmol, 881 mg, 1.0 equiv.), 2-chloroaniline (7.47 mmol, 0.72 mL, 3.0 equiv.), pyridine (2.97 mmol, 0.24 mL, 1.2 equiv.). **5k** was isolated as a colorless solid (0.15 g, 20%). **IR** (KBr) 3201, 1584, 1471, 1437, 1309, 1287, 1249 1079, 1061, 1032, 958, 751, 717, 678, 620 cm⁻¹. **¹H NMR** (CDCl₃, 400 MHz) δ 8.26-8.21 (m, 4H), 7.49 - 7.43 (m, 6H), 7.38-7.29 (m, 2H), 6.92 (t, *J* = 7.5 Hz, 1H), 6.76 (t, *J* = 7.7, 1H), 2.37 (brs, 1H). **¹³C NMR** (CDCl₃, 100 MHz) δ 142.8, 142.7, 132.2, 129.8, 129.2, 128.2, 126.9, 122.5, 121.4; one aromatic signal was missing probably due to overlap. **HRMS** (ESI) *m/z*: [M+H]⁺ Calcd for C₁₈H₁₆N₂SCl⁺: 327.0717; Found 327.0715. **Rf** 0.5 (hexane/AcOEt = 2:1).



N-(naphthalen-1-yl)-1,1-diphenyl-λ⁶-sulfondiimine (5l): Prepared according to **GP-F** using diphenylsulfiliminium mesitylenesulfonate (2.49 mmol, 1.0 g, 1.0 equiv.), Na₂CO₃ (12.47 mmol, 1.3 g, 5.0 equiv.), Selectfluor® (2.49 mmol, 881 mg, 1.0 equiv.), naphthalen-1-amine (7.47 mmol, 973 mg, 3.0 equiv.), pyridine (2.97 mmol, 0.24 mL, 1.2 equiv.). **5l** was isolated as a colorless solid (0.13 g, 18%). **IR** (KBr) 3198, 1568, 1396, 1270, 1240, 1186, 1113, 1078, 937, 769, 727 cm⁻¹. **¹H NMR** (CDCl₃, 400 MHz) δ 8.77 (d, *J* = 8.2 Hz, 1H), 8.29-8.24 (m, 4H), 7.77 (d, *J* = 8.2 Hz, 1H), 7.54-7.44 (m, 8H), 7.35 (d, *J* = 8.2 Hz, 1H), 7.22 (d, *J* = 7.2 Hz, 1H), 7.14 (t, *J* = 7.7 Hz, 1H), 2.35 (brs, 1H). **¹³C NMR** (CDCl₃, 100 MHz) δ 143.1, 142.0, 134.7, 132.1, 130.9, 129.2, 128.0, 127.8, 126.0, 125.7, 124.7, 124.0, 120.3, 115.4. **HRMS** (ESI) *m/z*: [M+H]⁺ Calcd for C₂₂H₁₉N₂S⁺: 343.1263; Found 343.1259. **Rf** 0.4 (hexane/AcOEt = 2:1).

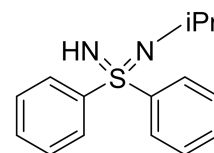


N-methyl-1,1-diphenyl-λ⁶-sulfondiimine (5m): Prepared according to **GP-F** using diphenylsulfiliminium mesitylenesulfonate (2.49 mmol, 1.0 g, 1.0 equiv.), Na₂CO₃ (12.47 mmol, 1.3 g, 5.0 equiv.), Selectfluor® (2.49 mmol, 881 mg, 1.0 equiv.), methanamine (7.47 mmol, 33 wt% in EtOH 1.0 mL, 3.0 equiv.), pyridine (2.97 mmol, 0.24 mL, 1.2 equiv.). **5m** was isolated as a colorless solid (0.1 g, 19%). **IR** (KBr) 3152, 2909, 2852, 2786, 1444, 1181, 1089, 1091, 995, 837, 757, 716, 688 cm⁻¹. **¹H NMR** (CDCl₃, 400 MHz) δ 8.10-8.04 (m, 4H), 7.52-7.39 (m, 6H), 2.80 (s, 3H). **¹³C NMR** (CDCl₃, 100 MHz) δ 142.4, 131.7 129.0, 127.9, 29.1. **HRMS** (ESI) *m/z*: [M+H]⁺ Calcd for C₁₃H₁₅N₂S⁺: 231.0950; Found 231.0947. **Rf** 0.2 (hexane/AcOEt = 2:1).



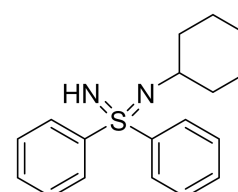
N-isopropyl-1,1-diphenyl-λ⁶-sulfondiimine (5n): Prepared according to **GP-F** using

diphenylsulfiliminium mesitylenesulfonate (2.49 mmol, 1.0 g, 1.0 equiv.), Na₂CO₃ (12.47 mmol, 1.3 g, 5.0 equiv.), Selectfluor® (2.49 mmol, 881 mg, 1.0 equiv.), propan-2-amine (7.47 mmol, 0.6 mL, 3.0 equiv.), pyridine (2.97 mmol, 0.24 mL, 1.2 equiv.). **5n** was isolated as a colorless solid (50 mg, 9%). **IR** (KBr) 3202, 2969, 2924, 2858, 1442, 1177, 1142, 1069, 982, 758, 709, 689 cm⁻¹. **¹H NMR** (CDCl₃, 400 MHz) δ 8.13-8.08 (m, 4H), 7.49-7.39 (m, 6H), 3.52-3.45 (m, 1H), 1.87 (brs, 1H), 1.25-1.19 (m, 6H). **¹³C NMR** (CDCl₃, 100 MHz) δ 143.7, 131.5, 128.8, 128.0, 45.2, 27.0. **HRMS** (ESI) m/z: [M+H]⁺ Calcd for C₁₅H₁₉N₂S⁺: 259.1263; Found 259.1261. **Rf** 0.3 (hexane/AcOEt = 2:1).

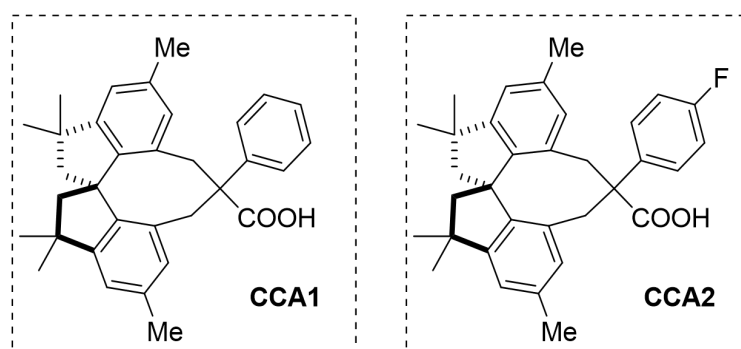
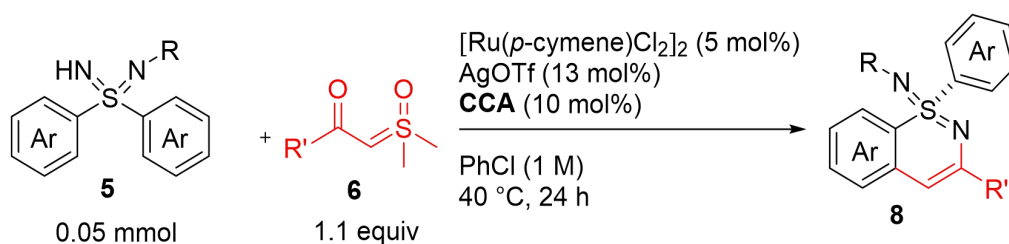


N-cyclohexyl-1,1-diphenyl-λ⁶-sulfondiimine (5o): Prepared according to **GP-F**

using diphenylsulfiliminium mesitylenesulfonate (2.49 mmol, 1.0 g, 1.0 equiv.), Na₂CO₃ (12.47 mmol, 1.3 g, 5.0 equiv.), Selectfluor® (2.49 mmol, 881 mg, 1.0 equiv.), cyclohexanamine (7.47 mmol, 0.8 mL, 3.0 equiv.), pyridine (2.97 mmol, 0.24 mL, 1.2 equiv.). **5o** was isolated as a colorless solid (0.18 g, 26%). **IR** (KBr) 3302, 3062, 2913, 2850, 1473, 1445, 1167, 1087, 1082, 962, 696, 679 cm⁻¹. **¹H NMR** (CDCl₃, 400 MHz) δ 8.12-8.07 (m, 4H), 7.46-7.39 (m, 6H), 3.17-3.09 (m, 1H), 1.89-1.82 (m, 2H), 1.75-1.67 (m, 3H), 1.57-1.39 (m, 3H), 1.29-1.13 (m, 3H). **¹³C NMR** (CDCl₃, 100 MHz) δ 144.2, 131.2, 128.8, 128.0, 52.8, 37.4, 25.8, 25.4. **HRMS** (ESI) m/z: [M+H]⁺ Calcd for C₁₆H₂₃N₂S⁺: 299.1576; Found 299.1574. **Rf** 0.5 (hexane/AcOEt = 2:1).



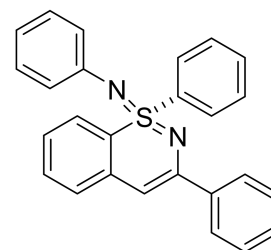
4.4. Ru(II)-catalyzed enantioselective C–H alkylation/cyclization

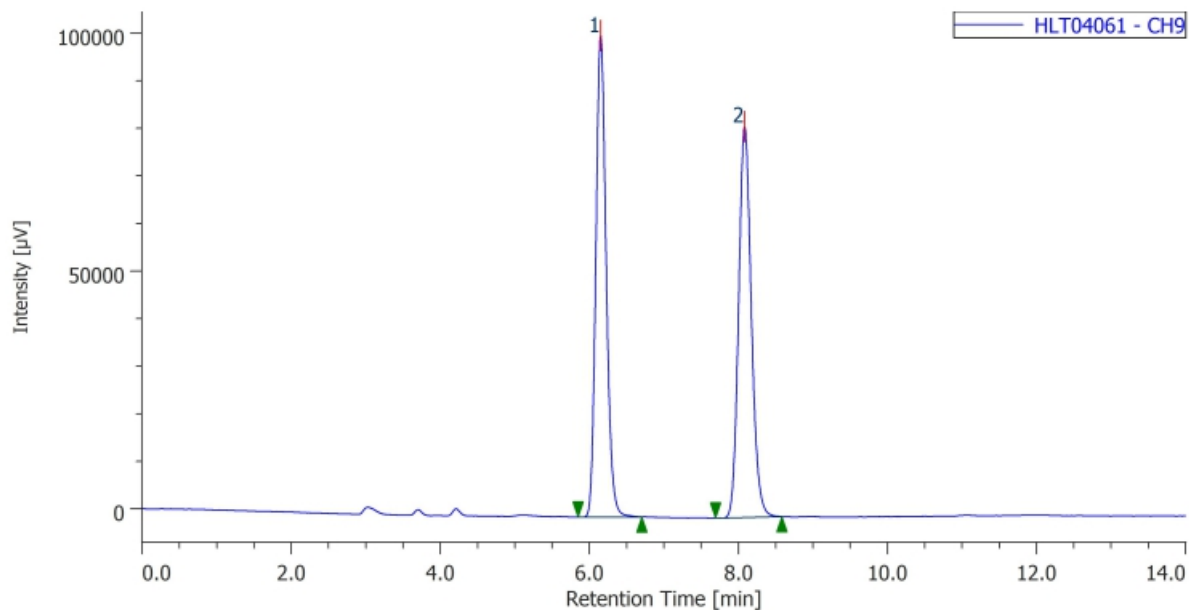


General Procedure G: Ru(II)-catalyzed enantioselective C–H alkylation/cyclization

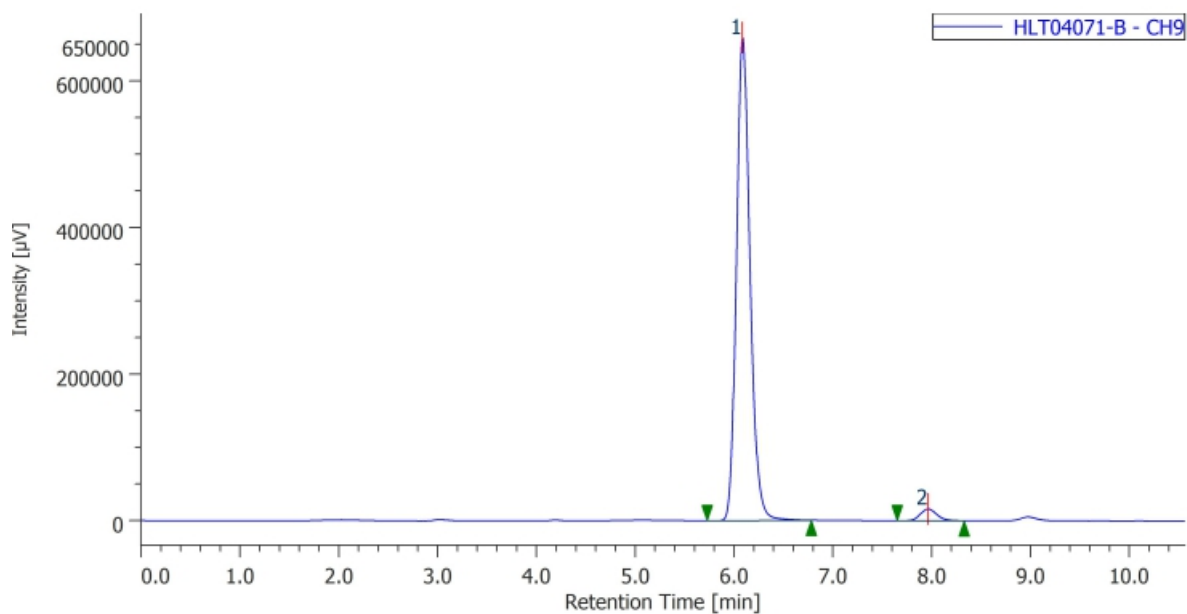
In an argon-filled glovebox, a screw-capped test tube was charged with chiral carboxylic acid **CCA** (0.005 mmol, 10 mol%), [Ru(*p*-cymene)Cl₂]₂ (1.6 mg, 0.0025 mmol, 5 mol%), AgOTf (1.6 mg, 0.0065 mmol, 13 mol%), sulfondiimine **5** (0.05 mmol, 1.0 equiv.), and sulfoxonium ylide **6** (0.055 mmol, 1.1 equiv.). After the addition of chlorobenzene (0.05 mL), the test tube was capped and brought out of the glovebox. The reaction mixture was stirred at 40 °C for 24 h. The resulting mixture was directly purified by silica gel column chromatography (hexane/AcOEt) to afford **8**.

(S)-N,1,3-triphenyl-1λ⁶-benzo[e][1,2]thiazin-1-imine (8aa): Prepared according to **GP-G** using compound **5a** (0.05 mmol, 14.6 mg, 1.0 equiv.), **6a** (0.055 mmol, 10.8 mg, 1.1 equiv.), **CCA2** (0.005 mmol, 2.4 mg, 10 mol%). **8aa** was isolated as a yellow solid (16.5 mg, 84%). **IR** (KBr) 3055, 2957, 2923, 1585, 1530, 1483, 1472, 1445, 1362, 1283, 1256, 1117, 1040, 752, 691 cm⁻¹. **¹H NMR** (CDCl₃, 400 MHz) δ 8.21 (m, 2H), 8.02-7.98 (m, 2H), 7.58-7.53 (m, 3H), 7.46-7.34 (m, 5H), 7.30 (d, *J* = 7.2 Hz, 1H), 7.15-7.09 (m, 1H), 7.09-7.04 (m, 2H), 6.87 - 6.80 (m, 3H), 6.63 (s, 1H). **¹³C NMR** (CDCl₃, 100 MHz) δ 149.2, 144.6, 143.0, 139.7, 139.1, 132.5, 132.1, 128.9, 128.8, 128.7, 128.5, 128.3, 126.5, 126.4, 126.3, 125.9, 123.5, 121.5, 116.3, 96.4. **HPLC** (chiral column: DAICEL CHIRALPAK IF; solvent: hexane/2-propanol = 4/1; flow rate: 1.0 mL/min; detection: at 254 nm): *t_R* = 6.09 min (major) and 7.97 min (minor). **HRMS** (ESI) *m/z*: [M+Na]⁺ Calcd for C₂₆H₂₀N₂SNa⁺: 415.1239; Found 415.1235. [**α**]_D^{22.1} = +142.1 (*c* = 0.25, CHCl₃). **R_f** 0.5 (hexane/AcOEt = 2:1).



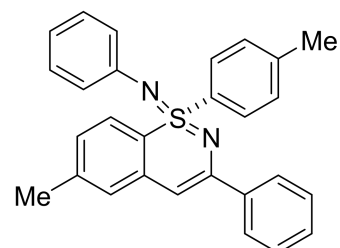


#	ピーク名	CH	tR [min]	Area%
1	Unknown	9	6.150	50.045
2	Unknown	9	8.080	49.955

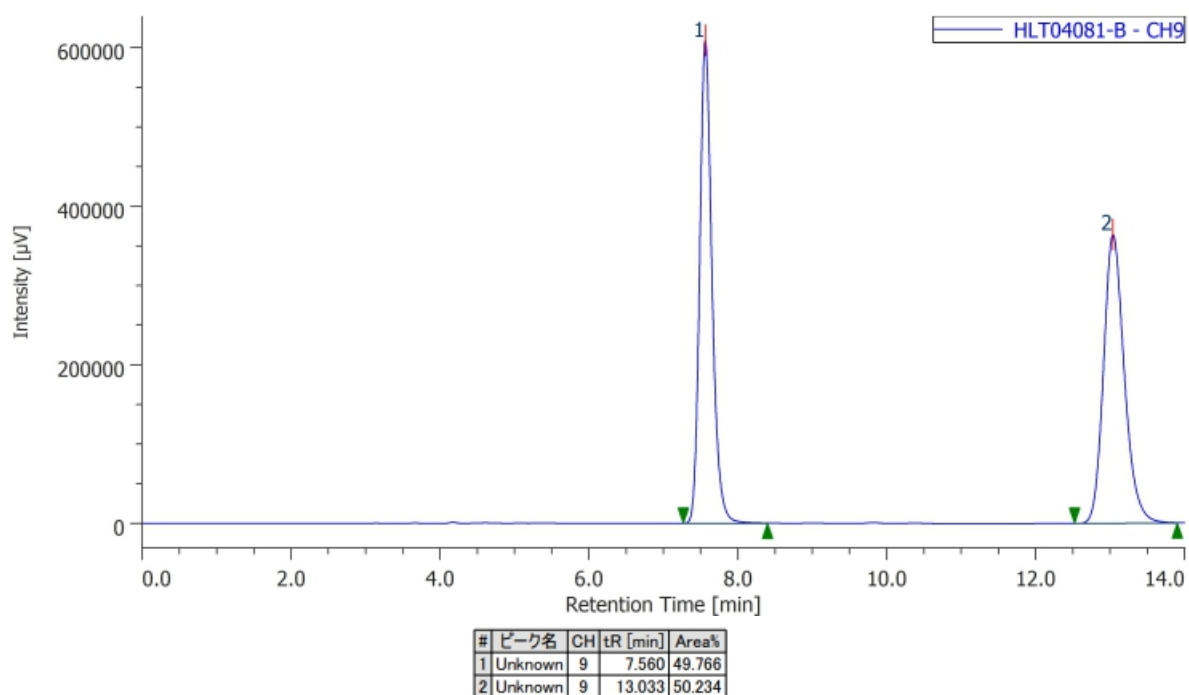


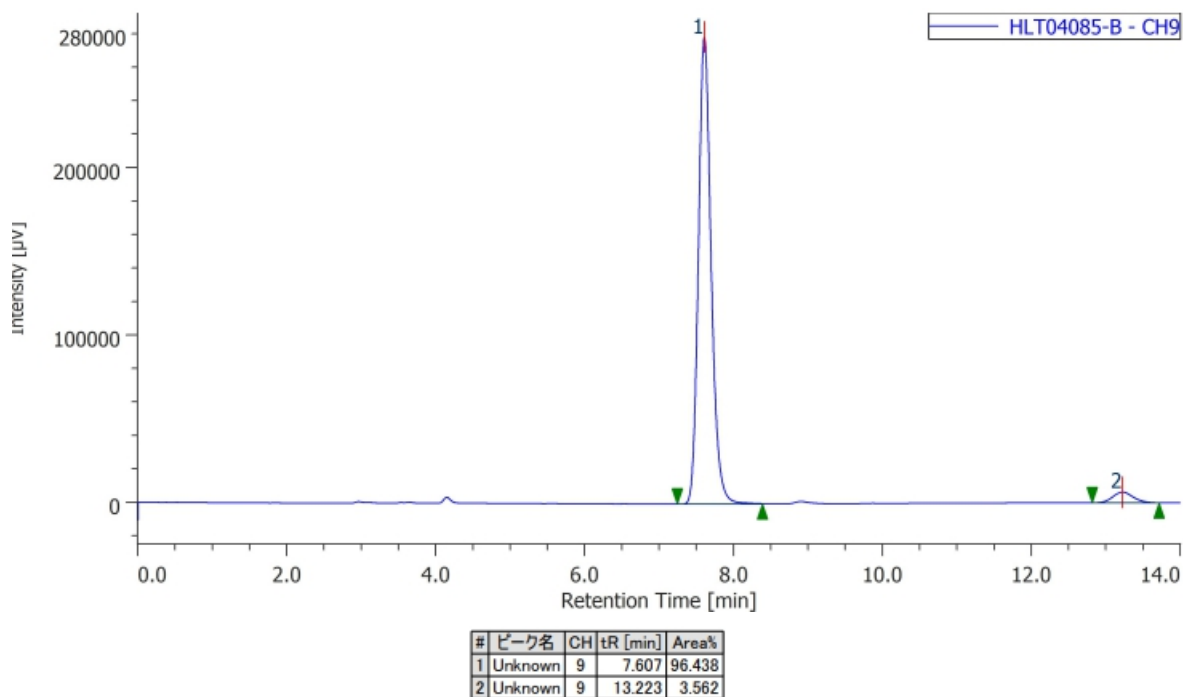
#	ピーク名	CH	tR [min]	Area%
1	Unknown	9	6.083	97.113
2	Unknown	9	7.963	2.887

(S)-6-methyl-N,3-diphenyl-1-(p-tolyl)-1λ⁶-benzo[e][1,2]thiazin-1-imine (8ba): Prepared according to GP-G using compound **5b** (0.05 mmol, 16.0 mg, 1.0 equiv.), **6a** (0.055 mmol, 10.8 mg, 1.1 equiv.), **CCA2** (0.005 mmol, 2.4 mg, 10 mol%). **8ba** was isolated as a yellow solid (14.7 mg, 70%). IR (KBr) 3051, 2954, 2915, 1591, 1534, 1485, 1468, 1352, 1282, 1259, 1115, 1088, 1013, 754, 695

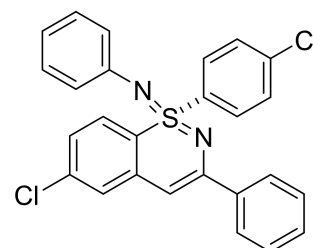


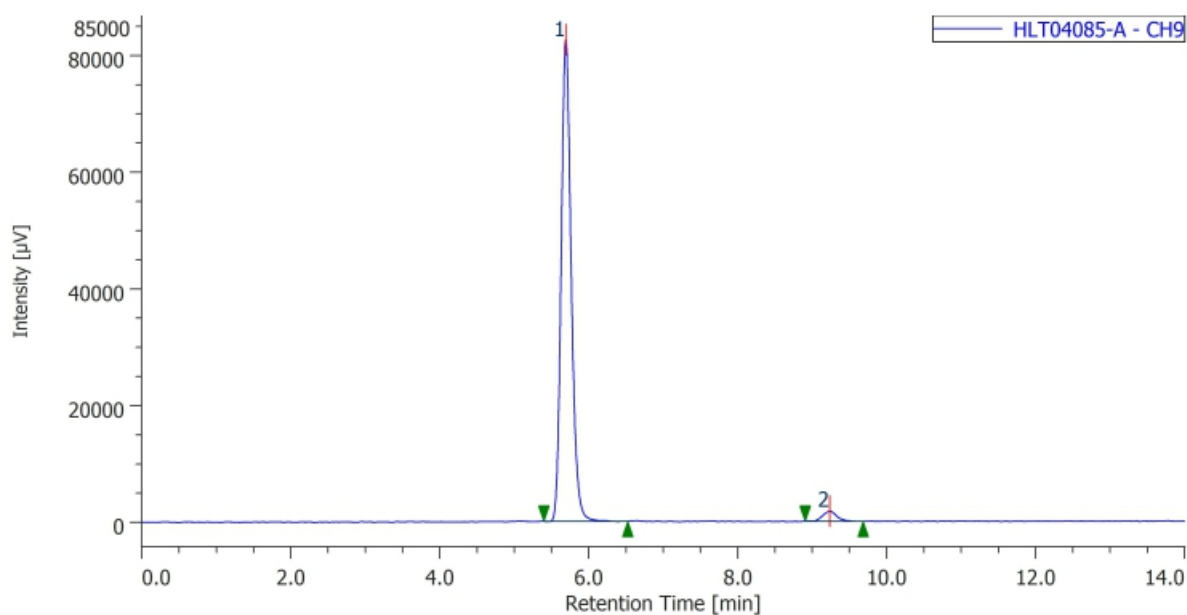
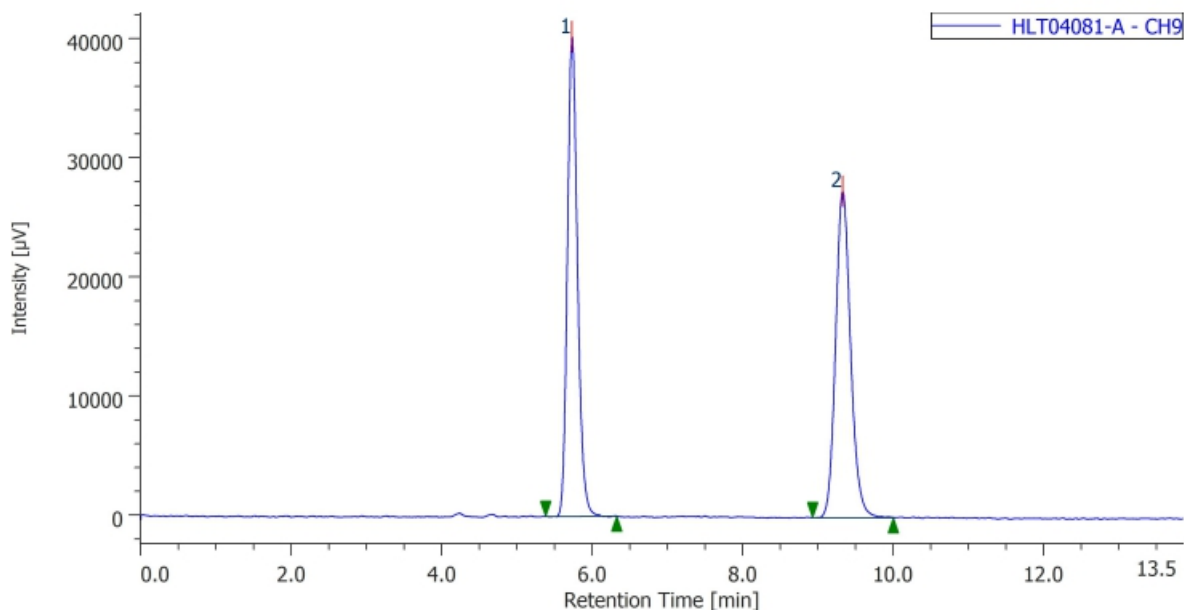
cm⁻¹. **¹H NMR** (CDCl₃, 400 MHz) δ 8.03 (d, *J* = 8.6 Hz, 2H), 7.99 (dd, *J* = 8.2, 1.4 Hz, 2H), 7.42-7.30 (m, 6H), 7.08-7.03 (m, 3H), 6.94-6.90 (m, 1H), 6.85-6.79 (m, 3H), 6.56 (s, 1H), 2.41 (s, 3H), 2.30 (s, 3H). **¹³C NMR** (CDCl₃, 100 MHz) δ 149.2, 144.9, 143.3, 142.6, 140.5, 139.8, 139.3, 129.5, 128.8, 128.6, 128.5, 128.3, 127.8, 126.5, 126.1, 125.8, 123.4, 121.3, 113.9, 96.2, 21.6, 21.4. **HPLC** (chiral column: DAICEL CHIRALPAK IF; solvent: hexane/2-propanol = 4/1; flow rate: 1.0 mL/min; detection: at 254 nm): t_R = 7.61 min (major) and 13.22 min (minor). **HRMS** (ESI) m/z: [M+H]⁺ Calcd for C₂₈H₂₅N₂S⁺: 421.1733; Found 421.1726. [α]_D^{19.1} = +218.1 (*c* = 0.25, CHCl₃). **Rf** 0.5 (hexane/AcOEt = 3:1).



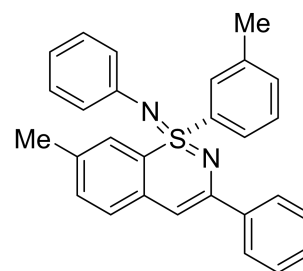


(S)-6-chloro-1-(4-chlorophenyl)-N,3-diphenyl-1 λ ⁶-benzo[e][1,2]thiazin-1-imine (8ca): Prepared according to **GP-G** using compound **5c** (0.05 mmol, 18.0 mg, 1.0 equiv.), **6a** (0.055 mmol, 10.8 mg, 1.1 equiv.), **CCA2** (0.005 mmol, 2.4 mg, 10 mol%). **8ca** was isolated as a yellow solid (12.0 mg, 52%). **IR** (KBr) 1567, 1484, 1390, 1257, 1083, 821, 757, 694, 669 cm^{-1} . **¹H NMR** (CDCl_3 , 400 MHz) δ 8.10-8.07 (m, 2H), 7.98-7.95 (m, 2H), 7.54-7.51 (m, 2H), 7.45-7.36 (m, 3H), 7.33 (d, $J = 8.6$ Hz, 1H), 7.29 (d, $J = 2.3$ Hz, 1H), 7.10-7.05 (m, 3H), 6.86 (t, $J = 7.2$ Hz, 1H), 6.81 (dd, $J = 8.4$, 1.1 Hz, 2H), 6.56 (s, 1H). **¹³C NMR** (CDCl_3 , 100 MHz) δ 150.6, 143.8, 141.3, 141.2, 139.6, 138.6, 138.5, 129.9, 129.3, 129.2, 129.0, 128.5, 127.4, 126.7, 126.6, 125.6, 123.4, 122.1, 114.0, 95.7. **HPLC** (chiral column: DAICEL CHIRALPAK IF; solvent: hexane/2-propanol = 4/1; flow rate: 1.0 mL/min; detection: at 350 nm): $t_R = 5.69$ min (major) and 9.23 min (minor). **HRMS** (ESI) m/z : $[\text{M}+\text{H}]^+$ Calcd for $\text{C}_{26}\text{H}_{19}\text{N}_2\text{SCl}_2^+$: 461.0641; Found 461.0631. $[\alpha]_D^{23.3} = +88.7$ ($c = 0.25$, CHCl_3). **Rf** 0.8 (hexane/AcOEt = 3:1).

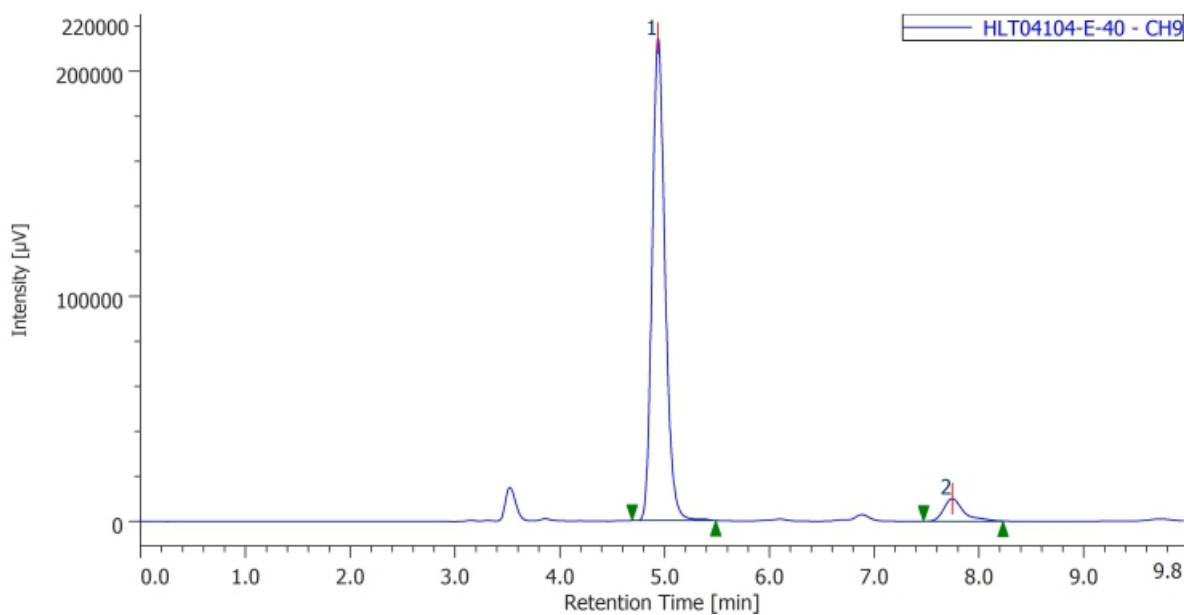
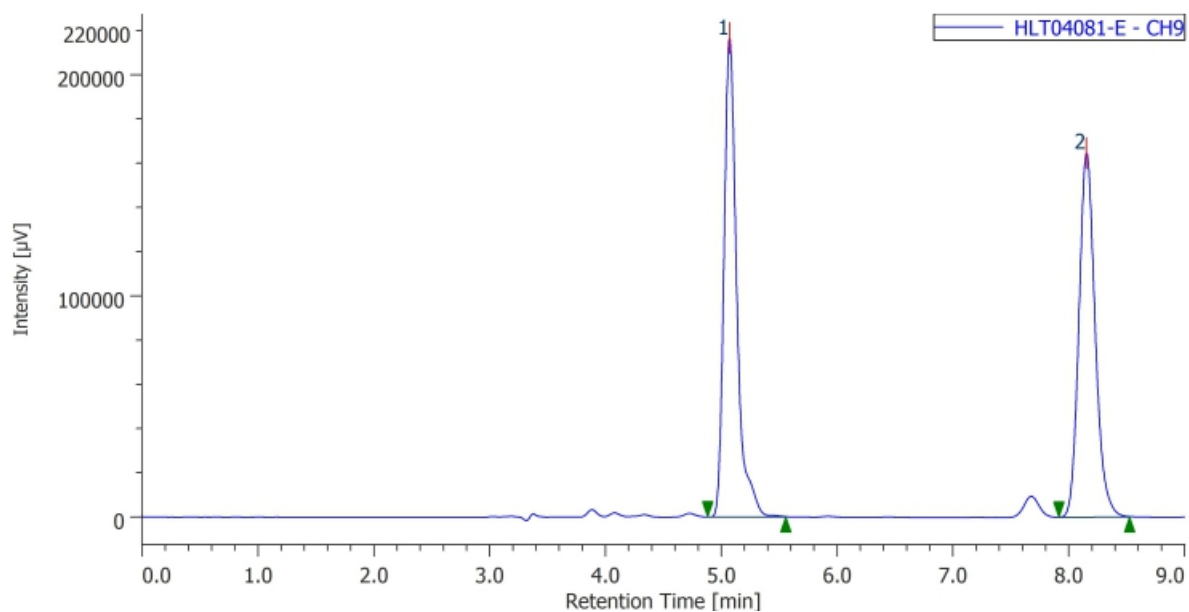




(S)-7-methyl-N,3-diphenyl-1-(m-tolyl)-1 λ^6 -benzo[e][1,2]thiazin-1-imine (8da): Prepared according to GP-G using compound **5d** (0.05 mmol, 16.0 mg, 1.0 equiv.), **6a** (0.055 mmol, 10.8 mg, 1.1 equiv.), **CCA1** (0.005 mmol, 2.4 mg, 10 mol%). **8da** was isolated as a yellow solid (14.3 mg, 68%). IR (KBr) 3051, 3023, 2947, 1588, 1483, 1358, 1285, 1255, 1114, 1037, 758, 685 cm^{-1} . ^1H NMR (CDCl_3 , 400 MHz) δ 7.99-7.96 (m, 4H), 7.45-7.32 (m, 6H), 7.22-7.19 (m, 2H), 7.06 (t, $J =$



7.9 Hz, 2H), 6.83-6.80 (m, 3H), 6.61 (s, 1H), 2.43 (s, 3H), 2.23 (s, 3H). ^{13}C NMR (CDCl_3 , 125 MHz) δ 148.2, 144.8, 143.0, 139.3, 139.1, 137.3, 136.5, 133.7, 133.3, 128.8, 128.7, 128.4, 128.3, 126.4, 126.3, 125.9, 125.2, 123.3, 121.3, 116.2, 96.2, 21.5, 21.3; one aromatic signal was missing probably due to overlap. **HPLC** (chiral column: DAICEL CHIRALPAK IF; solvent: hexane/2-propanol = 2/1; flow rate: 1.0 mL/min; detection: at 254 nm): t_R = 4.94 min (major) and 7.74 min (minor). **HRMS** (ESI) m/z : $[\text{M}+\text{Na}]^+$ Calcd for $\text{C}_{28}\text{H}_{24}\text{N}_2\text{SNa}^+$: 443.1352; Found 443.1548. $[\alpha]_D^{20.8} = +107.8$ ($c = 0.25$, CHCl_3). **Rf** 0.6 (hexane/AcOEt = 3:1).



(S)-7-(tert-butyl)-1-(3-(tert-butyl)phenyl)-N,3-diphenyl-1λ⁶-benzo[e][1,

2]thiazin-1-imine (8ea): Prepared according to GP-G using compound 5e

(0.05 mmol, 16.0 mg, 1.0 equiv.), 6a (0.055 mmol, 10.8 mg, 1.1 equiv.),

CCA1 (0.005 mmol, 2.4 mg, 10 mol%). 8ea was isolated as a yellow oil

(17.2 mg, 68%). IR (neat) 2962, 2934, 2927, 1592, 1486, 1360, 1290,

1256, 1127 cm⁻¹. ¹H NMR (CDCl₃, 400 MHz) δ 8.25 (s, 1H), 8.01 (d, *J* = 6.8 Hz, 2H), 7.86-7.83 (m, 1H),

7.56 (d, *J* = 8.6 Hz, 1H), 7.48-7.34 (m, 6H), 7.23 (d, *J* = 8.6 Hz, 1H), 7.08-7.03 (m, 2H), 6.94 (d, *J* = 8.6 Hz,

2H), 6.82 (t, *J* = 7.2 Hz, 1H), 6.57 (s, 1H), 1.33 (s, 9H), 1.19 (s, 9H). ¹³C NMR (CDCl₃, 100 MHz) δ 152.2,

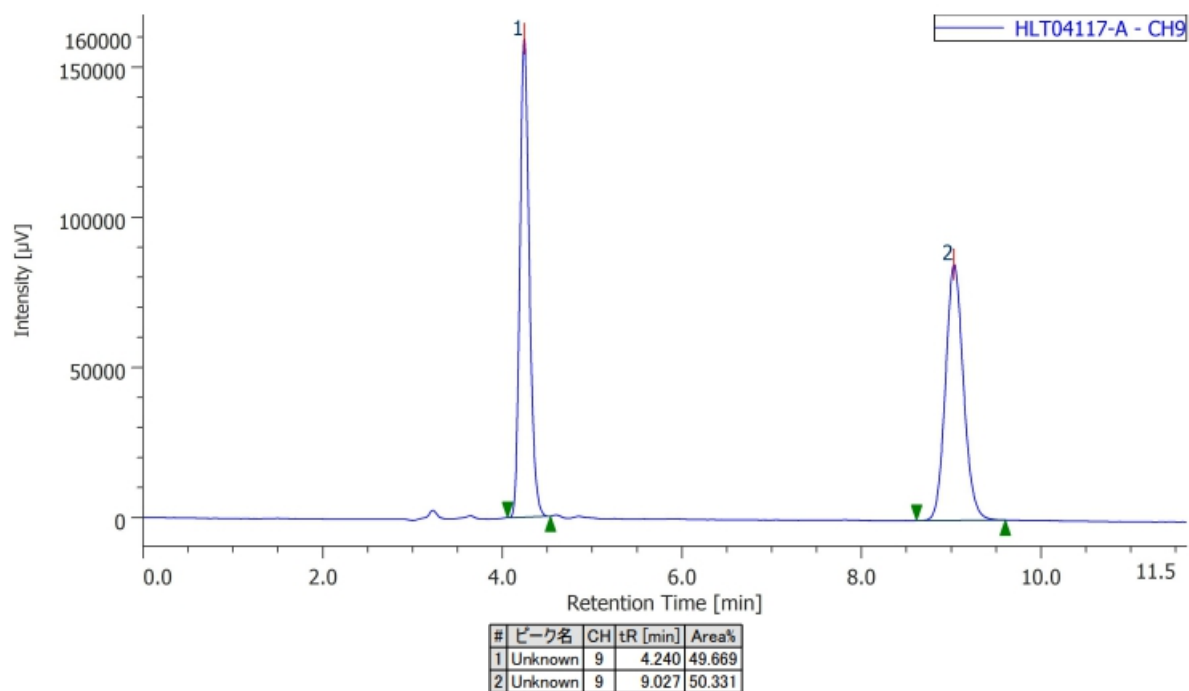
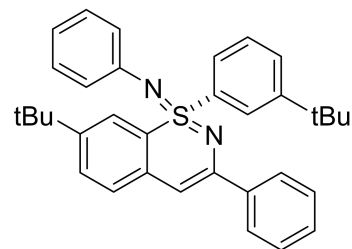
149.6, 148.3, 145.1, 142.4, 139.4, 137.2, 130.0, 129.4, 128.8, 128.7, 128.4, 128.3, 126.4, 126.2, 125.8,

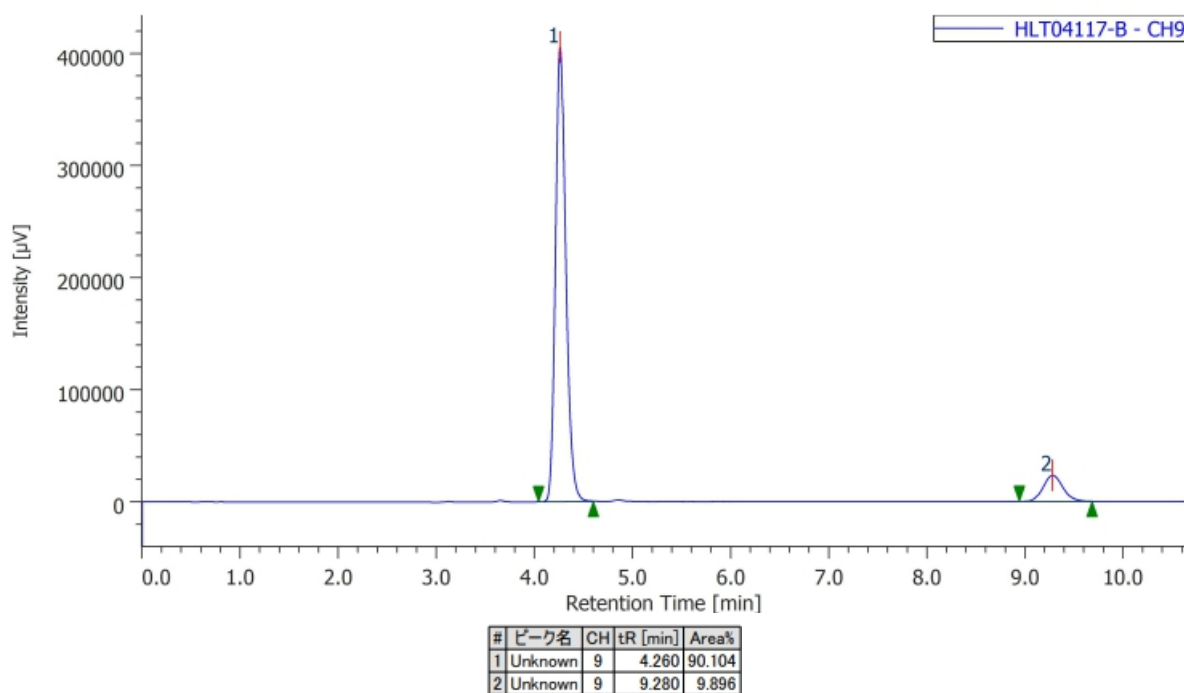
124.8, 124.0, 121.6, 121.5, 116.0, 96.4, 35.1, 34.7, 31.2, 30.9. HPLC (chiral column: DAICEL

CHIRALPAK IF; solvent: hexane/2-propanol = 4/1; flow rate: 1.0 mL/min; detection: at 254 nm): t_R = 4.24

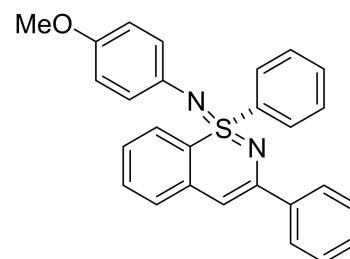
min (major) and 9.28 min (minor). HRMS (ESI) m/z: [M+H]⁺ Calcd for C₃₄H₃₇N₂S⁺: 505.2672; Found

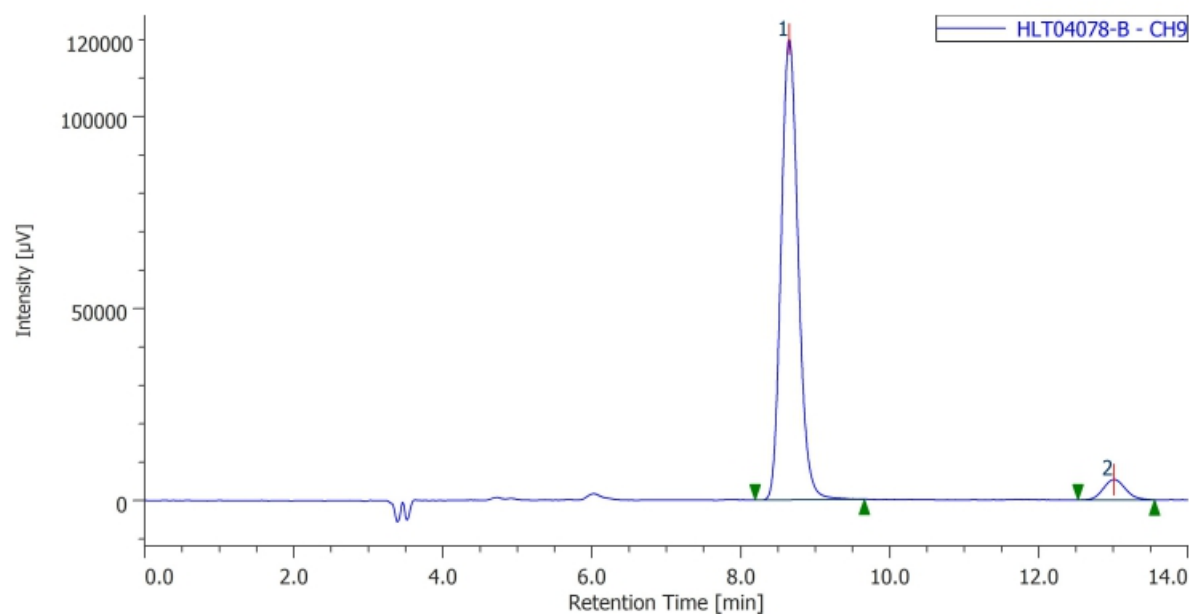
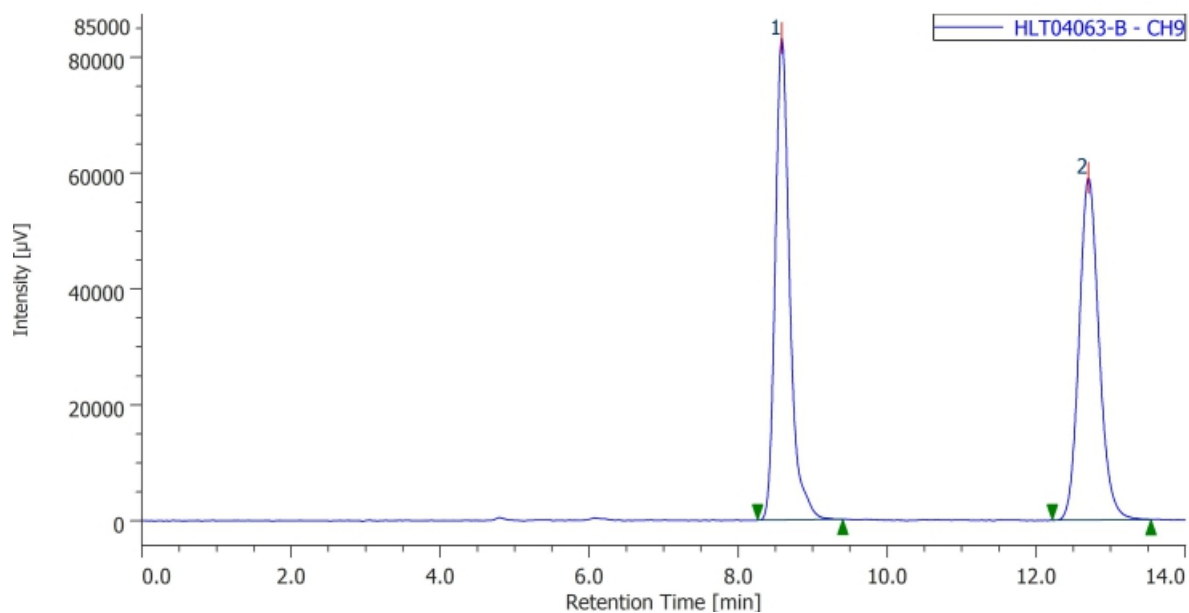
505.2666. [α]_D^{23.4} = +157.0 (*c* = 0.25, CHCl₃). R_f 0.8 (hexane/AcOEt = 3:1).



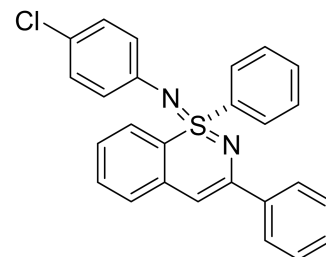


(S)-N-(4-methoxyphenyl)-1,3-diphenyl-1λ⁶-benzo[e][1,2]thiazin-1-imine (8fa): Prepared according to GP-G using compound **5f** (0.05 mmol, 16.1 mg, 1.0 equiv.), **6a** (0.055 mmol, 10.8 mg, 1.1 equiv.), **CCA2** (0.005 mmol, 2.4 mg, 10 mol%). **8fa** was isolated as a yellow solid (12.7 mg, 60%). **IR** (KBr) 2957, 2925, 2851 1665, 1572, 1501, 1470, 1445, 1363, 1260, 1236, 1101, 1030, 801, 684 cm⁻¹. **¹H NMR** (CDCl₃, 400 MHz) δ 8.18-8.15 (m, 2H), 8.00 (d, *J* = 8.1 Hz, 2H), 7.55-7.53 (m, 3H), 7.45-7.34 (m, 5H), 7.28 (d, *J* = 8.1 Hz, 1H), 7.12 (t, *J* = 7.4 Hz, 1H), 6.79 (d, *J* = 7.2 Hz, 2H), 6.61 (d, *J* = 7.2 Hz, 2H), 6.58 (s, 1H), 3.65 (s, 3H). **¹³C NMR** (CDCl₃, 100 MHz) δ 154.8, 149.2, 142.9, 139.8, 139.2, 137.5, 132.4, 132.1, 128.9, 128.7, 128.6, 128.3, 126.5, 126.4, 126.2, 126.0, 124.5, 116.4, 114.2, 96.3, 55.3. **HPLC** (chiral column: DAICEL CHIRALPAK IF; solvent: hexane/2-propanol = 4/1; flow rate: 1.0 mL/min; detection: at 350 nm): t_R = 8.65 min (major) and 13.00 min (minor). **HRMS** (ESI) m/z: [M+H]⁺ Calcd for C₂₇H₂₃N₂SO⁺: 423.1526; Found 423.1519. [α]_D^{20.1} = +28.3 (*c* = 0.25, CHCl₃). **Rf** 0.5 (hexane/AcOEt = 3:1).

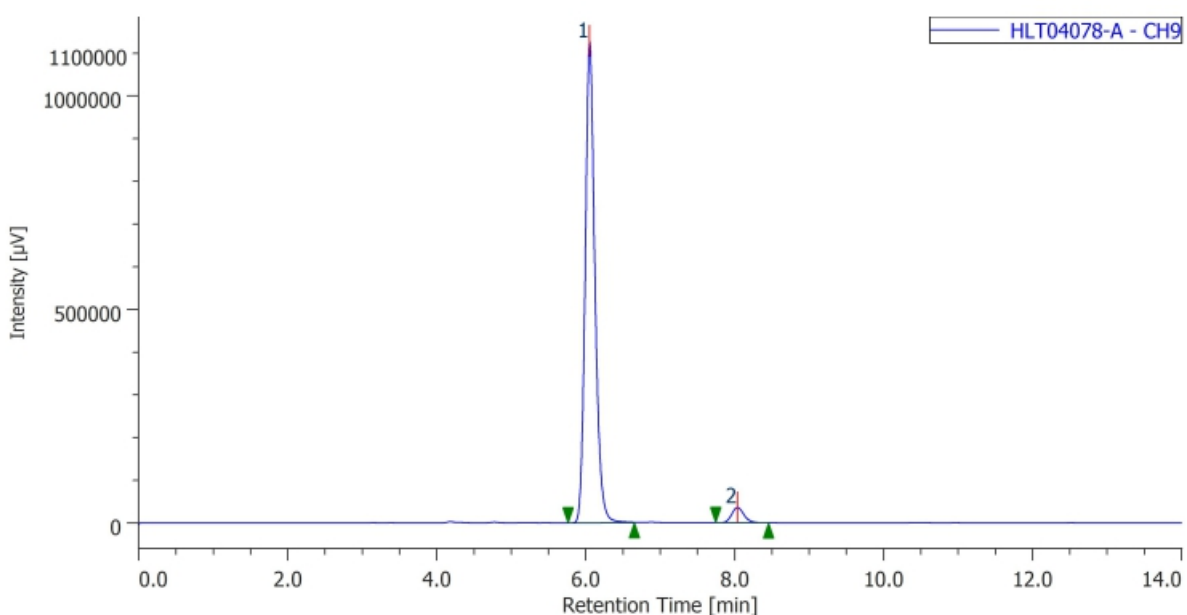
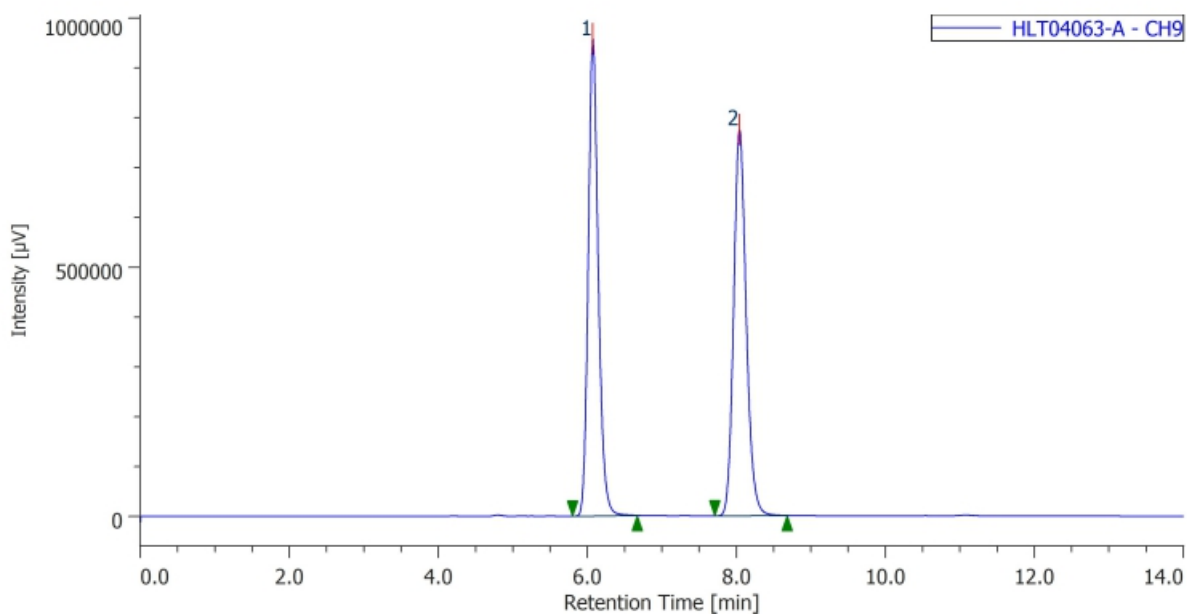




(S)-N-(4-chlorophenyl)-1,3-diphenyl-1 λ^6 -benzo[e][1,2]thiazin-1-imine (8ga): Prepared according to GP-G using compound **5g** (0.05 mmol, 16.3 mg, 1.0 equiv.), **6a** (0.055 mmol, 10.8 mg, 1.1 equiv.), **CCA2** (0.005 mmol, 2.4 mg, 10 mol%). **8ga** was isolated as a yellow solid (13.8 mg, 65%). IR (KBr) 1584, 1530, 1484, 1446, 1362, 1277, 1250, 1116, 1085, 824, 755 cm^{-1} . ^1H NMR (CDCl_3 , 400 MHz) δ 8.17-8.15 (m, 2H), 7.99 (d, $J = 8.3$ Hz, 2H), 7.58-7.56 (m, 3H),

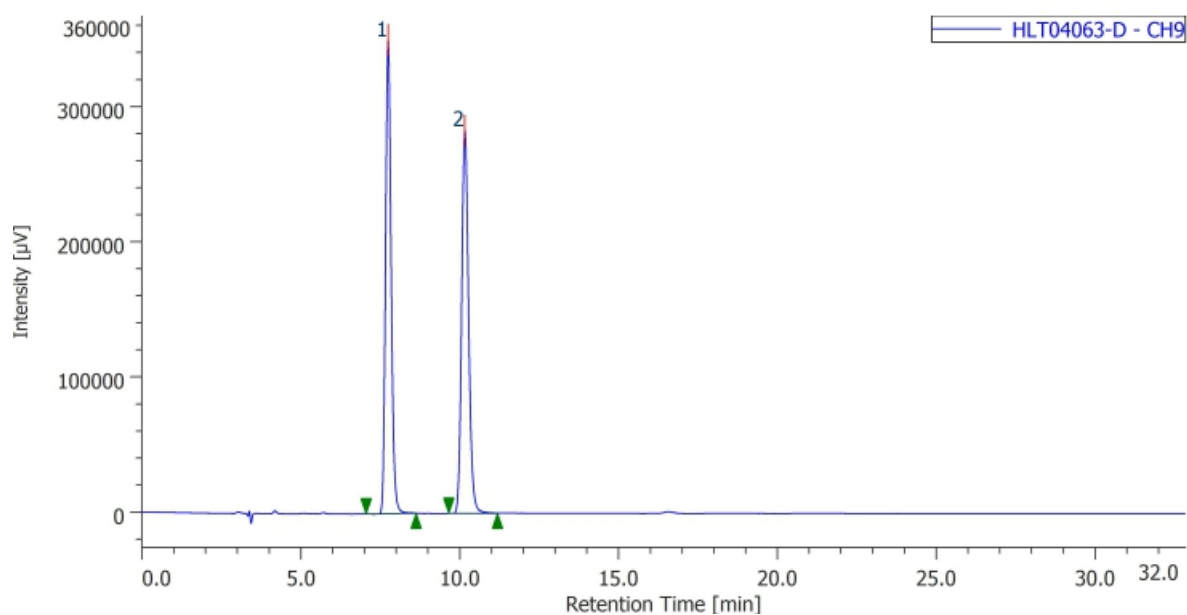
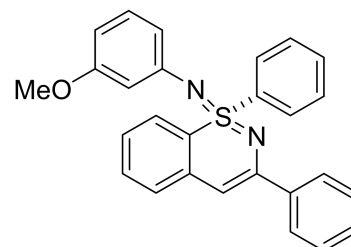


7.44-7.36 (m, 5H), 7.31 (d, $J = 7.9$ Hz, 1H), 7.14 (t, $J = 7.5$ Hz, 1H), 7.01 (d, $J = 8.7$ Hz, 2H), 6.76 (d, $J = 8.6$ Hz, 2H), 6.64 (s, 1H). ^{13}C NMR (CDCl_3 , 125 MHz) δ 149.0, 147.6, 143.4, 142.7, 139.7, 138.9, 132.7, 132.3, 129.0, 128.8, 128.6, 128.4, 126.8, 126.5, 126.5, 125.8, 124.6, 115.8, 96.5; one aromatic signal was missing probably due to overlap. **HPLC** (chiral column: DAICEL CHIRALPAK IF; solvent: hexane/2-propanol = 4/1; flow rate: 1.0 mL/min; detection: at 254 nm): $t_R = 6.05$ min (major) and 8.03 min (minor). **HRMS** (ESI) m/z : $[\text{M}+\text{H}]^+$ Calcd for $\text{C}_{26}\text{H}_{20}\text{N}_2\text{SCl}^+$: 427.1030; Found 427.1028. $[\alpha]_D^{21.5} = +155.6$ ($c = 0.25$, CHCl_3). **Rf** 0.5 (hexane/AcOEt = 3:1).

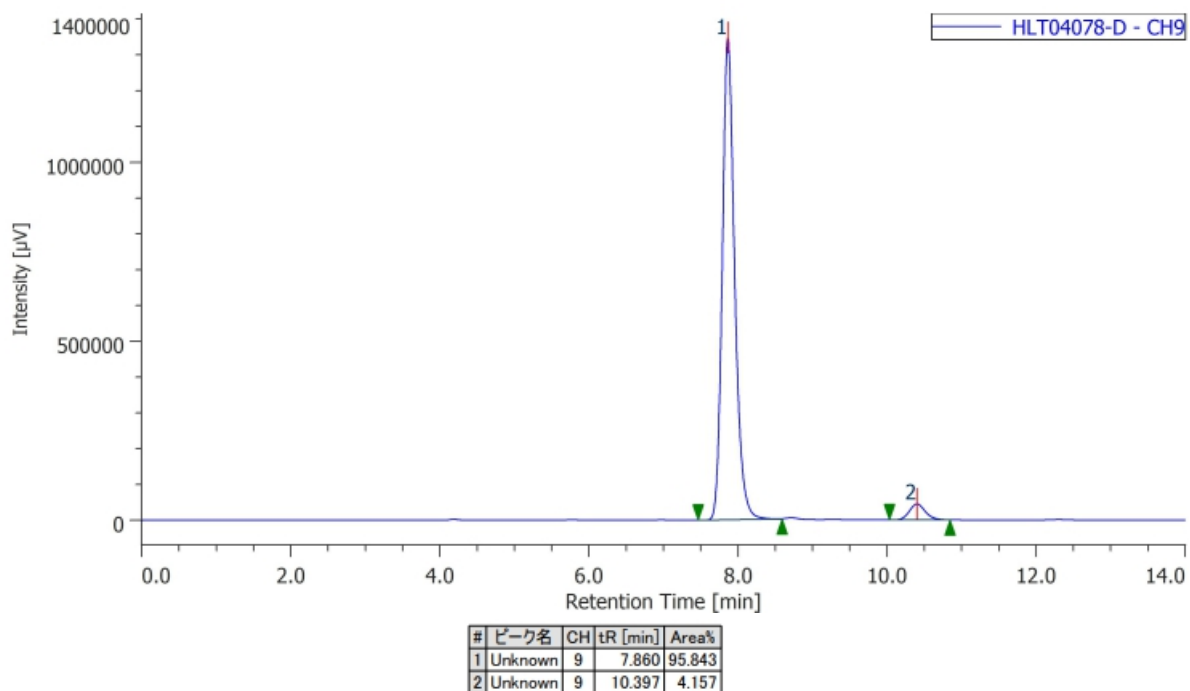


#	ピーク名	CH	tR [min]	Area%
1	Unknown	9	6.050	96.060
2	Unknown	9	8.033	3.940

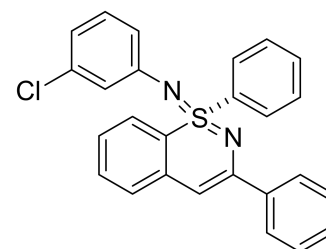
(S)-N-(3-methoxyphenyl)-1,3-diphenyl-1 λ 6-benzo[e][1,2]thiazin-1-imine (8ha): Prepared according to **GP-G** using compound **5h** (0.05 mmol, 16.1 mg, 1.0 equiv.), **6a** (0.055 mmol, 10.8 mg, 1.1 equiv.), **CCA2** (0.005 mmol, 2.4 mg, 10 mol%). **8ha** was isolated as a yellow solid (15.8 mg, 75%). **IR** (KBr) 3056, 2928, 1585, 1530, 1471, 1445, 1362, 1282, 1209, 1162, 1116, 1085, 758, 720 cm^{-1} . **^1H NMR** (CDCl_3 , 400 MHz) δ 8.20-8.18 (m, 2H), 8.01-7.98 (m, 2H), 7.58-7.54 (m, 3H), 7.44-7.33 (m, 5H), 7.30 (d, $J = 7.2$ Hz, 1H), 7.14-7.10 (m, 1H), 6.97-6.93 (m, 1H), 6.64 (s, 1H), 6.46-6.39 (m, 3H), 3.58 (s, 3H). **^{13}C NMR** (CDCl_3 , 100 MHz) δ 160.0, 149.1, 145.9, 142.8, 139.7, 139.1, 132.6, 132.2, 129.4, 128.9, 128.7, 128.7, 128.3, 126.5, 126.4, 126.4, 125.9, 116.3, 115.9, 108.3, 108.3, 96.4, 54.9. **HPLC** (chiral column: DAICEL CHIRALPAK IF; solvent: hexane/2-propanol = 4/1; flow rate: 1.0 mL/min; detection: at 254 nm): $t_R = 7.86$ min (major) and 10.40 min (minor). **HRMS** (ESI) m/z : $[\text{M}+\text{H}]^+$ Calcd for $\text{C}_{27}\text{H}_{23}\text{N}_2\text{SO}^+$: 423.1526; Found 423.1520. $[\alpha]_D^{22.3} = +145.3$ ($c = 0.25$, CHCl_3). **Rf** 0.6 (hexane/AcOEt = 3:1).

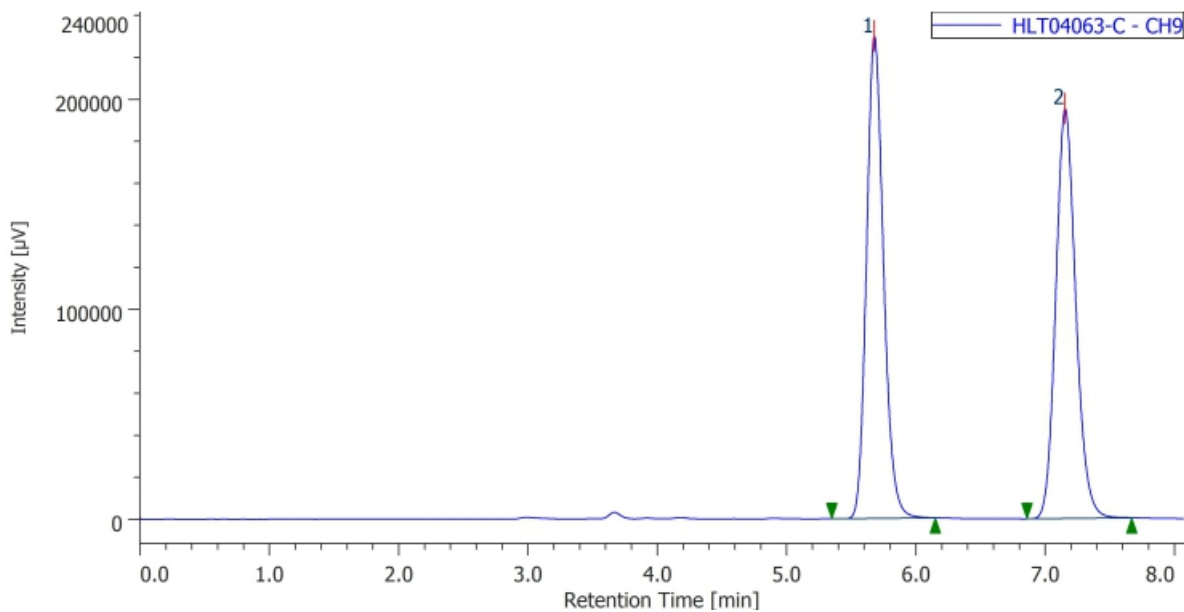


#	ピーク名	CH	tR [min]	Area%
1	Unknown	9	7.743	49.888
2	Unknown	9	10.157	50.112

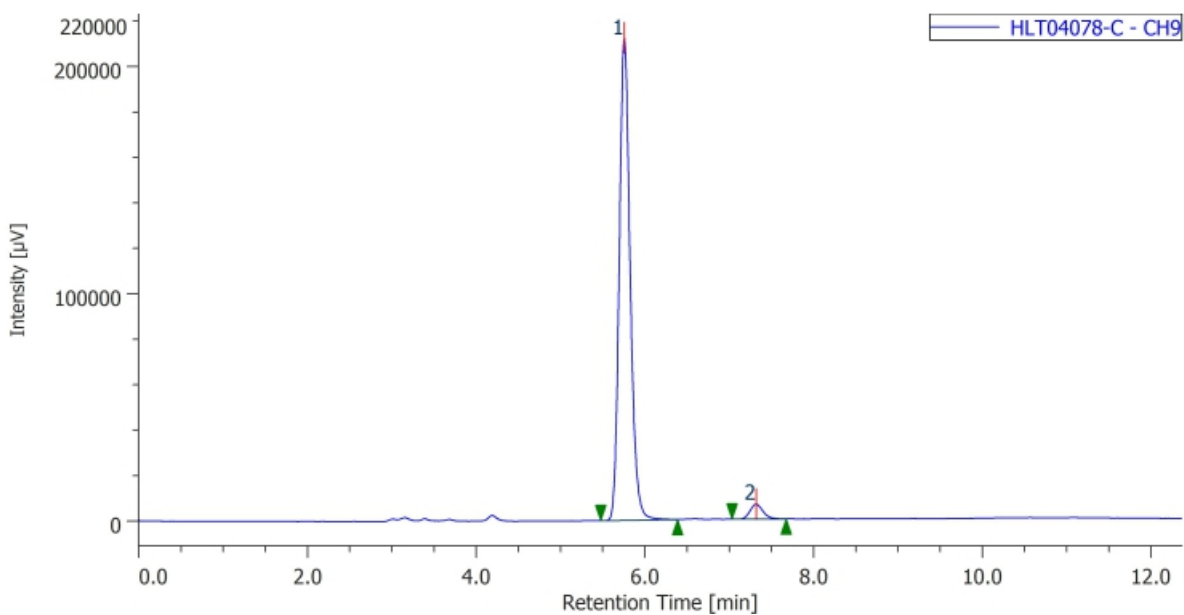


(S)-N-(3-chlorophenyl)-1,3-diphenyl-1 λ ⁶-benzo[e][1,2]thiazin-1-imine (8ia): Prepared according to GP-G using compound **5i** (0.05 mmol, 16.3 mg, 1.0 equiv.), **6a** (0.055 mmol, 10.8 mg, 1.1 equiv.), **CCA2** (0.005 mmol, 2.4 mg, 10 mol%). **8ia** was isolated as a yellow solid (14.9 mg, 70%). IR (KBr) 1584, 1530, 1469, 1445, 1263, 1238, 1115, 1022, 936, 757, 684 cm⁻¹. ¹H NMR (CDCl₃, 400 MHz) δ 8.18-8.14 (m, 2H), 7.99 (d, J = 8.2 Hz, 2H), 7.58-7.54 (m, 3H), 7.44-7.36 (m, 5H), 7.32 (d, J = 8.2 Hz, 1H), 7.14 (t, J = 7.5 Hz, 1H), 6.96-6.91 (m, 2H), 6.81-6.77 (m, 1H), 6.67 (s, 1H), 6.64-6.60 (m, 1H). ¹³C NMR (CDCl₃, 100 MHz) δ 149.1, 146.1, 142.6, 139.7, 138.9, 134.2, 132.7, 132.4, 129.6, 129.0, 128.8, 128.6, 128.4, 126.6, 126.5, 125.8, 125.3, 124.0, 121.5, 121.0, 115.8, 96.6. HPLC (chiral column: DAICEL CHIRALPAK IF; solvent: hexane/2-propanol = 4/1; flow rate: 1.0 mL/min; detection: at 350 nm): t_R = 5.75 min (major) and 7.32 min (minor). HRMS (ESI) m/z : [M+H]⁺ Calcd for C₂₆H₂₀N₂SCl⁺: 427.1030; Found 427.1027. $[\alpha]_D^{22.3}$ = +118.1 (c = 0.25, CHCl₃). R_f 0.5 (hexane/AcOEt = 3:1).





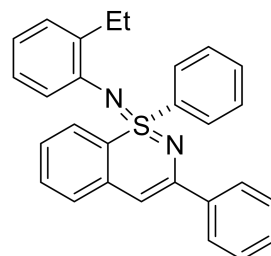
#	ピーク名	CH	tR [min]	Area%
1	Unknown	9	5.677	50.030
2	Unknown	9	7.150	49.970



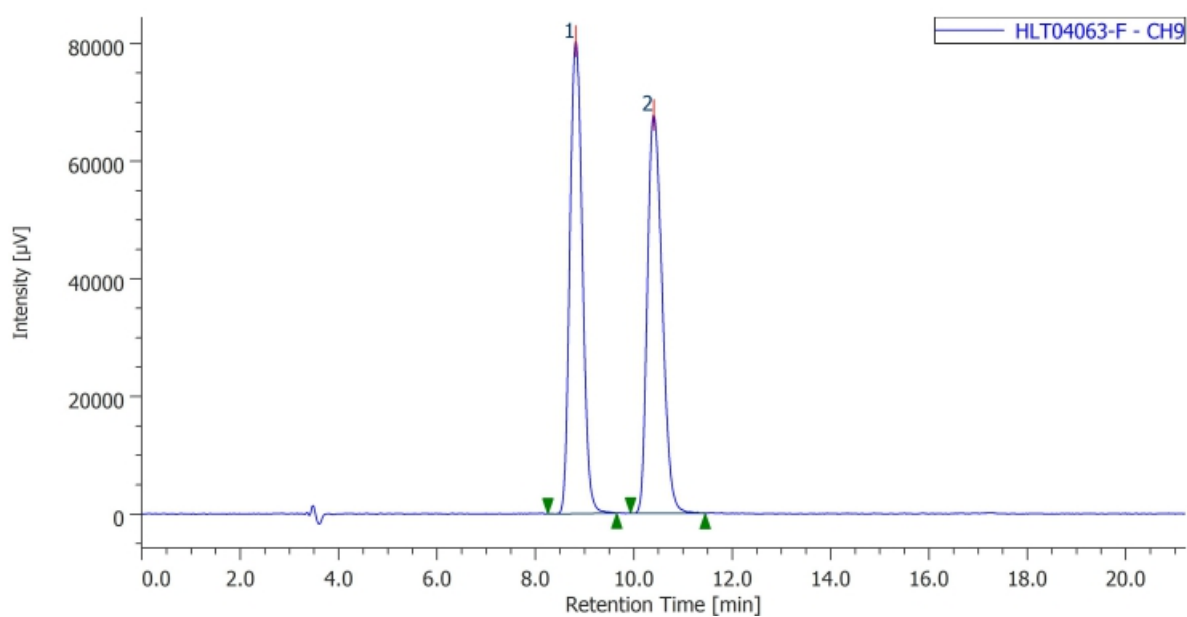
#	ピーク名	CH	tR [min]	Area%
1	Unknown	9	5.753	96.409
2	Unknown	9	7.317	3.591

(S)-N-(2-ethylphenyl)-1,3-diphenyl-1 λ ⁶-benzo[e][1,2]thiazin-1-imine (8ja):

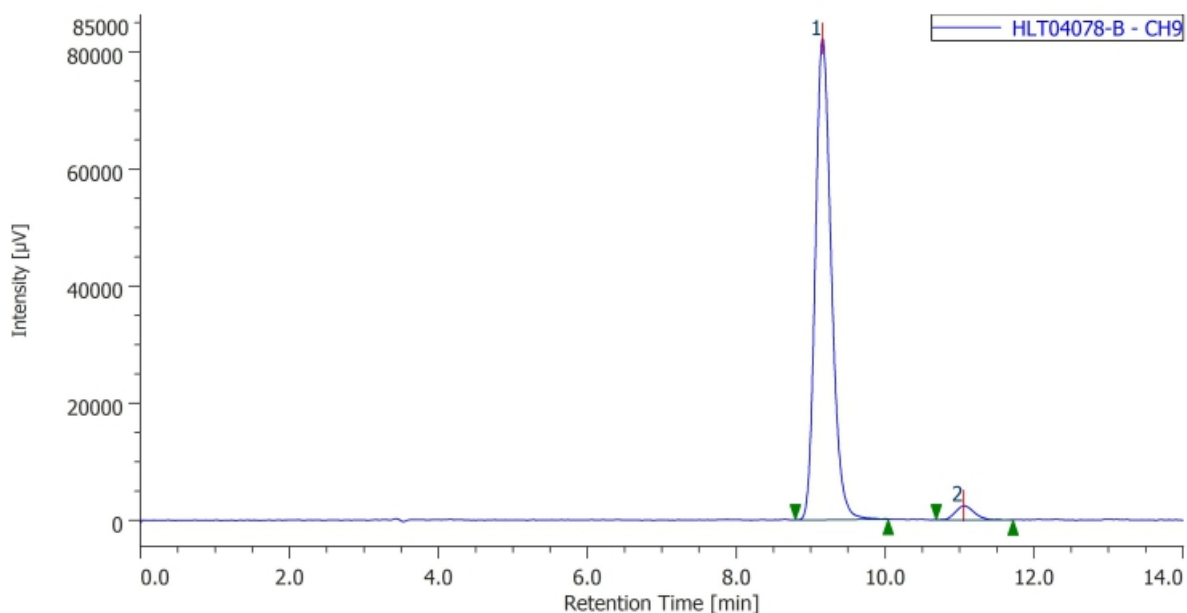
Prepared according to GP-G using compound **5j** (0.05 mmol, 16.0 mg, 1.0 equiv.), **6a** (0.055 mmol, 10.8 mg, 1.1 equiv.), **CCA2** (0.005 mmol, 2.4 mg, 10 mol%). **8ja** was isolated as a yellow amorphous (13.4 mg, 65%). IR (neat) 3059, 2959, 2925, 1583, 1530, 1472, 1446, 1363, 1281, 1257, 1126, 767, 753, 685 cm^{-1}



¹H NMR (CDCl₃, 400 MHz) δ 8.20-8.18 (m, 2H), 7.99 (dd, *J* = 8.1, 1.3 Hz, 2H), 7.58-7.54 (m, 3H), 7.42-7.29 (m, 6H), 7.12-7.04 (m, 2H), 6.80-6.74 (m, 2H), 6.66 (s, 1H), 6.36-6.34 (m, 1H), 2.98-2.87 (m, 2H), 1.33 (t, *J* = 7.6 Hz, 3H). **¹³C NMR** (CDCl₃, 100 MHz) δ 149.3, 144.0, 142.3, 140.0, 139.2, 138.9, 132.4, 132.1, 128.9, 128.7, 128.6, 128.3, 126.5, 126.3, 126.1, 125.8, 121.5, 120.6, 116.6, 96.3, 25.5, 14.5; two aromatic signals were missing probably due to overlap. **HPLC** (chiral column: DAICEL CHIRALPAK IF; solvent: hexane/2-propanol = 49/1; flow rate: 1.0 mL/min; detection: at 350 nm): *t_R* = 9.16 min (major) and 11.05 min (minor). **HRMS** (ESI) *m/z*: [M+H]⁺ Calcd for C₂₈H₂₅N₂S⁺: 421.1733; Found 421.1727. **[α]_D^{18.7}** = +70.5 (*c* = 0.25, CHCl₃). **R_f** 0.7 (hexane/AcOEt = 3:1).

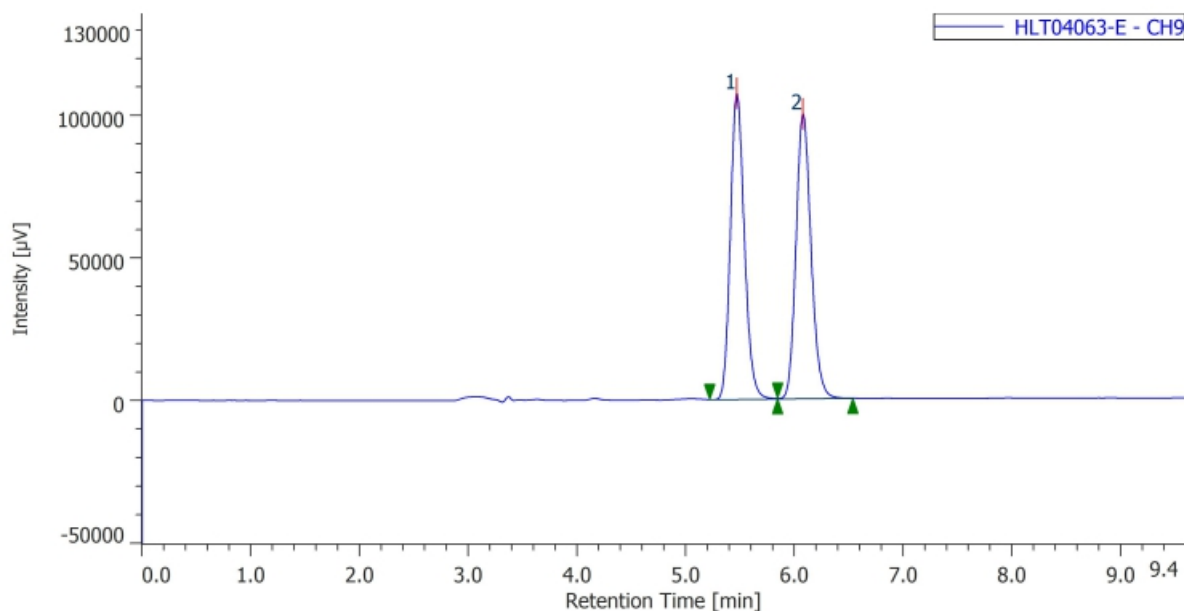
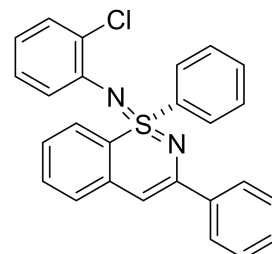


#	ピーク名	CH	tR [min]	Area%
1	Unknown	9	8.817	50.050
2	Unknown	9	10.400	49.950

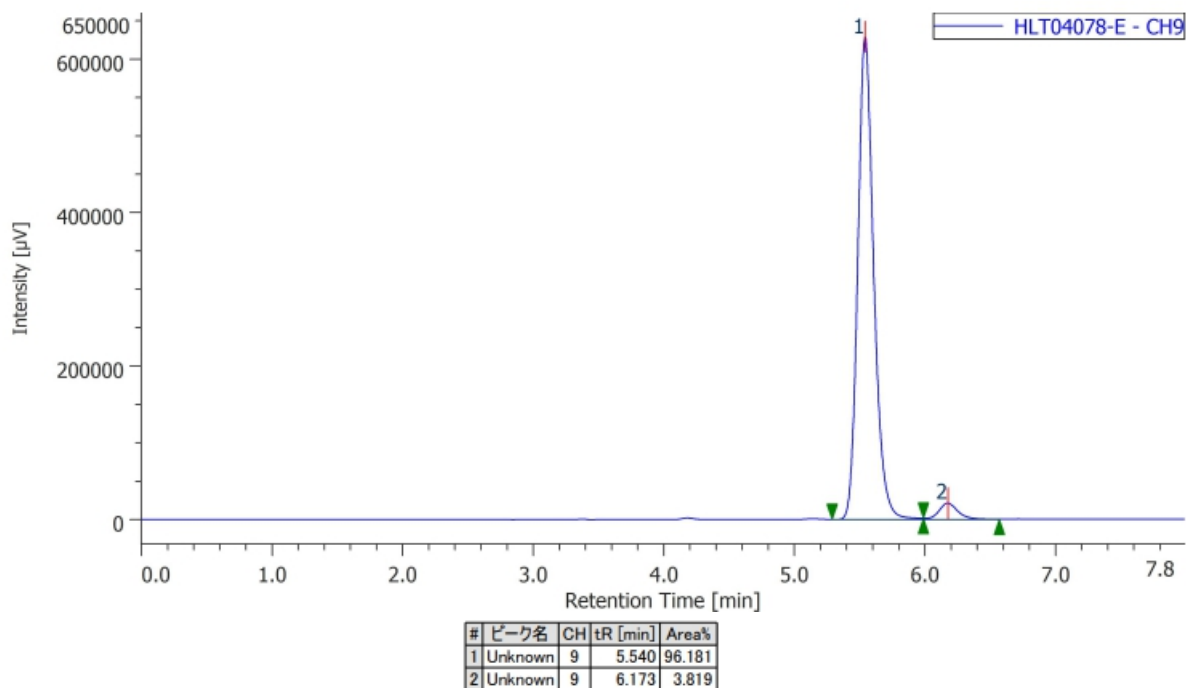


#	ピーク名	CH	tR [min]	Area%
1	Unknown	9	9.157	96.618
2	Unknown	9	11.050	3.382

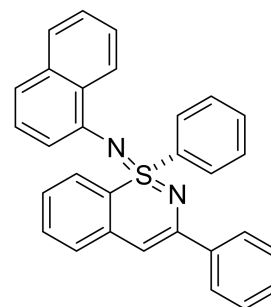
(S)-N-(2-chlorophenyl)-1,3-diphenyl-1 λ ⁶-benzo[e][1,2]thiazin-1-imine (8ka): Prepared according to **GP-G** using compound **5k** (0.05 mmol, 16.3 mg, 1.0 equiv.), **6a** (0.055 mmol, 10.8 mg, 1.1 equiv.), **CCA2** (0.005 mmol, 2.4 mg, 10 mol%). **8ka** was isolated as a yellow solid (14.9 mg, 70%). **IR** (KBr) 1583, 1530, 1471, 1362, 1308, 1280, 1249, 1116, 1019, 751, 720, 679 cm⁻¹. **¹H NMR** (CDCl₃, 400 MHz) δ 8.31-8.29 (m, 2H), 8.04-8.02 (m, 2H), 7.58-7.56 (m, 3H), 7.47-7.33 (m, 5H), 7.30-7.27 (m, 2H), 7.13-7.09 (m, 1H), 6.82 (td, $J = 7.7, 1.8$ Hz, 1H), 6.74 (td, $J = 7.6, 1.7$ Hz, 1H), 6.67 (s, 1H), 6.57 (dd, $J = 7.9, 1.6$ Hz, 1H). **¹³C NMR** (CDCl₃, 100 MHz) δ 148.7, 143.3, 141.8, 139.9, 138.9, 132.7, 132.4, 129.8, 129.7, 129.0, 128.9, 128.8, 128.4, 127.0, 126.6, 126.5, 126.4, 126.0, 122.4, 122.3, 115.8, 96.4. **HPLC** (chiral column: DAICEL CHIRALPAK IF; solvent: hexane/2-propanol = 4/1; flow rate: 1.0 mL/min; detection: at 254 nm): $t_R = 5.54$ min (major) and 6.17 min (minor). **HRMS** (ESI) m/z : $[M+H]^+$ Calcd for C₂₆H₂₀N₂SCl⁺: 427.1030; Found 427.1025. $[\alpha]_D^{22.6} = +69.6$ ($c = 0.25$, CHCl₃). **Rf** 0.5 (hexane/AcOEt = 3:1).

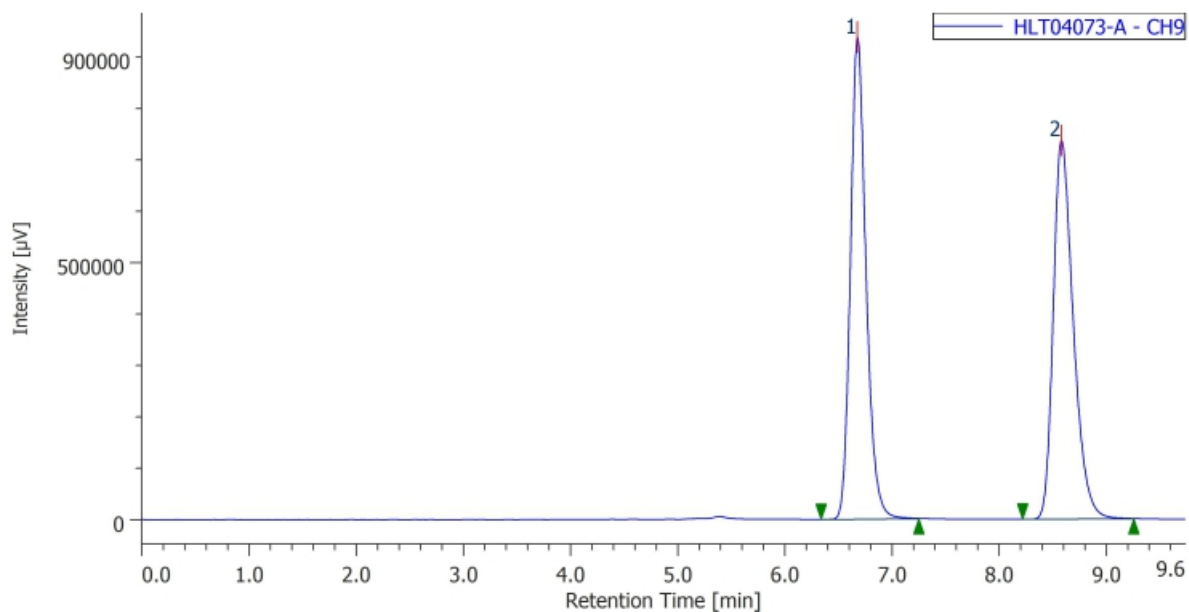


#	ピーク名	CH	tR [min]	Area%
1	Unknown	9	5.470	49.960
2	Unknown	9	6.077	50.040

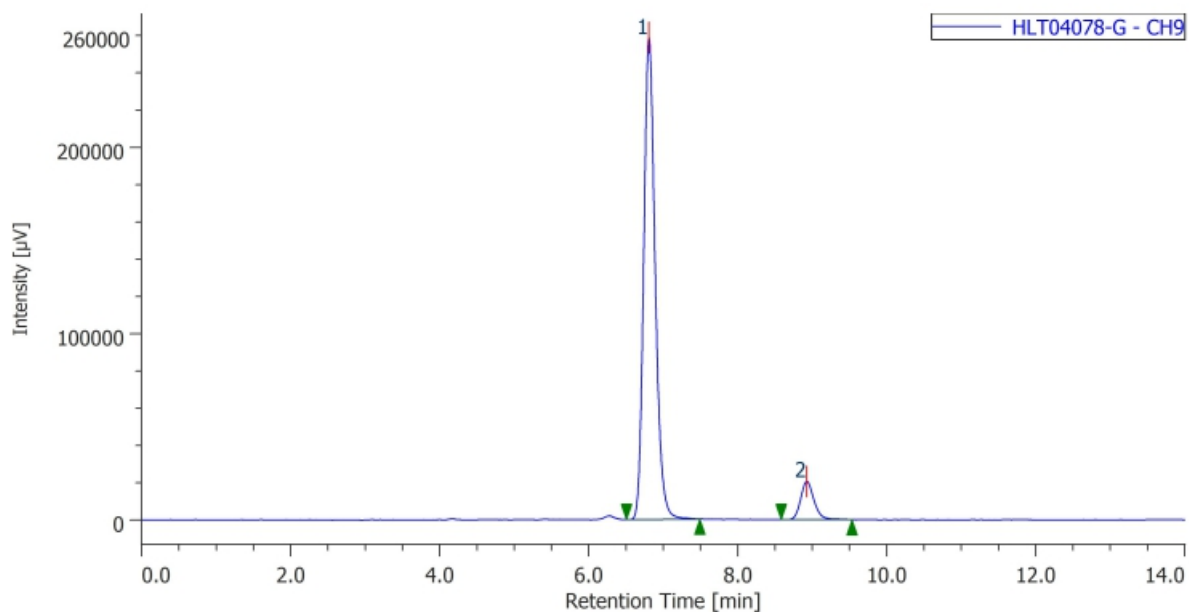


(S)-N-(naphthalen-1-yl)-1,3-diphenyl-1λ⁶-benzo[e][1,2]thiazin-1-imine (8la): Prepared according to **GP-G** using compound **5I** (0.05 mmol, 17.1 mg, 1.0 equiv.), **6a** (0.055 mmol, 10.8 mg, 1.1 equiv.), **CCA2** (0.005 mmol, 2.4 mg, 10 mol%). **8la** was isolated as a yellow solid (11.9 mg, 54%). **IR** (KBr) 1570, 1530, 1470, 1394, 1362, 1278, 1112, 794, 750, 684 cm⁻¹. **¹H NMR** (CDCl₃, 400 MHz) δ 8.72 (d, *J* = 7.7 Hz, 1H), 8.33-8.29 (m, 2H), 8.04-8.00 (m, 2H), 7.72 (d, *J* = 8.2 Hz, 1H), 7.63-7.60 (m, 3H), 7.54-7.49 (m, 1H), 7.48-7.30 (m, 8H), 7.05 (t, *J* = 7.9 Hz, 2H), 6.70 (s, 1H), 6.49 (d, *J* = 6.3 Hz, 1H). **¹³C NMR** (CDCl₃, 100 MHz) δ 149.3, 143.6, 141.1, 140.1, 139.1, 134.6, 132.6, 132.3, 130.9, 129.0, 128.7, 128.6, 128.4, 127.7, 126.5, 126.5, 126.3, 126.0, 125.8, 125.8, 124.8, 124.3, 121.3, 115.9, 115.6, 96.5. **HPLC** (chiral column: DAICEL CHIRALPAK IF; solvent: hexane/2-propanol = 4/1; flow rate: 1.0 mL/min; detection: at 320 nm): t_R = 6.80 min (major) and 8.92 min (minor). **HRMS** (ESI) m/z: [M+H]⁺ Calcd for C₃₀H₂₃N₂S⁺: 443.1576; Found 443.1571. [α]_D^{19.9} = +9.3 (*c* = 0.25, CHCl₃). **Rf** 0.6 (hexane/AcOEt = 3:1).



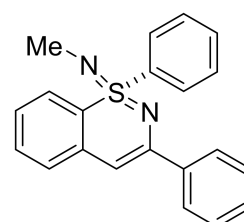


#	ピーク名	CH	tR [min]	Area%
1	Unknown	9	6.673	49.737
2	Unknown	9	8.577	50.263

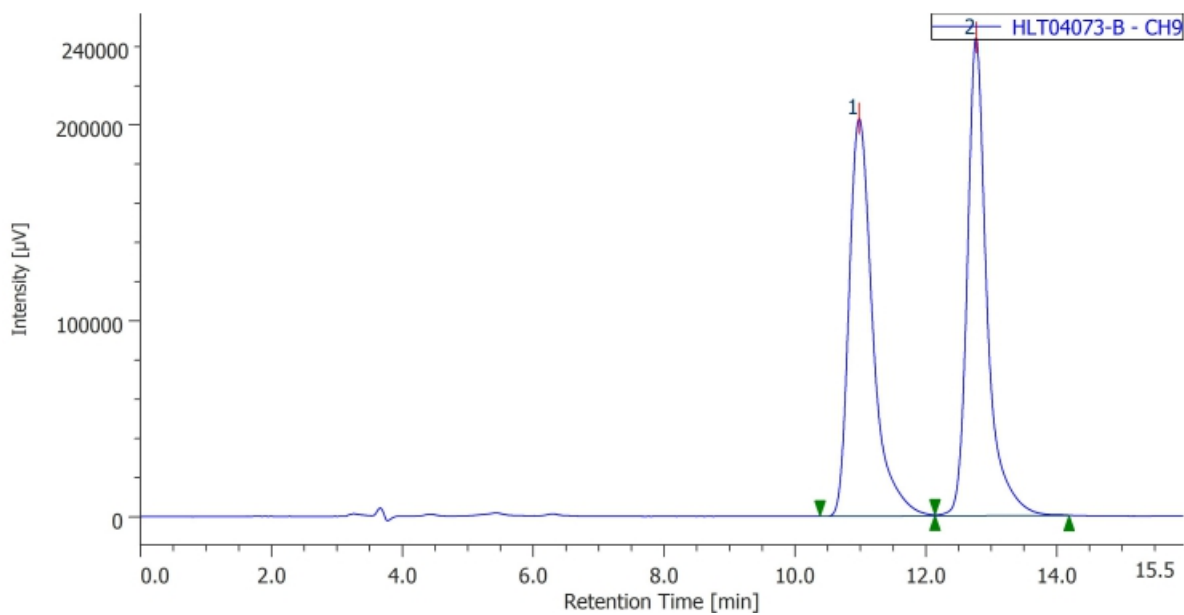


#	ピーク名	CH	tR [min]	Area%
1	Unknown	9	6.803	91.461
2	Unknown	9	8.923	8.539

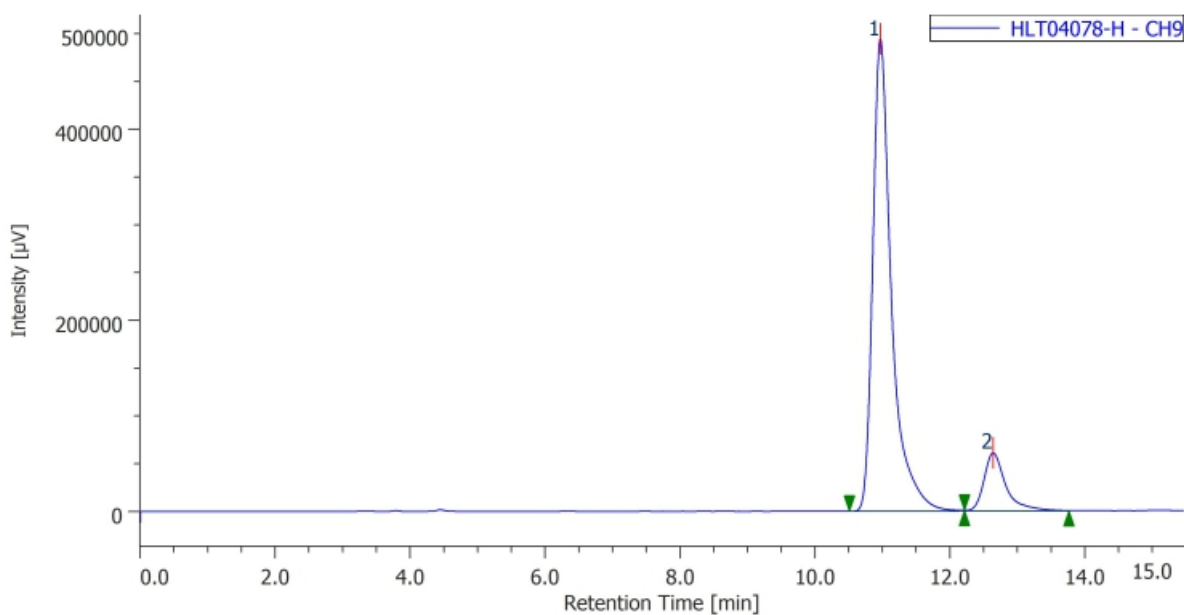
(S)-N-methyl-1,3-diphenyl-1 λ ⁶-benzo[e][1,2]thiazin-1-imine (8ma**):** Prepared according to **GP-G** using compound **5m** (0.05 mmol, 11.5 mg, 1.0 equiv.), **6a** (0.055 mmol, 10.8 mg, 1.1 equiv.), **CCA2** (0.005 mmol, 2.4 mg, 10 mol%). **8ma** was isolated as a yellow solid (13.2 mg, 80%). IR (KBr) 3056, 2861, 1582, 1528, 1471, 1445, 1361, 1199, 1102, 947, 766 cm⁻¹. ¹H NMR (CDCl₃, 400 MHz) δ 8.04-7.95 (m, 4H), 7.52-7.36 (m, 8H)



7.33 (d, $J = 7.2$ Hz, 1H), 7.21 (t, $J = 7.5$ Hz, 1H), 6.52 (s, 1H), 2.75 (s, 3H). ^{13}C NMR (CDCl_3 , 100 MHz) δ 150.2, 142.5, 140.0, 139.4, 132.3, 132.0, 128.8, 128.6, 128.3, 127.8, 126.5, 126.3, 126.0, 125.8, 115.3, 96.1, 29.6. **HPLC** (chiral column: DAICEL CHIRALPAK IA; solvent: hexane/2-propanol = 19/1; flow rate: 1.0 mL/min; detection: at 254 nm): $t_R = 11.00$ min (major) and 12.64 min (minor). **HRMS** (ESI) m/z : $[\text{M}+\text{H}]^+$ Calcd for $\text{C}_{21}\text{H}_{19}\text{N}_2\text{S}^+$: 331.1263; Found 331.1257. $[\alpha]_D^{19.8} = -130.0$ ($c = 0.25$, CHCl_3). **Rf** 0.2 (hexane/AcOEt = 3:1).

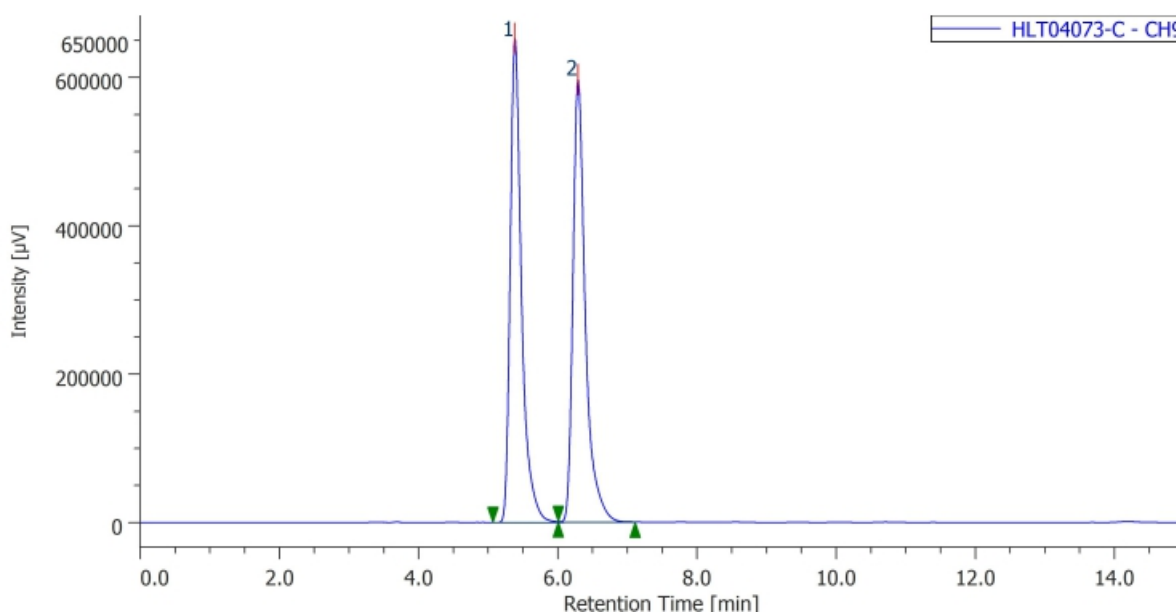
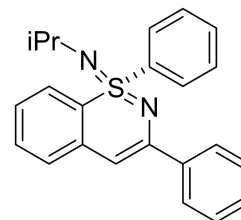


#	ピーク名	CH	tR [min]	Area%
1	Unknown	9	10.977	50.072
2	Unknown	9	12.763	49.928

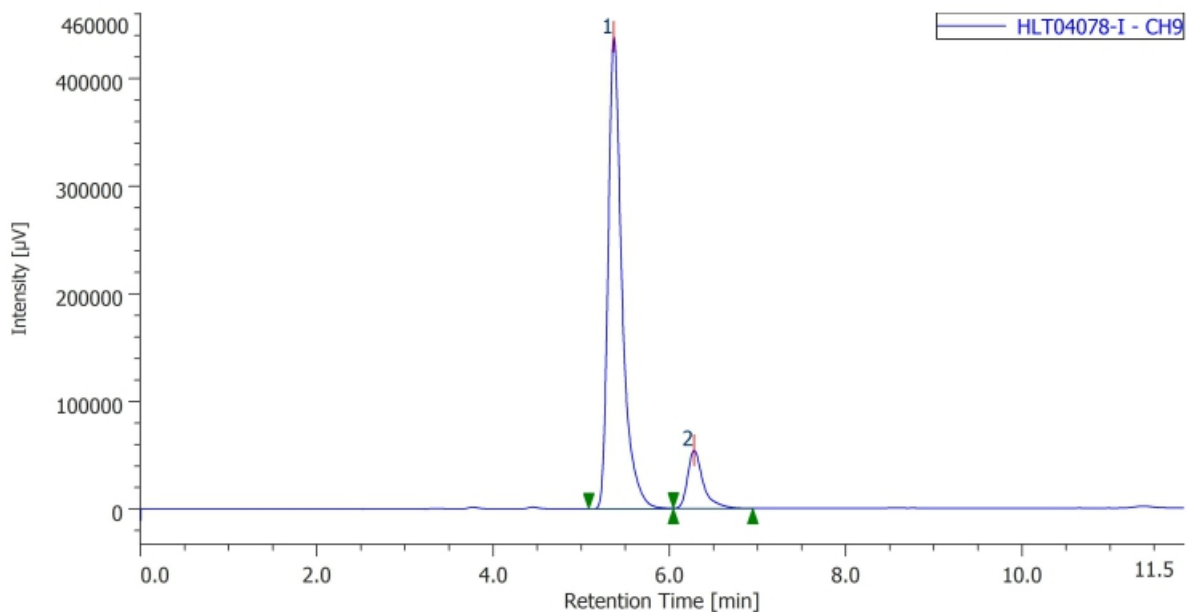


#	ピーク名	CH	tR [min]	Area%
1	Unknown	9	10.967	87.592
2	Unknown	9	12.637	12.408

(S)-N-isopropyl-1,3-diphenyl-1 λ^6 -benzo[e][1,2]thiazin-1-imine (8na): Prepared according to GP-G using compound **5n** (0.05 mmol, 12.9 mg, 1.0 equiv.), **6a** (0.055 mmol, 10.8 mg, 1.1 equiv.), **CCA2** (0.005 mmol, 2.4 mg, 10 mol%). **8na** was isolated as a yellow solid (14.4 mg, 79%). **IR** (KBr) 3061, 2965, 2922, 2857, 1571, 1530, 1473, 1445, 1366, 1287, 1181, 1116, 940, 821, 756, 682 cm^{-1} . **$^1\text{H NMR}$** (CDCl_3 , 400 MHz) δ 8.08-8.00 (m, 4H), 7.51-7.46 (m, 3H), 7.44-7.33 (m, 5H), 7.32-7.29 (m, 1H), 7.19-7.14 (m, 1H), 6.52 (s, 1H), 3.30-3.24 (m, 1H), 1.18 (d, $J = 6.3$ Hz, 3H), 1.09 (d, $J = 6.3$ Hz, 3H). **$^{13}\text{C NMR}$** (CDCl_3 , 100 MHz) δ 149.6, 142.6, 139.7, 139.6, 132.1, 131.6, 128.7, 128.5, 128.4, 128.3, 126.5, 126.1, 125.9, 125.7, 117.3, 95.6, 46.0, 26.4, 26.1. **HPLC** (chiral column: DAICEL CHIRALPAK IA; solvent: hexane/2-propanol = 19/1; flow rate: 1.0 mL/min; detection: at 254 nm): $t_R = 5.37$ min (major) and 6.28 min (minor). **HRMS** (ESI) m/z : $[\text{M}+\text{H}]^+$ Calcd for $\text{C}_{23}\text{H}_{23}\text{N}_2\text{S}^+$: 359.1576; Found 359.1572. $[\alpha]_D^{23.1} = +227.1$ ($c = 0.25$, CHCl_3). **Rf** 0.5 (hexane/AcOEt = 3:1).



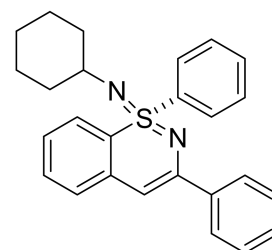
#	ピーク名	CH	tR [min]	Area%
1	Unknown	9	5.380	49.871
2	Unknown	9	6.290	50.129

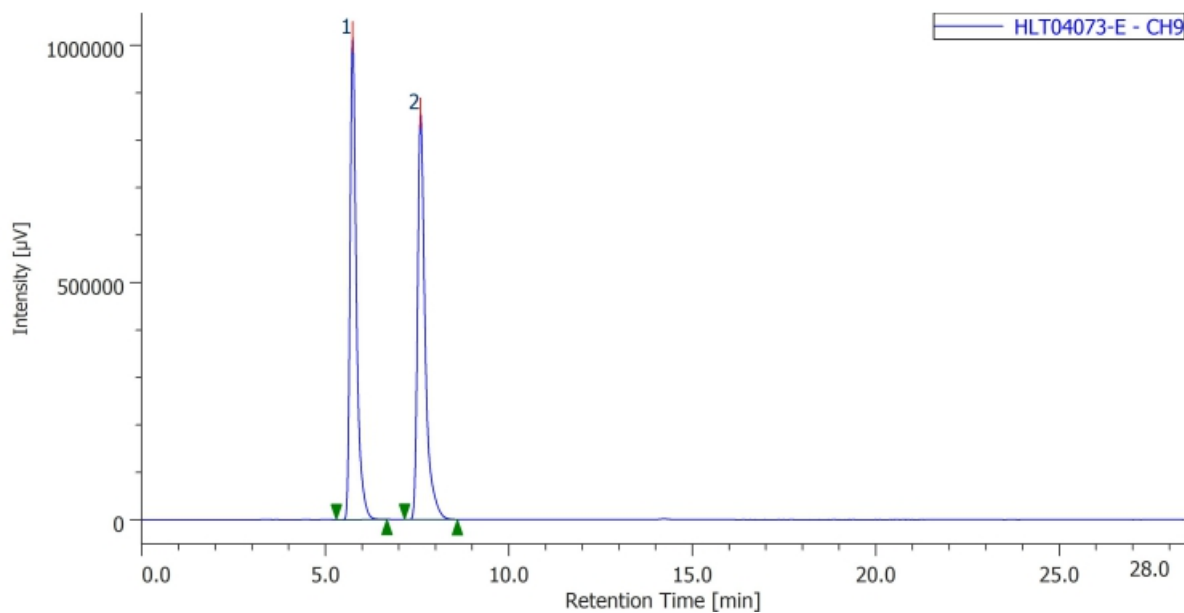


#	ピーク名	CH	tR [min]	Area%
1	Unknown	9	5.367	87.803
2	Unknown	9	6.277	12.197

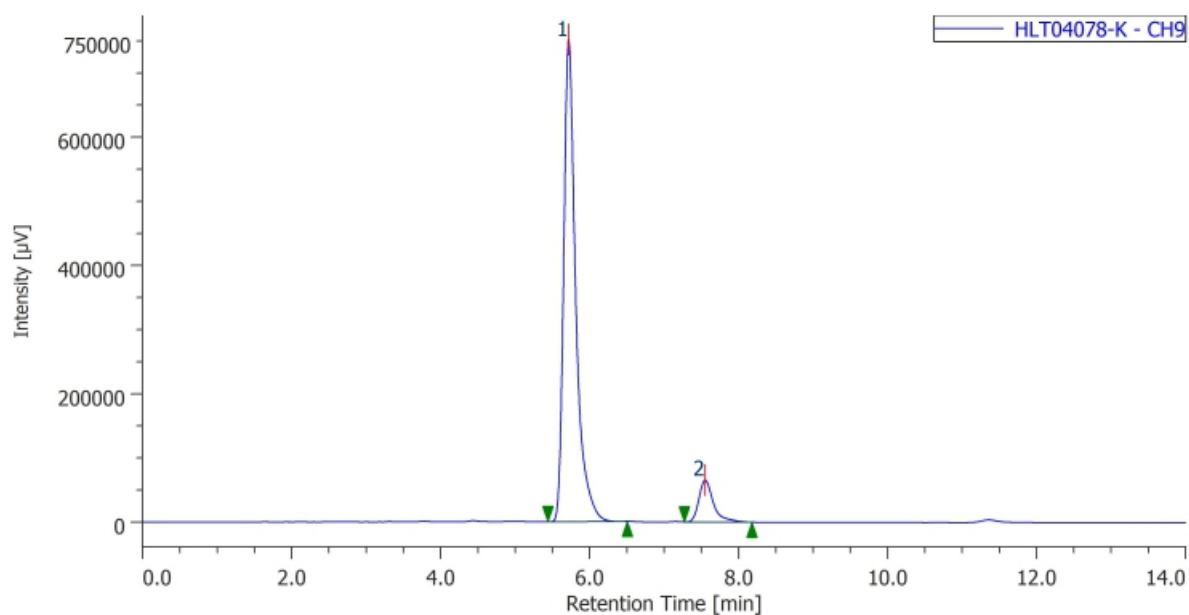
(S)-N-cyclohexyl-1,3-diphenyl-1 λ ⁶-benzo[*e*][1,2]thiazin-1-imine (80a): Prepared according to GP-G using compound **5o** (0.05 mmol, 14.9 mg, 1.0 equiv.), **6a** (0.055 mmol, 10.8 mg, 1.1 equiv.), **CCA2** (0.005 mmol, 2.4 mg, 10 mol%). **80a** was isolated as a yellow solid (14.3 mg, 72%). IR (KBr) 3059, 2926, 2850, 1571, 1527, 1472, 1444, 1366, 1181, 1106, 945, 765, 720 cm⁻¹. ¹H NMR (CDCl₃, 400 MHz) δ 8.05-7.98 (m, 4H), 7.49-7.45 (m, 3H), 7.44-7.33 (m, 5H), 7.30 (d, *J* = 7.2 Hz, 1H), 7.15 (t, *J* = 7.4 Hz, 1H), 6.51 (s, 1H), 2.99-2.90 (m, 1H), 1.86-1.79 (m, 1H), 1.70-1.58 (m, 3H), 1.52-1.34 (m, 3H), 1.19-1.05 (m, 3H). ¹³C NMR (CDCl₃, 100 MHz) δ 149.6, 143.0, 139.8, 139.5, 132.0, 131.6, 128.7, 128.4, 128.3, 128.2, 126.5, 126.1, 126.0, 125.6, 117.7, 95.6, 53.4, 36.7, 36.2, 25.8, 25.3, 25.2.

HPLC (chiral column: DAICEL CHIRALPAK IA; solvent: hexane/2-propanol = 19/1; flow rate: 1.0 mL/min; detection: at 254 nm): t_R = 5.72 min (major) and 7.55 min (minor). **HRMS** (ESI) m/z: [M+H]⁺ Calcd for C₂₆H₂₇N₂S⁺: 399.1889; Found 399.1886. [α]_D^{23.6} = +195.2 (*c* = 0.25, CHCl₃). **Rf** 0.5 (hexane/AcOEt = 3:1).





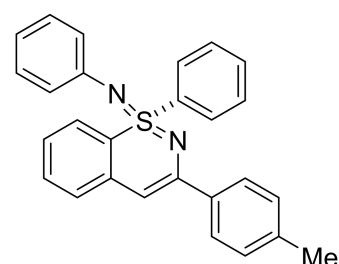
#	ピーク名	CH	tR [min]	Area%
1	Unknown	9	5.740	49.730
2	Unknown	9	7.593	50.270



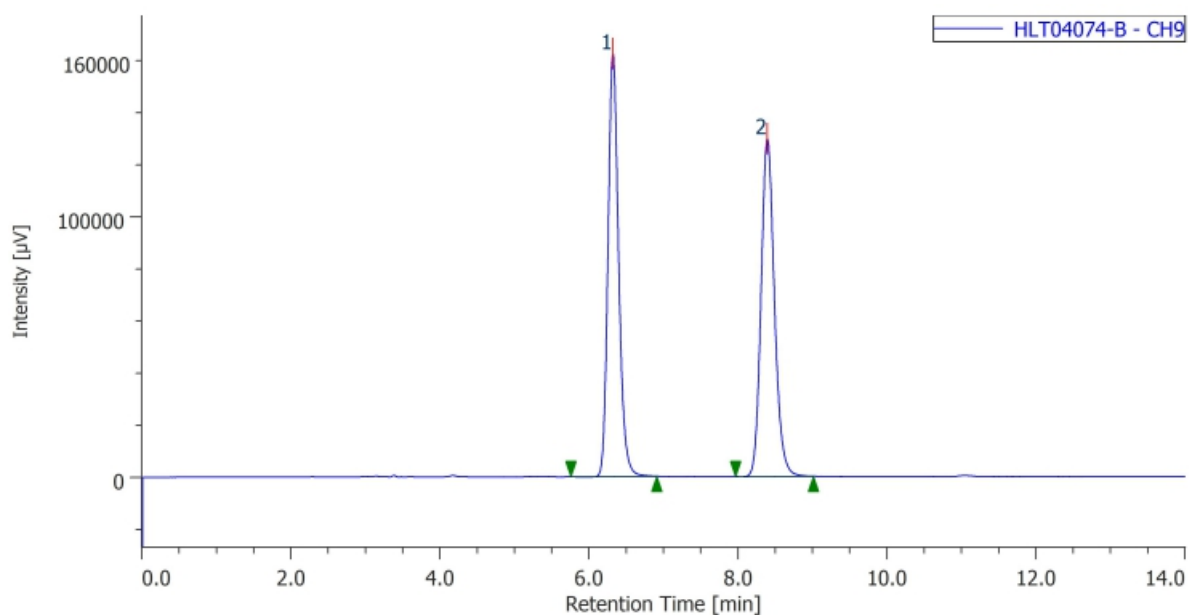
#	ピーク名	CH	tR [min]	Area%
1	Unknown	9	5.717	90.486
2	Unknown	9	7.547	9.514

(S)-N,1-diphenyl-3-(p-tolyl)-1λ⁶-benzo[e][1,2]thiazin-1-imine (8ab)

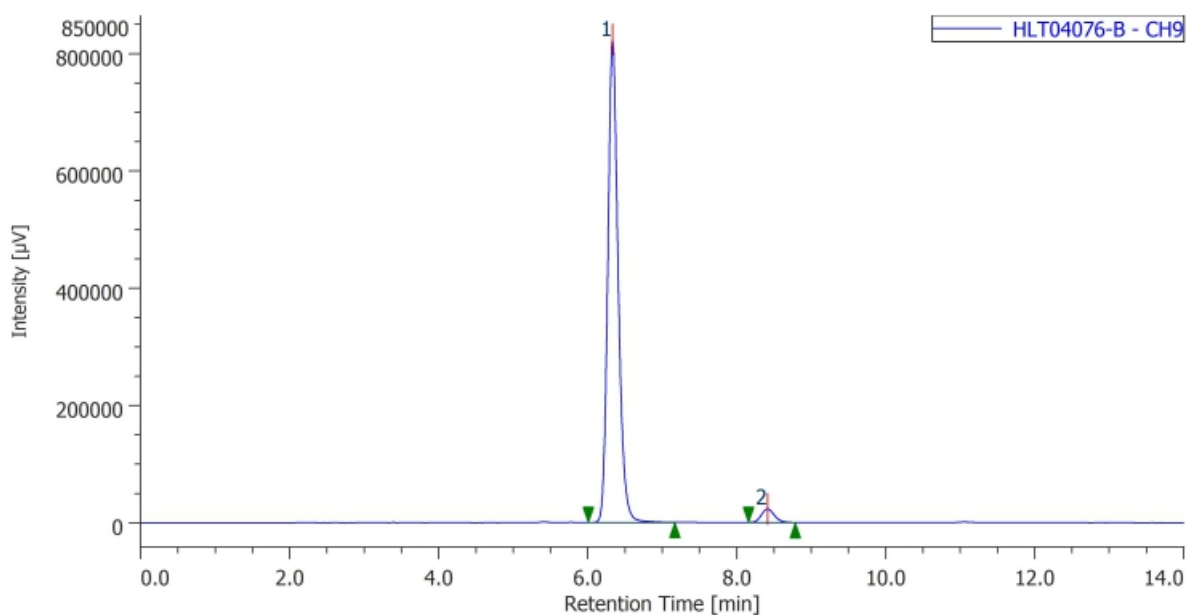
Prepared according to GP-G using compound **5a** (0.05 mmol, 14.6 mg, 1.0 equiv.), **6b** (0.055 mmol, 11.6 mg, 1.1 equiv.), **CCA2** (0.005 mmol, 2.4 mg, 10 mol%). **8ab** was isolated as a yellow solid (14.6 mg, 72%). IR (KBr)



3056, 1579, 1506, 1471, 1283, 1256, 1116, 1086, 749, 682, 607 cm^{-1} . **^1H NMR** (CDCl_3 , 400 MHz) δ 8.19-8.16 (m, 2H), 7.90 (d, $J = 8.2$ Hz, 2H), 7.56-7.53 (m, 3H), 7.43 (d, $J = 8.2$ Hz, 1H), 7.35 (td, $J = 7.6$, 1.1 Hz, 1H), 7.28 (d, $J = 6.8$ Hz, 1H), 7.22 (d, $J = 8.2$ Hz, 2H), 7.12-7.03 (m, 3H), 6.86-6.80 (m, 3H), 6.60 (s, 1H), 2.38 (s, 3H). **^{13}C NMR** (CDCl_3 , 100 MHz) δ 149.2, 144.7, 143.1, 139.9, 138.8, 136.3, 132.5, 132.1, 129.1, 128.9, 128.8, 128.5, 126.4, 126.3, 126.1, 125.9, 123.5, 121.5, 116.1, 95.8, 21.3. **HPLC** (chiral column: DAICEL CHIRALPAK IF; solvent: hexane/2-propanol = 4/1; flow rate: 1.0 mL/min; detection: at 254 nm): $t_R = 6.33$ min (major) and 8.41 min (minor). **HRMS** (ESI) m/z : $[\text{M}+\text{Na}]^+$ Calcd for $\text{C}_{27}\text{H}_{22}\text{N}_2\text{SNa}^+$: 429.1396; Found 429.1394. $[\alpha]_D^{22.6} = +150.2$ ($c = 0.25$, CHCl_3). **Rf** 0.5 (hexane/AcOEt = 3:1).

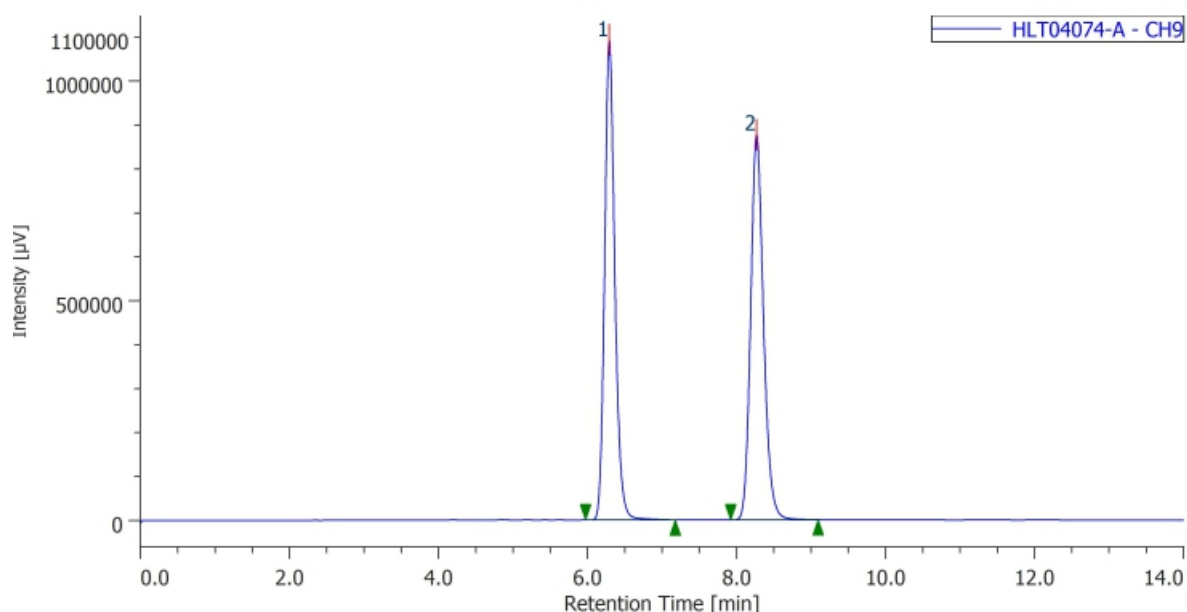
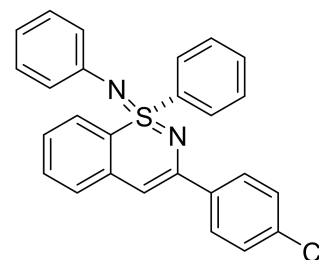


#	ピーク名	CH	tR [min]	Area%
1	Unknown	9	6.320	49.816
2	Unknown	9	8.390	50.184

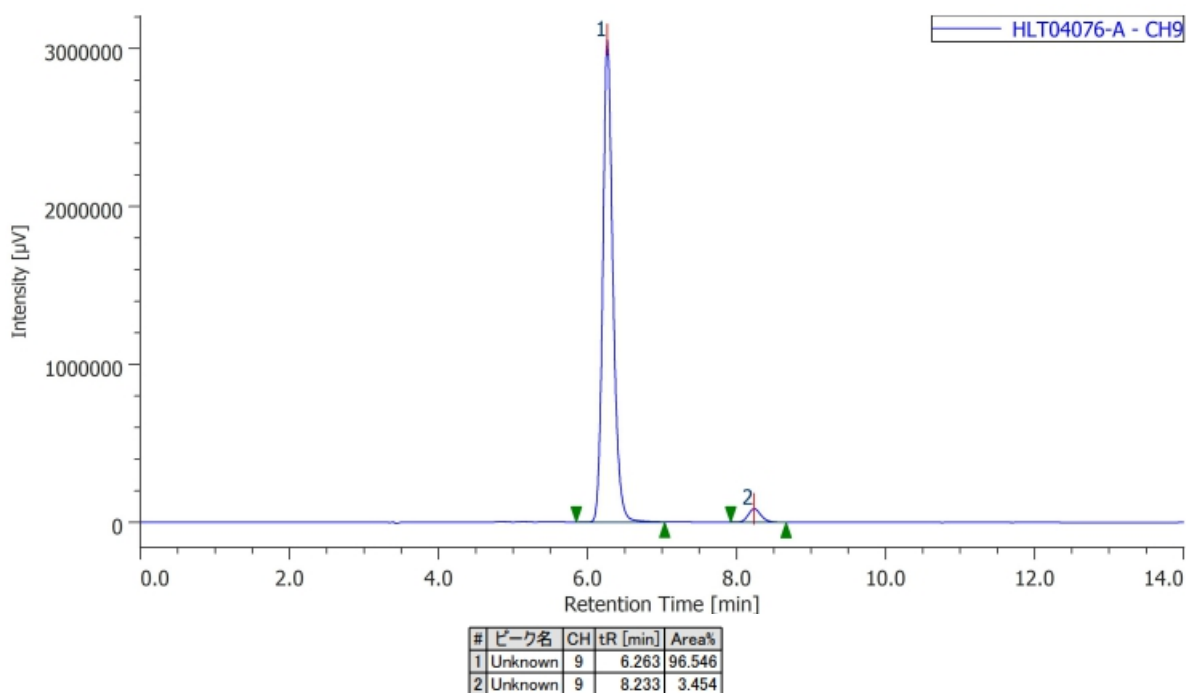


#	ピーク名	CH	tR [min]	Area%
1	Unknown	9	6.330	96.543
2	Unknown	9	8.410	3.457

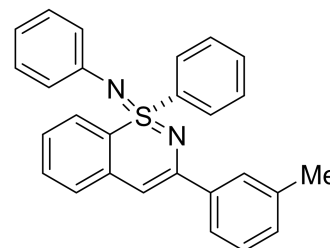
(S)-3-(4-chlorophenyl)-N,1-diphenyl-1 λ ⁶-benzo[e][1,2]thiazin-1-imine (8ac): Prepared according to **GP-G** using compound **5a** (0.05 mmol, 14.6 mg, 1.0 equiv.), **6c** (0.055 mmol, 12.7 mg, 1.1 equiv.), **CCA2** (0.005 mmol, 2.4 mg, 10 mol%). **8ac** was isolated as a yellow solid (18.3 mg, 86%). **IR** (KBr) 1579, 1531, 1471, 1402, 1283, 1256, 1115, 1086, 756 cm⁻¹. **¹H NMR** (CDCl₃, 400 MHz) δ 8.18-8.15 (m, 2H), 7.93 (d, J = 8.2 Hz, 2H), 7.58-7.55 (m, 3H), 7.43 (d, J = 8.2 Hz, 1H), 7.40-7.36 (m, 3H), 7.29 (d, J = 8.2 Hz, 1H), 7.14 (t, J = 7.5 Hz, 1H), 7.06 (t, J = 7.5 Hz, 2H), 6.85-6.80 (m, 3H), 6.60 (s, 1H). **¹³C NMR** (CDCl₃, 125 MHz) δ 147.9, 144.4, 142.8, 139.5, 137.6, 134.6, 132.6, 132.2, 129.0, 128.9, 128.6, 128.5, 127.8, 126.6, 126.4, 125.9, 123.5, 121.7, 116.5, 96.4. **HPLC** (chiral column: DAICEL CHIRALPAK IF; solvent: hexane/2-propanol = 4/1; flow rate: 1.0 mL/min; detection: at 254 nm): t_R = 6.26 min (major) and 8.23 min (minor). **HRMS** (ESI) m/z : [M+Na]⁺ Calcd for C₂₆H₁₉N₂SClNa⁺: 449.0850; Found 449.0845. **$[\alpha]_D^{22.9}$** = +127.5 (c = 0.25, CHCl₃). **Rf** 0.6 (hexane/AcOEt = 3:1).

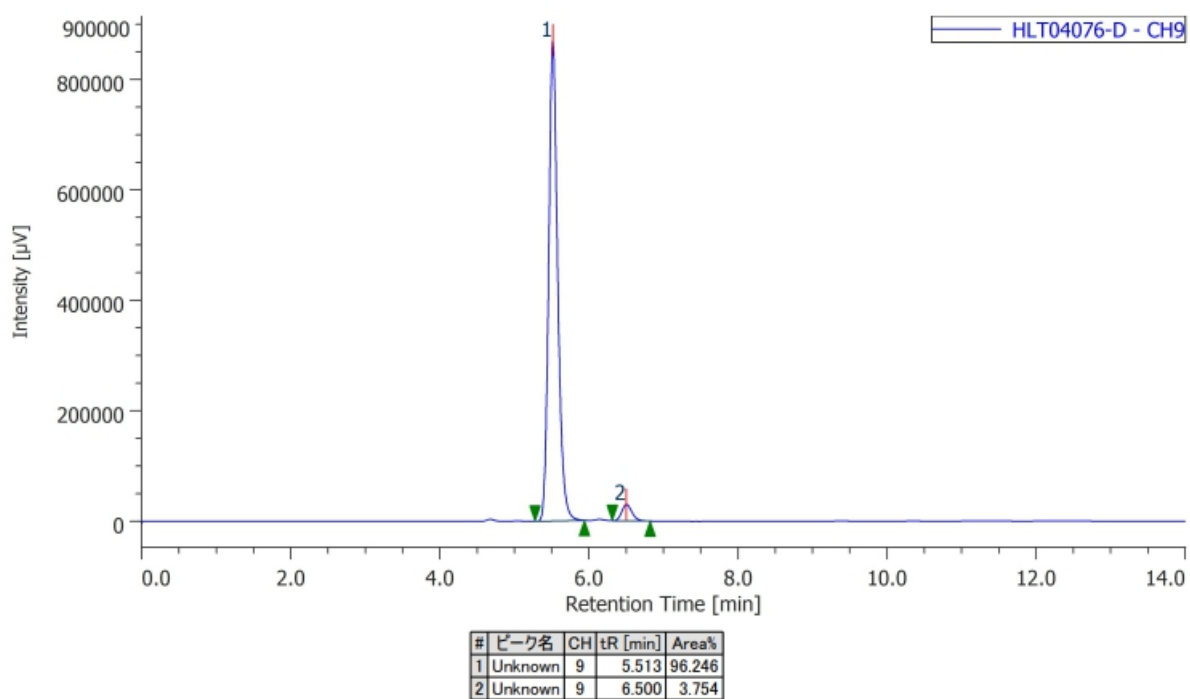
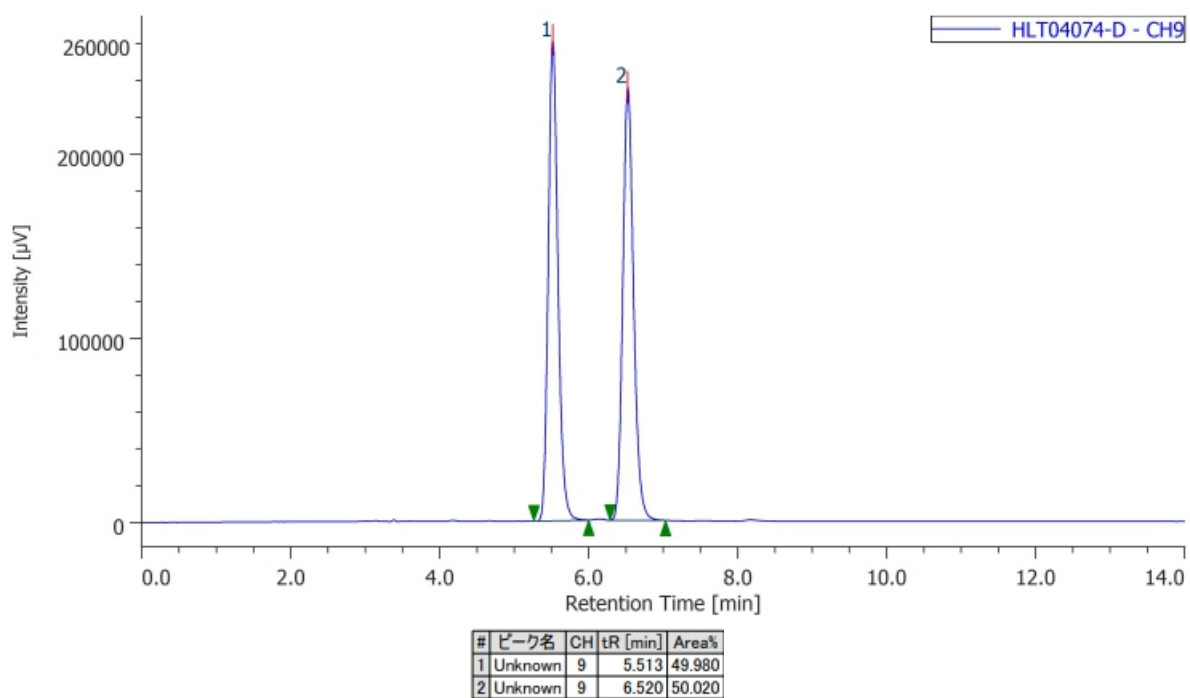


#	ピーク名	CH	tR [min]	Area%
1	Unknown	9	6.290	49.711
2	Unknown	9	8.267	50.289

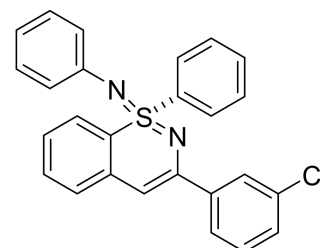


(S)-N,1-diphenyl-3-(m-tolyl)-1λ⁶-benzo[e][1,2]thiazin-1-imine (8ad): Prepared according to **GP-G** using compound **5a** (0.05 mmol, 14.6 mg, 1.0 equiv.), **6d** (0.055 mmol, 11.6 mg, 1.1 equiv.), **CCA2** (0.005 mmol, 2.4 mg, 10 mol%). **8ad** was isolated as a yellow solid (15.2 mg, 75%). **IR** (KBr) 1590, 1573, 1529, 1471, 1286, 1257, 1116, 1086, 754 cm⁻¹. **¹H NMR** (CDCl₃, 400 MHz) δ 8.19-8.17 (m, 2H), 7.83-7.78 (m, 2H), 7.56-7.55 (m, 3H), 7.42 (d, *J* = 7.7 Hz, 1H), 7.38-7.28 (m, 3H), 7.18 (d, *J* = 7.2 Hz, 1H), 7.12-7.04 (m, 3H), 6.85-6.83 (m, 3H), 6.62 (s, 1H), 2.40 (s, 3H). **¹³C NMR** (CDCl₃, 125 MHz) δ 149.4, 144.6, 143.1, 139.1, 138.0, 132.5, 132.1, 129.5, 128.9, 128.8, 128.8, 128.7, 128.2, 127.2, 126.4, 126.3, 125.9, 123.6, 123.4, 121.5, 116.2, 96.3, 21.5. **HPLC** (chiral column: DAICEL CHIRALPAK IF; solvent: hexane/2-propanol = 4/1; flow rate: 1.0 mL/min; detection: at 254 nm): t_R = 5.51 min (major) and 6.50 min (minor). **HRMS** (ESI) m/z: [M+Na]⁺ Calcd for C₂₇H₂₂N₂SNa⁺: 429.1396; Found 429.1390. [α]_D^{20.0} = +231.0 (*c* = 0.25, CHCl₃). **Rf** 0.5 (hexane/AcOEt = 3:1).

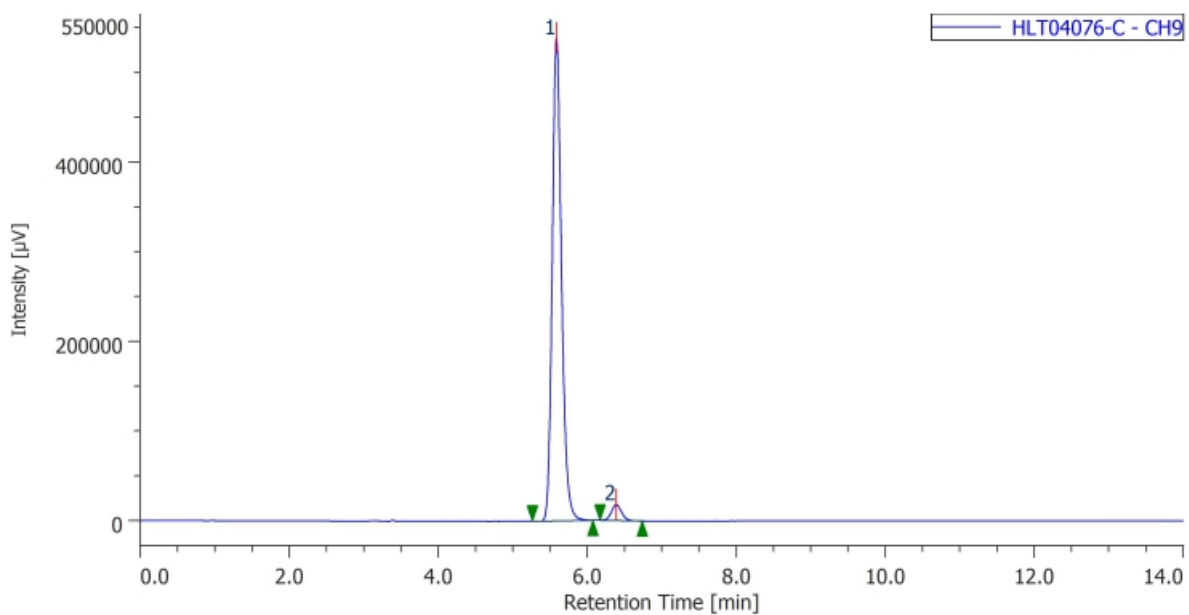
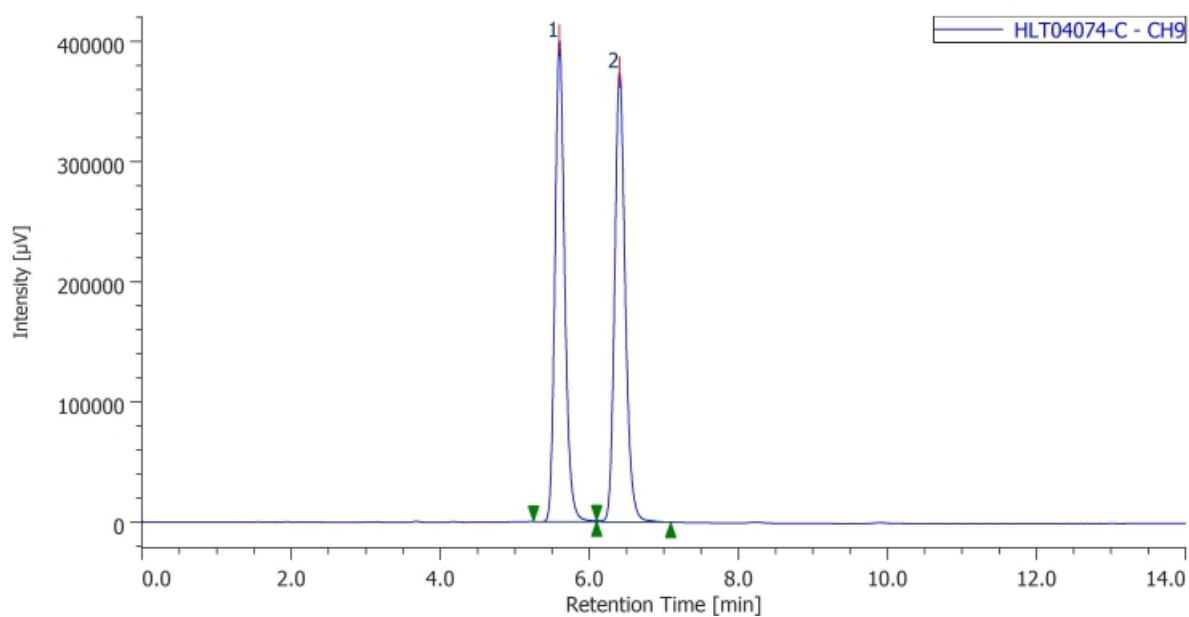




(S)-3-(3-chlorophenyl)-N,1-diphenyl-1 λ ⁶-benzo[e][1,2]thiazin-1-imine (8ae): Prepared according to GP-G using compound **5a** (0.05 mmol, 14.6 mg, 1.0 equiv.), **6e** (0.055 mmol, 12.7 mg, 1.1 equiv.), **CCA2** (0.005 mmol, 2.4 mg, 10 mol%). **8ae** was isolated as a yellow solid (16.9 mg, 80%). IR (KBr) 1591, 1472, 1261, 1116, 1085, 948, 748 cm^{-1} . ^1H NMR (CDCl_3 , 400 MHz) δ 8.19-8.16 (m, 2H) 7.99 (s, 1H), 7.88-7.86 (m, 1H), 7.59-7.57 (m, 3H), 7.45-7.37 (m, 2H).



7.34-7.30 (m, 3H), 7.15 (t, $J = 7.5$ Hz, 1H), 7.07 (t, $J = 7.0$ Hz, 2H), 6.86-6.81 (m, 3H), 6.62 (s, 1H). ^{13}C NMR (CDCl_3 , 100 MHz) δ 147.6, 144.4, 142.7, 141.0, 139.4, 134.4, 132.7, 132.3, 129.5, 129.0, 128.9, 128.6, 126.8, 126.6, 126.5, 125.9, 124.6, 123.4, 121.7, 116.6, 96.9; one aromatic signal was missing probably due to overlap. HPLC (chiral column: DAICEL CHIRALPAK IF; solvent: hexane/2-propanol = 4/1; flow rate: 1.0 mL/min; detection: at 254 nm): $t_R = 5.58$ min (major) and 6.39 min (minor). HRMS (ESI) m/z : $[\text{M}+\text{Na}]^+$ Calcd for $\text{C}_{26}\text{H}_{19}\text{N}_2\text{SClNa}^+$: 449.0850; Found 449.0847. $[\alpha]_D^{20.7} = +132.8$ ($c = 0.25$, CHCl_3). Rf 0.5 (hexane/AcOEt = 3:1).



(S)-N,1-diphenyl-3-(o-tolyl)-1 λ ⁶-benzo[e][1,2]thiazin-1-imine (8af): Prepared

according to **GP-G** using compound **5a** (0.05 mmol, 14.6 mg, 1.0 equiv.), **6f**

(0.055 mmol, 11.6 mg, 1.1 equiv.), **CCA2** (0.005 mmol, 2.4 mg, 10 mol%). **8af**

was isolated as a yellow solid (18.3 mg, 90%). **IR** (KBr) 1577, 1528, 1469,

1358, 1255, 1116, 1086, 758, 720 cm⁻¹. **¹H NMR** (CDCl₃, 500 MHz) δ

8.21-8.19 (m, 2H), 7.57-7.56 (m, 3H), 7.49-7.47 (m, 1H), 7.42-7.37 (m, 2H).

7.26-7.19 (m, 4H), 7.15-7.09 (m, 3H), 6.88-6.83 (m, 3H), 6.19 (s, 1H), 2.42 (s, 3H). **¹³C NMR** (CDCl₃, 100

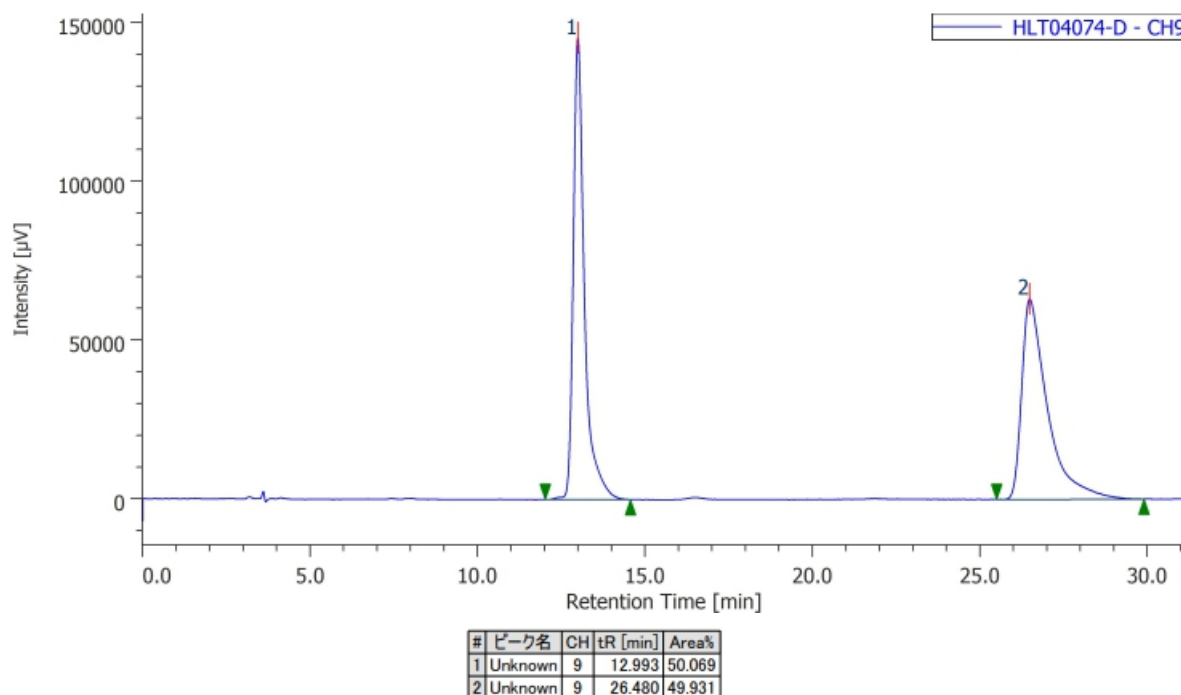
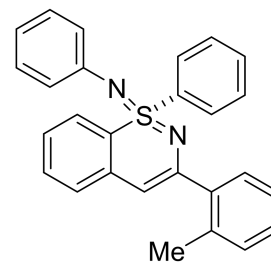
MHz) δ 152.2, 144.4, 142.8, 140.6, 139.6, 136.0, 132.5, 132.2, 130.7, 129.0, 128.9, 128.8, 128.7, 128.0,

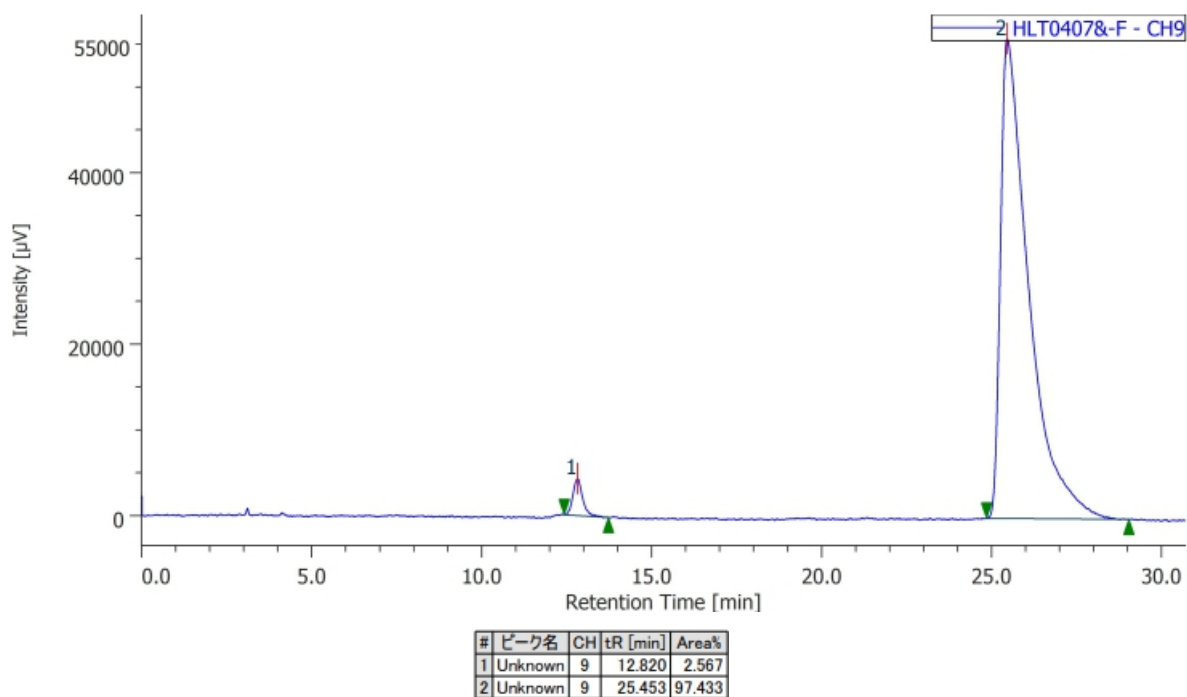
126.4, 126.0, 125.9, 125.6, 123.5, 121.5, 115.4, 99.6, 20.5. **HPLC** (chiral column: DAICEL CHIRALPAK

IA; solvent: hexane/2-propanol = 9/1; flow rate: 1.0 mL/min; detection: at 300 nm): t_R = 12.82 min (minor)

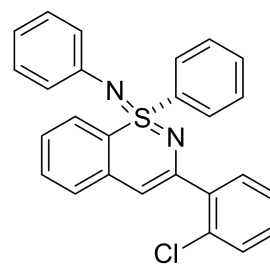
and 25.45 min (major). **HRMS** (ESI) m/z : [M+H]⁺ Calcd for C₂₇H₂₃N₂S⁺: 407.1577; Found 407.1571.

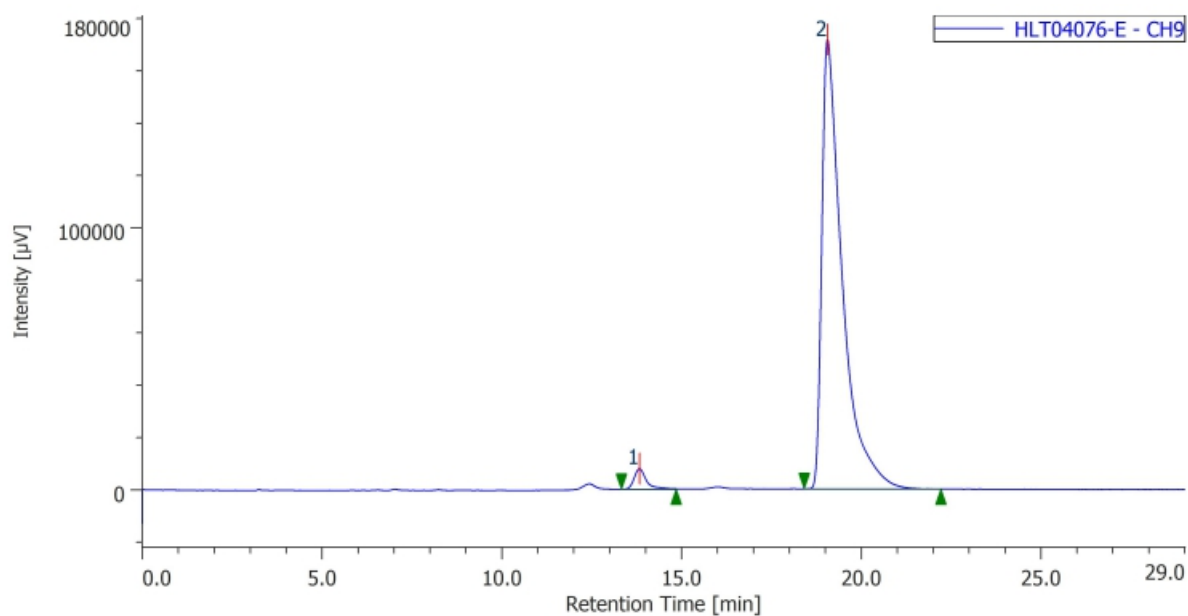
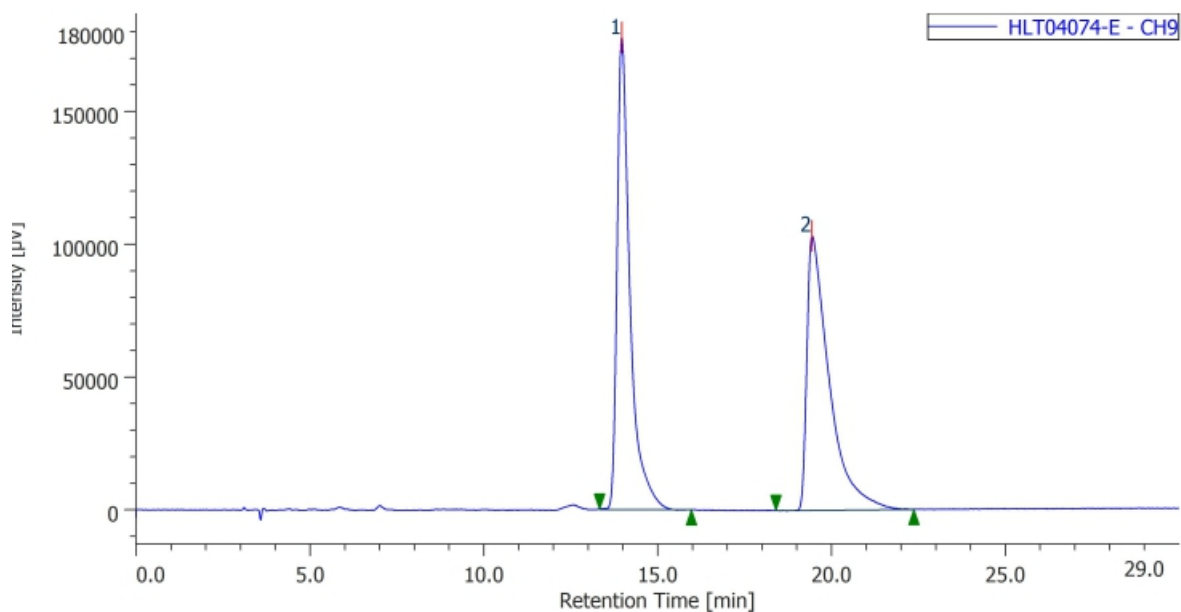
$[\alpha]_D^{18.9}$ = +125.3 (c = 0.25, CHCl₃). **Rf** 0.5 (hexane/AcOEt = 3:1).



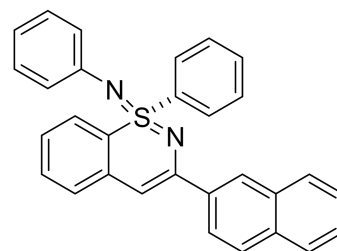


(S)-3-(2-chlorophenyl)-N,1-diphenyl-1 λ ^6-benzo[e][1,2]thiazin-1-imine (8ag): Prepared according to **GP-G** using compound **5a** (0.05 mmol, 14.6 mg, 1.0 equiv.), **6g** (0.055 mmol, 12.7 mg, 1.1 equiv.), **CCA2** (0.005 mmol, 2.4 mg, 10 mol%). **8ag** was isolated as a yellow solid (16.9 mg, 80%). **IR** (KBr) 1579, 1482, 1469, 1359, 1287, 1261, 1115, 1078, 751 cm^{-1} . **^1H NMR** (CDCl_3 , 500 MHz) δ 8.26-8.24 (m, 2H), 7.60-7.57 (m, 4H), 7.44-7.42 (m, 2H), 7.41-7.37 (m, 1H), 7.29-7.24 (m, 3H), 7.18-7.14 (m, 1H), 7.13-7.10 (m, 2H), 6.89-6.86 (m, 3H), 6.37-6.36 (m, 1H). **^{13}C NMR** (CDCl_3 , 100 MHz) δ 148.6, 144.3, 142.8, 139.5, 139.1, 132.6, 132.2, 132.2, 130.9, 130.1, 129.1, 128.9, 128.8, 126.8, 126.7, 126.2, 126.0, 123.6, 121.7, 116.0, 100.8; one aromatic signal was missing probably due to overlap. **HPLC** (chiral column: DAICEL CHIRALPAK IA; solvent: hexane/2-propanol = 9/1; flow rate: 1.0 mL/min; detection: at 254 nm): t_R = 13.82 min (minor) and 19.05 min (major). **HRMS** (ESI) m/z : $[\text{M}+\text{Na}]^+$ Calcd for $\text{C}_{26}\text{H}_{19}\text{N}_2\text{SClNa}^+$: 449.0850; Found 449.0845. $[\alpha]_D^{19.8}$ = +208.9 (c = 0.25, CHCl_3). **Rf** 0.6 (hexane/AcOEt = 3:1).

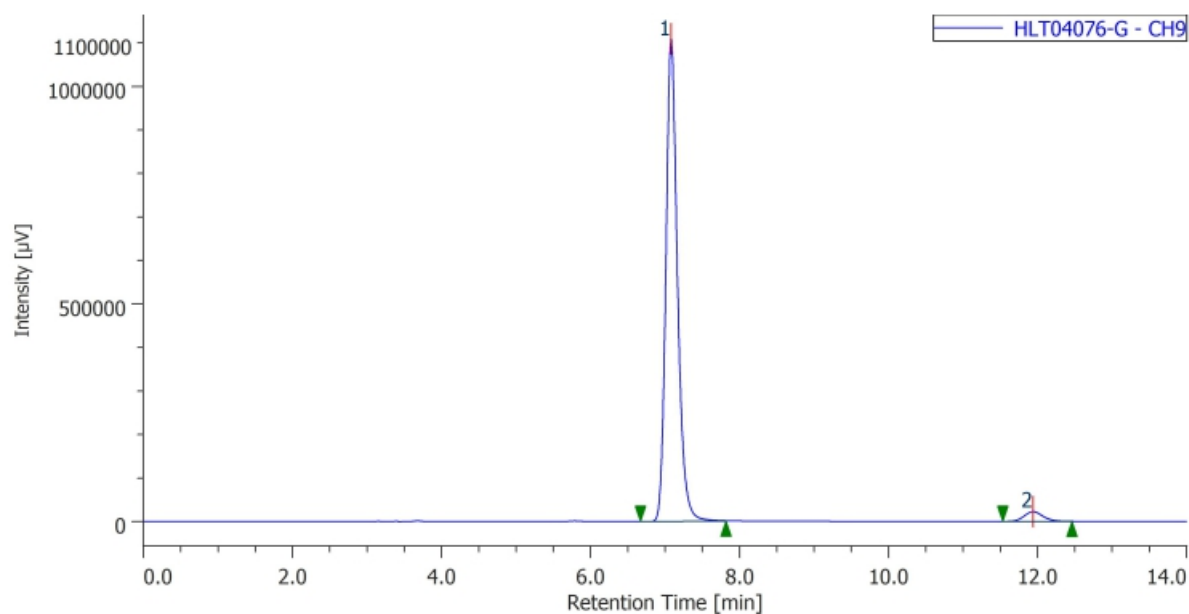
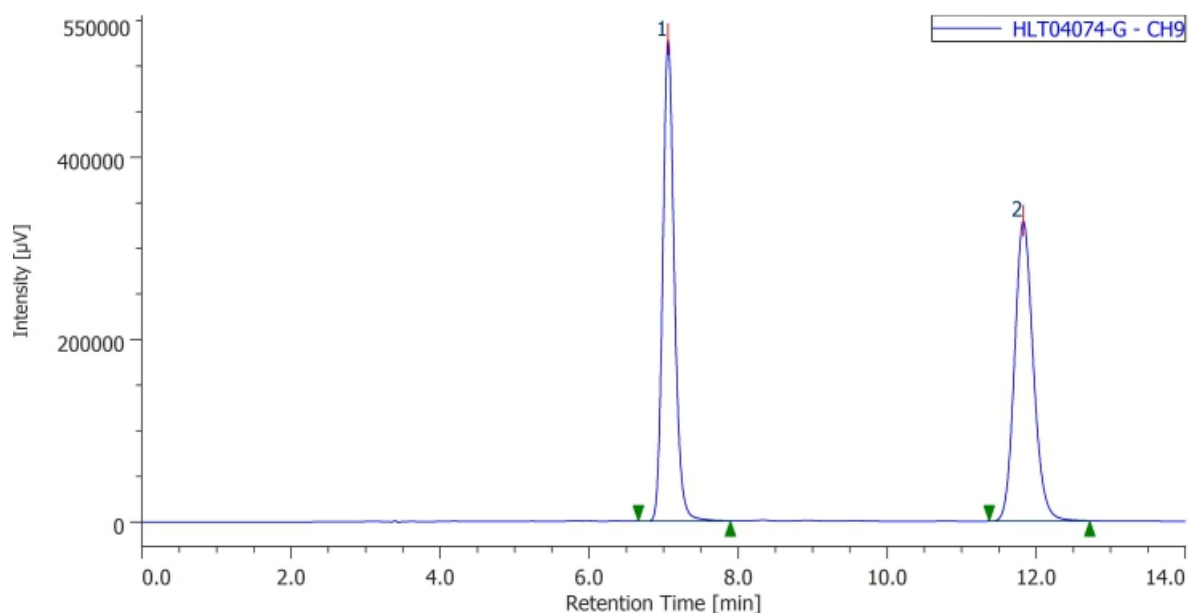




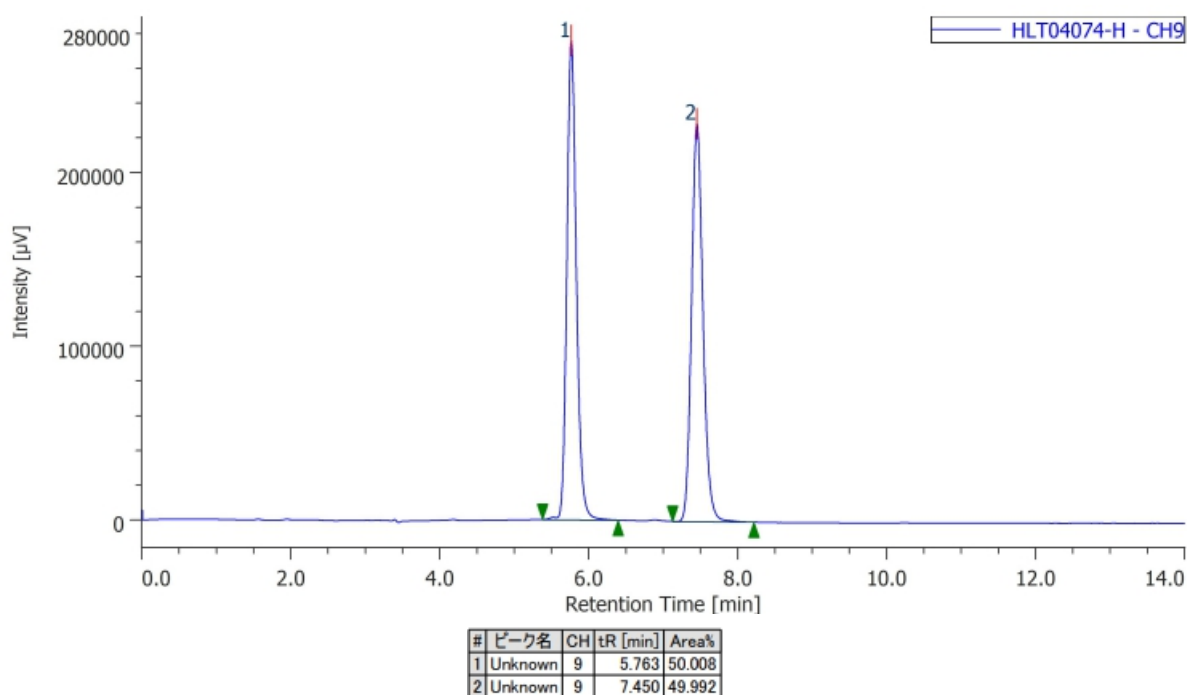
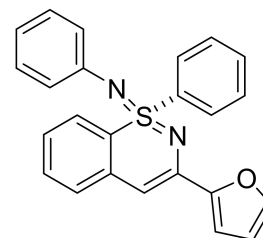
(S)-3-(naphthalen-2-yl)-N,1-diphenyl-1λ⁶-benzo[e][1,2]thiazin-1-imine (8ah): Prepared according to GP-G using compound **5a** (0.05 mmol, 14.6 mg, 1.0 equiv.), **6h** (0.055 mmol, 13.6 mg, 1.1 equiv.), **CCA2** (0.005 mmol, 2.4 mg, 10 mol%). **8ah** was isolated as a yellow solid (16.1 mg, 75%). IR (KBr) 3854, 3751, 3649, 3055, 1576, 1527, 1472, 1374, 1259, 1114, 755 cm⁻¹. ¹H NMR (CDCl₃, 400 MHz) δ 8.56 (s, 1H), 8.24-8.21 (m, 2H), 8.08 (dd, *J* = 8.6,

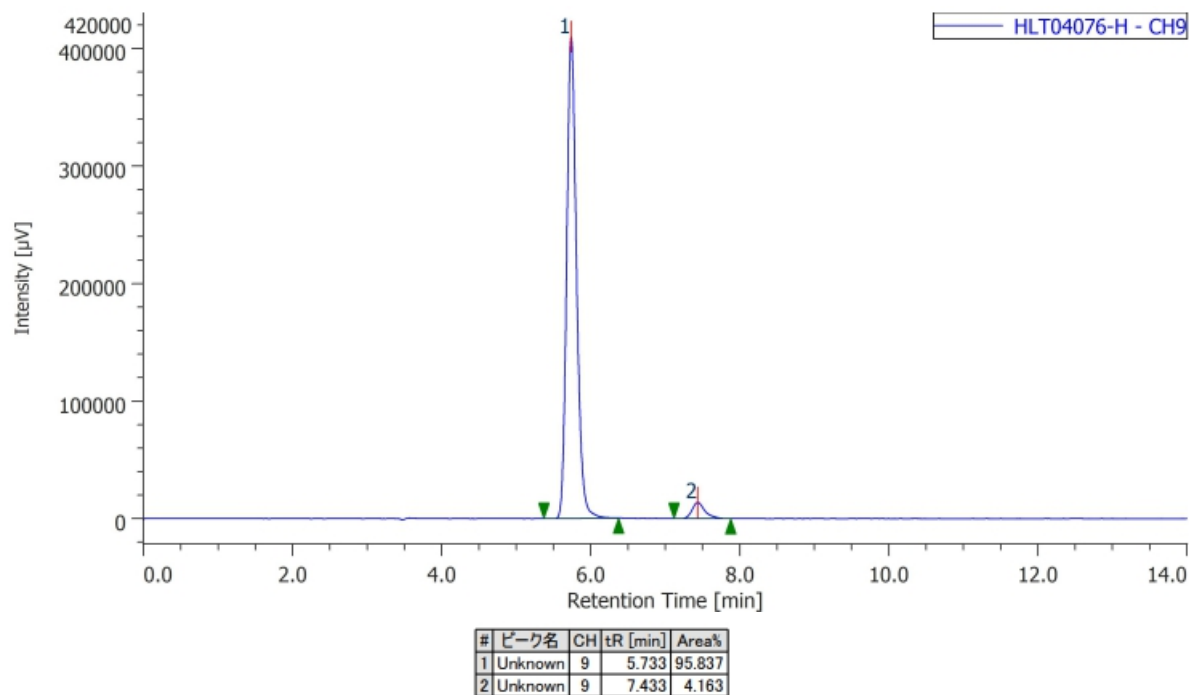


1.8 Hz, 1H), 7.92-7.83 (m, 3H), 7.59-7.56 (m, 3H), 7.49-7.45 (m, 3H), 7.42-7.37 (m, 1H), 7.36-7.33 (m, 1H), 7.16-7.12 (m, 1H), 7.09-7.03 (m, 2H), 6.90 - 6.87 (m, 2H), 6.90-6.81 (m, 1H), 6.79 (s, 1H). ¹³C NMR (CDCl₃, 125 MHz) δ 148.9, 144.6, 143.0, 139.8, 136.3, 133.6, 133.4, 132.6, 132.2, 129.0, 128.9, 128.8, 128.6, 127.8, 127.5, 126.5, 126.4, 126.3, 126.2, 126.1, 126.0, 124.0, 123.5, 121.6, 116.5, 96.9. HPLC (chiral column: DAICEL CHIRALPAK IF; solvent: hexane/2-propanol = 4/1; flow rate: 1.0 mL/min; detection: at 254 nm): t_R = 7.08 min (major) and 11.94 min (minor). HRMS (ESI) m/z: [M+H]⁺ Calcd for C₃₀H₂₃N₂S⁺: 443.1577; Found 443.1573. [α]_D^{20.5} = +69.5 (c = 0.25, CHCl₃). R_f 0.5 (hexane/AcOEt = 3:1).

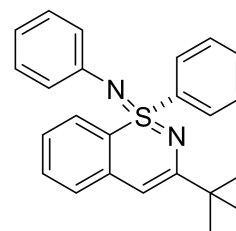


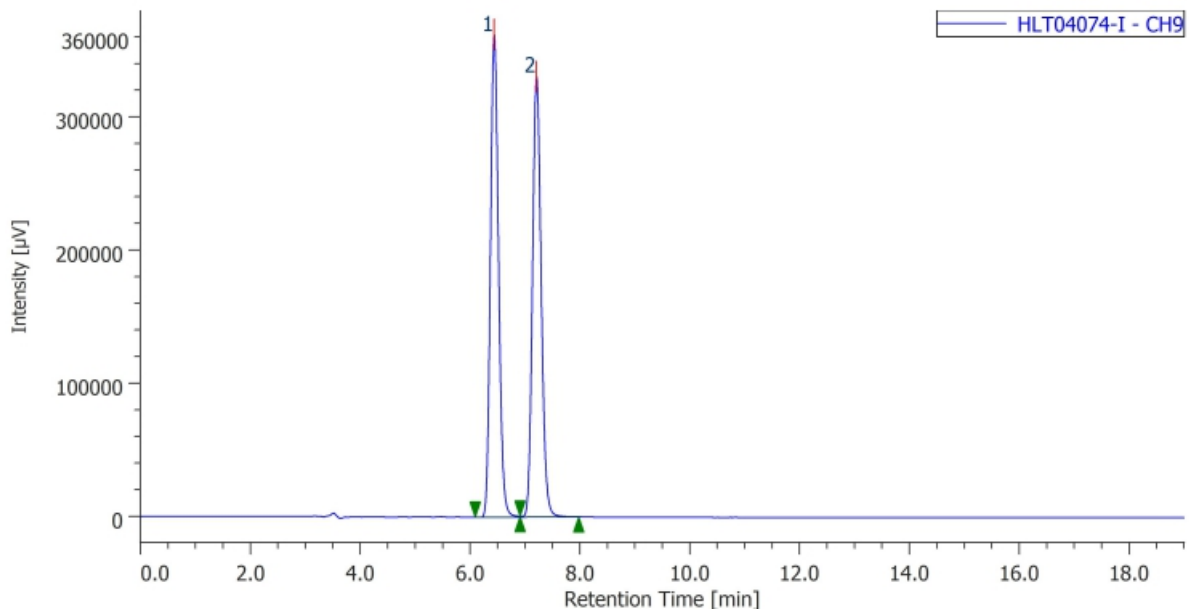
(S)-3-(furan-2-yl)-N,1-diphenyl-1 λ ^6-benzo[e][1,2]thiazin-1-imine (8ai): Prepared according to **GP-G** using compound **5a** (0.05 mmol, 14.6 mg, 1.0 equiv.), **6i** (0.055 mmol, 10.2 mg, 1.1 equiv.), **CCA2** (0.005 mmol, 2.4 mg, 10 mol%). **8ai** was isolated as a yellow solid (14.3 mg, 75%). **IR** (KBr) 1586, 1526, 1483, 1468, 1310, 1292, 1261, 1216, 1119, 1086, 795, 752, 737 cm⁻¹. **¹H NMR** (CDCl₃, 500 MHz) δ 8.18-8.15 (m, 2H), 7.57-7.54 (m, 3H), 7.49 (dd, J = 1.8, 0.9 Hz, 1H), 7.41 (d, J = 8.1 Hz, 1H), 7.36-7.33 (m, 1H), 7.27 (d, J = 6.9 Hz, 1H), 7.11-7.06 (m, 3H), 6.90 (dd, J = 3.3, 0.9 Hz, 1H), 6.88-6.82 (m, 3H), 6.63 (s, 1H), 6.48 (dd, J = 3.3, 1.8 Hz, 1H). **¹³C NMR** (CDCl₃, 125 MHz) δ 153.5, 144.5, 143.0, 142.9, 140.7, 139.6, 132.6, 132.2, 128.9, 128.9, 128.5, 126.4, 126.2, 126.0, 123.6, 121.6, 117.0, 111.9, 109.2, 94.6. **HPLC** (chiral column: DAICEL CHIRALPAK IF; solvent: hexane/2-propanol = 4/1; flow rate: 1.0 mL/min; detection: at 300 nm): t_R = 5.73 min (major) and 7.43 min (minor). **HRMS** (ESI) m/z : [M+Na]⁺ Calcd for C₂₄H₁₈N₂SONa⁺: 405.1032; Found 405.1028. $[\alpha]_D^{19.5}$ = +103.2 (c = 0.25, CHCl₃). **Rf** 0.5 (hexane/AcOEt = 3:1).



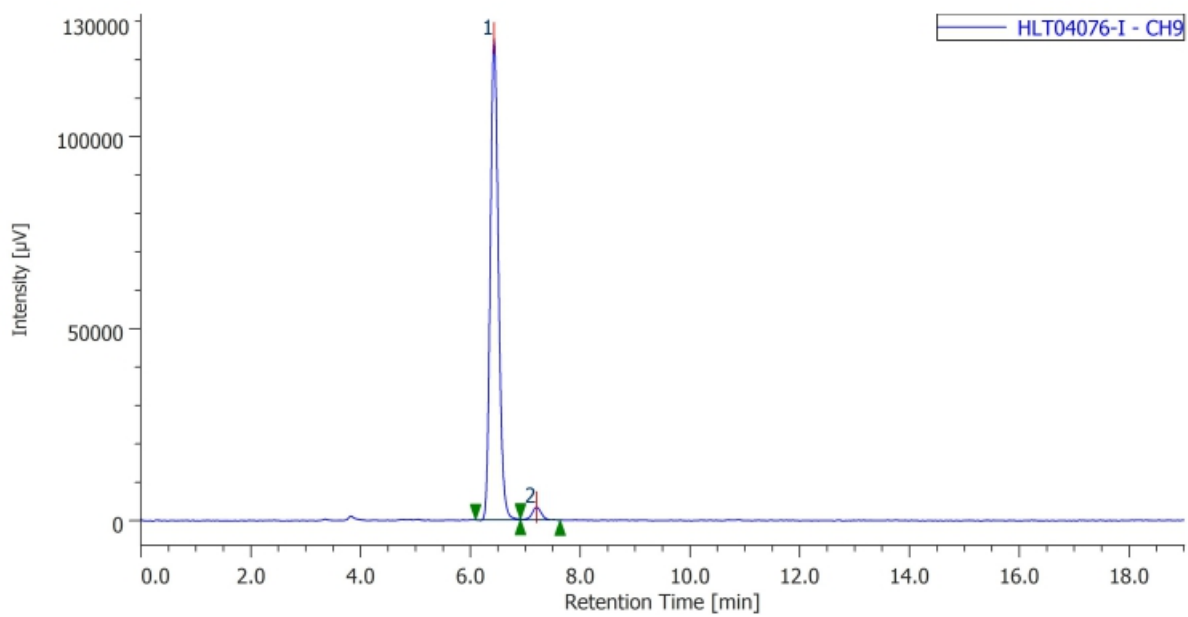


(S)-3-(tert-butyl)-N,1-diphenyl-1 λ ⁶-benzo[e][1,2]thiazin-1-imine (8aj): Prepared according to **GP-G** using compound **5a** (0.05 mmol, 14.6 mg, 1.0 equiv.), **6j** (0.055 mmol, 9.7 mg, 1.1 equiv.), **CCA2** (0.005 mmol, 2.4 mg, 10 mol%). **8aj** was isolated as a yellow oil (12.3 mg, 66%). **IR** (neat) 2960, 2924, 1577, 1532, 1486, 1472, 1350, 1283, 1257, 1148, 1087, 748, 719 cm^{-1} . **¹H NMR** (CDCl_3 , 500 MHz) δ 8.13 - 8.11 (m, 2H), 7.56 - 7.54 (m, 3H), 7.38 (d, $J = 8.1$ Hz, 1H), 7.31 - 7.28 (m, 1H), 7.18-7.16 (m, 1H), 7.09 - 7.04 (m, 3H), 6.85-6.81 (m, 1H), 6.79 - 6.76 (m, 2H), 6.03-6.03 (m, 1H), 1.33 (s, 9H). **¹³C NMR** (CDCl_3 , 125 MHz) δ 162.0, 144.9, 143.6, 139.9, 132.3, 131.9, 128.8, 128.6, 128.4, 126.1, 125.8, 125.8, 123.5, 121.3, 115.1, 93.0, 38.1, 29.1. **HPLC** (chiral column: DAICEL CHIRALPAK IF; solvent: hexane/2-propanol = 97/3; flow rate: 1.0 mL/min; detection: at 300 nm): $t_R = 6.43$ min (major) and 7.21 min (minor). **HRMS** (ESI) m/z : $[\text{M}+\text{H}]^+$ Calcd for $\text{C}_{24}\text{H}_{25}\text{N}_2\text{S}^+$: 373.1733; Found 373.1730. $[\alpha]_D^{21.0} = +185.4$ ($c = 0.25$, CHCl_3). **Rf** 0.7 (hexane/AcOEt = 3:1).



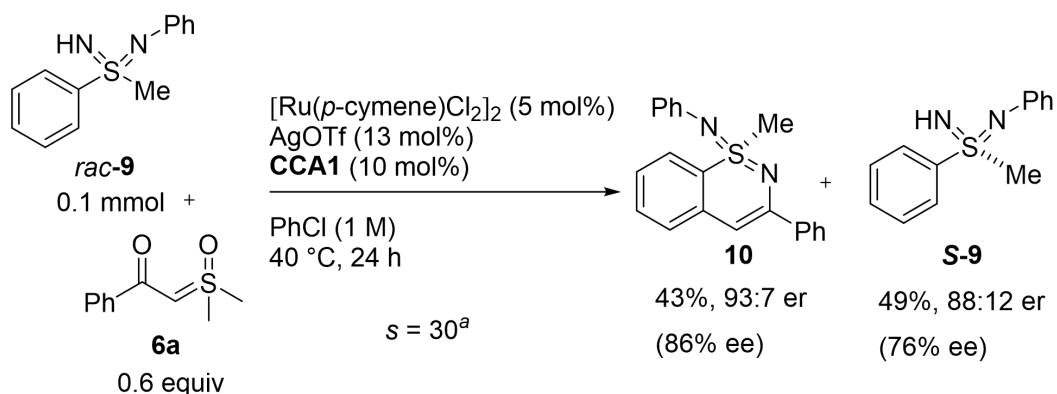


#	ピーク名	CH	tR [min]	Area%
1	Unknown	9	6.437	50.516
2	Unknown	9	7.207	49.484



#	ピーク名	CH	tR [min]	Area%
1	Unknown	9	6.427	97.050
2	Unknown	9	7.207	2.950

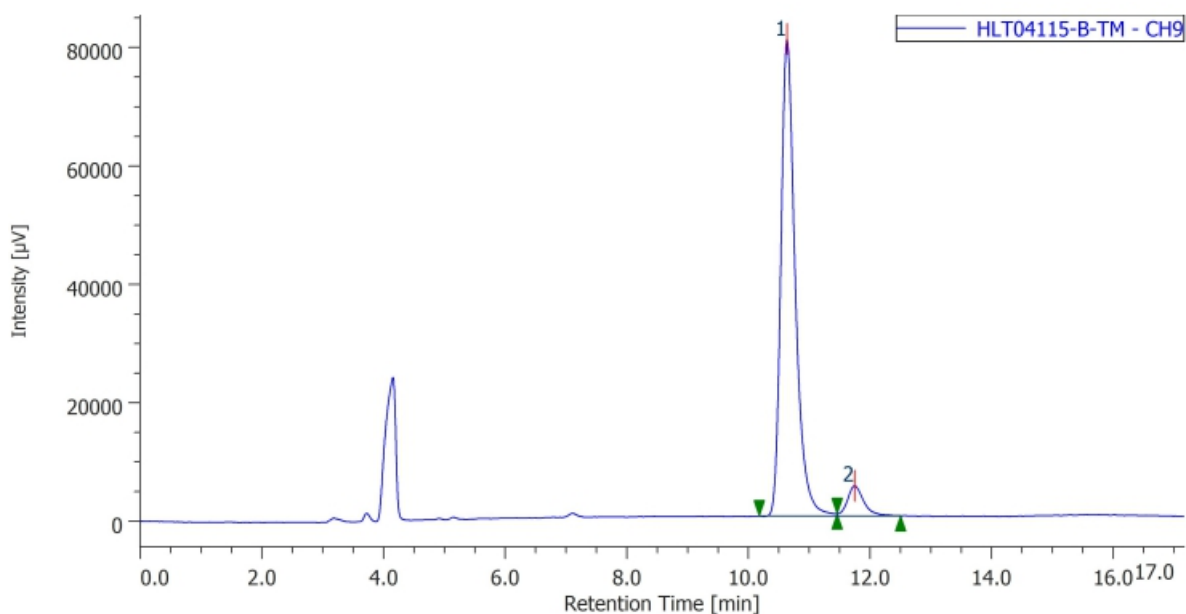
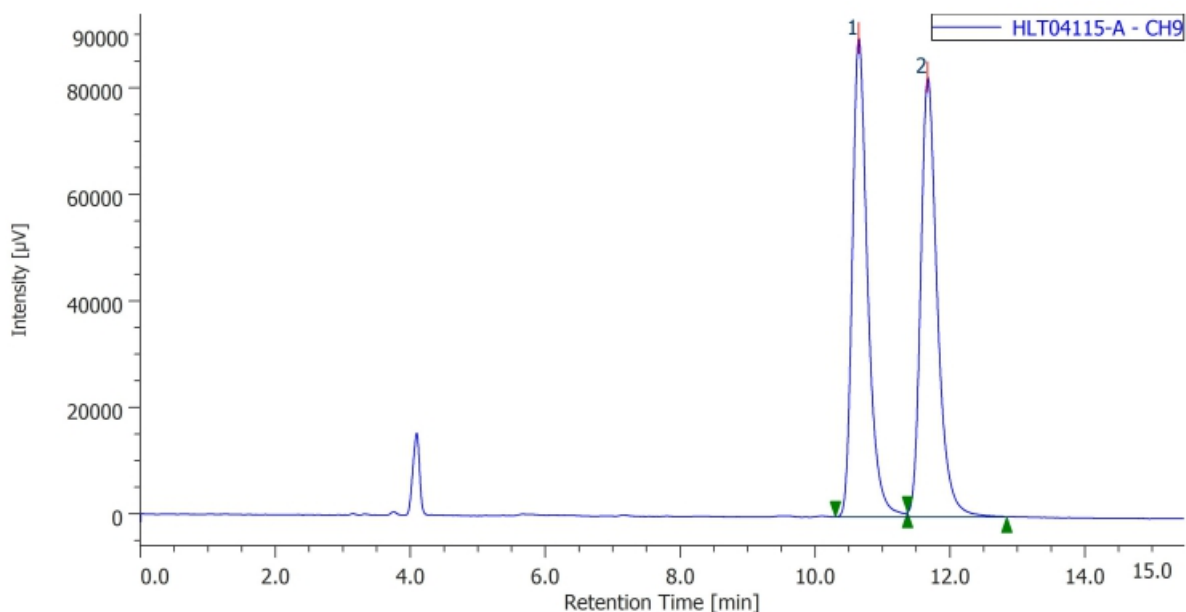
4.5. Kinetic resolution of racemic sulfondiimine



a) Selectivity factor is given: $S = \ln[(1 - C)(1 - ee_5)] / \ln[(1 - C)(1 + ee_5)]$, $C = ee_5 / (ee_5 + ee_6)$

In an argon-filled glovebox, a screw-capped test tube was charged with chiral carboxylic acid **CCA1** (4.8 mg, 0.01 mmol, 10 mol%), $[Ru(p\text{-cymene})Cl_2]_2$ (3.2 mg, 0.005 mmol, 5 mol%), AgOTf (3.2 mg, 0.013 mmol, 13 mol%), sulfondiimine **rac-9** (23.0 mg, 0.1 mmol, 1.0 equiv.), and sulfoxonium ylide **6a** (11.8 mg, 0.06 mmol, 0.6 equiv.). After the addition of chlorobenzene (0.1 mL), the test tube was capped and brought out of the glovebox. The reaction mixture was stirred at 40 °C for 24 h. The resulting mixture was directly purified by silica gel column chromatography (hexane/AcOEt) to afford **10** and **S-9**.

(S)-1-methyl-N,3-diphenyl-1λ⁶-benzo[e][1,2]thiazin-1-imine (10): **10** was isolated as a yellow oil (14.2 mg, 43%). IR (KBr) 1571, 1530, 1472, 1364, 1284, 1256, 1117, 1041, 758, 694 cm^{-1} . ¹H NMR (CDCl₃, 400 MHz) δ 7.93-7.90 (m, 2H), 7.74 (d, $J = 8.2$ Hz, 1H), 7.47-7.33 (m, 4H), 7.29-7.25 (m, 2H), 7.04-7.00 (m, 2H), 6.81 (t, $J = 7.5$ Hz, 1H), 6.74-6.71 (m, 2H), 6.48 (s, 1H), 3.66 (s, 3H). ¹³C NMR (CDCl₃, 100 MHz) δ 149.2, 144.9, 140.0, 138.9, 132.8, 128.8, 128.8, 128.3, 126.5, 126.4, 126.4, 124.8, 123.0, 121.6, 114.8, 96.5, 50.1. HPLC (chiral column: DAICEL CHIRALPAK IF; solvent: hexane/2-propanol = 19/1; flow rate: 1.0 mL/min; detection: at 254 nm): $t_R = 10.62$ min (major) and 11.72 min (minor). HRMS (ESI) m/z : $[M+Na]^+$ Calcd for C₂₁H₁₈N₂SNa⁺: 353.1083; Found 353.1075. $[\alpha]_D^{24.7} = -8.5$ ($c = 0.25$, CHCl₃). Rf 0.8 (hexane/AcOEt = 3:1).



(S)-1-methyl-N,1-diphenyl- λ^6 -sulfanediimine (S-9): S-9 was isolated as a pale brown solid (11.3 mg,

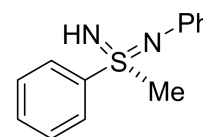
49%). IR (KBr) 3120, 3106, 1595, 1485, 1284, 1256, 1088, 1060, 963, 768, 756, 735

cm⁻¹. ¹H NMR (CDCl₃, 400 MHz) δ 8.19 (d, *J* = 8.2 Hz, 2H), 7.63-7.55 (m, 3H), 7.17

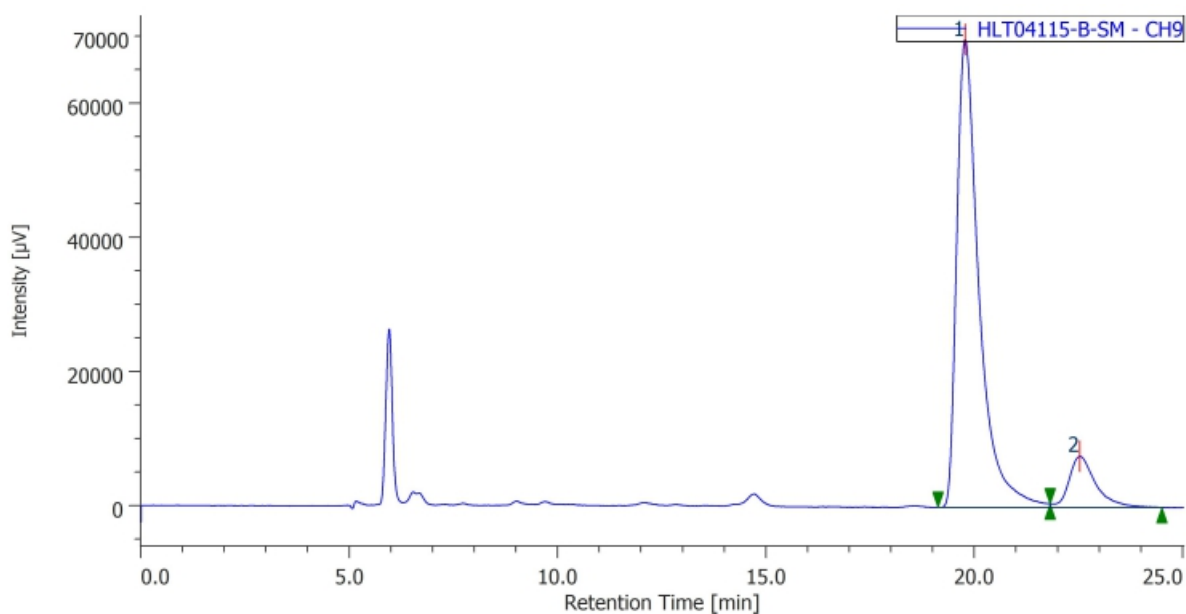
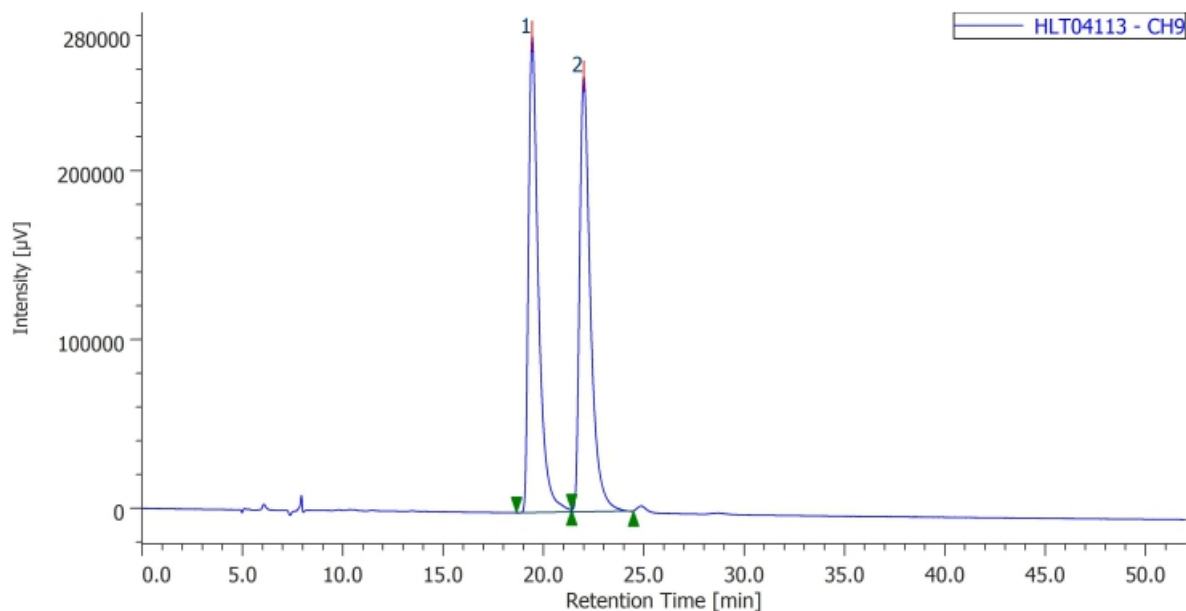
(t, *J* = 7.5 Hz, 2H), 7.09 (d, *J* = 8.2 Hz, 2H), 6.89 (t, *J* = 7.2 Hz, 1H), 3.27 (s, 3H), 2.17

(brs, 1H). ¹³C NMR (CDCl₃, 100 MHz) δ 145.9, 142.0, 132.7, 129.4, 129.0, 127.8,

123.1, 121.0, 48.3. HPLC (chiral column: DAICEL CHIRALPAK IA; solvent: hexane/2-propanol = 9/1;

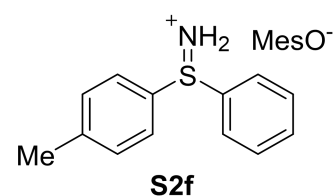


flow rate: 0.6 mL/min; detection: at 254 nm): $t_R = 19.77$ min (major) and 22.53 min (minor). **HRMS** (ESI) m/z : $[M+H]^+$ Calcd for $C_{13}H_{15}N_2S^+$: 231.0951; Found 231.0947. $[\alpha]_D^{23.0} = -41.0$ ($c = 0.25$, $CHCl_3$). **Rf** 0.8 (hexane/AcOEt = 3:1).



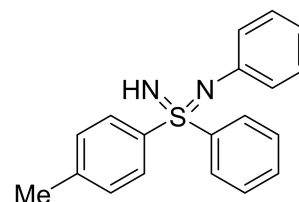
4.6. Parallel kinetic resolution of sulfondiimine

(4-tolyl-phenyl)sulfiliminium mesitylenesulfonate (S2f): Prepared according to **GP-F** using (4-tolylphenyl) sulfide (3.5 mmol, 750 mg, 1.0 equiv.), **S2f** was isolated as a colorless solid (1.3 g, 72%). **IR** (KBr) 3042,

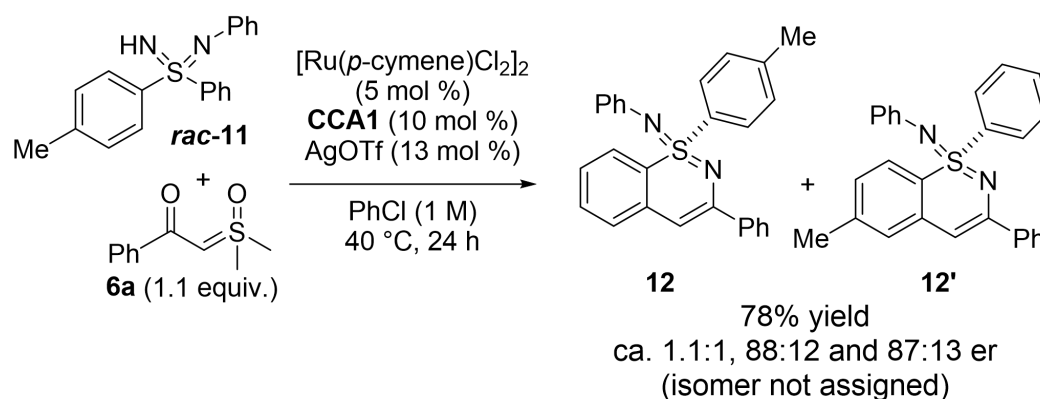


1603, 1445, 1218, 1189, 1176, 1085, 676 cm^{-1} . $^1\text{H NMR}$ (CDCl_3 , 400 MHz) δ 7.73 (d, $J = 7.5$ Hz, 2H), 7.65 (d, $J = 8.4$ Hz, 2H), 7.58-7.46 (m, 3H), 7.42 (t, $J = 7.5$ Hz, 2H), 7.21 (d, $J = 8.0$ Hz, 2H), 6.76 (s, 2H), 2.53 (s, 6H), 2.34 (s, 3H), 2.22 (s, 3H). $^{13}\text{C NMR}$ (CDCl_3 , 100 MHz) δ 144.2, 138.3, 137.1, 133.4, 132.8, 130.9, 130.5, 130.1, 130.0, 129.9, 128.6, 128.2, 67.0, 22.9, 21.5, 20.7. **HRMS** (ESI) m/z : $[\text{M-MesO}]^+$ Calcd for $\text{C}_{13}\text{H}_{14}\text{NS}^+$: 216.0842; Found 216.0838.

N,1-diphenyl-1-(p-tolyl)- λ^6 -sulfondiimine (*rac*-11): Prepared according to **GP-F** using compound **S2f** (3.2 mmol, 1.3 g, 1.0 equiv.), Na_2CO_3 (16 mmol, 1.68 g, 5.0 equiv.), Selectfluor® (3.2 mmol, 1.13 g, 1.0 equiv.), aniline (9.6 mmol, 0.9 mL, 3.0 equiv.), pyridine (3.84 mmol, 0.3 mL, 1.2 equiv.). *rac*-11 was isolated as a colorless solid (0.27 g, 27%). **IR** (KBr) 3191, 3152, 3058,



1594, 1482, 1443, 1282, 1257, 1176, 1085, 1039, 949, 750 cm^{-1} . $^1\text{H NMR}$ (CDCl_3 , 400 MHz) δ 8.20-8.17 (m, 2H), 8.06 (d, $J = 7.9$ Hz, 2H), 7.47-7.45 (m, 3H), 7.26-7.24 (m, 2H), 7.17-7.11 (m, 4H), 6.87-6.83 (m, 1H), 2.36 (s, 3H). $^{13}\text{C NMR}$ (CDCl_3 , 100 MHz) δ 145.7, 143.4, 142.8, 139.8, 131.9, 129.8, 129.1, 128.8, 128.1, 127.9, 123.4, 120.7, 21.3. **HRMS** (ESI) m/z : $[\text{M}+\text{H}]^+$ Calcd for $\text{C}_{19}\text{H}_{19}\text{N}_2\text{S}^+$: 307.1264; Found 307.1257. **Rf** 0.4 (hexane/AcOEt = 3:1).



In an argon-filled glovebox, a screw-capped test tube was charged with chiral carboxylic acid **CCA1** (4.8 mg, 0.01 mmol, 10 mol%), $[\text{Ru}(p\text{-cymene})\text{Cl}_2]_2$ (3.2 mg, 0.005 mmol, 5 mol%), AgOTf (3.2 mg, 0.013 mmol, 13 mol%), sulfondiimine *rac*-11 (30.6 mg, 0.1 mmol, 1.0 equiv.), and sulfoxonium ylide **6a** (11.8 mg, 0.06 mmol, 0.6 equiv.). After the addition of chlorobenzene (0.1 mL), the test tube was capped and brought out of the glovebox. The reaction mixture was stirred at 40 °C for 24 h. The resulting mixture was directly purified by silica gel column chromatography (hexane/AcOEt) to afford an inseparable mixture of

12 and **12'** as a yellow solid (15.8 mg, 78%, ca. 1.1:1 ratio). Due to the structural similarity and inseparable nature, the ^1H and ^{13}C NMR signals could not be assigned and the structure of the isomers were not assigned.

(S)-N,3-diphenyl-1-(p-tolyl)-1 λ ⁶-benzo[e][1,2]thiazin-1-imine

and

(S)-6-methyl-N,1,3-triphenyl-1 λ ⁶-benzo[e][1,2]thiazin-1-imine (12** and **12'**, not assigned):**

IR (KBr) 1585, 1531, 1486, 1471, 1445, 1282, 1256, 1114, 1088, 754 cm^{-1} .

^1H NMR (CDCl_3 , 400 MHz) δ 8.17-8.14 (m, 2H), 8.05 (d, $J = 8.5$ Hz, 2H),

8.01-7.89 (m, 4H), 7.54-7.52 (m, 3H), 7.43-7.33 (m, 11H), 7.28 (d, $J = 7.0$

Hz, 1H), 7.13-7.03 (m, 6H), 6.94 (d, $J = 8.4$ Hz, 1H), 6.87-6.79 (m, 6H),

6.62 (s, 1H), 6.57 (s, 1H), 2.42 (s, 3H), 2.31 (3H). **^{13}C NMR** (CDCl_3 , 100

MHz) δ 149.3, 149.2, 144.8, 144.7, 143.5, 143.4, 142.8, 140.0, 139.6, 139.3,

132.3, 132.0, 129.6, 128.9, 128.8, 128.8, 128.7, 128.6, 128.4, 128.3, 127.9,

126.5, 126.5, 126.3, 126.2, 126.2, 125.9, 125.8, 123.5, 123.5, 121.4, 121.4,

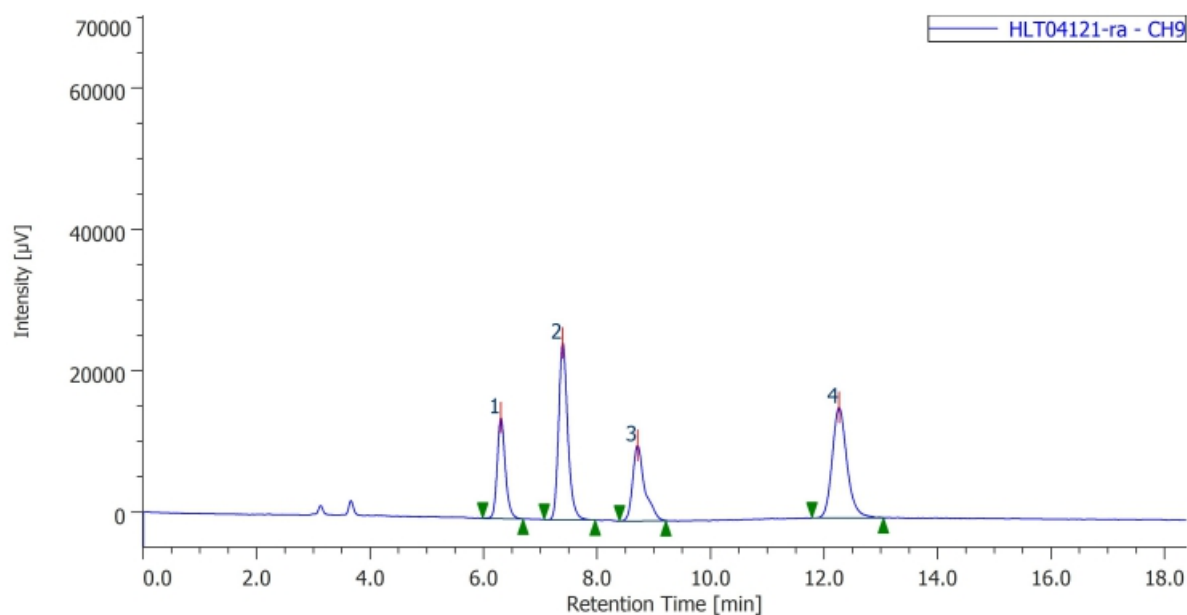
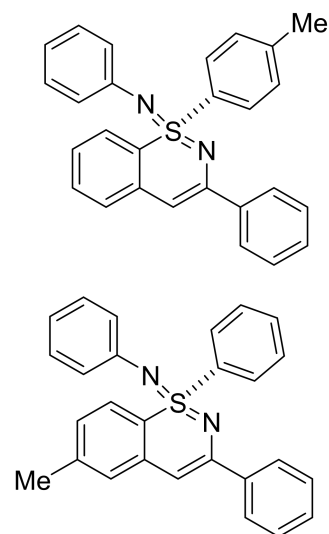
116.6, 113.7, 96.3, 96.3, 21.6, 21.5. (four aromatic signals were missing

probably due to overlap) **HPLC** (chiral column: DAICEL CHIRALPAK IF;

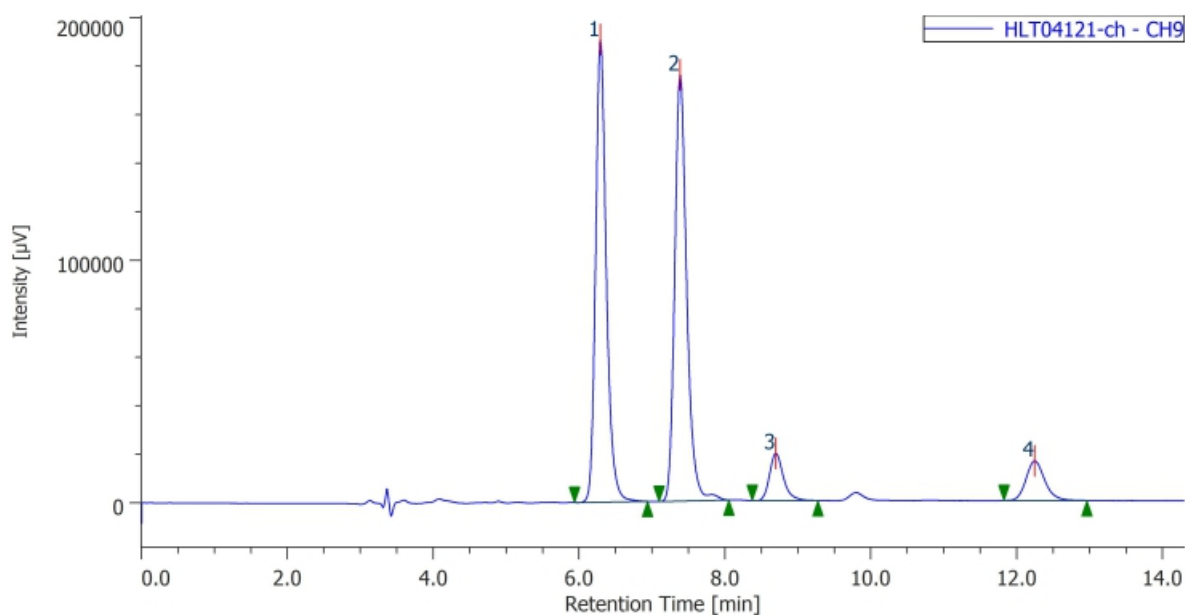
solvent: hexane/2-propanol = 4/1; flow rate: 1.0 mL/min; detection: at 250 nm): $t_{\text{R}} = 6.29$ min (major), 7.38

(major), 8.70 (minor), 12.24 (minor). **HRMS** (ESI) m/z : $[\text{M}+\text{Na}]^+$ Calcd for $\text{C}_{27}\text{H}_{22}\text{N}_2\text{SNa}^+$: 429.1396;

Found 429.1389. $[\alpha]_{\text{D}}^{22.0} = +87.7$ ($c = 0.25$, CHCl_3). **Rf** 0.7 (hexane/AcOEt = 2:1).



#	ピーク名	CH	tR [min]	Area%
1	Unknown	9	6.300	16.486
2	Unknown	9	7.393	32.569
3	Unknown	9	8.710	18.216
4	Unknown	9	12.260	32.729

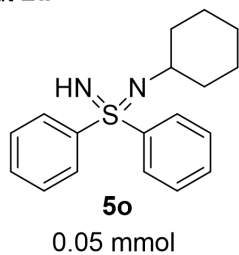


#	ピーク名	CH	tR [min]	Area%
1	Unknown	9	6.290	43.132
2	Unknown	9	7.383	44.637
3	Unknown	9	8.697	5.759
4	Unknown	9	12.243	6.473

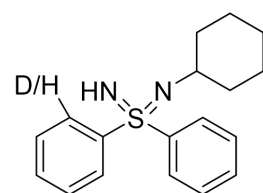
4.7. H/D exchange experiments

Without 6a: To a screw-cap vial were added **CCA2** (2.4 mg, 0.005 mmol, 10 mol%) and CD₃OD (ca. 0.2 mL), and the mixture was stirred for 30 min at room temperature. The mixture was concentrated in vacuo and moved into an argon-filled glovebox. The vial was charged with [Ru(*p*-cymene)Cl₂]₂ (1.6 mg, 0.0025 mmol, 5 mol%), AgOTf (1.6 mg, 0.0065 mmol, 13 mol%) and sulfondiimine **5o** (14.9 mg, 0.05 mmol, 1.0 equiv.). After the addition of chlorobenzene (0.5 mL) and CD₃OD (10.0 equiv.), the test tube was capped and brought out of the glovebox. The reaction mixture was stirred at 40 °C for 24 h. The resulting mixture was directly purified by silica gel column chromatography (hexane/AcOEt) to afford **5o** (12.2 mg, 82%). The ¹H NMR analysis of the recovered **5o** indicated no H/D exchange.

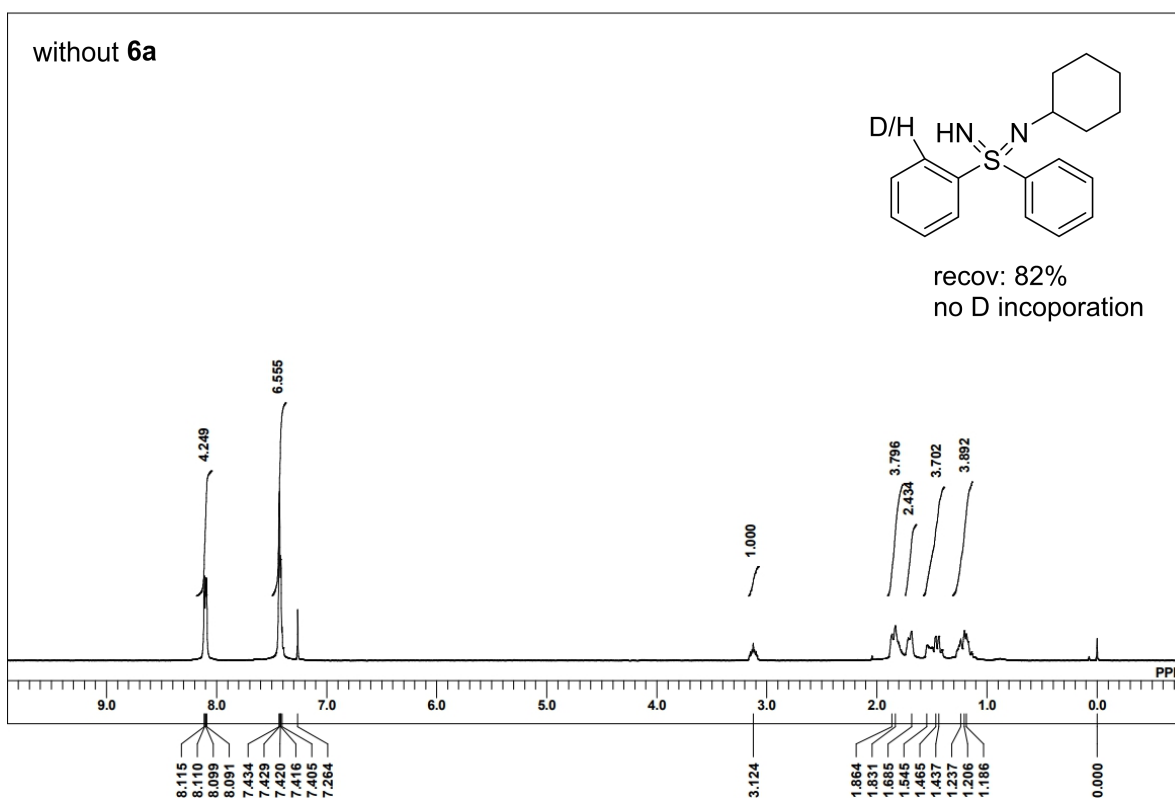
Without **2a**



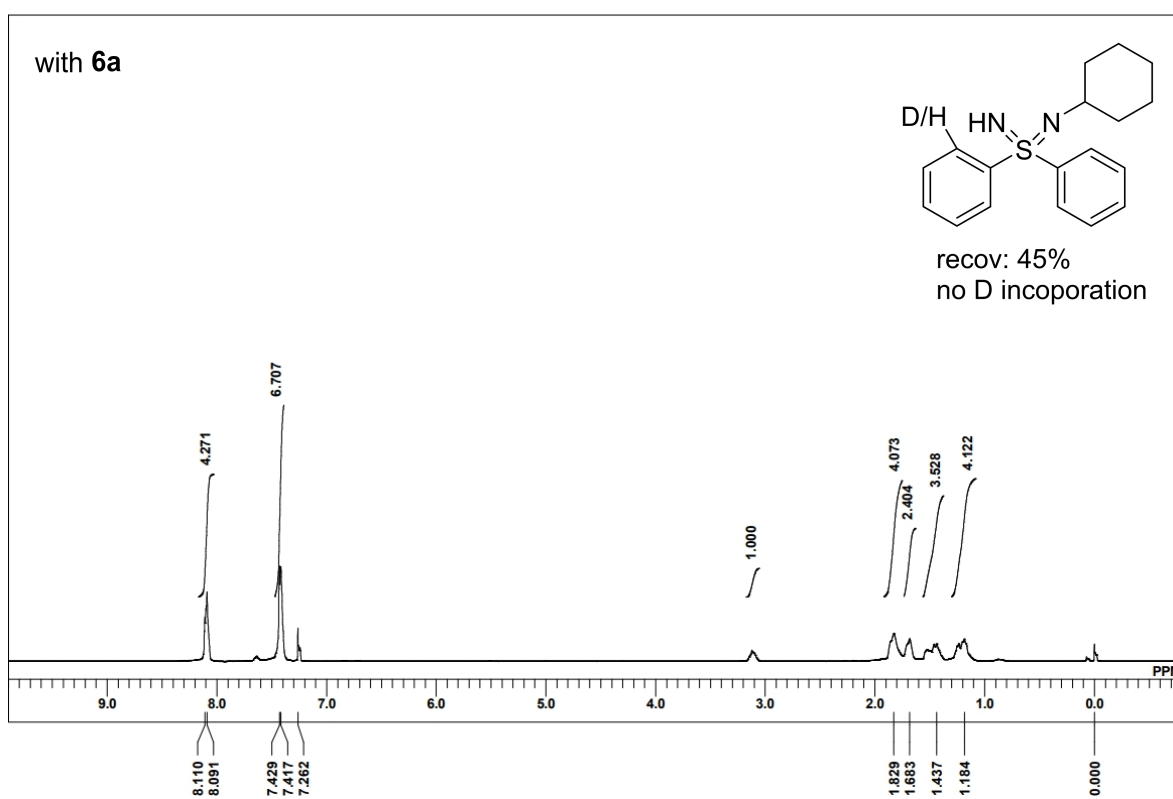
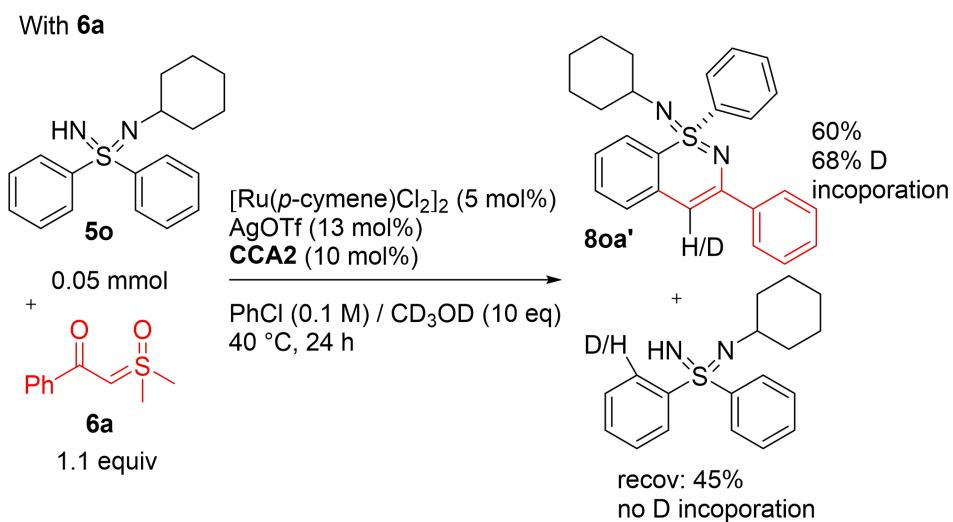
[Ru(*p*-cymene)Cl₂]₂ (5 mol%)
AgOTf (13 mol%)
CCA2 (10 mol%)
PhCl (1 M) /CD₃OD (10 eq)
40 °C, 24 h

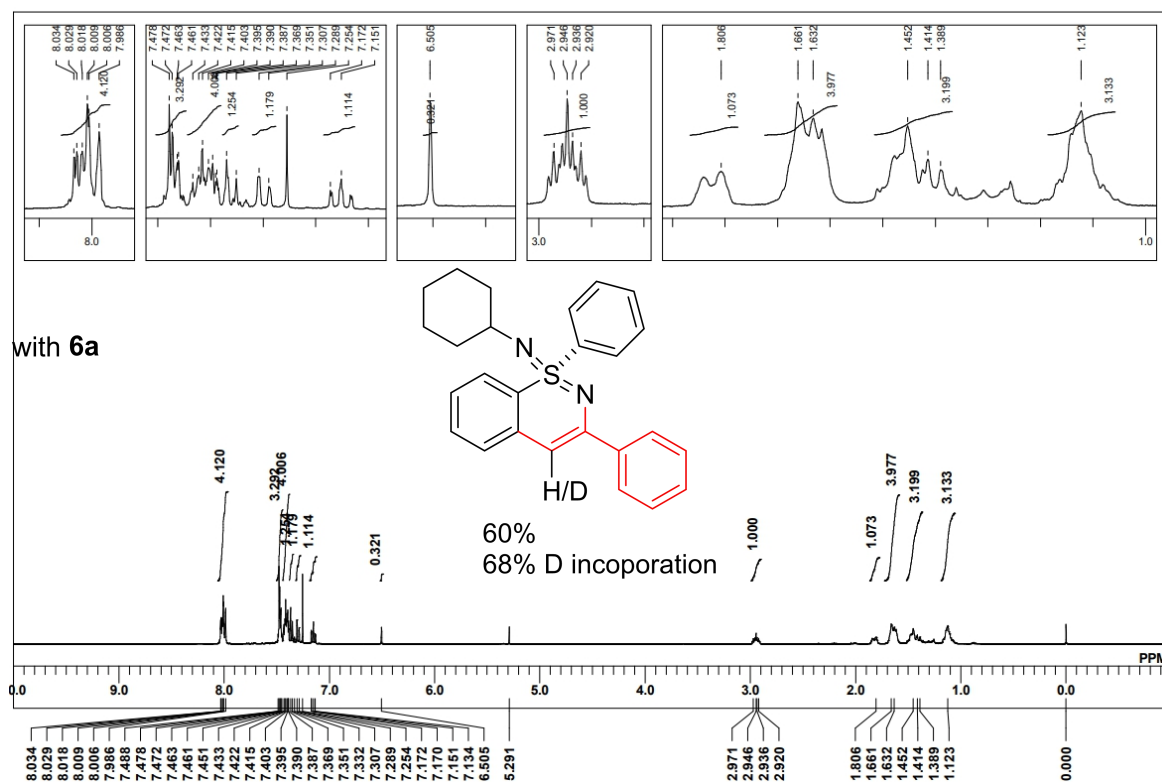


recov: 82%
no D incorporation



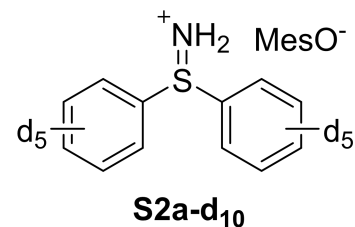
With 6a: To a screw-cap vial were added **CCA2** (2.4 mg, 0.005 mmol, 10 mol%) and CD₃OD (ca. 0.2 mL), and the mixture was stirred for 30 min at room temperature. The mixture was concentrated in vacuo and moved into an argon-filled glovebox. The vial was charged with [Ru(*p*-cymene)Cl₂]₂ (1.6 mg, 0.0025 mmol, 5 mol%), AgOTf (1.6 mg, 0.0065 mmol, 13 mol %), sulfondiimine **5o** (14.9 mg, 0.05 mmol, 1.0 equiv.), and sulfoxonium ylide **6a** (10.8 mg, 0.055 mmol, 1.1 equiv.). After the addition of chlorobenzene (0.5 mL) and CD₃OD (10.0 equiv.), the test tube was capped and brought out of the glovebox. The reaction mixture was stirred at 40 °C for 24 h. The resulting mixture was directly purified by silica gel column chromatography (hexane/AcOEt) to afford **8oa'** (12.0 mg, 60%) and **5o** (6.7 mg, 45%, with a small amount of some impurity). The ¹H NMR analysis of the recovered **5o** indicated no H/D exchange.



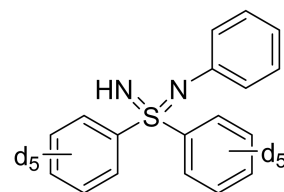


4.8. Kinetic isotopic effect

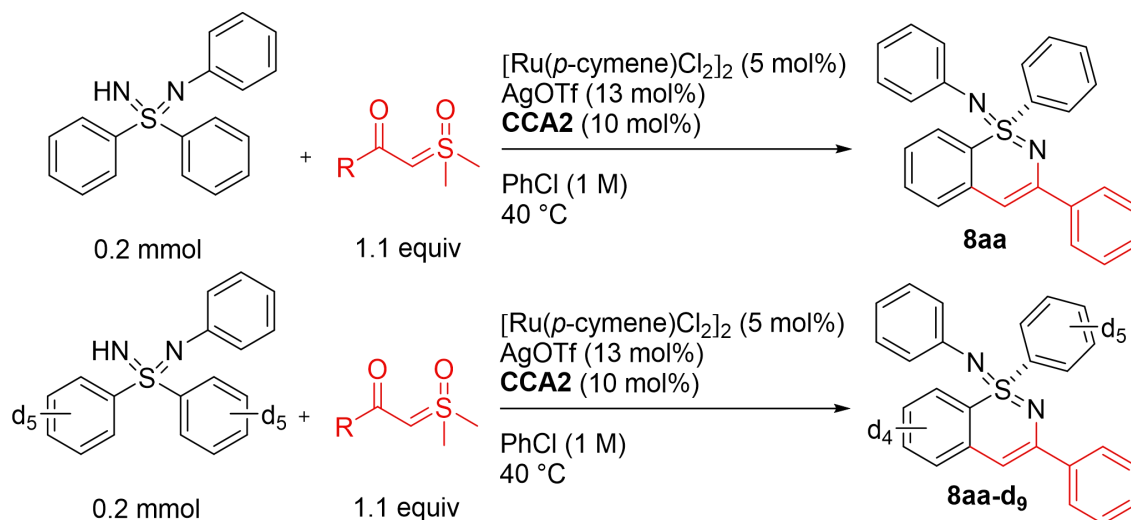
Bis(phenyl- d_5)sulfiliminium mesitylenesulfonate ($S2a-d_{10}$) : Prepared according to GP-F using bis(phenyl- d_5) sulfide (3.51 mmol, 690 mg, 1.0 equiv.), $S2a-d_{10}$ was isolated as a colorless solid (1.4 g, 96%). **IR** (KBr) 2989, 1603, 1455, 1320 1223, 1084, 1077, 1020, 682, 665 cm^{-1} . **1H NMR** ($CDCl_3$, 400 MHz) δ 7.62 (brs, 2H), 7.77 (s, 2H), 2.52 (s, 6H), 2.22 (s, 3H). **^{13}C NMR** ($CDCl_3$, 100 MHz) δ 139.6, 138.4, 137.1, 132.9, 132.5 (t, $J = 23.5$ Hz), 130.6, 129.7 (t, $J = 25.4$ Hz), 128.0 (t, $J = 25.8$ Hz), 22.9, 20.7. **HRMS** (ESI) m/z : $[M-MesO]^+$ Calcd for $C_{12}H_{10}D_{10}NS^+$: 212.1313; Found 212.1309.



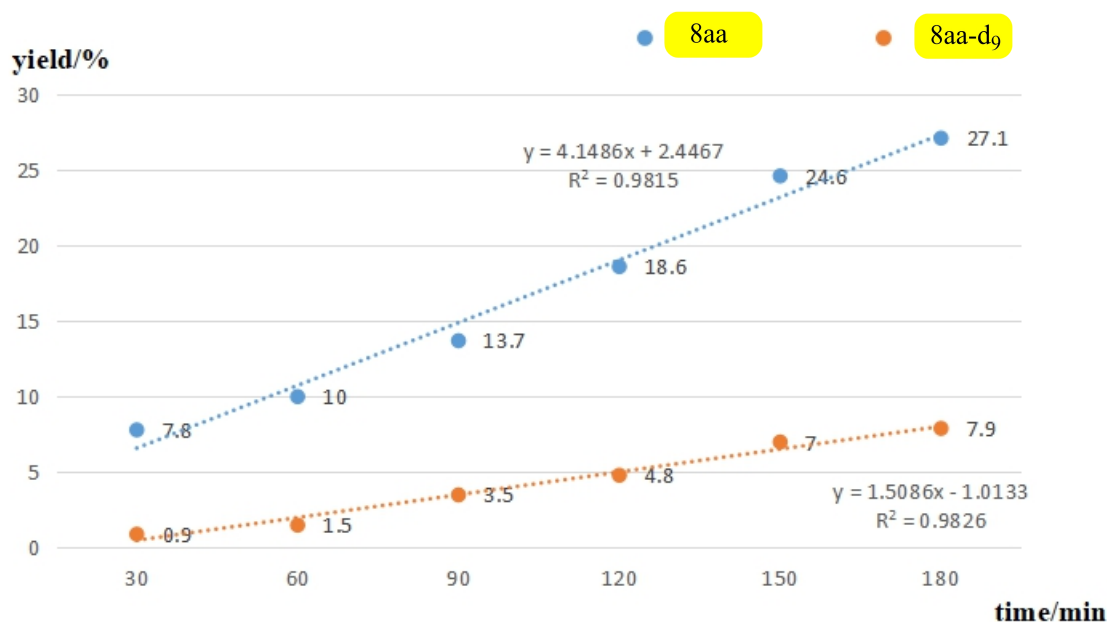
N-Phenyl-S,S-di(phenyl- d_5) sulfondiimine ($5a-d_{10}$) : Prepared according to GP-F using compound $S2a-d_{10}$ (3.2 mmol, 1.3 g, 1.0 equiv.), Na_2CO_3 (16.0 mmol, 1.7 g, 5.0 equiv.), Selectfluor (3.2 mmol, 1.14 g, 1.0 equiv.), aniline (9.6 mmol, 0.90 mL, 3.0 equiv.), pyridine (3.81 mmol, 0.33 mL, 1.2 equiv.). $5a-d_{10}$ was isolated as a brown solid (0.30 g, 31%). **IR** (KBr) 3169, 1597, 1485, 1294, 1263, 1056, 964 817, 750, 692 cm^{-1} . **1H NMR** ($CDCl_3$, 400 MHz) δ 7.18-7.11 (m, 4H), 6.85 (t, $J = 6.3$ Hz, 1H), 2.22 (brs,



¹H). ¹³C NMR (CDCl₃, 100 MHz) δ 145.7, 142.9, 131.5 (t, *J* = 23.5 Hz), 128.8, 128.6 (t, *J* = 24.0 Hz), 127.6 (t, *J* = 25.4 Hz), 123.3, 120.8. HRMS (ESI) *m/z*: [M+Na]⁺ Calcd for C₁₈H₆D₁₀N₂SNa⁺: 325.1554; Found 325.1549. Rf 0.3 (hexane/AcOEt = 3:1).



In an argon-filled glovebox, a screw-capped test tube was charged with chiral carboxylic acid **CCA2** (9.6 mg, 0.02 mmol, 10 mol%), [Ru(*p*-cymene)Cl₂]₂ (6.4 mg, 0.01 mmol, 5 mol%), AgOTf (6.4 mg, 0.026 mmol, 13 mol%), sulfondiimine **5** (0.2 mmol, 1.0 equiv.), and sulfoxonium ylides **6a** (0.22 mmol, 43.2 mg, 1.1 equiv.). After the addition of chlorobenzene (0.2 mL), the test tube was stirred at 40 °C in the glovebox. An aliquot of the mixture (25 μL) was taken by syringe at each reaction time (30, 60, 90, 120, 180 min) and filtrated through Celite using ethyl acetate. The yield was calculated by ¹H NMR analysis using CHBr₂CHBr₂ as the internal standard.



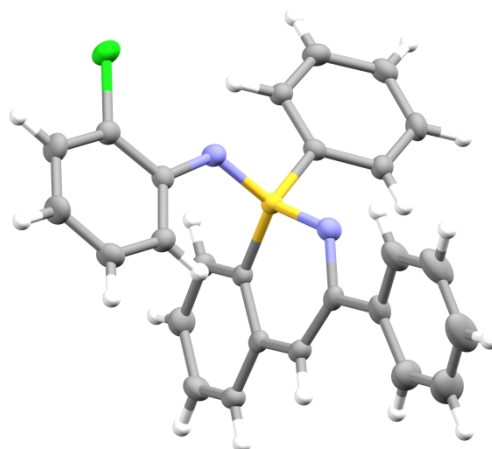
4.9.1 Determination of the absolute configuration

A single crystal of **8ka** suitable for X-ray crystallography was grown by slow vapor diffusion of pentane to a solution of **8ka** in ethyl acetate. Single crystal X-ray diffraction analysis was performed on a Rigaku R-Axis RAPID/S equipped with an imaging plate area detector, a graphite-monochromated Cu-K α radiation source ($\lambda = 1.5418 \text{ \AA}$) and a low temperature system using cold nitrogen stream (133 K). The detailed data were available in a crystallographic information file (CIF) deposited in CCDC (@@@@).

Table 1. Crystal data and structure refinement for **8ka**.

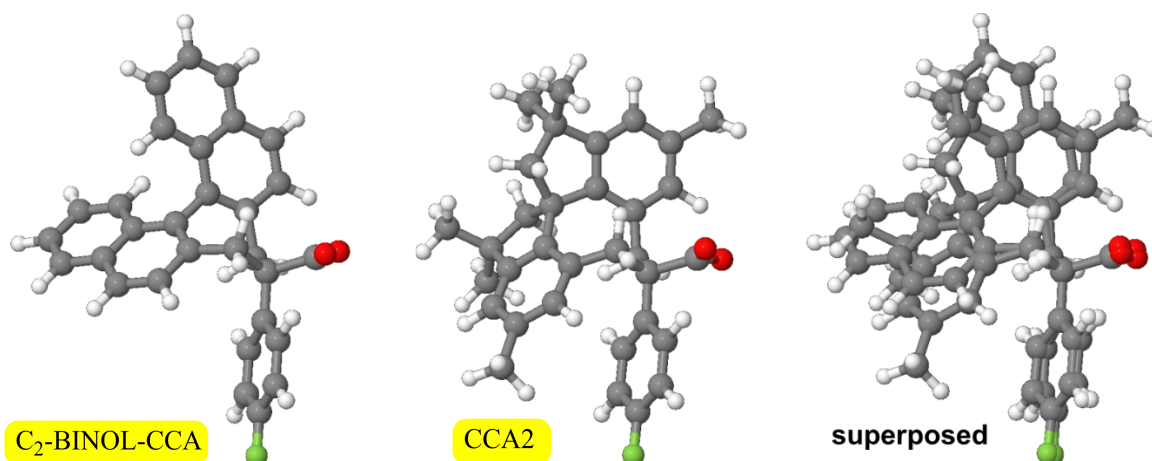
Identification code	8ka	
Empirical formula	C ₂₆ H ₁₉ Cl N ₂ S	
Formula weight	426.94	
Temperature	133(2) K	
Wavelength	1.54187 \AA	
Crystal system	Orthorhombic	
Space group	P2 ₁ 2 ₁ 2 ₁	
Unit cell dimensions	a = 9.5685(2) \AA	a = 90 \AA
	b = 13.1219(2) \AA	b = 90 \AA
	c = 16.8024(3) \AA	g = 90 \AA
Volume	2109.66(7) \AA^3	
Z	4	
Density (calculated)	1.344 Mg/m ³	
Absorption coefficient	2.637 mm ⁻¹	
F(000)	888	
Crystal size	0.428 x 0.348 x 0.295 mm ³	
Theta range for data collection	4.275 to 68.224 $^\circ$	
Index ranges	-11 \leq h \leq 11, -15 \leq k \leq 15, -20 \leq l \leq 20	
Reflections collected	24033	
Independent reflections	3844 [R(int) = 0.0396]	
Completeness to theta = 67.687 $^\circ$	100.0 %	
Absorption correction	Semi-empirical from equivalents	
Max. and min. transmission	1.0000 and 0.7999	
Refinement method	Full-matrix least-squares on F ²	
Data / restraints / parameters	3844 / 0 / 272	
Goodness-of-fit on F ²	1.071	
Final R indices [I > 2 σ (I)]	R1 = 0.0248, wR2 = 0.0656	
R indices (all data)	R1 = 0.0250, wR2 = 0.0658	
Absolute structure parameter	0.053(3)	

Extinction coefficient 0.0025(3)
 Largest diff. peak and hole 0.206 and -0.205 e.Å⁻³



4.9.2 Determination of the absolute configuration DFT calculation of the structures of chiral carboxylic acids

The structures of **C₂-BINOL-CCA** and **CCA2** as their carboxylate anion forms were optimized with ω B97X-D functional^[S6] and def2-SVP basis set^[S7] using Gaussian 16 Rev. C.01 program.^[S8] The structures and superposed structures with their carbonyl carbon atom, α -carbon atom, and adjacent carbon atom of the α -aryl moiety are shown below.



Cartesian coordinates of **C₂-BINOL-CCA** and **CCA2**:

C₂-BINOL-CCA : charge=-1, multiplicity=1							
C	0.95186900	0.77246700	0.27268200	C	2.54883400	2.23916500	-0.98533000
C	-0.20282500	0.66294000	1.04086200	C	0.79263300	3.23445100	0.39351100
C	1.44509000	2.06530600	-0.10009800	C	-1.53748000	-1.24431100	0.03306600
C	-0.81761800	-0.68661500	1.29720800	H	1.52740700	-0.64302700	2.13132400
C	-0.84671700	1.83975200	1.50357200	H	-0.04365900	-1.40747800	1.59455400
C	1.58255200	-0.49015600	-0.21847900	C	-0.35852700	3.08653000	1.21030100
				H	-1.75659000	1.73119000	2.09918500

C	0.78730800	-1.37227000	-0.93790100	C	3.79585163	-0.34950243	0.74672078
C	2.92694600	-0.85210300	0.12471000	H	3.25111923	1.76596635	1.12064919
C	3.00007500	3.49084200	-1.32574900	H	2.27417330	0.57498859	1.99022123
H	3.03384300	1.35468300	-1.40074900	C	0.39341329	1.38255151	0.38798556
C	1.29095200	4.51686500	0.03192100	C	1.72831673	-0.75068399	-0.44264362
C	0.65323300	-1.02867700	-1.20991700	C	1.43664322	3.03866892	-1.03270811
C	-2.90503400	-0.58147700	-0.11289700	H	3.11416953	1.67267895	-1.50957454
H	-0.86410800	3.98252400	1.58059100	H	1.55272704	1.19963360	-2.18998669
C	1.31364600	-2.62197700	-1.35637500	C	4.27892384	-0.98072291	2.05851388
C	3.75763100	-0.04330000	0.95287600	C	5.01829054	0.13216750	-0.05135691
C	3.45497500	-2.09035900	-0.34826300	C	2.94672340	-1.31630378	-0.06281646
C	2.37223900	4.64785900	-0.80343400	C	-0.65283770	0.83710729	1.14921446
H	3.84634800	3.59454600	-2.00914000	C	0.32885483	2.70838438	-0.04464919
H	0.78503500	5.40240400	0.42691100	C	0.73965325	-1.54263916	-1.04457616
H	-1.05440800	-1.66834200	-2.00557700	C	0.87011363	3.63831704	-2.32631781
H	-0.68954600	0.02205100	-1.53624800	C	2.45458106	4.02284874	-0.43476277
C	-3.27539700	0.22294000	-1.19631200	H	4.99942287	-1.79327465	1.87236833
C	-3.86408300	-0.78192600	0.89800800	H	4.77900594	-0.22755793	2.69034646
C	2.61483000	-2.96001500	-1.09384000	H	3.43425074	-1.40162881	2.62434257
H	0.62993500	-3.31615300	-1.84835900	H	5.69254907	-0.71274693	-0.26458236
C	5.04530200	-0.41599700	1.25448400	H	5.58726670	0.88724816	0.51651579
H	3.35476200	0.88597600	1.35823100	H	4.73098201	0.57199953	-1.01604564
C	4.79460700	-2.44321700	-0.02700700	C	3.24554934	-2.64283626	-0.36167062
H	2.74154900	5.63938200	-1.07663500	C	-0.84277541	-0.64769623	1.30365775
C	-4.53381300	0.82717400	-1.26856300	C	-1.66508573	1.70944250	1.56442769
H	-2.57956700	0.39420500	-2.01759100	C	-0.70381999	3.55099754	0.36081171
C	-5.11948600	-0.18734700	0.84392000	C	-0.66606912	-1.03439527	-1.23404558
H	-3.60317800	-1.46494300	1.71070100	C	1.05154412	-2.87665189	-1.32326048
H	3.01358700	-3.92329300	-1.42358100	H	0.42825737	4.63226090	-2.15033743
C	5.57850400	-1.62625100	0.74993000	H	1.66567428	3.75317191	-3.08136349
H	5.65897200	0.22297000	1.89420900	H	0.08667450	2.98996425	-2.74729761
H	5.18665600	-3.39200600	-0.40409100	H	1.97227002	4.98962996	-0.21845342
C	-5.43849500	0.62009500	-0.24180400	H	3.28377184	4.20593044	-1.13818397
H	-4.81372600	1.45627500	-2.11579700	H	2.87989608	3.65058083	0.50698947
H	-5.86104900	-0.35221500	1.62830500	C	2.29790214	-3.43424019	-1.01528781
H	6.60468100	-1.91359200	0.99213600	H	4.20325866	-3.07736176	-0.05643149
F	-6.65009500	1.20314200	-0.29831800	C	-1.52900787	-1.24264621	0.03312822
C	-1.77655600	-2.82112300	0.25452000	H	-1.47969962	-0.88885309	2.16306418
O	-2.09120600	-3.13372100	1.41530400	H	0.10577989	-1.17474948	1.47231154
O	-1.63175000	-3.52990800	-0.75369800	C	-1.70673970	3.05903506	1.19859726
				H	-2.49494824	1.29532928	2.14481080
				H	-0.74681809	4.58622232	0.00679264
CCA2: charge=-1, multiplicity=1				H	-1.16443165	-1.58802099	-2.04033086
C	1.68899348	0.73073959	-0.08386583	H	-0.62257547	0.02937338	-1.51129389
C	2.77326311	0.77986409	1.02981243	H	0.25038680	-3.50603122	-1.71873990
C	2.03588596	1.63337742	-1.29995400	H			

C	2.56906969	-4.88210614	-1.33641933
C	-2.90613123	-0.59078471	-0.11157848
C	-2.86911576	3.91756695	1.62762147
H	3.52784504	-5.21919479	-0.91455024
H	2.60226167	-5.04883027	-2.42543196
H	1.77064139	-5.52488974	-0.93519974
C	-3.20228665	0.40044763	-1.05288793
C	-3.91665883	-0.93165620	0.80465240
H	-3.80489950	3.55618094	1.17099049
H	-3.00849757	3.88789441	2.71965782
H	-2.72971778	4.96764569	1.33068278
C	-4.43896797	1.04954603	-1.07542944
H	-2.45240460	0.70616877	-1.78253433
C	-5.15410376	-0.29626575	0.79919349
H	-3.70005176	-1.72239433	1.52846519
C	-5.39858123	0.69686006	-0.14151576
H	-4.65800107	1.83017903	-1.80660787
H	-5.93457081	-0.56455181	1.51417985
F	-6.58924445	1.32509845	-0.14611849
C	-1.78393091	-2.81348007	0.25313925
O	-1.92178860	-3.16492517	1.43762334
O	-1.86429499	-3.48477419	-0.78908759

5. Reference for experimental section

- [S1] (a) Lu, B.; Li, C.; Zhang, L. *J. Am. Chem. Soc.* **2010**, *132*, 14070. (b) Fukagawa, S.; Yoshino, T.; Matsunaga, S. *Angew. Chem. Int. Ed.* **2019**, *58*, 18154.
- [S2] (a) Chanthamath, S.; Takaki, S.; Shibatomi, K. and Iwasa, S. *Angew. Chem. Int. Ed.* **2013**, *52*, 5818. (b) Hellmuth, T.; Frey, W. and Peters, R. *Angew. Chem. Int. Ed.* **2015**, *54*, 2788.
- [S3] (a) Tota, A.; Zenzola, M.; Chawner, J. S. *Chem. Commun.* **2017**, *53*, 348. (b) Vaitla, J.; Bayer, A.; Hopmann, K. H. *Angew. Chem. Int. Ed.* **2017**, *56*, 4277. (c) Kato, Y.; Lin, L-Q.; Kojima, M.; Yoshino, T.; Matsunaga, S. *ACS Catal.* **2021**, *11*, 4271.
- [S4] Zhou, T. ; Qian, P.-F.; Li, J.-Y.; Zhou, Y.-B.; Li, H.-C.; Chen, H.-Y.; Shi, B.-F. *J. Am. Chem. Soc.* **2021**, *143*, 6810.
- [S5] (a) Candy, M.; Guyon, C.; Mersmann, S.; Chen, J.-R.; Bolm, C. *Angew. Chem. Int. Ed.* **2012**, *51*, 4440; (b) Yoshimura, T.; Ishikawa, H.; Fujie, T.; Takata, E.; Miyatake, R.; Kita, H.; Tsukurimichi, E. *Synthesis* **2008**, 1835.
- [S6] Chai, J.-D.; Head-Gordon, M. *Phys. Chem. Chem. Phys.* **2008**, *10*, 6615.
- [S7] Weigend, F.; Ahlrichs, R. *Phys. Chem. Chem. Phys.* **2005**, *7*, 3297.
- [S8] Gaussian 16, Revision C.01, Frisch, M. J.; Trucks, G. W.; Schlegel, H. B.; Scuseria, G. E.; Robb, M. A.; Cheeseman, J. R.; Scalmani, G.; Barone, V.; Petersson, G. A.; Nakatsuji, H.; Li, X.; Caricato, M.; Marenich, A. V.; Bloino, J.; Janesko, B. G.; Gomperts, R.; Mennucci, B.; Hratchian, H. P.; Ortiz, J. V.; Izmaylov, A. F.; Sonnenberg, J. L.; Williams-Young, D.; Ding, F.; Lipparini, F.; Egidi, F.; Goings, J.; Peng, B.; Petrone, A.; Henderson, T.; Ranasinghe, D.; Zakrzewski, V. G.; Gao, J.; Rega, N.; Zheng, G.; Liang, W.; Hada, M.; Ehara, M.; Toyota, K.; Fukuda, R.; Hasegawa, J.; Ishida, M.; Nakajima, T.; Honda, Y.; Kitao, O.; Nakai, H.; Vreven, T.; Throssell, K.; Montgomery, J. A.; Peralta, Jr., J. E.; Ogliaro, F.; Bearpark, M. J.; Heyd, J. J.; Brothers, E. N.; Kudin, K. N.; Staroverov, V. N.; Keith, T. A.; Kobayashi, R.; Normand, J.; Raghavachari, K.; Rendell, A. P.; Burant, J. C.; Iyengar, S. S.; Tomasi, J.; Cossi, M.; Millam, J. M.; Klene, M.; Adamo, C.; Cammi, R.; Ochterski, J. W.; Martin, R. L.; Morokuma, K.; Farkas, O.; Foresman, J. B. and Fox, D. J. Gaussian, Inc., Wallingford CT, 2016.

Reference

- 【1】 For review about Cp*M(III) catalyzed C-H bond activation: a) Yoshino, T. *Bull. Chem. Soc. Jpn.* **2022**, *95*, 1280. b) Yoshino, T.; Matsunaga, S. *ACS Catal.* **2021**, *11*, 6455. c) Mas-Roselló, J.; Herraiz, A. G.; Audic, B.; Laverny, A.; Cramer, N. *Angew. Chem. Int. Ed.* **2021**, *60*, 13198. d) Yoshino, T.; Satake, S.; Matsunaga, S. *Chem. Eur. J.* **2020**, *26*, 7346. e) Peneau, A.; Guillou, C.; Chabaud, L. *Eur. J. Org. Chem.* **2018**, 5777. f) Park, J.; Chang, S. *Chem. Asian J.* **2018**, *13*, 1089. g) Piou, T.; Rovis, T. *Acc. Chem. Res.* **2018**, *51*, 170. h) Chirila, P. G.; Whiteoak, C. J. *Dalton Trans.* **2017**, *46*, 9721. i) Wang, S.; Chen, S.-Y.; Yu, X.-Q. *Chem. Commun.* **2017**, *53*, 3165. j) Yoshino, T.; Matsunaga, S. *Adv. Synth. Catal.* **2017**, *359*, 1245. k) Song, G.; Li, X. *Acc. Chem. Res.* **2015**, *48*, 1007. l) Satoh, T.; Miura, M. *Chem. Eur. J.* **2010**, *16*, 11212.
- 【2】 a) Ueura, K.; Satoh, T.; Miura, M.; *Org. Lett.* **2007**, *9*, 1407. b) Ueura, K.; Satoh, T.; Miura, M. *J. Org. Chem.* **2007**, *72*, 5362.
- 【3】 a) Yoshino, T.; Ikemoto, H.; Matsunaga, S.; Kanai, M. *Angew. Chem. Int. Ed.* **2013**, *52*, 2207. b) Sun, B.; Yoshino, T.; Matsunaga, S.; Kanai, M. *Adv. Synth. Catal.* **2014**, *356*, 1491.
- 【4】 Hyster, T. K.; Knçrr, L.; Ward, T. R.; Rovis, T. *Science*, **2012**, *338*, 500.
- 【5】 a) Ye, B.; Cramer, N. *Science*, **2012**, *338*, 504. b) Ye, B.; Cramer, N. *J. Am. Chem. Soc.* **2013**, *135*, 636.
- 【6】 Tian, M.; Bai, D.; Zheng, G.; Chang, J.; Li, X. *J. Am. Chem. Soc.* **2019**, *141*, 9527.
- 【7】 a) Zheng, J.; Cui, W.-J.; Zheng, C.; You, S.-L. *J. Am. Chem. Soc.* **2016**, *138*, 5242. b) For other applications of Rh-3, see: Zheng, J.; Wang, S.-B.; Zheng, C.; You, S.-L. *Angew. Chem. Int. Ed.* **2017**, *56*, 4540. c) Li, T.; Zhou, C.; Yan, X.; Wang, J. *Angew. Chem. Int. Ed.* **2018**, *57*, 4048.
- 【8】 a) Jia, Z.-J.; Merten, C.; Gontla, R.; Daniliuc, C. G.; Antonchick, A. P.; Waldmann, H. *Angew. Chem. Int. Ed.* **2017**, *56*, 2429. b) Trifonova, E. A.; Ankudinov, N. M.; Mikhaylov, A. A.; D. A. Chusov, D. A.; Nelyubina, Y. V.; Perekalin, D. S. *Angew. Chem. Int. Ed.* **2018**, *57*, 7714. c) Ozols, K.; Jang, Y.-S.; Cramer, N. *J. Am. Chem. Soc.* **2019**, *141*, 5675. d) Mas-Roselló, J.; Smejkal, T.; Cramer, N. *Science* **2020**, *368*, 1098.
- 【9】 For review about carboxylate-assisted mechanism: a) Ackermann, L. *Chem. Rev.* **2011**, *111*, 1315. b) Ackermann, L. *Acc. Chem. Res.* **2014**, *47*, 281. c) Park, H. S.; Fan, Z.-L.; Zhu, R.-Y. and Yu, J.-Q. *Angew. Chem.* **2020**, *132*, 2. d) Shao, Q.; Wu, K.; Zhuang, Z.; Qian, S.; Yu, J.-Q. *Acc. Chem. Res.* **2020**, *53*, 833.
- 【10】 a) Shi, B.-F.; Mangel, N.; Zhang, Y.-H. and Yu, J.-Q. *Angew. Chem. Int. Ed.* **2008**, *47*, 4882. b) Liu, Y.-H.; Li, P.-X.; Yao, Q.-J.; Zhang, Z.-Z.; Huang, D.-Y.; Le, M.-D.; Song, H.; Liu, L. and Shi, B.-F. *Org. Lett.* **2019**, *21*, 1895.
- 【11】 Gwon, D.; Park, S.; Chang, S. *Tetrahedron* **2015**, *71*, 4504.
- 【12】 Jang, Y.-S.; Dieckmann, M.; Cramer, N. *Angew. Chem. Int. Ed.* **2017**, *56*, 15088.
- 【13】 a) Gomez-Gallego, M.; Sierra, M. A. *Chem. Rev.* **2011**, *111*, 4857. b) Simmons, E. M.; Hartwig, J. F. *Angew. Chem., Int. Ed.* **2012**, *51*, 3066.
- 【14】 Lin, L.-Q.; Fukagawa, S.; Sekine, D.; Tomita, E.; Yoshino, T.; Matsunaga, S. *Angew. Chem. Int. Ed.* **2018**, *57*, 12048.
- 【15】 a) Satake, S.; Kurihara, T.; Nishikawa, K.; Mochizuki, T.; Hatano, M.; Ishihara, K.; Yoshino, T.; Matsunaga, S. *Nat. Catal.* **2018**, *1*, 585. b) Kurihara, T.; Kojima, M.; Yoshino, T.; Matsunaga, S. *Asian J. Org. Chem.* **2020**, *9*, 368.
- 【16】 Fukagawa, S.; Kato, Y.; Tanaka, R.; Kojima, M.; Yoshino, T.; Matsunaga, S. *Angew. Chem. Int. Ed.*

- 2019, 58, 1153.
- 【17】 a) Fukagawa, S.; Kojima, M.; Yoshino, T.; Matsunaga, S. *Angew. Chem. Int. Ed.* **2019**, *58*, 18154. b) Kato, Y.; Lin, L.; Kojima, M.; Yoshino, T.; Matsunaga, S. *ACS Catal.* **2021**, *11*, 4271. c) Sekine, D.; Ikeda, K.; Fukagawa, S.; Kojima, M.; Yoshino, T.; Matsunaga, S. *Organometallics* **2019**, *38*, 3921. d) Hirata, Y.; Sekine, D.; Kato, Y.; Lin, L.; Kojima, M.; Yoshino, T.; Matsunaga, S. *Angew. Chem., Int. Ed.* **2022**, *61*, e202205341. e) Zhou, Y.-B.; Zhou, T.; Qian, P.-F.; Li, J.-Y.; Shi, B.-F. *ACS Catal.* **2022**, *12*, 9806.
- 【18】 For the racemic sample: a) For racemic reactions, see: Tan, P. W.; Mak, A. M.; Sullivan, M. B.; Dixon, D. J.; Seayad, J. *Angew. Chem. Int. Ed.* **2017**, *56*, 16550. b) Wang, H.; Tang, G.; Li, X. *Angew. Chem. Int. Ed.* **2015**, *54*, 13049. c) Huang, J.; Huang, Y.; Wang, T.; Huang, Q.; Wang, Z.; Chen, Z. *Org. Lett.* **2017**, *19*, 1128.
- 【19】 For reviews about transition-metal catalyzed direct addition of C–H bonds to polar multiple bonds: a) Kakiuchi, F.; Kochi, T. *Synthesis* **2008**, 3013. b) Colby, D. A.; Tsai, A. S.; Bergman, R. G.; Ellman, J. A. *Acc. Chem. Res.* **2012**, *45*, 814. c) Yan, G.; Wu, X.; Yang, M. *Org. Biomol. Chem.* **2013**, *11*, 5558. d) Zhang, X.-X.; Chen, K.; Shi, Z.-J. *Chem. Sci.* **2014**, *5*, 2146. e) Yang, L. and Huang, H.-M. *Chem. Rev.* **2015**, *115*, 3468. f) Fagnou, K. and Lautens, M. *Chem. Reviews*, **2003**, *103*, 195. g) Hargrave, J. D.; Allen, J. C. and Frost, C. G. *Chem. Asian J.*, **2010**, *5*, 386.
- 【20】 a) Kakiuchi, F.; Murai, S. *Acc. Chem. Res.* **2002**, *35*, 826. b) Sakai, M.; Hayashi, H.; Miyaura, N. *Organometallics* **1997**, *16*, 4229. c) Yang, L.; Correia, C. A. and Li, C.-J. *Org. Biomol. Chem.* **2011**, *9*, 7176.
- 【21】 Shi, X.-Y.; Li, C.-J. *Org. Lett.* **2013**, *15*, 1476.
- 【22】 Yang, L.; Qian, B.; Huang, H. *Chem. Eur. J.* **2012**, *18*, 9511.
- 【23】 For the paper about Rh(III)-catalyzed C(sp³)–H activation: a) Hu, X.-H.; Yang, X. F.; Loh, T.-P. *ACS Catal.* **2016**, *6*, 5930. b) Liu, B.; Li, B.; Wang, B. *Chem. Commun.* **2015**, *51*, 16334. c) Hou, W.; Yang, Y.; Wu, Y.; Feng, H.; Li, Y.; Zhou, B. *Chem. Commun.* **2016**, *52*, 9672. d) Huang, X.; You, J. *Chem. Lett.* **2015**, *44*, 1685. e) Kang, T.; Kim, Y.; Lee, D.; Wang, Z.; Chang, S. *J. Am. Chem. Soc.* **2014**, *136*, 4141. f) Gao, P.; Guo, W.; Xue, J.; Zhao, Y.; Yuan, Y.; Xia, Y.; Shi, Z. *J. Am. Chem. Soc.* **2015**, *137*, 12231. g) Wang, N.; Li, R.; Li, L.; Xu, S.; Song, H.; Wang, B. *J. Org. Chem.* **2014**, *79*, 5379. h) Xu, S.; Song, H.; Wang, B. *Angew. Chem., Int. Ed.* **2014**, *53*, 4191. i) Tang, C.; Zou, M.; Liu, J.; Wen, X.; Sun, X.; Zhang, Y.; Jiao, N. *Chem. Eur. J.* **2016**, *22*, 11165. j) Kim, H.; Park, G.; Park, J.; Chang, S. *ACS Catal.* **2016**, *6*, 5922. k) Huang, X.; Wang, Y.; Lan, J.; You, J. *Angew. Chem., Int. Ed.* **2015**, *54*, 9404. l) Wang, X.; Yu, D.-G.; Glorius, F. *Angew. Chem., Int. Ed.* **2015**, *54*, 10280. m) Wang, H.; Tang, G.; Li, X. *Angew. Chem., Int. Ed.* **2015**, *54*, 13049.
- 【24】 Rh(III)-catalyzed racemic C(sp³)–H alkylations of 8-alkylquinolines: a) Han, S.; Park, J.; Kim, S.; Lee, S. H.; Sharma, S.; Mishra, N. K.; Jung, Y. H.; Kim, I. S. *Org. Lett.* **2016**, *18*, 4666. b) Liu, B.; Hu, P.; Zhou, X.; Bai, D.; Chang, J.; Li, X.; *Org. Lett.* **2017**, *19*, 2086. c) Han, S.; Ma, W.; Zhang, Z.; Liu, L.; Tang, M.; Li, J. *J. Org. Chem.* **2017**, *6*, 1014. d) Kumar, R.; Kumar, R.; Parmar, D.; Gupta, S. S.; Sharma, U. *J. Org. Chem.* **2020**, *85*, 1181.
- 【25】 For the review about Ru-catalyzed C–H activation: a) Arockiam, P. B.; Bruneau, C.; Dixneuf, P. H. *Chem. Rev.* **2012**, *112*, 5879. (b) Ackermann, L. *Acc. Chem. Res.* **2014**, *47*, 281. (c) De Sarkar, S.; Liu, W.; Kozhushkov, S. I.; Ackermann, L. *Adv. Synth. Catal.* **2014**, *356*, 1461. (d) Leitch, J. A.; Frost, C. G. *Chem. Soc. Rev.* **2017**, *46*, 7145. (e) Shan, C.; Zhu, L.; Qu, L. B.; Bai, R.; Lan, Y. *Chem. Soc. Rev.* **2018**, *47*, 7552.
- 【26】 Murai, S.; Kakiuchi, F.; Sekine, S.; Tanaka, Y.; Kamatani, A.; Sonoda, M.; Chatani, N. *Nature*.

- 1993, 366, 529.
- 【27】 Oi, S.; Fukita, S.; Hirata, N.; Watanuki, N.; Miyano, S.; Inoue, Y. *Org. Lett.* **2001**, *3*, 2579.
- 【28】 For the review about enantioselective Ru(II)-catalyzed C–H functionalization: Liang, H.; Wang, J. *Chem. Eur. J.* **2023**, *29*, e20220246.
- 【29】 Simonetti, M.; Cannas, D. M.; Just-Baringo, X.; Vitorica-Yrezabal, I. J.; Larrosa, I. *Nat. Chem.* **2018**, *10*, 724.
- 【30】 Liang, H.; Guo, W.; Li, J.; Jiang, J.; Wang, J. *Angew. Chem. Int. Ed.* **2022**, *61*, e202204926.
- 【31】 Pototskiy, R. A.; Boym, M. A.; Nelyubina, Y. V.; Perekalin, D. S. *Synthesis* **2021**, *54*, 4721.
- 【32】 Li, Z.-Y.; Lakmal, H. H. C.; Qian, X.; Zhu, Z.; Donnadiou, B.; McClain, S. J.; Xu, X.; Cui, X. *J. Am. Chem. Soc.* **2019**, *141*, 15730.
- 【33】 Li, G.; Liu, Q.; Vasamsetty, L.; Guo, W.; Wang, J. *Angew. Chem. Int. Ed.* **2020**, *59*, 3475.
- 【34】 Dhawa, U.; Connon, R.; Oliveira, J. C. A.; Steinbock, R.; Ackermann, L. *Org. Lett.* **2021**, *23*, 2760.
- 【35】 Li, Y.; Liou, Y.-C.; Oliveira, J. C. A.; Ackermann, L. *Angew. Chem. Int. Ed.* **2022**, *61*, e202212595.
- 【36】 Zhou, T.; Qian, P.-F.; Li, J.-Y.; Zhou, Y.-B.; Li, H.-C.; Chen, H.-Y.; Shi, B.-F. *J. Am. Chem. Soc.* **2021**, *143*, 6810.
- 【37】 Qian, P.-F.; Zhou, T.; Li, J.-Y.; Zhou, Y.-B.; Shi, B.-F. *ACS Catal.* **2022**, *12*, 13876.
- 【38】 For the review about sulfone: a) Ilardi, E. A.; Vitaku, E.; Njardarson, J. T. *J. Med. Chem.* **2014**, *57*, 2832. b) Zhao, C.; Rakesh, K. P.; Ravidar, L.; Fang, W.-Y.; Qin, H.-L. *Eur. J. Med. Chem.* **2019**, *162*, 679. For the review about sulfoximine: a) Bizet, V.; Hendriks, C. M. M.; Bolm, C. *Chem. Soc. Rev.* **2015**, *44*, 3378. b) Frings, M.; Bolm, C.; Blum, A.; Gnam, C. *Eur. J. Med. Chem.* **2017**, *126*, 225. c) Bull, J. A.; Degennaro, L.; Luisi, R.; *Synlett* **2017**, *28*, 2525. d) Ghosh, P.; Ganguly, B.; Das, S. *Asian J. Org. Chem.* **2020**, *9*, 2035. e) Andresini, M.; Tota, A.; Degennaro, L.; Bull, J. A.; Luisi, R. *Chem. Eur. J.* **2021**, *27*, 17293.
- 【39】 Dong, W.; Wang, L.; Parthasarathy, K.; Pan, F.; Bolm, C. *Angew. Chem. Int. Ed.* **2013**, *52*, 11573.
- 【40】 Parthasarathy, K.; Bolm, C. *Chem. Eur. J.* **2014**, *20*, 1.
- 【41】 Li, Y.; Dong, L. *Org. Biomol. Chem.* **2017**, *15*, 9983.
- 【42】 Hanchate, V.; Muniraj, N.; Prabhu, K. R. *J. Org. Chem.* **2019**, *84*, 8248.
- 【43】 Shen, B.; Wan, B.; Li, X. *Angew. Chem. Int. Ed.* **2018**, *57*, 15534.
- 【44】 Sun, Y.; Cramer, N. *Angew. Chem. Int. Ed.* **2018**, *57*, 15539.
- 【45】 Brauns, M.; Cramer, N. *Angew. Chem. Int. Ed.* **2019**, *58*, 8902.
- 【46】 Mukherjee, K.; Grimblat, N.; Sau, S.; Ghosh, K.; Shankar, M.; Gandon, V.; Sahoo, A. K. *Chem. Sci.* **2021**, *12*, 14863.
- 【47】 Li, J.-Y.; Xie, P.-P.; Zhou, T.; Qian, P.-F.; Zhou, Y.-B.; Li, H.-C.; Hong, X.; Shi, B.-F. *ACS Catal.* **2022**, *12*, 9083.
- 【48】 Song, S.-Y.; Zhou, X.; Ke, Z.; Xu, S. *Angew. Chem. Int. Ed.* **2023**, *62*, e202217130.
- 【49】 Xie, H. S.; Lan, J. Y.; Gui, J.; Chen, F. J.; Jiang, H. F.; Zeng, W. *Adv. Synth. Catal.* **2018**, *360*, 3534.
- 【50】 Bohmann, R. A.; Schöbel, J.-H.; Unoh, Y.; Miura, M.; Bolm, C. *Adv. Synth. Catal.* **2019**, *361*, 2000.
- 【51】 Huang, L.-T.; Fukagawa, S.; Kojima, M.; Yoshino, T.; Matsunaga, S. *Org. Lett.* **2020**, *22*, 8256.
- 【52】 Huang, L.-T.; Hirata, Y.; Kato, Y.; Lin, L.; Kojima, M.; Yoshino, T.; Matsunaga, S. *Synthesis*. **2021**, *54*, 4703.
- 【53】 Huang, L.-T.; Kitakawa, Y.; Yamada, K.; Kamiyama, F.; Kojima, M.; Yoshino, T.; Matsunaga, S. doi: 10.1002/anie.202305480.

